

Methods for the determination of possible damage

to people and objects resulting from release of hazardous materials

CPR 16E

First edition 1992

Methods for the determination of possible damage

to people and objects resulting from releases of hazardous materials

CPR 16E

This report, which has been prepared under the auspices of the Committee for the Prevention of Disasters caused by Dangerous Substances, is published at the request of

The Director-General of Labour
The Director-General for Environmental Protection
The Director-General for Public Order and Security
The Director-General for Transport

The Labour Inspectorate sees this report as an "Information Sheet" issued by this Inspectorate.

Voorburg, December 1989

The Director-General of Labour

ir. A.J. Roos

CIP-data of the Royal Library, The Hague

Methods

Methods for the determination of possible damage to people and objects resulting from releases of hazardous materials/Committee for the Prevention of Disasters caused by dangerous substances.

The Hague: Directorate-General of Labour of the Ministry of Social Affairs and Employment. III. (CPR. ISSN 0921-9633; 16)

ISBN 90-5307-052-4

SISO 614.3 UDC 614.87

Subject: Hazardous materials

Research performed by TNO - The Netherlands Organisation of Applied Scientific Research

Listing of authors

Chapter 1. Damage caused by heat radiation	Ir. C.J.H. van den Bosch, et al. – Institute of Environmental and Energy Research Ir. L. Twilt – Center of fire research
Chapter 2. The consequences of explosion effects on structures	Ir. W.P.M. Merx – Prins Maurits Laboratory
Chapter 3. The consequences of explosion effects on humans	Ir. W.P.M. Merx – Prins Maurits Laboratory
Chapter 4. Survey study of the products which can be released during a fire	C.M.A. Jansen – Institute of Environmental and Energy Research
Chapter 5. Damage caused by acute intoxication	Drs. D. de Weger, et al. – Institute of Environmental and Energy Research Drs. P.G.J. Reuzel – Institute CIVO Toxicology and Nutrition and Food Research
Chapter 6. Protection against toxic substances by remaining indoors	D. v. Leeuwen – Prins Maurits Laboratory
Chapter 7. Population data	Ing. J.M. Blom-Bruggeman – Institute of Environmental and Energy Research

Contents

Introduction

Damage models for the purposes of risk analysis (a framework)

- 1. Damage caused by heat radiation**
- 2. The consequences of explosion effects on structures**
- 3. The consequences of explosion effects on humans**
- 4. Survey study of the products which can be released during a fire**
- 5. Damage caused by acute intoxication**
- 6. Protection against toxic substances by remaining indoors**
- 7. Population data**

Introduction

Extend and Limitations of the "Green Book"

The so-called "Green Book" hereby presented contains a number of models, the extend and limitations of which are determined by: on one side, the knowledge about the effect-damage relations which is available and, on the other side, the budget limitations for the development of this book. In a number of cases, the knowledge available, from a strictly scientific point of view, was not sufficiently adequate to provide a back-up for the models presented in the book. An example of this is the use of data about toxicity, in the effect-damage models. On the basis of suggestions provided by the researches concerning the models to be applied, and pending more information, an agreement has been reached, within the CPR (Committee for the Prevention of Disasters), regarding the modelling which is presently applicable. In general, this present book about damage models must be considered as one corresponding to the time period of the investigations. Even when it was ready to be printed, some new results of investigations became available which, in turn, permitted to provide a better understanding of some of the subjects in question. This, for example, applies to models for "toxic combustion products" and to models for "damage caused by explosions".

The "Green Book" has been developed under a limited budget and, due to the needs of clarity and standardization, the cost of years of research was not justified. The budget limitations, coupled with time limitations, find, in the opinion of the CPR, their logical repercussions in a number of models presented. An example of this is the chapter "Population data".

In summary, it is the view of the CPR that this book must be regarded as a series of recommendations for the use of the damage models, and it must further be noted that for budgetary, practical and pragmatical reasons, it has sometimes recourse to generalizations over and above the specific knowledge of possibilities which is available. Nevertheless, the CPR feels that the book properly serves the purposes of clarity and standardization related to damage models, notwithstanding the fact that valid reasons remain for further expansion and revision of the models in the future.

Voorburg, December 1989

The chairman of the committee for the Prevention of Disasters due to Dangerous Substances

Ir. E. Rombouts

Damage models for purposes of risk analysis

A framework

In the hereby presented book ("Green Book"), damage models are presented (also called vulnerability models) for the purpose of determining the possible damage to people and objects due to the release of dangerous substances. The use of these damage models is in general preceded by the application of the so-called effect models. An important standard reference, in this respect, in which these effect models are described, is the "Yellow book" (1). It deals with the calculation of concentrations of a given substance in the atmosphere, the calculation of heat radiation intensities and the calculation of overpressures due to an explosion. All of the above-mentioned effects are functions of the distance to the release point. These calculated effects, with the help of the damage models, can then be applied for the determination of damage which may be caused to people or objects.

Jointly with the book on "probabilities" ("Red Book") (2), the "Yellow Book" (1), this "Green Book" forms part of a series of standards for purposes of risk analysis. Risk analysis, as such, is not an exact science in all respects. It has, however, been shown that the application of the above-mentioned models can lead to a better insight of the risks of the handling of dangerous substances and, consequently, can be a help in reducing these risks.

In view of the relatively substantial uncertainties which are introduced, it is nevertheless recommended to be prudent in the interpretation of the results of a risk analysis.

An estimate of the uncertainties related to the application of the damage models presented is made, in as much as possible, during the presentation of the models themselves (see, for this, the chapters in question). These uncertainties must then be applied to the entire process of risk analysis. Uncertainties are also introduced into the probability determination of undesirable events as well as into the calculation of the effects. In the COVO study and in the LPG integrated study, the following uncertainty factors are globally mentioned: a factor of 10-100 in the probabilities and a factor of 10 in the consequences. In the "uncertainties of the effect calculations in risk studies" (3) a closer treatment has been conducted with regard to the uncertainty-parameters of the effect-models. A factor which spreads from 2 to 6 is indicated in this case.

In the application of the damage models, the user must realize that the results of the effect calculations (departure point for the damage calculation) are uncertain. Furthermore, the damage calculations themselves introduce additional uncertainties.

These uncertainties are of different types:

a. Model uncertainties

Important, in this case, is the difference of the vulnerability of people among themselves and of structures among themselves.

b. Parameter uncertainties

In this case, the following, for example, is essential: population data, toxicity data, duration of exposure (escape possibilities) etc.

In order to obtain an adequate evaluation of safety distances between installations, or between installations or transport routes and housing, the damage calculations, however, can certainly play a role.

The above is also the case for disaster combatment plans. By comparing various calculation results applied to the same models, the differences which can be observed can help reducing the degree of uncertainty. A relative use (comparisons between different locations/safety measures/transport routes, etc.) leads, consequently, to the best results.

It is worth recommending, when dealing with the damage models, to quantify, as close as possible, the influence of the uncertainties. This, or further research, will help reducing the magnitude of these uncertainties.

The results obtained must serve the purpose of obtaining a higher degree of safety. There is, apart from this, also a number of other techniques available (process safety analysis, HAZOP, safety audits, etc). A proper risk management requires that all knowledge and experience be up to date, that the installation itself is safe, that maintenance is adequate, etc. Furthermore, a proper evaluation of the possible damage due to an undesirable event also belongs to the field of good risk management. The models hereby presented can help, in this respect. These models reflect the knowledge, in this area, which was available by year 1987.

References

1. Methods for the Calculation of Physical Effects of the escape of dangerous material (liquids and gases). The "Yellow Book" DGA, OP 15E, 1979. (second edition, CPR 14E, 1991)
2. Methods for the Determining and the Processing Probabilities. DGA, CPR 12E, 1988.
3. The Uncertainty of Effect Calculations in Risk Studies. AVIV, January 1986.

Chapter 1

Damage caused by heat radiation

Contents

	Page
List of symbols	5
1. Introduction	6
1.1 Models	6
1.2 Description of chapters	6
1.3 Identification chart	7
1.4 Procedure for the calculation of damages due to heat radiation	7
2. The effects of heat radiation on people	11
2.1 Introduction	11
2.2 Characterization of the injury	11
2.3 Consequences of burns	12
2.4 Physical properties of the skin	13
2.5 A calculation model for the injury due to heat radiation	14
2.5.1 Introduction	14
2.5.2 Model for heat transfer	15
2.6 Experimental determination of injury caused by heat radiation	17
3. Statistical model for injury due to heat radiation	19
3.1 Introduction	19
3.2 Relationship between the heat load and the degree of burns	19
3.3 Determination of the extend of the damage with the help of probit functions	22
4. The influence of clothing on the extend of personal injury due to heat radiation	25
4.1 Introduction	25
4.2 The ignition of clothing	25
4.3 The protective effect of clothing	28
5. Options for the exposure duration of people subjected to heat radiation from a fire	30
5.1 Introduction	30
5.2 Influence of the composition of the exposed group	30
5.3 Influence of the conditions of the fire	31
5.4 Data from literature about exposure duration and a calculation procedure	32
6. Damages consequent to a flash fire	35
6.1 Introduction	35
6.2 The progress of a flash fire	35
6.3 Material damage due to a flash fire	36
6.4 Personal injury due to a flash fire	36
6.5 Conclusion	36
7. Material damages due to heat radiation	37
7.1 Introduction	37
7.2 The critical radiation intensity	38

7.3	Closer analysis of material damages	40
7.3.1	General	40
7.3.2	Wood	41
7.3.3	Synthetic materials	42
7.3.4	Glass	42
7.3.5	Steel	43
7.3.6	Evaluation	44
8.	Considerations regarding the results	46
9.	References	48
Appendix A.		
	Fatal injury, in the vicinity of a fireball or of a pool-fire caused by heat radiation.	51
Appendix B.		
	Examples of calculations of the exposure duration.	54
Appendix C.		
	Considerations with regard to a non-stationary character of the heat flux.	58

Symbols

A	: contents per unit length	[m ³]
A	: probit constant	
a	: absorption coefficient	[-]
a _t	: temperature-equalizing coefficient	[m ² s ⁻¹]
b	: see Figure 7.2	[m]
B	: probit constant	
c	: specific heat	[Jkg ⁻¹ K ⁻¹]
d	: thickness	[m]
D _s	: radiation dose	[s · (Wm ⁻²)n]
h	: see Figure 7.2	[m]
n	: concentration exponent in dose calculation	[-]
N ₀	: population density	[m ⁻²]
N ₁	: number of fatalities inside the fireball	[-]
N ₂	: the same outside the fireball	[-]
P	: probability	[-]
Pr	: probit	[-]
Q	: heat quantity	[Jm ⁻²]
q	: heat-flux absorbed	[Wm ⁻²]
q _i	: heat-flux inwards	[Wm ⁻²]
q _o	: intensity of heat radiation	[Wm ⁻²]
R	: radius of a fireball	[m]
r	: distance to the center of the fireball	[m]
s _i	: see Figure 7.2	[m]
s _u	: see Figure 7.2	[m]
Y	: temperature	[K]
t	: time	[s]
t _c	: exposure duration	[s]
t _{eff}	: effective exposure duration	[s]
t _r	: duration of reaction	[s]
T ₀	: ambient temperature	[K]
u	: speed of escape	[ms ⁻¹]
x	: distance (penetration depth)	[m]
x	: distance to the center of the fire	[m]
x ₀	: initial distance from the fire	[m]
α	: convective heat transfer coefficient	[Wm ⁻² K]
Δ	: relationship N ₂ /N ₁	[-]
ζ	: r/R	[-]
λ	: heat conduction coefficient	[Wm ⁻¹ K ⁻¹]
ρ	: specific mass	[kg m ⁻³]
σ	: Stephan Boltzman constant	[Wm ⁻² K ⁻⁴]

Introduction

1.1 Models

In Chapter 6 ("Heat radiation") of the Yellow Book [1] models are presented for the calculation of the heat radiation intensity for different types of fires. In the revision of the Yellow Book [2], a lot of data has been added. The effects of a fire are expressed in terms of radiation levels as functions of distance and time.

Different situations can be foreseen whereby, as consequence of a calamity, the amount of heat generated can be so large that damage to the surroundings of non-negligible magnitude can develop. This damage can manifest itself in the form of burns due to exposure and by deformation and weakening of materials, due to overheating. In addition (among others, due to auto-ignition) secondary fires may develop.

The most known models for the calculation of damage due to heat radiation are presented in the "Vulnerability Model" of the U.S. Coast Guard [3]. These models are of limited intent and, in addition, their application in the Netherlands is also of limited nature, among other reasons due to the difference between types of construction in the Netherlands and in the U.S. Furthermore, the models described in [3] are almost totally based on the analysis of damage due to nuclear explosions. There is, however, a justifiable doubt about the similarity of damage due to nuclear explosions and of damage due to fires of, for instance, hydrocarbons.

The models described in this report are suitable for conditions in the Netherlands and are based on conventional fires.

1.2 Description of Paragraphs

Paragraph 2 provides a general description of the effects of heat radiation on skin. It characterizes, first, the types of injury due to burns and their consequences. This follows by a description of skin properties and, finally, a model is presented for the calculation of the temperature variations in the skin due to heat radiation.

In Paragraph 3 a statistical characterization of personal injuries due to heat radiation is presented. With the help of the presented profit functions, it is possible to calculate the magnitude of the injury. The above departing from known exposure duration and radiation intensity.

Paragraph 4 deals with the influence of clothing on the extend of the injury. It provides, at the same time, values of radiation intensity whereby the clothing ignites, for different materials. The protective effect is expressed by a reduction factor of the extend of the damage.

Paragraph 5 provides indications for the determination of the effective exposure duration. Considerations are given, in this case, to the escape possibilities of people exposed to radiation as well as to the influence of the surroundings. The influence of escape possibilities on the extend of the damage is estimated.

In Paragraph 6 the consequences of a flash fire are analyzed. Due to the quick character of the burning process, the damage due to heat radiation outside of the flammable cloud are of limited nature.

Paragraph 7 gives global values for critical radiation intensities for materials: wood, synthetic materials, glass and uncoated steel. These are values whereby, for materials suitable for the outer faces of buildings or installations, damage must be considered for long term exposures. With regard to the damage itself, a difference is made between two levels of damage.

1.3 Identification Chart

With the help of the identification chart given in Figure 1.1 it is possible to establish under which conditions the values given in this report are applicable for the determination of damage due to heat radiation. The numbers outside of the blocks refer to the applicable paragraphs of this chapter.

1.4 Procedure for the Calculation of Damage due to Heat Radiation

In this paragraph, with reference to the identification chart of Figure 1.1, it is shown how the calculation of damage to people due to heat radiation must be conducted.

Determine the amount of victims within the flame area (See Appendix A)

- a. Calculate the dimensions of the flame (R)
- b. Determine the population density in the flame area
- c. The number of victims inside the flame area is calculated as follows:

$$N_1 = N_0 * \pi R^2 \quad (D.1)$$

Assumptions:

- homogenous distribution of the people
- all people outside

Determine the maximum effective exposure duration of a victim (t_{eff}) (See Paragraph 5 and Appendix B)

Determine the following quantities:

- Radius of a flame area (R) (Flame area = radius of a fireball or of a pool fire).
- Radiation intensity at the flame surface (q_0). (For instance with the help of the Yellow Book [1].
- Radiation intensity as function of the distance to the boundary of the flame (for instance with the help of a computer program [19]. The safe distance (x_v) is deducted from this.
- Maximum escape time (t_c) from the boundary of the flame (R) to x_v (at this distance, the radiation intensity is taken equal to 1 kW/m²), (Appendix B).
- Duration of the fire (t_0).
- Effective exposure duration (t_{eff}) inclusive of escape possibilities (Appendix B and Paragraph 5.4).

Assumptions:

- Speed of escape $u = 4$ m/s
- Reaction time $t_r = 5$ s
- The speed of escape calculated is valid for all persons exposed. Consequently, it represents an overestimation.

Determine the number of victims outside of the flame area (N_2), (See Appendix A).

$$N_2 = \int_R^{\infty} p(r) * N_o * 2\pi r dr \quad (D.2)$$

where

$$p(r) = F_k * \frac{1}{2} \left[1 + \operatorname{erf} \left(\frac{Pr-5}{\sqrt{2}} \right) \right] \quad (D.3)$$

(F_k is a reduction factor related to an eventual protection possibility of clothing, see below.)

Determine the influence of clothing (see Paragraph 4)

a. The clothing does not ignite

A reduction factor of the percentage of victims:

$F_k = 0.14$ is given, for the influence of clothing, in Paragraph 4.3, in which it is assumed that the clothing does not ignite. The dimensions of the 100% lethality area are, consequently, equal to the dimensions of the flame.

Assumptions:

- The skin protected by clothing remains unharmed.
- Average age distribution for the population exposed.
- Fully dressed, which means that only the face, the neck and the under-arms can suffer burns.

b. The clothing does ignite

Assumption:

- The injury is fatal when the clothing does ignite.

Consider that ignition occurs when the heat radiation dose received (D_{sk}) is higher than $2.5 * 10^4 \text{ kW}^2\text{m}^{-4}\text{s}$ (see Paragraph 4.2). We then determine the distance to the origin (R_k) at which this dose is surpassed, inclusive of escape considerations. Thereby we set the value of the exponent n in the dose equal to 2.7 (the maximum measured value, see Paragraph 4.2).

$$D_{sk} = q_o^{2.7} * t_r + t_r \int^{t_c} q(t)^{2.7} * dt \quad (D.4)$$

where

$$q(t) = q_o \left(\frac{x_o}{x_o + u(t - t_r)} \right)^2$$

and

t_r = reaction time = 5 s

From this given dose we can now calculate the time by which this dose will be reached, with the help of:

$$D_{sk} \geq 2.5 * 10^4 = (q_o)^{2.7} * t_r + \int_{t_r}^{t_c} \left[q_o * \frac{x_o}{x_o + u * (t - t_r)} \right]^{2.7} * dt \quad (D.5)$$

with

$$t_c = \left(\frac{x_v - x_o}{u} \right) + t_r \quad (D.6)$$

where x_v = distance when $q = 1 \text{ kW/m}^2$, and

x_o = starting location of the victim in relation to the boundary of the flame

From this, x_o can be determined by iteration. This value of x_o is, in the same time, the minimum value of x_o in the Formulas (B.3), (B.4) and (B.5). The corresponding value of R_k follows from:

$$R_k = R + x_o \quad (D.7)$$

The influence of clothing which ignites is evaluated by an increase of the surface which is located "inside" the flame area (= 100% fatal injury area). Therefore R has to be replaced by R_k in (D.1). In this manner, "double-countings" (consequences of the burning of the clothing and direct radiation effect) are, in the same time, avoided.

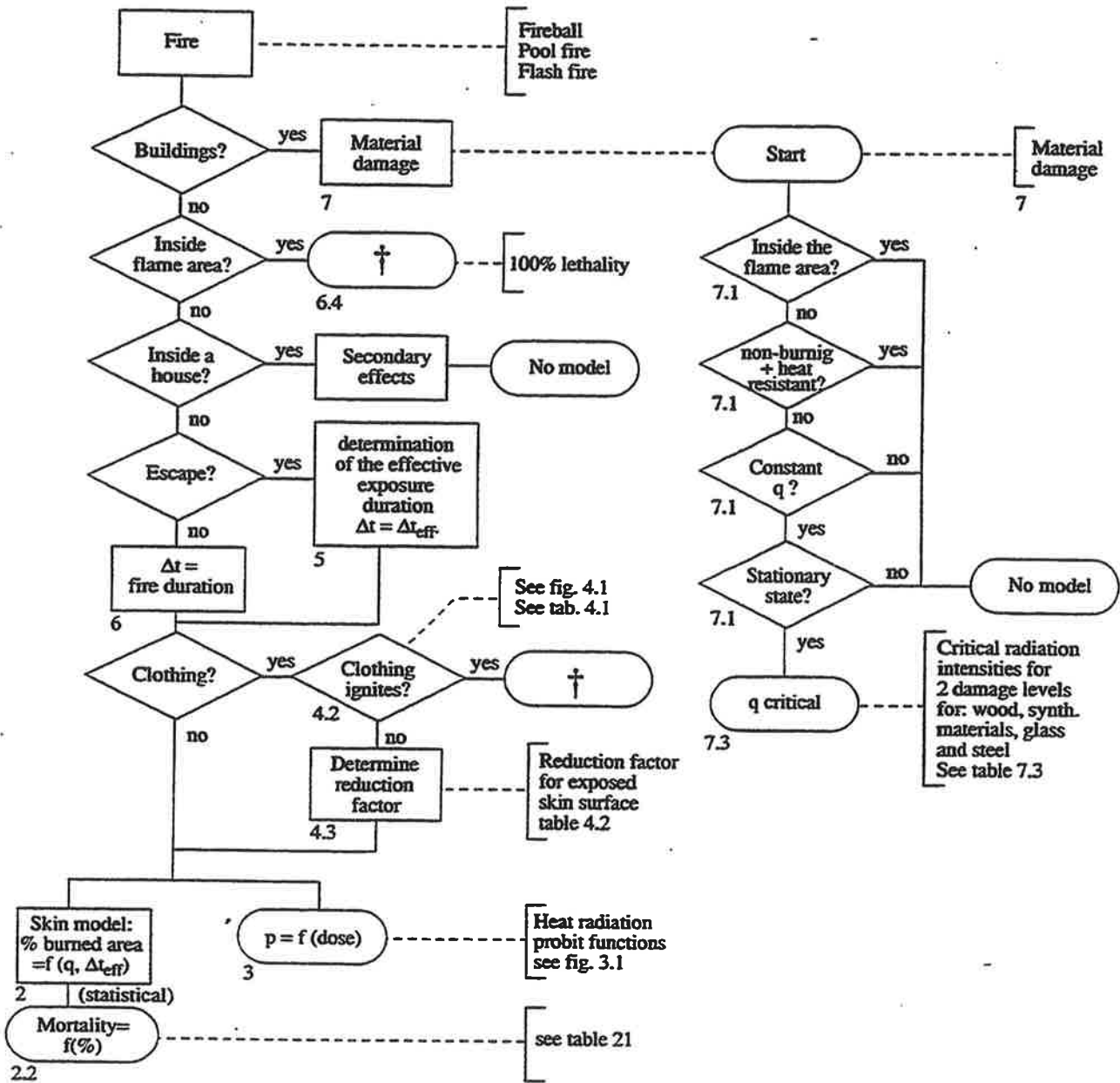


Fig. 1.1 Identification chart for damage due to heat radiation. The numbers under the blocks refer to the corresponding paragraphs.

The effects of heat radiation on people

2.1 Introduction

Heat radiation has a twofold effect on people. Physiological effects manifest themselves, primarily, by staying in hot, humid conditions. These effects are:

- Increase of the heart-beat
- Sweating (transpiration)
- Rise of the body temperature

These effects only play a role by a long term exposure and will not be further considered.

Pathological effects of heat radiation are related to the development of burns due to heat transfer to the skin. The process is relatively easy to describe for an unprotected skin. For a skin protected by clothing it is more complicated.

The development of burns on parts of the body which are protected by clothing is mainly caused by the ignition of the clothing. This phenomenon will be treated separately (Paragraph 4.2).

After the characterization of the seriousness of the injury due to heat radiation (burns) (Paragraph 2.2) and the explanation of the most essential physical properties of the skin (Paragraph 2.3), a model will be presented for the calculation of the depth of the burns, as function of the radiation dose to which the skin is exposed (Paragraph 2.4).

2.2 Characterization of the Injury

The injury caused to the skin by the heat radiation is normally defined as: first, second or third degree burn. This determines to what extent and to which depth the skin has been damaged. A published description of burns and of the consequent reactions of the body, as well as the corresponding therapy, is given in the book "Burns" [4]. The degrees of burns previously indicated have been taken from this book.

Figure 2.1 (also taken from [4]) gives a cross-section of the skin. The upper layer, the epidermis, has among others, the function of cell-formation; the recovery from burns takes place from the basale cell layer (stratum basale). In case of burns of the dermis, the recovery takes place from bulges of the epidermis in the dermis (see Figure 2.1).

A first degree burn is superficial and is characterized by a red, dry and painful skin. At a second degree burn the epidermis (thickness 0.07- 0.12 mm) is burned; this type of burn is characterized by blister formation and a wet skin, which is also red. A third degree burn extends to the dermis (thickness 1-2 mm) in which, among others, hair roots and free nerve extremities are present; the burned skin is absent of feeling, dry and has a white, yellow or black colour. Only within the range of a second degree burns a difference is still made between superficial or deep burns.

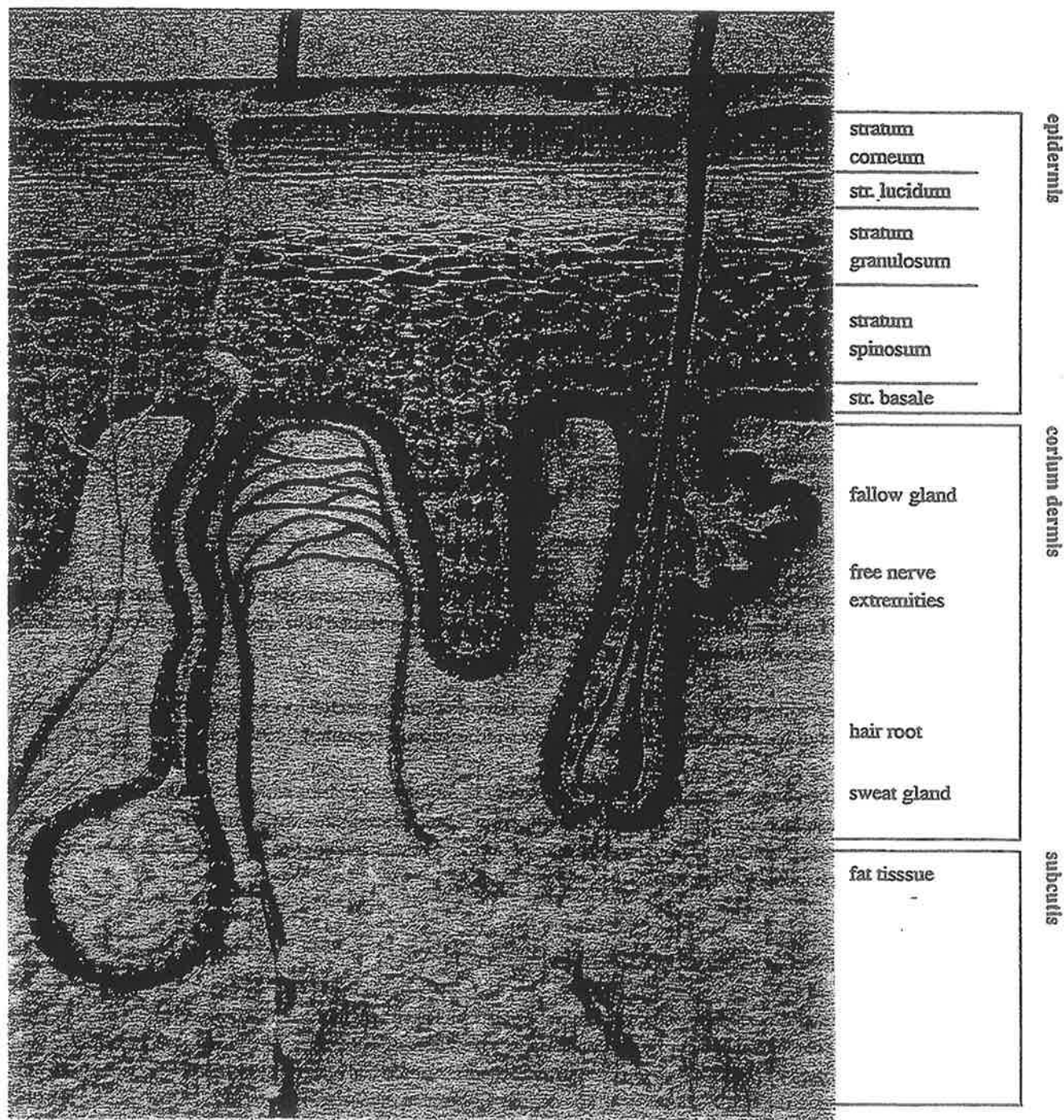


Fig. 2.1 Cross-section of the skin (schematic).

2.3

Consequences of Burns

Second and third degree burns can lead to disability. Their treatment, also related to the burn-sickness after a few hours, often requires clinical help in a specialized hospital. A realistic probability of mortality is also present.

An estimate of this probability is made on the basis of the portion of the skin surface which has been burned and depends, also, on the age of the person affected. Table 2.1 (taken from [4]) gives a relationship between the mortality probability and these parameters. This relationship (according to Bull [5] and Fisher) is used to estimate the survival possibilities of patients, among others by the "Brandwondencentrum" in Beverwijk, The Netherlands.

It can be seen, from this table, that by a 50% burn of the skin surface, a child between 0 to 9 years old

has a 80% probability of survival, a grown-up person aged 30 to 35 has a 50% probability and a person older than 60 years will practically certainly die.

Table 2.1 Relationship between age, percentage of burned area and mortality. (From The Lancet, 20 Nov. 1971).

% Body area burned	Age (yr)																
	0-4	5-9	10-14	15-19	20-24	25-29	30-34	35-39	40-44	45-49	50-54	55-59	60-64	65-69	70-74	75-79	80
93+	1	1	1	1	1	1	1	1	1	1	1	1	1	1	1	1	1
88-92	.9	.9	.9	.9	1	1	1	1	1	1	1	1	1	1	1	1	1
83-87	.9	.9	.9	.9	.9	.9	1	1	1	1	1	1	1	1	1	1	1
78-82	.8	.8	.8	.8	.9	.9	.9	.9	1	1	1	1	1	1	1	1	1
73-77	.7	.7	.8	.8	.8	.8	.9	.9	.9	1	1	1	1	1	1	1	1
68-72	.6	.6	.7	.7	.7	.8	.8	.8	.9	.9	.9	1	1	1	1	1	1
63-67	.5	.5	.6	.6	.6	.7	.7	.8	.8	.9	.9	.9	1	1	1	1	1
58-62	.4	.4	.4	.5	.5	.6	.6	.7	.7	.8	.9	.9	1	1	1	1	1
53-57	.3	.3	.3	.4	.4	.5	.5	.6	.7	.7	.8	.9	.9	1	1	1	1
48-52	.2	.2	.3	.3	.3	.3	.4	.5	.6	.6	.7	.8	.9	1	1	1	1
43-47	.2	.2	.2	.2	.2	.3	.3	.4	.4	.5	.6	.7	.8	1	1	1	1
38-42	.1	.1	.1	.1	.2	.2	.2	.3	.3	.4	.5	.6	.8	.9	1	1	1
33-37	.1	.1	.1	.1	.1	.1	.2	.2	.3	.3	.4	.5	.7	.8	.9	1	1
28-32	0	0	0	0	.1	.1	.1	.1	.2	.2	.3	.4	.6	.7	.9	1	1
23-27	0	0	0	0	0	0	.1	.1	.1	.2	.2	.3	.4	.6	.7	.9	1
18-22	0	0	0	0	0	0	0	.1	.1	.1	.1	.2	.3	.4	.6	.8	.9
13-17	0	0	0	0	0	0	0	0	0	.1	.1	.1	.2	.3	.5	.6	.7
8-12	0	0	0	0	0	0	0	0	0	0	.1	.1	.1	.2	.3	.5	.5
3-7	0	0	0	0	0	0	0	0	0	0	0	0	.1	.1	.2	.3	.4
0-2	0	0	1	0	0	0	0	0	0	0	0	0	0	.1	.1	.2	.2

The curing time for deep second or third degree burns can be set at, respectively, 14-21 and 21 days. Formation of blisters is considered to be superficially of second degree.

2.4

Physical Properties of the Skin

The physical properties of the skin are strongly dependent on the part of the human skin considered. This is especially important with regard to the skin thickness.

Stoll [6] indicates the following average values:

Table 2.2 Average values for physical properties of the skin of a man of 70 kgs and 1.7 m.

weight, M	4 kg
surface, A	1.8 m ²
volume, V	3.6 * 10 ⁻³ m ³
water contents, -	70 - 75% (mass)
specific mass, ρ	110 kg . m ⁻³
thickness, d	0.05-5 mm (in the main 1-2 mm)

The most important property of the skin in relation to wounds caused by heat radiation is the temperature-equalizing coefficient a_t ,

$$a_t = \frac{\lambda}{\rho c} [m^2 \cdot s^{-1}] \quad (2.0)$$

with:

λ : heat conducting coefficient [Wm⁻¹K⁻¹]
 ρ : specific mass [kg . m⁻³]
 c : specific heat [J . kg⁻¹K⁻¹]

This coefficient determines the speed by which the energy is absorbed by the skin and its temperature rise.

Another quantity which determines the extend of the temperature rise is the so-called thermal slowness: $\lambda \rho c$ [J²m⁻⁴s⁻¹K⁻²]. A heat conductivity model for the skin is given by Hardee and Lee [7]. Even though, sometimes, the thermal properties for water are used for the thermal properties of the skin, measurements show that these properties can vary very substantially. A number of measured values is given in Table 2.3.

Table 2.3 Thermal properties of human skin. From [7].

	λ [W/mK]	ρc [J/m ³ K]	a_t [m ² /s]	$\lambda \rho c$ [W/m ⁴ K ²]
Perkins et al [8]	0.764	3.35x10 ⁶	0.228x10 ⁻⁶	2.56x10 ⁶
Mitchell [32]	0.591	4.19x10 ⁶	0.141x10 ⁻⁶	2.47x10 ⁶
Stoll [6]	0.628	3.68x10 ⁶	0.171x10 ⁻⁶	2.31x10 ⁶

A preference, in [7], is given to the values given by Perkins et al [8].

The absorption coefficient, a , shows which part of the radiation is being absorbed. From tests by Stoll and Chianta [9] with (blackened) skin a 94% absorption is indicated. In view of the small value of the reflected part a full absorption of the radiation can be considered.

2.5

A Calculation Model for the Injury due to Heat Radiation

2.5.1

Introduction

Burns develop due to the temperature rise of the skin caused by heat transfer into the skin. At the heat supply produced by heat radiation due to a fire, the energy absorption is practically total ("see physical properties of the skin"). Dependent on the magnitude of the temperature rise and on the depth of penetration, more or less serious burns can develop, see Paragraph 2.2. A model is presented by Hardee and Lee [7], whereby the temperature in the skin is calculated as a function of time and location. By

comparing the calculated temperatures to the limit values of a given degree of burn we can obtain an idea of the extend of the burn consequent to exposure to a heat load.

2.5.2

Model for Heat Transfer

The heat transfer into the skin by radiation due to a fire can be considered as a one-dimensional heat transfer problem, see Figure 2.2.

A part of the radiation received will be reflected on the upper surface of the skin. Depending on the condition of the skin, this reflection can be larger or smaller. The heat-flux which goes through q follows from:

$$q = a * q_i \quad (2.1)$$

with a being the absorption coefficient.

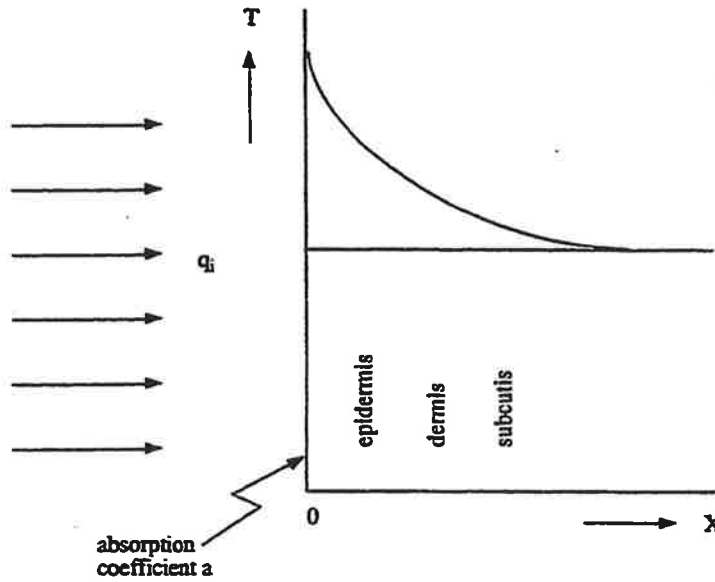


Fig. 2.2 One-dimensional model for heat transfer into the skin.

When the skin is assumed to be a half-infinite medium, whereby for $0 \leq t \leq t_c$ the heat-flux q is constant, we can then calculate for $t \leq t_c$ the temperature path with (see [7]):

$$T(t, x) - T_i = \frac{2q}{\sqrt{\lambda \rho c}} \sqrt{t} \operatorname{ierfc} \left(\frac{x}{\sqrt{4a_t t}} \right) \quad (2.2)$$

with T_i : the initial temperature [K]
 $T(t, x)$: temperature of the skin at depth x as a function of time
 x : the penetration depth [m]
 ierfc : integrated complementary error function
 t : exposure duration

$$\operatorname{ierfc}(z) = \int_z^\infty \left(\frac{2}{\sqrt{\pi}} \right) \int_{z_1}^\infty \exp(-\eta^2) d\eta dz_1 \quad (2.3)$$

The total amount of heat, Q , in the skin consequent to a heat pulse lasting time t_c is :

$$Q = q * t_c \quad (2.4)$$

By the end of the exposure duration this heat quantity will be stored in the upper layer of the skin. For $t > t_c$ the heat diffuses further into the skin and gives, then, a temperature rise. The temperature path, for $t > t_c$, follows from:

$$T(t) - T_i = \frac{2q}{\sqrt{\lambda \rho c}} \left[\sqrt{t} * \operatorname{ierfc} \left(\frac{x}{\sqrt{4a_t t}} \right) - \sqrt{t - t_c} * \operatorname{ierfc} \left(\frac{x}{\sqrt{4a_t (t - t_c)}} \right) \right] \quad (2.5)$$

The above derivation does not take into account the fact that some heat, in the skin, will be taken away due to blood-streaming in the blood vessels. The physical properties of the skin given in Paragraph 2.4 have been determined experimentally. By using these data the heat transfer due to blood streaming is implicitly taken into account. When the exposure duration is really long (for example > 1 minute), then the above model, due to the disregarding of the heat loss by blood-streaming, gives an overestimation.

It is concluded, in [7], on the basis of data obtained from literature, that burns develop when the temperature rise is at least equal to 9K. The depth of the burn follows from the calculation of the depth until the temperature rise has at least reached this value of 9K.

If the burn is limited to the thickness of the epidermis ($x \approx 0.12$ mm) it is considered to be a first degree burn. If the dermis is affected ($x \approx 2$ mm) this means a second degree burn. At greater depths third degree burns develop. The criteria are put together in Table 2.4.

Table 2.4 Criteria for the seriousness of the burns.

Degree of burn	Depth until $\Delta T = 9K$ (mm)
First	< 0.12
Second	< 2

On the basis of these criteria, Hardee and Lee [7] have derived the radiation dose (in kJ/m^2) as a function of the exposure duration, for second and third degree burns, with the help of Formulas (2.2) and (2.5); the results have been tested versus experimental results (see Figure 2.3).

Model [7] shows a reasonable agreement with the experimental results given in Figure 2.3. However, on the basis of an analysis of further experimental results, Hymes [10] concluded that the results of the Hardee and Lee model [7] (such as previously presented) are not backed-up by all experimental results. In a discussion about the results, Hardee and Lee [7] gave several reasons why experimental results (may) depart from the theory (minimum values up to 4 to 6 times higher).

- The wave length of the radiation used has an influence on the absorption coefficient a (50 to 85%) and can be reflected when dealing with a radiation source of very high temperature. For example: a nuclear explosion [12], of 4000°C [8], versus up to 2000 to 2300°C in [7].
- The artificial “blackening” of the skin increases the absorption coefficient.
- Very intense heat sources can lead to the carbonizing of the upper skin layer, which provides protection against deeper burns.

Furthermore, simulation tests with a synthetic skin (see Paragraph 2.6) seem to indicate that the heat loss through blood cannot be neglected.

Since, in actual practice, it is not certain how large the absorption coefficient might be, it is worth recommending to consider, for this half-uncertainty, a value of 1 (one).

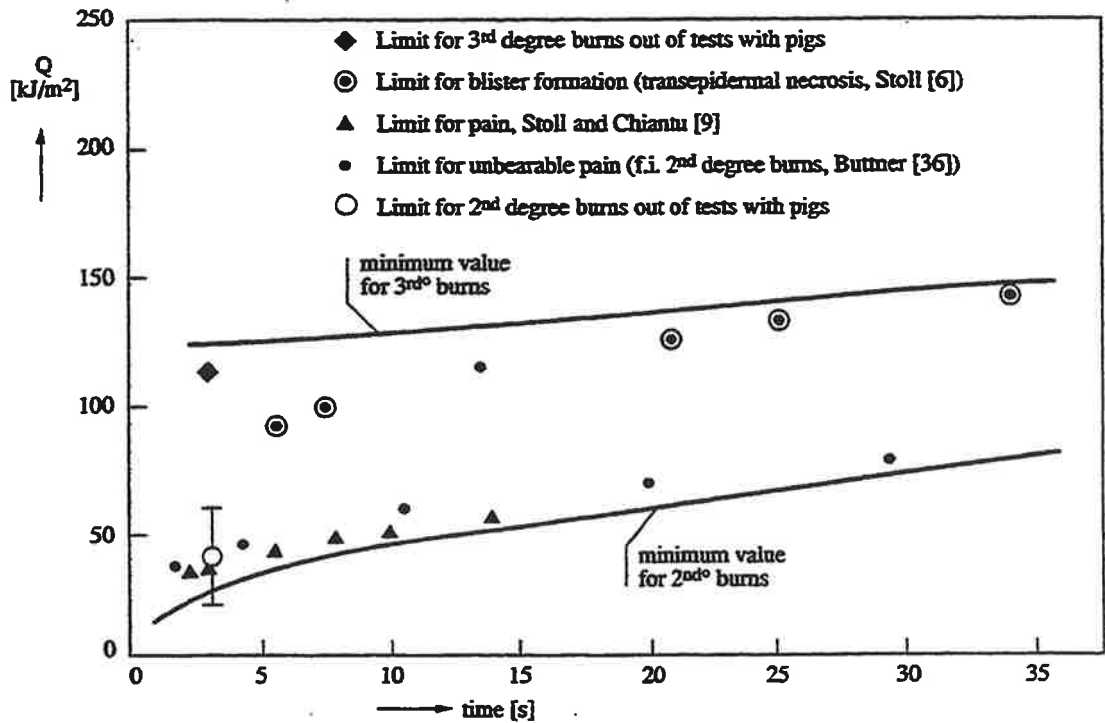


Fig. 2.3 Minimum values of the heat load (radiation dose) absorbed by the skin for second and third degree burns, for a given time duration (according to the model of Hardee and Lee [7]), and experimental results.

2.6

Experimental Determination of Injury caused by Heat Radiation

Tests indicate that there is a relationship between the heat-flux and the time after which this heat-flux leads to an unbearable pain, this by exposure to radiation of an unprotected skin. See Figure 2.4 [33]. The highest heat-flux that the skin can absorb during a long time without feeling pain is about 1 kW/m^2 . This value is in the range of the heat-flux received from a mid-day sunshine in the summer. Even though no pain is felt, a tissue damage will take place for an extended exposure period to this radiation intensity. If pain is felt, the person exposed must try and protect the exposed part of the skin from the radiation source.

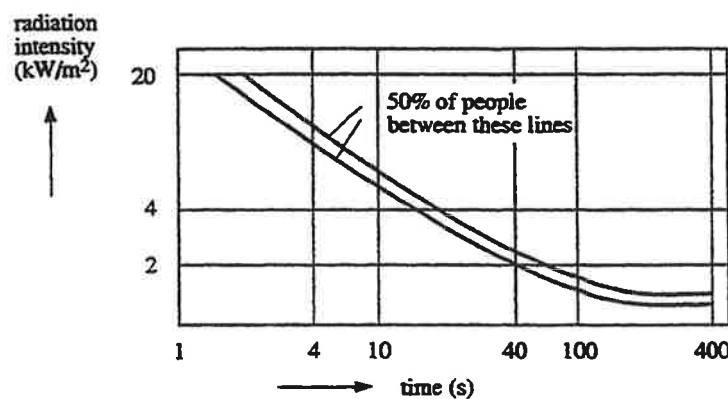


Fig. 2.4 Time for unbearable pain according to [33].

For a skin protected by clothing, the starting-point, normally, is a temperature-criterium. It is considered, in this case, that a temperature of 45°C can just be tolerated, for an extended period of exposure, without leading to a sensation of pain. Higher values are, of course, acceptable for shorter exposure durations. The above is illustrated in Figure 2.5.

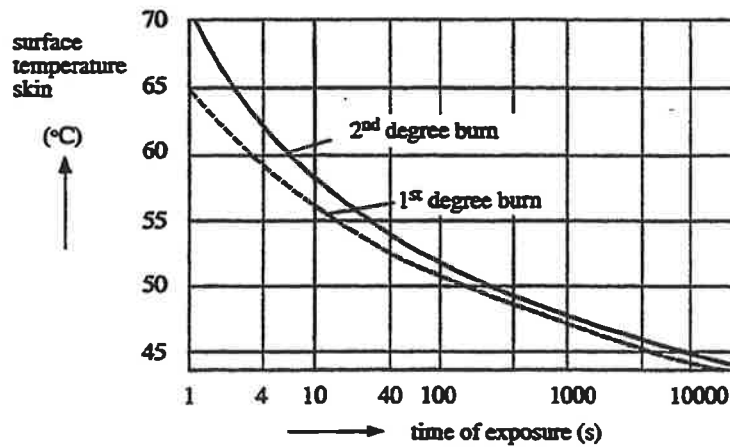


Fig. 2.5 The critical surface temperature of the skin as function of the time of exposure.

The Center of Fire Research of the TNO, jointly with the TNO Institute of the physiology of the Senses, have developed a skin model with which the protective properties of clothing, under different conditions, can be evaluated. This skin model is an artificial skin made out of synthetic materials layers and copper. The back-side of this skin is maintained at a temperature of 37°C by means of a water circuit. This artificial skin, on which the clothing is stretched, is exposed to a previously established heat load, while the temperature on the surface of the skin is being registered. As soon as a temperature of 45°C is reached, the heat load is removed. The skin temperature keeps going-up before the temperature goes down. See Figure 2.6. A combination of radiation load and convective heat load on the clothing is possible.

A more complete description of the model and the measurement procedure are given in [34], [35].

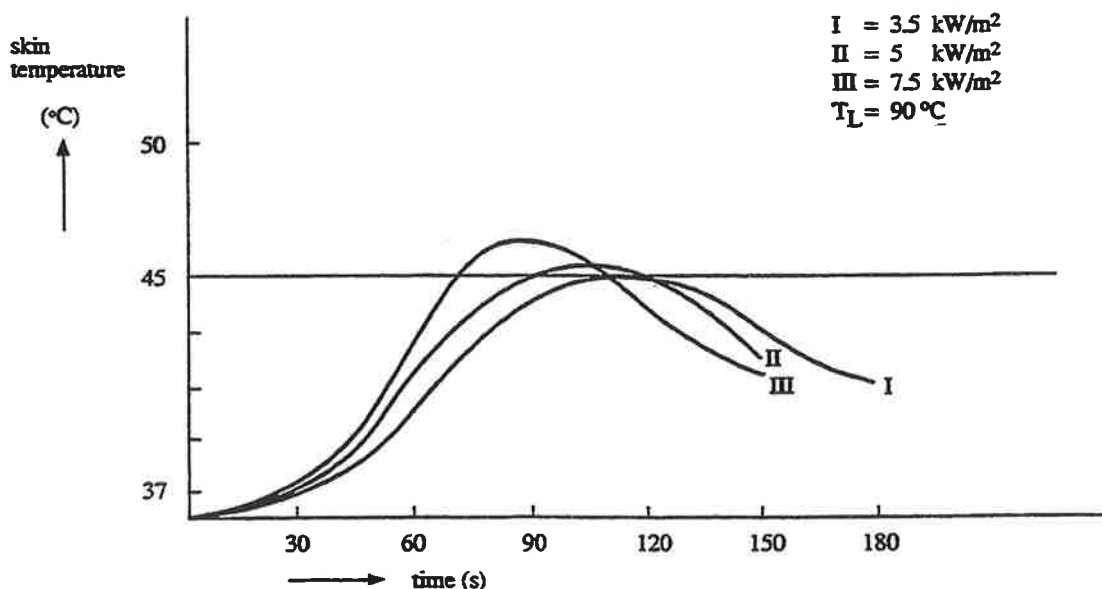


Fig. 2.6 Skin temperature as a function of time, for a skin protected by clothing, for different values of the radiation intensity and an air temperature of 90°C; after reaching the critical temperature (= 45°C), the radiation and the hot air-flow are removed.

Statistical model for injury due to heat radiation

3.1 Introduction

In a quantitative risk-analysis, the magnitude of the damage is used to express the seriousness of a given situation. With regard to injuries caused by heat radiation, this means that a model is required which, on the basis of a calculation of the radiation load (intensity and duration), will allow us to determine what the nature and magnitude of the injury is going to be.

This paragraph is dedicated to the analysis of the probability of the injury with the help of probit functions¹. In it, the probability of a injury of a given type will be expressed in relation to the radiation load.

The types of injuries will be:

- First, second and third degree burns
- Fatal injury

On the basis of the calculated radiation load, the probit function (-s) and population data can be used to determine the magnitude of the damage. Protection by clothing, buildings, presence inside a house, etc. will be handled in Paragraph 4.4 and in Paragraph 4.5.

3.2 Relationship between the Heat Load and the Degree of Burns

The "Vulnerability Model" [3] uses information from [12], which is based on data for nuclear explosions. From lethality data for different magnitudes of nuclear weapons a probit function can be derived:

$$\text{Probit} = -38.48 + 2.56 * \ln(t * q^{4/3}) \quad (3.1)$$

with:

t in seconds
q in W/m²

For injuries which are not fatal we only are interested in the limit values; for first degree burns it appears, from measurements by nuclear explosions (see [3]) that the 1% limit values can best be expressed by $t * q^{1.15}$ (instead of $t * q^{4/3}$). According to [3], for first degree burns, the limit value is equal to:

$$t * q^{1.15} = 5.5 * 10^5 \left(\text{in s} * \left(\text{W/m}^2 \right)^{1.15} \right) \quad (3.2)$$

¹ See, for instance, Finney [11].

For second degree burns due to a nuclear explosion, the following, according to [3] is valid :

$$t * q^{4/3} = 8.7 * 10^6 \left(\text{in s} * \left(\text{W/m}^2 \right)^{4/3} \right) \quad (3.3)$$

The wave-length of a heat radiation due to nuclear explosions is mainly within the range of the visible + the UV part ($< 1 \mu\text{m}$) of the spectrum. By fires of hydrocarbons and similar, the wave-length is principally within the infra-red area ($> 1 \mu\text{m}$). The more the wave-length increases, the deeper the radiation penetrates into the skin (compare, for instance, a micro-wave-oven, with a wave-length of $\approx 0.1 - 1 \text{ mm}$) and the damage mechanism, then, is different; a radiation with a higher wave-length leads to a warming-up at a greater depth. When this warming-up process exceeds certain limits this, in turn, leads to deeper burns (higher degree) than due to radiation with a shorter wave-length.

It results, from the above, that, for fires of hydrocarbons and similar, the radiation dose required for a given degree of damage is lower than the radiation dose from, for instance, nuclear explosions.

In what follows, in this paragraph, we shall present probit-functions for "fires of hydrocarbons".

On the basis of data given by Stoll et al [9], as a continuation of [3], the following probit-functions are presented in [13], whereby, with reference to [3], limit values are adapted to fires of hydrocarbons.

The 1% limit value for the doses for first-degree burns appears to be, on the basis of measurements [9] to be lower, by a factor of 2.23, for infra-red radiation as compared to UV-radiation (compare 3.4 and 3.2).

First-degree burn:

$$\text{Probit} = -39.83 + 3.0186 \ln (t * q^{4/3}) \quad (3.4)$$

Assuming that the same factor is valid for lethality, it follows, consequently [9]:

lethality:

$$\text{Probit} = -36.38 + 2.56 \ln (t * q^{4/3}) \quad (3.5)$$

If we apply the same adaptation to second-degree burns, the limit value will be:

$$t * q^{4/3} = 3.9 * 10^6 \left(\text{in s} * \left(\text{W/m}^2 \right)^{4/3} \right) \quad (3.6)$$

In case of insufficiency of adequate data, it becomes necessary to make an assumption with regard to the variation of the probit-function. It is often assumed that, for different types of damage, with similar conditions of exposure, the gradient of the probit-function are equal, (compare the probit function for a second-degree burn and lethality due to radiation, Figure 3.1).

If we thus assume that the gradient of the probit-function for second-degree burns is similar to the gradient of first-degree burns, we then obtain, for a second-degree burn:

$$\text{Probit} = -43.14 + 3.0186 \ln (t * q^{4/3}) \quad (3.7)$$

These probit-functions are presented, in Figure 3.1, as probability of a certain injury as a function of the radiation dose. Hereby, the relationship between the value of the probit-function and of the corresponding percentage is used, (see Table 3.1). This percentage indicates:

- The % of the affected population which receives an injury in accordance with the probit-function corresponding to it, or
- the probability that an individual incurs this corresponding injury.

In Figure 3.1 and in the values of the probit-functions the influence of clothing or of escape possibilities is not taken into account. Refer, for this, to the following paragraphs.

By the determination of the extend of the damage with the help of the % presented, the possibility of adding (doubling) the calculated effects must be considered. See Paragraph 3.3. It nevertheless, depends, among others, on the fractions for second and third degree burns, whether the affected person will die or not.

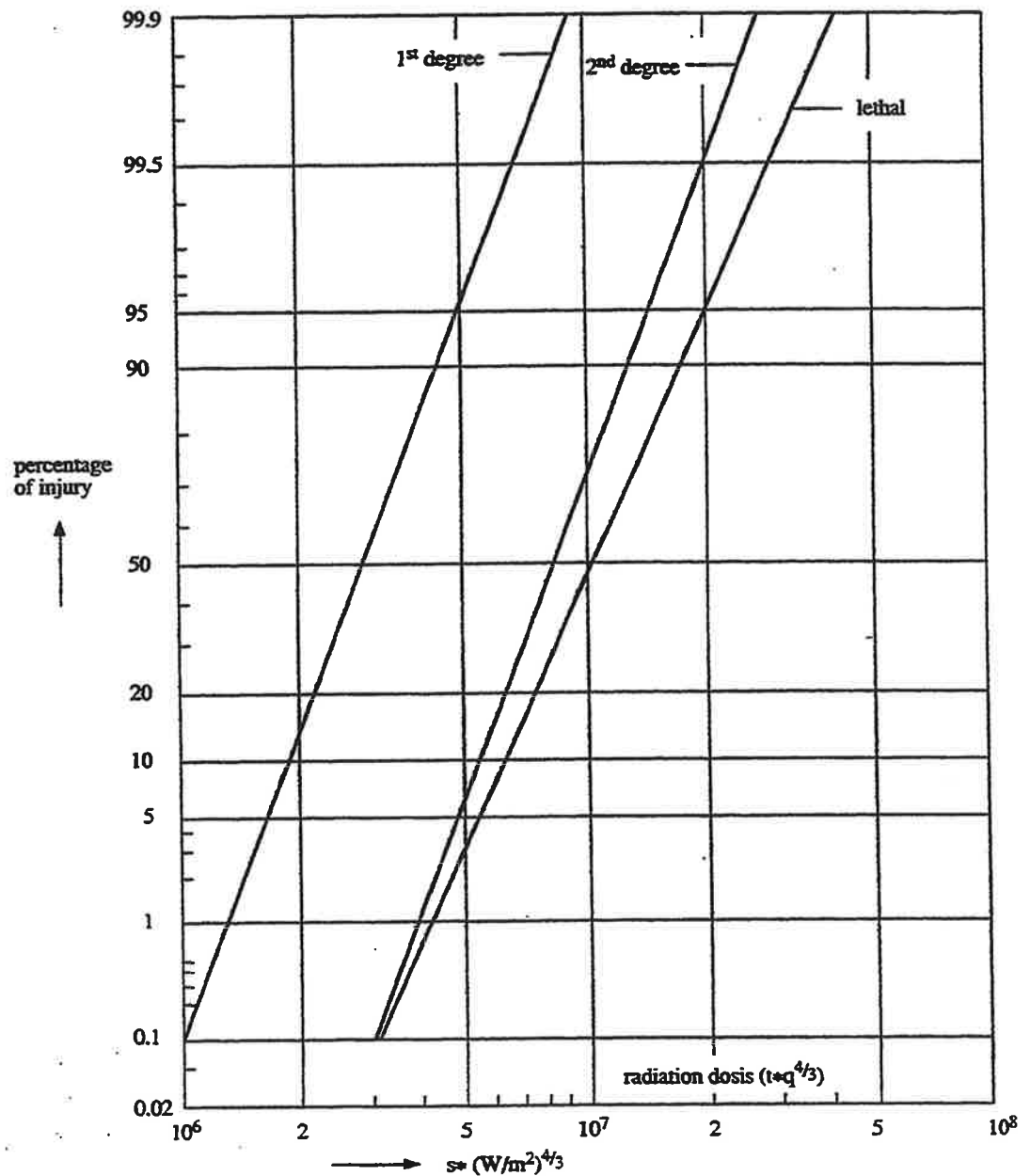


Fig. 3.1 Probit-functions for heat radiation from fires of hydrocarbons without the influence of clothing.

Table 3.1 Relationship between the percentage and the value of the probit-function.

%	0	1	2	3	4	5	6	7	8	9
0	-	2.67	2.95	3.12	3.25	3.36	3.45	3.52	3.59	3.66
10	3.72	3.77	3.82	3.87	3.92	3.96	4.01	4.05	4.08	4.12
20	4.16	4.19	4.23	4.26	4.29	4.33	4.36	4.39	4.42	4.45
30	4.48	4.50	4.53	4.56	4.59	4.61	4.64	4.67	4.69	4.72
40	4.75	4.77	4.80	4.82	4.85	4.87	4.90	4.92	4.95	4.97
50	5.00	5.03	5.05	5.08	5.10	5.13	5.15	5.18	5.20	5.23
60	5.25	5.28	5.31	5.33	5.36	5.39	5.41	5.44	5.47	5.50
70	5.52	5.55	5.58	5.61	5.64	5.67	5.71	5.74	5.77	5.81
80	5.84	5.88	5.92	5.95	5.99	6.04	6.08	6.13	6.18	6.23
90	6.28	6.34	6.41	6.48	6.55	6.64	6.75	6.88	7.05	7.33
-	0.0	0.1	0.2	0.3	0.4	0.5	0.6	0.7	0.8	0.9
99	7.33	7.37	7.41	7.46	7.51	7.58	7.65	7.75	7.88	8.09

3.3

Determination of the Extend of the Damage with the Help of Probit functions

(The value of the probit function corresponds to the fraction of the total of the affected population in one of the classes of damage belonging to this probit function at a certain load.)

With the help of the probit-functions, the affected fraction of the total of the population in question is determined with relation to the class of injury. We principate from a given radiation-dose. Due to the definition of the probit-function (independent classes) "double-effect calculations" take place: These are people who fall, on an equal basis, within several classes of injury. Due to this, there are in reality less victims than shown by the summation over all classes.

As an example (see Figure 3.1):

Radiation dosis = $5 \cdot 10^6 \text{ s} \cdot (\text{W} \cdot \text{m}^{-2})^{1.25}$

Affected percentage of the total population:

First-degree	=	96%
Second-degree	=	5%
Third-degree	=	<u>3%</u>
Total		104%

This would give a total percentage of affected persons higher than the totality of the population in question.

Causes for double-effect calculations:

1. A single damage mechanism, due to a single event, causes, through escalation, victims in different classes of injury. Hereby the fraction of victims in a certain class of damage is also included in all subsequent (= more serious) classes.

For example: a toxic gas cloud can produce death, a recoverable injury or irritation. A victim of the "death" class is, at the same time, included in the "recoverable" and "irritation" classes, and a victim of the "recoverable" class is, in the same time, included in the "irritation" class.

2. Several damage mechanisms, due to the same event, produce, at the same time, victims in the same class of injury (for example, an explosion can kill due to either a direct hit or blast overpressure).

3. Several events, occurring at different times, all theoretically produce damage to the same person, while the first event may, actually, produce such a major damage that the consequent events do not really add anything more to it. This means that this first event in fact, reduces the size of the affected population. For example: a person killed by a toxic gas cannot be further "damaged" by an explosion which follows.

– Correction for double-effect calculations See Annex G from [30].

– Correction for cause 1.

The cumulative effect can be corrected by deducting the fractions of population which suffered more serious damage from the class which suffered relatively small damage. For example, the percentage of people affected by exclusively first-degree burns can be established by deducting, from the calculated percentage (with the help of the probit-function) the percentage of second and third degree burns.

– Correction for cause 2.

This phenomenon can be improved with the help of the "Venn-diagram" (see Figure 3.2). Data A gives all the victims, in a certain damage class, who suffered as consequence of damage mechanism A, the same for data B for mechanism B. If the corresponding fractions are called F(A) and F(B), the total fraction, in this class, is then given by the product of F(A) and F(B), see for instance [31].

Therefore, for the calculation of the total number of victims, using the sum of victims due to mechanism A and of victims due to mechanism B, a reduction by a factor equal to $(1 - F_A * F_B)$ can be made.

– Correction for cause 3.

The correct fraction F_i of people killed, as consequence of the event at time t_i , can be found, from the calculated value of F_i with the help of a probit- function, by discounting the remaining affected population which, as consequence of previous events at times t_1, t_2, \dots, t_{i-1} , is decreased:

$$F_i^{correction} = F_i * \frac{1}{1 - F_1 - F_2 - \dots - F_{i-1}}$$

Note: F_i to F_1 are always referred to the original population.

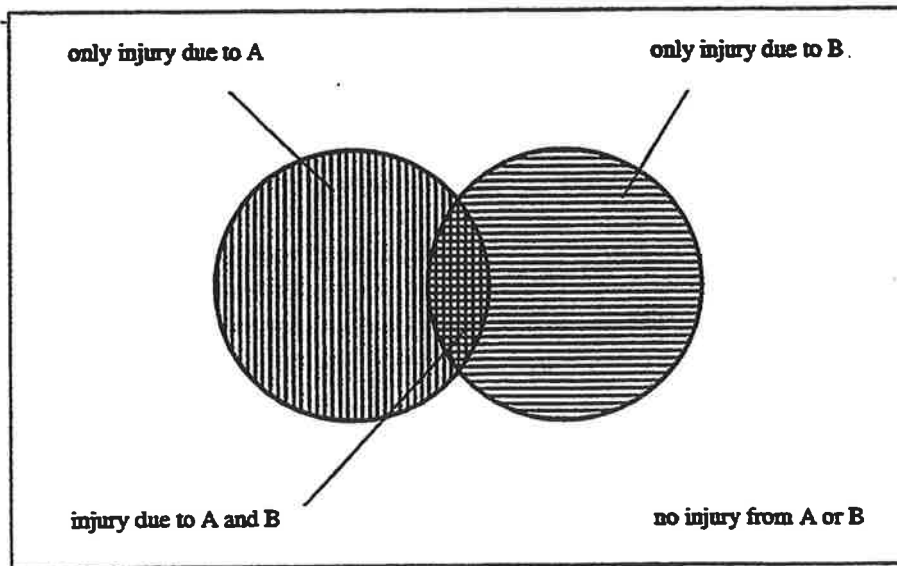


Fig. 3.2 A Venn diagram of two simultaneous damage mechanisms; the four resulting classes of injury are shown in the figure.

The influence of clothing on the extend of personal injury due to heat radiation

4.1 Introduction

In practically all cases, people who might be exposed to heat radiation and who are located in the open (outside of houses) will be wearing clothing. This clothing will certainly have a positive influence in reducing the extend of the burns due to radiation. In Paragraph 4.3 an evaluation will be made to determine to which extend the number of fatal victims can be reduced due to clothing. The protective effect of clothing is dependent on various factors. In the case of good reflective properties of the outer part of the clothing the heat can only penetrate to a minor extend.

A small heat-conducting ability and a high heat capacity of the clothing will result in a slow rise of the temperature on the inside of the clothes. Air layers between various pieces of clothing and between clothing and skin also improve substantially the resistance to heat. Humidity in the clothing, however, decreases the resistance to heat, due to the heat transfer of the hot water vapour.

If the radiation intensity is so large that the clothing itself may ignite, then any possible escape is practically meaningless and the probability of burns due to the burning clothing is very high. For this reason, an investigation is carried-out, in Paragraph 4.2, to determine by which radiation dose the clothing will ignite.

4.2 The Ignition of Clothing

For samples of given materials (covers of furniture, 3* cotton, 1* rayon), and for three radiation levels, the time required for ignition is experimentally determined in [14]. In agreement with other damage mechanisms, it can be assumed that the non-ignition of a sample is dependent on the radiation dose D_s , to be defined as:

$$D_s = t_c * q^n \quad (4.1)$$

From data out of [14] it follows that the exponent n , for the four samples, is practically equal to 2. The radiation dose, as defined in 4.1 increases when the thickness of the material increases. The value lies, roughly, between $2.5 * 10^4$ and $4.5 * 10^4 \text{ kW}^2\text{m}^{-4}\text{s}$.

Since materials which normally cover furniture can be looked upon as heavy materials, it is considered that, for average clothing, we can depart from a dose equal to $2.5 * 10^4 \text{ kW}^2\text{m}^{-4} \text{ s}$. For a exposure duration equal to 60 seconds this corresponds to a radiation intensity of 20 kW/m^2 , and for a exposure duration of 10 seconds to 50 kW/m^2 .

Hymes [10] uses the results of an investigation carried-out by Wulff [15] to determine the properties of 20 different (daily) clothing materials, see Table 4.1. The exponent n seems to vary, for these materials, between about 1.0 to 2.7. The cause of the difference with [14] is not known². It can be seen, from

² Hilado and Murphy [14] had investigated materials applicable to furniture coverage, while Wulff had investigated samples of materials used for clothing.

Table 4.1 that 10-40% of the incoming radiation penetrates. On the average, 50% are reflected, 30% penetrate and 20% are absorbed by the clothing material. The time required for ignition, with or without an ignition source, is compared in Figure 4.1, with the time required to produce third-degree burns in an unprotected skin. It appears that the time required for auto-ignition is practically always longer than the time required to produce third-degree burns in an (unprotected) skin.

For certain applications (upholstery, night-clothing) materials are sometimes used which are less flammable than normally. Such materials, then, will only ignite for a higher radiation dose. However, in the practice, it must be considered that a person exposed to heat radiation will be wearing normal clothes.

Explanations with reference to Figure 4.1

In Table 4.1, the time of exposure required for auto-ignition of the twenty different materials is set versus different heat radiation loads, based on the results given by Wulff [15].

For purposes of comparison, in the figures also shown are the curves corresponding to the fire with an ignition source and to third-degree burns.

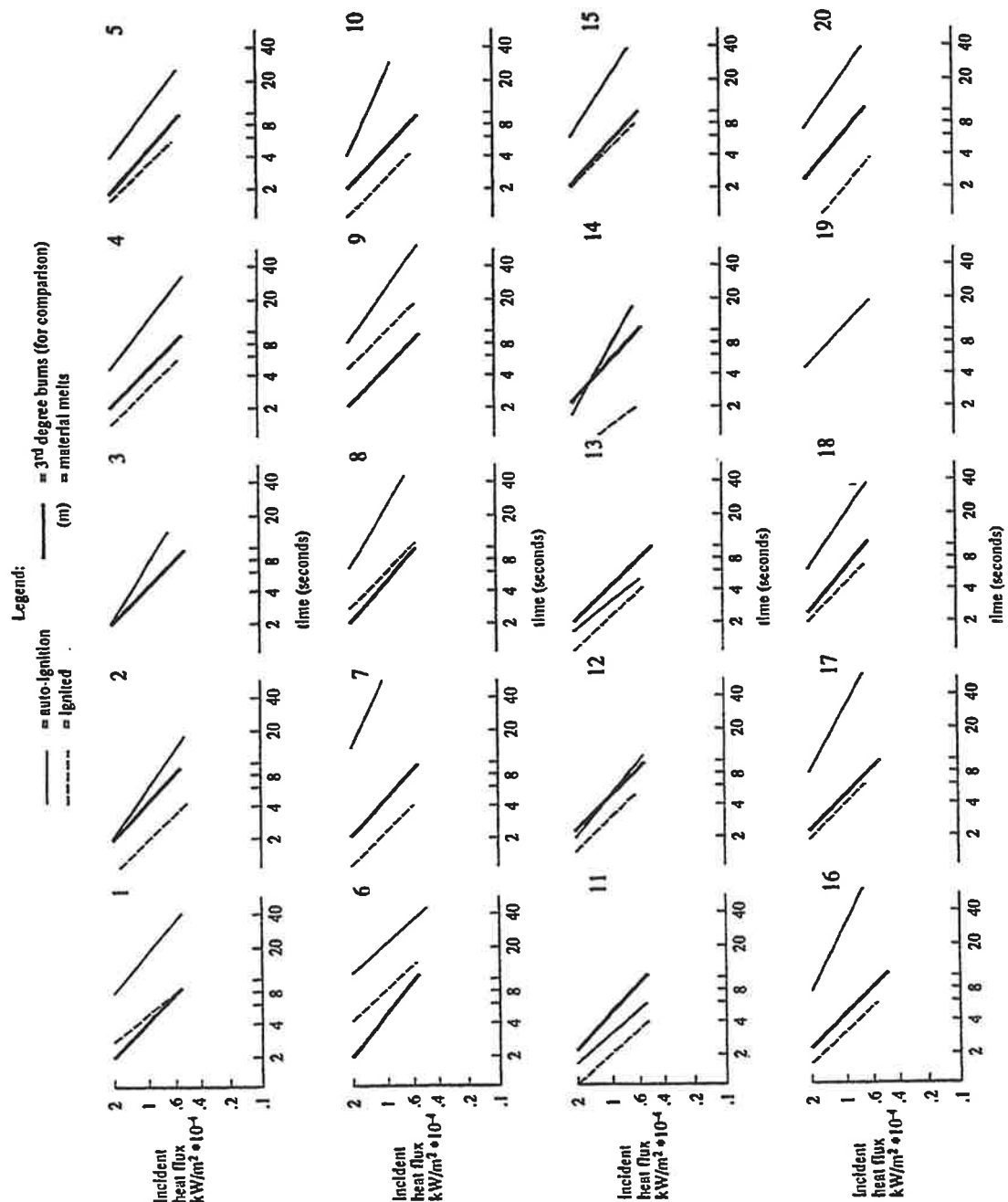


Fig. 4.1 Time required for the ignition of the clothing material referred to in Table 4.1 (taken from [10]).

Table 4.1 (taken from [10]) Properties of Typical Everyday clothing materials.

Material no. and description	Fibre type	Colour	Finish	Specific mass mg/mm ²	Limiting oxygen index (%)	Material thickness mm	Heat conduction coefficient (90°C) (mW/mm ² ·°C ⁻¹)	Specific heat (130°C) (W·s·g ⁻¹ ·°C ⁻¹)	Char temp (°C)T _c	Mean auto ignition (I) or melting(m) temp °C T _{1,m}	Piloted ignition temp (°C)	Optical response to i.r. source: 0.6 - 2.5 μm (percent of incoming flux)			Heats of combustion		Index for non plotted ignition dose calculated from Wulff date (24)
												Reflected	Transmitted	Absorbed	KJ/g	J/mm ³	
1. Slacks	65/35 PE/Cotton	White	Durable pressed	0.24	18	0.46	0.16	1.35	219	413 l	334	52.2	28.9	18.9	11.1	2.7	2.32
2. Woven blouse	% PE	Yellow		0.08	19	0.20	0.22	1.42	134	258 m		50.1	34.6	15.3			1.49
3. Double knit	100% PE	White		0.21	20	0.95	0.06	1.30	134	250 m		61.9	23.8	14.3			1.68
4. Denim	100% Cotton	Navy blue		0.30	17	0.58	0.13	1.37	162	290 l	285	49.1	13.7	37.2	13.4	3.9	1.49
5. Jersey T-shirt	100% Cotton	White		0.14	17	0.53	0.12	1.54	162	305 l	306	52.1	29.6	18.3	13.2	1.8	1.89
6. Slacks	65/35 PE Cotton	White		0.24	17	0.48	0.15	1.29	219	413 l	341	58.1	28.4	13.5	11.7	2.8	2.56
7. Jersey tube knit	100% Acrylic	Gold		0.15	16	0.79	0.08	1.81	230	242 m		54.9	15.9	29.2	20.9		2.42
8. Jersey T-Shirt	65/35 PE Cotton	White		0.16	17	0.62	0.09	1.59	230	435 l	310	56.0	27.6	16.4	13.2	2.1	1.64
9. Terry cloth	100% Cotton	White		0.27	16	2.0	0.03	1.49	162	302 l	294	62.3	23.1	14.6			1.80
10. Batiste	100% Cotton	Purple		0.07	16	0.10	0.03	1.84	230	438 l	345	40.6	39.4	20.0	13.0	0.8	2.67
11. Tricot	80/20 Acetate/Nylon	White		0.11	18	0.61	0.08	1.45	134	228 m		50.8	32.9	16.3	16.0		0.98
12. Tricot	100% Nylon	White		0.09	20	0.27	0.18	2.19	134	246 m		39.7	43.3	17.0			1.28
13. Tricot	100% Acetate	White	Durable pressed	0.09	18	0.30	0.16	1.72	134	230 m		44.3	39.0	16.7	15.2		1.23
14. Tafeta	100% Nylon	White		0.06	25	0.11	0.28	1.78	134	241 m		34.8	43.4	21.8			2.25
15. Slacks	65/35 PE Cotton	Brown		0.23	18	0.42	0.15	1.32	247	422 l	335	42.3	33.1	25.6	10.0	2.3	1.72
16. Shirt	50/50 PE Cotton	White		0.13	18	0.32	0.20	1.34	247	355 l	335	49.9	29.4	20.7	11.6	1.5	2.67
17. Batiste	65/35 PE Cotton	White		0.09	18	0.19	0.25	1.50	252	472 l	378	46.4	37.2	16.4	12.4	1.0	3.22
18. Flannel	100% Cotton	White		0.13	17	0.71	0.07	1.66	162	305 l	286	57.3	25.1	17.6	13.7	1.7	1.96
19. Flannel	100% Cotton	White	Fire retardant	0.15	25	0.69	0.08	1.65	252	488 l	322	60.2	19.7	20.1	5.6		1.22
20. Flannel	100% Wool	Navy blue		0.20	26	0.72	0.07	1.27	252	471 l	323	36.5	10.2	53.3	9.3		1.16

The Protective Effect of Clothing

The formation of wounds on parts of the body which are protected by clothing requires a higher dose of radiation than for unprotected skin. Since it is assumed that serious burns on skin protected by clothing can only occur if the clothing itself is ignited, it is then logical to deduct that the chances of survival of persons exposed to radiation who are protected by clothing is very substantially improved.

A review of the percentage of surfaces affected by burns, for different parts of the body, is given in [4], as function of the age of the person (Table 4.2).

Table 4.2 Review of the percentages of surfaces affected by burns as function of age.

Burns	1 year	1-4	5-9	10-14	15	grown-up
Head	19	17	13	11	9	7
Neck	2	2	2	2	2	2
Trunk(front)	13	13	13	13	13	13
Trunk(back)	13	13	13	13	13	13
Behind(right)	2½	2½	2½	2½	2½	2½
Behind(left)	2½	2½	2½	2½	2½	2½
Genitals	1	1	1	1	1	1
Right upper-arm	4	4	4	4	4	4
Left upper-arm	4	4	4	4	4	4
Right under-arm	3	3	3	3	3	3
Left under-arm	3	3	3	3	3	3
Right hand	2½	2½	2½	2½	2½	2½
Left hand	2½	2½	2½	2½	2½	2½
Right upper-leg	5½	6½	8	8½	9	9½
Left upper-leg	5½	6½	8	8½	9	9½
Right lower-leg	5	5	5½	6	6½	7
Left lower-leg	5	5	5½	6	6½	7
Right foot	3½	3½	3½	3½	3½	3½

If it is considered that due to the presence of clothing, only the face, neck, under-arms and hands can be affected by burns, then the percentage of burns on the skin of the human body is, at the maximum, equal to 20% of the total skin surface. (This figure can, eventually, be refined with regard to age and population group in question).

Table 4.3 Connection between age and mortality for an approximate 20% burn of the surface of the body.

Body area burned %	Age (years)																
	0-4	5-9	10-14	15-19	20-24	25-29	30-34	35-39	40-44	45-49	50-54	55-59	60-64	65-69	70-74	75-79	80+
18-22	0.0	0.0	0.0	0.0	0.0	0.0	0.0	0.1	0.1	0.1	0.1	0.2	0.3	0.4	0.6	0.8	0.9

*) According to table 2.1.

**) The mortality increases by more advanced age.

It can be seen, from the above, that despite the protective effect of clothing, a part of the people exposed will be fatally affected by the radiation dose (0% younger than 35, 10% between 35 and 55, and increasing to 90% for persons older than 80). If the exposed group, with reference to age, has the same composition as that of the dutch population, this means that 14% of the people exposed, despite

the protective effect of clothing, will receive such burns that they will die as a consequence of them.

The protective effect of clothing is only valid as long as the clothing has not reached an auto-ignition temperature. On the basis of the effective exposure duration and of the corresponding radiation level, it is possible to determine, using Figure 4.1, whether the clothing will ignite (this depending on the type of clothing, in accordance with Table 4.1).

It would appear reasonable, in this, to consider a situation whereby ignition sources are present (piloted ignition).

Without ignition of the clothing, the extend to which first, second or third degree burns will occur, from a global point of view, must be taken equal to 14% (= the fraction of the always unprotected skin area) of the values calculated with the help of probit-functions, corresponding to the classes of injury produced by radiation doses **without** protective clothing (Paragraph 3). In this case, it is quite clear that the choice for a probability of mortality is equal to 1 (one).

Options for the exposure duration of people subjected to heat radiation from a fire

5.1 Introduction

In the case of fires, for instance, pool fires or flares, the type of injury to people, due to heat radiation, is determined by the exposure duration to the radiation. In the determination of the extent of the injury, the possible choices or options with regards to this exposure duration are therefore majorly important. It is obvious that the exposure duration, within a given situation, is dependent on so many (incidental) circumstances that, in fact, it is certainly not possible to establish any specific rules, regarding this exposure duration, allowing us to evaluate the degree of the damage. Apart from environment circumstances (escape routes or sheltering available), the exposure duration also depends on the composition of the exposed group.

In this paragraph, the various facets related to the exposure duration will be discussed, facets which play a role during a fire. On the basis of information available, a recommendation will then be given for a choice of a exposure duration as safe and responsible as possibly obtainable.

5.2 Influence of the Composition of the Exposed Group

Injuries of a certain importance (for example first-degree burns or higher) can only be provoked on persons located very close to a fire. The radiation level, roughly, increases in proportion to the square of the distance to the fire. This means that only the group of people located in the direct vicinity to the fire is of importance in the evaluation of their behaviour in case of a fire situation.

If a calamity occurs, the speed at which people will search for escape possibilities is strongly dependent on the knowledge the affected persons may have with regard to the seriousness of the situation. This means, for instance, that workers in a refinery, will, probably, behave much more effectively in their search for protection than children playing outside, in case a fire suddenly develops in their surrounding. It is quite true, for everyone, that a human being naturally tries to protect himself from physical dangers. In the case of exposure of a sensitive group (for instance, scholars, sick people, handicapped or old people) the exposure duration, generally, will be longer, since escape possibilities are of limited nature.

People who, in an exposed group, will find themselves inside a house will, by this fact, receive so much protection against radiation that victims, among them, are not likely. However, there could be victims inside houses if in the houses, themselves, secondary types of fires can develop.

The age distribution of the exposed group also plays a role in the determination of the exposure duration. The readiness and possibility to know how to handle the situation, as well as the uncontrolled type of behaviour due to panic, are also, in all probability, dependent on the age of the people exposed.

The distribution of the population in the Netherlands is given in Figure 5.1.

composition

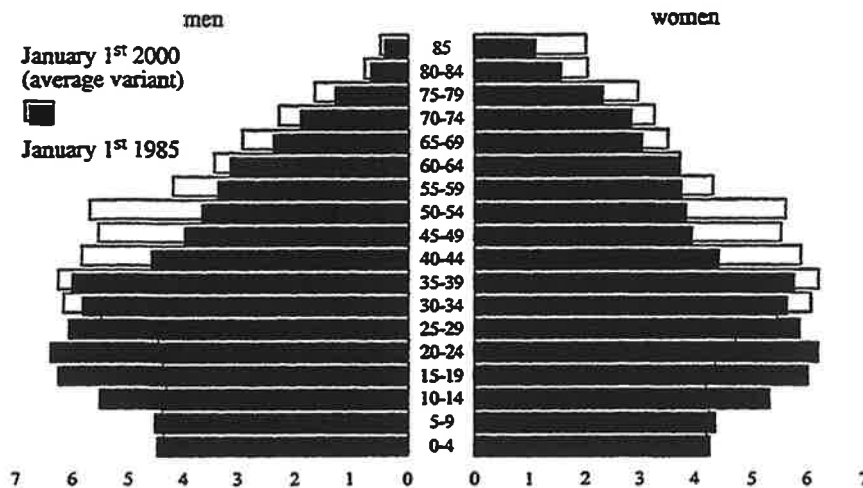


Fig. 5.1 Population distribution in the Netherlands (CBS data, 1985).

If we acknowledge the fact that children younger than 10 or people older than 65 will be less efficient in either escaping or seeking shelter than the “average” exposed people, this means that for about 25% of the population the exposure duration will, in turn, be longer than average.

Whenever it can be previously established that the exposed group, in a given situation, departs from the average with regard to its composition, it is then obvious that options are open for the determination of this departure from the “average” exposure duration.

By choosing the reaction time and the speed of escape for a sub-group, the effective exposure duration for a group can be determined using the method described in Paragraph 5.4. These (different) exposure durations can then be used to determine the extend of the damage with the help of probit functions, as has been handled previously in Paragraphs 3 and 4.

It is very useful, in a risk analysis, to differentiate between groups of population. Examples of such different groups can be as follows:

- People who are treated in hospitals, nursing homes, etc.
- Residents of houses for old-age people.
- Children in schools.
- Vacationers on beaches or in campings.

Investigations with regard to the sensitive groups of population must be based on considerations regarding the possibilities, of the people in question, to seek and find protection.

To a major extend, protection against excessive exposure to heat radiation is offered by presence inside houses or buildings. This means that, in the first place, groups which can be most sensitive to heat radiation must be found in areas where many people (may) be present and where protection possibilities are very limited (for example, vacationers).

5.3

Influence of the Conditions of the Fire

When a calamity occurs, the moment at which a fire starts is very important with regard to probability and duration of the exposure to heat radiation. When the full extend of the fire, due to a given calamity, is only reached a certain time after the start of the calamity (the moment when the critical situation is discovered and alarm is given), then, most of the time, the people who are present have ample time at their disposal to seek and find locations which are safe.

When, however, a fire develops suddenly, without pre-warning, such fire may, in given circumstances, obstruct the possible escape routes. In these conditions, the exposure duration is, in principle, the same as the duration of the fire itself.

If people exposed to heat radiation try to escape to locations in which the radiation level becomes harmless, then the extend and magnitude of the fire become important considerations, see Paragraph 5.4.

Escape from the fire is easier in areas in which few obstacles are present on the escape route. This means that escape in an open area, in which no buildings are present, will be the simplest and the quickest.

If shelter is sought, then presence of buildings will, on the other hand, also be of advantage. Such a condition offers many possibilities to seek protection behind the "shadow" of an obstacle.

In most cases, the presence of obstacles will be advantageous with regard to time requirements for the finding of adequate protection. It is, therefore, logical to couple this time with the density of the building in the area under consideration. Three environment categories are defined, in this respect:

1. **Urban areas:** Areas with city buildings, adjoining buildings, industrial areas.
2. **Built-up areas:** For instance, the built-up centers of villages.
3. **Open areas:** Flat land, arable land, agricultural land, with wide-spread housing.

In urban areas and, to a lesser extend, in built-up areas, the exposure duration is mainly determined by the time span which is required to find an acceptable shelter.

In open areas, the exposure duration depends on the time span required to escape to locations of harmless radiation level, locations in which no injury can be incurred.

5.4

Data from Literature about Exposure Duration and a Calculation Procedure

It would appear that no much data, with proper back-up, are available in literature to enable us to properly select of exposure duration. For very short fires, such as a BLEVE-fireball, for instance, the fire duration is considered, which means that neither escape nor sheltering are taken into account.

Reference [16] recommends a value of 30 seconds for the exposure duration of people in an urban area. For other remaining conditions, reference [16] emphatically points to the fact that exposure duration is strongly dependent on prevailing circumstances. The choice or option is then left to the users of the models and, in a given example, it is shown how strongly the extend of the damage is dependent on the exposure duration which has been chosen [16, p. 28]. It follows, from this, that the extend of the damage (dead or wounded person) is fully dependent on this exposure duration (increase of the damage with a factor 40 to 50).

Hymes [10] analyzed the accident in Los Alfaques, in Spain. From this analysis he deduced that a person requires 5 seconds to react and, after that, can cover a distance of 30 meters per 5 seconds away from the fire (6 m/s). These values can be considered as representing as good an evaluation as obtained.

In the LNG - Integral study [17], and also in a few other quantitative risk analyses, an exposure duration of 60 seconds is indicated, irrespective of specific circumstances. However a 30 seconds figure is indicated, as an estimation, in other studies. The methodology of evaluation used in [17] leads to distances larger than 1000 meters at which fatal injuries due to heat radiation are still possible.

An analysis of the LPG disaster in Mexico-City (1984) [18] indicated the following: due to the high building density (closely spaced housing) and the protective possibilities coupled with it, the distances at which fatal injuries due to heat radiation were still possible were restricted to hundred to two-hundred meters outside the "major-damage" area (300 m radius). Thus, in the case of Mexico-City, the exposure duration was significantly lower than 60 seconds.

Selection of the exposure duration in the available literature is based exclusively on "engineering judgement".

It is customary, in risk-analysis, when data regarding a given parameter is insufficient, to use a pessimistic approach. This means, for the exposure duration, that the value selected will be longer than the one which can reasonably be expected. The values of 30-60 seconds represent, consequently, in many cases an overestimating, (see [17] with regard to [18]).

If, in the determination of a (global) exposure duration escape possibilities are taken into account, it is then logical, in principle, to also take into account the radiation intensity which varies with time (decreases).

To simplify the procedure, the following (pessimistic) approach can be used:

- The exposure duration will be taken equal to the time required to react (5 s) plus the time required to reach a distance at which the radiation intensity is not higher than 1 kW/m².

The speed of escape, according to Hymes [10], is equal to 6 m/s. This value, when considering an average figure, appears to be on the high side. It is therefore proposed to use an average value of 4 m/s. In the case when the exposed group under consideration departs from the average composition, it is then possible to select a different reaction time and a different escape speed, and that in either negative or positive directions. However, unless very concrete information is available, such a departure is highly speculative. An example is treated in Appendix B. In this treatment, an expression is derived for the effective exposure duration t_{eff} , in which escape possibilities are taken into account. This value of the effective exposure duration permits, in turn, to derive a proper value for the radiation intensity, which is expressed as follows:

$$D = q^{4/3} * t_{eff} \quad (5.1)$$

with

- q : the radiation intensity during the reaction time (t_r)
- t_{eff} : the effective exposure duration
- $t_{v,eff}$: the effective exposure duration during the escape

$$t_{eff} \cong t_r + \frac{3}{5} \frac{x_o}{u} \left\{ 1 - \left(1 + \frac{u}{x_o} * t_v \right)^{-5/3} \right\} = t_r + t_{v,eff} \quad (5.2)$$

with

- x_o : the distance to the center of the fire [m]
- u : the escape speed [m/s] (= 4 m/s)
- t_c : the total exposure duration ($t_c = t_r + t_v$)
- t_r : reaction time [s] (= 5 s)
- t_v : escape time ($t_v = (x_s - x_o)/u$)
- x_s : distance from the center of the fire to a location at which the radiation intensity is below the dangerous level (1 kW/m²)

With this approach, the influence of the extend of the fire on the exposure duration is brought into the calculation. For a less extensive fire, the escape route to be covered becomes shorter and, consequently, the radiation dose also decreases.

In the above approach, the eventual sheltering possibilities are not taken into account. This effect can be incorporated into the calculation by the selection of a maximum value for t_{eff} , dependent on the area (environment) considered.

In some cases the fire can be of limited duration. This, in turns, influences the radiation dose which is received. This effect can also be taken into consideration in the determination of t_{eff} by substituting, in (5.2), the value of t_c by the real fire duration, providing the latter is shorter than the escape time, see Appendix B.

Damages consequent to a flash fire

6.1 Introduction

As consequence of the escape of flammable materials, a flammable cloud of certain dimensions can form.

Ignition of this cloud can lead to the generation of significant overpressures as well as quick combustion can take place without these effects (flash fire). In both cases damages can be expected due to the combustion process. In the first place, material damages will develop due to direct flame contact inside the cloud and due to heat radiation. Next to this, personal injuries can be expected, also due to direct flame contact or heat radiation, as well as to the consequences of the effects of secondary fires. In what follows, only personal injuries will be considered.

6.2 The Progress of a Flash Fire

If, after the escape of a certain quantity of flammable material ignition is delayed for some time, then the combustion of the gas cloud which has formed will take place at a very high speed. If such speed is high enough it can lead to the development of a pressure or shock wave. Conditions for such an occurrence are discussed in the chapter "Vapour-cloud explosion" of the Yellow Book [1]. For the formation of the pressure or shock wave it is further necessary that either the cloud or part of it, to a certain extend, is enclosed or obstacles are present. A last requirement which can be mentioned is that only the part of the cloud in which the concentration lies between the explosive limits can contribute to an explosion.

The less the above requirements are fulfilled, the longer the combustion process will be and, also, the probability of explosion effects will be lower. However, independent of this, effects of direct flame contact and of heat radiation must anyway be considered.

Under optimum conditions, the outer expansion of the flame front can proceed at a speed of tens of meters per second. Results of a series of experiments conducted by the Lawrence Livermore Laboratory [20] show, for 40 M³ LNG spills on water, that, under the circumstances, the speed of propagation, **relative to the wind**, was in the range of 7 m/s. Taking into account a wind velocity of 5 m/s, the absolute speed of propagation of the flame front is equal to 2 m/s (against wind) or 12 m/s (in the direction of the wind). It can globally be established that the absolute speed of the flame front is equal to 1-10 m/s, providing flame acceleration due to presence of obstacles is not considered. The results of the Maplin Sands tests [21] confirm these conclusions, as well as the TNO tests [37].

The shape of a flammable gas cloud is, in practically all cases, extended in length in the direction of the wind, and its height is much smaller than its horizontal dimension. The thickness of the moving flame front depends on a number of (unknown) parameters, such as concentration and degree of turbulence, in the flame front. Generally, its height will be in the range of several meters.

During combustion the hot gases which form tend to expand and rise and, due to this, the height of the flame will be larger than that of the cloud.

It follows, from the above, that an object which is located outside of the cloud will, by the ignition of

the cloud, be subjected to heat radiation coming from a moving flame front. Objects inside the cloud will be subjected, for a short time, to direct flame contact.

6.3 Material Damage due to a Flash Fire

Buildings and objects inside the cloud will be subjected, for a short time, to the burning portion of the gas cloud. Combustible parts of the buildings will, due to this, catch fire. Combustible materials inside the buildings will (partially), due to radiation through windows, also catch fire. One and the other will lead to secondary fires inside the cloud.

If we consider that material damage inside the cloud is complete, then the extend of the damage outside the cloud (secondary fire due to heat radiation) is practically certainly negligible for a flash fire situation.

6.4 Personal Injury due to a Flash Fire

People who, at the moment of ignition of a cloud, will be located inside the cloud and outdoors will, due to direct flame contact, suffer at least very severe injuries. Due to this direct flame contact deep burns over major parts of the body will develop. The types of burns which can develop due to the ignition of the clothing are discussed in [10].

As first consideration, eventual attempts to escape the consequences, in case of ignition of the clothing, will end-up in attempts to extinguish the clothing. It is reasonable to assume that the skin-area with serious burns (second degree or worse) is equal to the area of the burning clothing. An American investigation has been conducted, in 5 hospitals, in a period between 1961 and 1966, whereby 179 people were treated for burns caused by burning clothing [38]. This investigation has shown that, in the case of burns caused by burning clothing, in 40% of the cases skin transplantations and extensive operational interventions had been necessary. Only in 5% of the cases in which the clothing did not catch fire admission to hospitals proved necessary. Even though the above results do not furnish a proof, they support the assumption that persons subjected to the ignition of the clothing will suffer from severe to very severe burns. In the case of ignition by a flash fire it could be expected that the major part of the clothing will catch fire. The extend of the skin-area which then will be affected will, in all probability, be so large that the persons who have been exposed will die as consequence of the burns.

People who, at the moment of ignition of the gas cloud, will be located inside houses will not be immediately subjected to direct flame contact. The flash fire will, however, lead to secondary fires on a large scale. The chances of survival of people inside houses will then be highly dependent on the prevailing conditions.

6.5 Conclusion

It can be concluded, from the above, that material damages due to a flash fire inside the cloud will be practically complete. Due to direct flame contact, secondary fires will develop on an extensive scale. Due to the short duration of the heat radiation outside the cloud, material damages, on the other hand, should be of limited nature outside of the cloud.

An appraisal of the extend of personal injuries due to a flash fire seems to reasonably indicate that all people who, at the moment of ignition of the cloud, will be located inside the cloud, will be mortally affected. Such an appraisal is valid for people outdoors (due to direct flame contact) as well as for people inside houses (due to secondary fires).

Due to the short exposure duration, the extend of personal injuries outside of the cloud will be relatively small versus the injuries incurred inside the cloud.

Material damages due to heat radiation

7.1 Introduction

The concept of material damages applies to damages to built up environments, including installations. Materials which are considered suitable for buildings play, consequently, an important role.

The following will be considered as critical:

- wood
- synthetic materials
- glass
- steel

The first two materials mentioned (wood and synthetic materials) are combustible and can, lead to secondary fires.

Glass is not combustible. However, glass panels can break under the influence of temperature changes. As glass is used in facades in large quantities, the breakage of this glass can lead to significant consequent damages.

Steel is also not a combustible material. However, when the temperature rises, the strength and stiffness of steel decrease rather rapidly. It is consequently foreseeable that a structural steel element can fail as consequence of heat radiation. Primarily in installations (for instance high tension masts) this, in turn, can lead to appreciable damages. Due to the above reason, attention will be given, in this study, to steel which is not protected against heat (so-called non coated steel).

Non combustible and heat resistant materials, such as masonry will not be considered. This is also valid for reinforced concrete and coated steel since, in such cases, heat radiation can lead to problems only in extreme situations, for instance if the object in consideration is located inside the flame or in its immediate vicinity. Furthermore, the level of radiation which may lead to damage will, then, be to a major extent dependent on the protective concrete layer or, respectively, appropriate coating. Due to the above, it is practically impossible, in these cases, to make a global appraisal. For an evaluation of protected (coated) steel constructions under arbitrary circumstances reference is made to [22].

With regard to damages we will differentiate between two levels:

- **Damage level 1:** Ignition of surfaces exposed to heat radiation and then breakages or other types of failures of structural elements.
- **Damage level 2:** Damages such as: serious discolouration of a certain surface of material, peeling off of paints and/or appreciable deformations of structural elements.

It will be clear that, for a given situation, the radiation required to reach damage level 1 will be higher than the one required for damage level 2.

The specific purpose of this investigation is to provide indications regarding the critical radiation intensities leading to damages of the above mentioned different materials and damage levels. In the evaluation of the effect of the radiation it will be assumed, that we are dealing with a constant radiation

intensity and an exposure of such duration that, on the surface of the materials under consideration, a stationary heat balance is established. Since this study is oriented towards a global appreciation of the damage mechanism, it must be based on strongly schematic heat flux models. For the previously mentioned different materials, in this respect, hypotheses will be made which will lead to the determination of the critical radiation intensities. See 7.3. However, first of all, we will take a closer look at the concept "critical radiation intensity", such as it is used in fire safety considerations, and, along with that, we will expand on this concept as required within the framework of this study.

7.2 The Critical Radiation Intensity

Surfaces of materials can catch fire as consequence of heat radiation. In this respect, the radiation intensity and the exposure duration are important. The longer the exposure duration will be, the smaller will be the radiation intensity required to ignite the surface of the material. Below a certain value of the radiation intensity ignition will not occur, no matter how long the exposure duration might be. This limiting value defines the concept "critical radiation intensity". See Figure 7.1. This critical radiation intensity, apart from the type of material under consideration, is dependent on the prevailing circumstances. The presence or absence of primary heat sources located on the surface of the material is of foremost importance in this respect. The following conditions are often differentiated [23] [24]:

- Presence of fire, in direct contact with the surface of the material;
- Presence of fire, without direct contact with the surface of the material;
- No presence of fire.

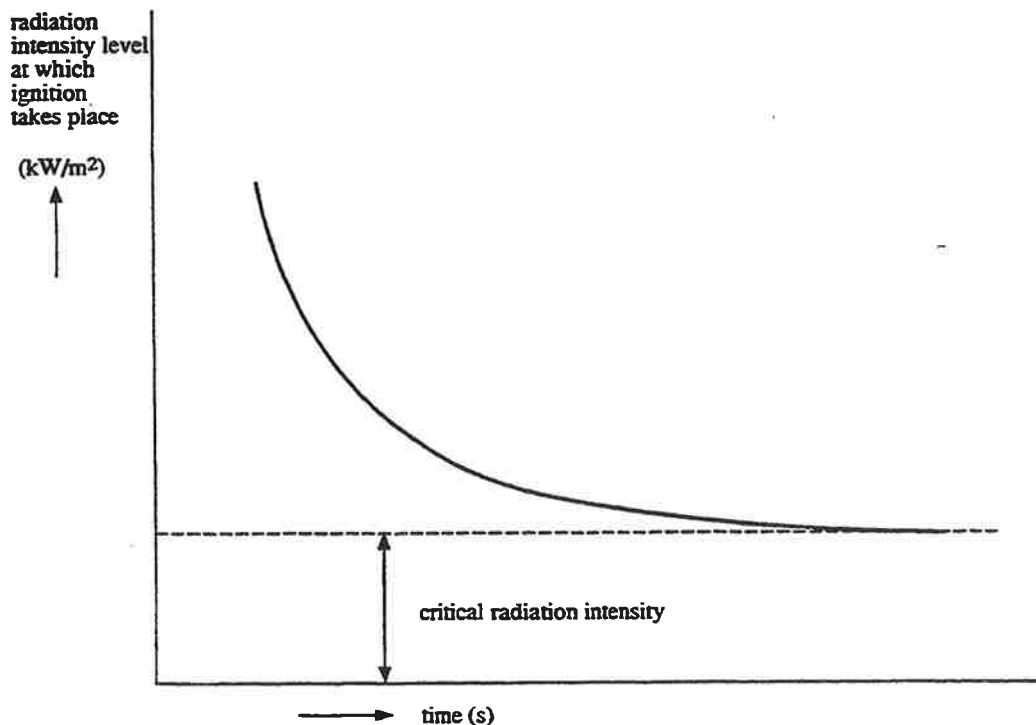


Fig. 7.1 The concept "critical radiation intensity".

An overview of values obtained experimentally for the critical radiation intensity, as defined above, for different materials, is given in Table 7.1, for the above mentioned conditions. Other factors which can influence the critical radiation intensity, such as thickness and constitution of the surface of the exposed material, possibilities of convective heat transfer (draught, position of the material surface) are not specified. This means that the values shown in Table 7.1 have only a global interest. It is well noticeable, looking at Table 7.1, that important differences of critical radiation intensity exist between the materials described. Also, the influence of primary heat sources is significant. In this respect, we

must remark that in a fire situation, in practice, the presence of primary heat sources cannot be excluded. Think, for instance, of sparks or flying brands. Generally speaking, however, in an evaluation of a possible “fire-spreading”³, it is not so that direct contact with the flame must be taken into account. For this reason, in fire safety evaluations, the values shown in the center column of table 7.1 are often the ones which are considered. Thus, for the critical radiation intensity of wood, the value of 15 kW/m² is the one which is normally retained.

Table 7.1 Some critical radiation intensities for different materials [23], [24].

Material	Critical radiation intensity [kW/m ²]		Without ignition flame
	With ignition flame; in contact with the surface	With ignition flame; without contact with the surface	
Wood	5	15	35
Hemp, jute, flax			40
Roofing material soaked in asphalt-bitumen	3		
Roofing material protected by aluminium plates	75		
Textile			35
Soft board		6	25
Hard board	5	10	30
Cork		3	23

The values of the critical radiation intensity shown above are based on the criterium that, for these values, the surface of the materials will ignite.

As already mentioned in Paragraph 7.1, this is, actually, only one of the possible damage mechanisms. Other damage mechanisms are as follows:

- The breakage or failure of structural elements without its surfaces actually burning; together with the ignition of the surface of materials, this type of damage belongs to the so-called “damage level 1” and is, in particular, important for glass and steel.
- Such a degree of discolouration or deformation of the surface of materials, even without initiation of fire, that the structural elements involved, are no longer useful and must either be replaced or repaired. This type of damage belongs to the so-called “damage level 2” and is, in particular, important for paint layers on wood, steel and synthetic materials.

Apart from the critical radiation intensity involving considerations of possible fire-spreading, no other critical radiation intensities, for the two damage mechanisms previously mentioned, are known from literature. However, it is possible to indicate global values of temperature levels at which these damage mechanisms take place. On the basis of these values, appraisals of the corresponding values of radiation intensities will be made in the next paragraph.

³ The concept “fire-spreading”, hereby, must be understood as a spreading, through outer air, of a fire to other objects.

7.3.1

General

With the help of a heat balance it is possible to establish a relationship between the radiation intensity acting on a given surface (q_i in W/m^2) and the temperature which will be reached on this surface (T in K). An important simplification can be achieved if we consider that, on this surface, a stationary heat flux is established.

If, in addition, we consider materials with poor heat conduction, such as wood or synthetic materials, we can then further simplify the heat balance condition by neglecting the heat conduction in the materials themselves. The heat balance equation then becomes:

$$a \cdot q_i - \epsilon \sigma (T)^4 - \alpha (T - T_0) = 0$$

with:

q_i = acting radiation intensity [Wm^{-2}]

T = temperature on the surface [K]

T_0 = ambient temperature [K]

a = absorption coefficient [-]

α = coefficient for convective heat transfer [$\text{Wm}^{-2}\text{K}^{-1}$]

σ = constant of Stephan-Boltzmann ($= 5.67 \times 10^{-8} \text{ Wm}^{-2} \text{ K}^{-4}$)

ϵ = emission coefficient [-]

Relation (7.1) should not be used for materials with good heat conducting properties, such as glass and steel, since in this case heat losses will develop on the object surfaces not exposed to radiation.

For a glass panel, the surface which will be exposed to radiation (= front part) is equal to the half of the total surface on which heat is discharged (= front part + back part). If then we further assume that temperature, in the glass, is uniformly distributed, we then find, for the heat balance:

$$a \cdot q_i - 2 \{ \epsilon \sigma (T)^4 + \alpha (T - T_0) \} = 0 \quad (7.2)$$

For structural steel elements the situation is somewhat more complicated, since the relation between the surface exposed to radiation versus the surface from which heat is discharged does not have a fixed value, but is dependent on the geometry of the element. Considering a structural steel element with an I shaped cross section, an illustration of the above is given in Figure 7.2.

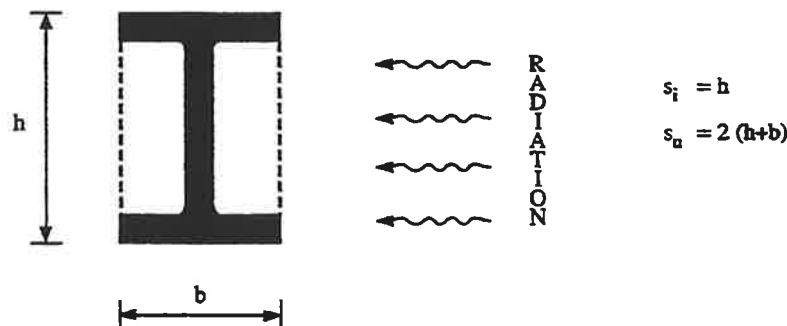


Fig. 7.2 Surfaces of a steel profile on which heat is supplied ($= s_i$) and from which heat is discharged (s_u).

From the point of view heat transfer through radiation, it is obvious that for the I profile we can schematically consider the rectangle forming the perimeter of the profile. For the condition such as

given in Figure 7.2, then, the surface to which the radiation heat is supplied, per unit length, will be: $S_i = h$; and the surface from which heat is discharged will be: $S_u = 2(h + b)$. For purposes of simplification, the rectangle forming the perimeter of the I profile will also be considered, schematically, for the convective heat transfer ($b \times h$), which, in addition, provides a conservative solution. If, again, we assume a uniform temperature distribution in the steel, the heat balance equation becomes:

$$a * q_i - \left(\frac{S_u}{S_i} \right) \{ \epsilon \sigma (T)^4 + \alpha (T - T_0) \} = 0 \quad (7.3)$$

If, in the above, we set $s_i = 1/2 s_u$ we return, logically, to the expression (7.2), derived for a glass panel.

With the help of (7.1), (7.2) or (7.3) we can now express the incident radiative heat flux q_i in terms of the upper surface temperature T , providing the following values can be estimated: the ambient temperature ($= T_0$), the absorption coefficient ($= a$), the emission coefficient ($= \epsilon$) and the convective heat transfer coefficient ($= \alpha$).

With regard to the above parameters the following hypotheses are made:

Ambient temperature ($= T_0$): In this case a conventional value of $T_0 = 293 \text{ K}$ is retained.

Absorption coefficient ($= a$): This value is dependent on the nature of the incident radiation and on the outer surface of the materials subjected to this radiation. For damage level 1 (combustion, collapse) it will be assumed that the material surface is scorched. In these conditions, a value of $a = 1.0$ can be considered. A smaller value can be used for damage level 2. Using data for solar radiation, a value $a = 0.7$ can be taken, which represents a conservative appraisal.

Emission coefficient ($= \epsilon$): This coefficient depends on the nature of the surface subjected to radiation and on the temperature on this surface. For the evaluation of the damage, a value of $\epsilon = 1$ is retained, valid for both damage level 1 and damage level 2.

Convection coefficient ($= \alpha$): This value is determined by the air flow which passes over the surface subjected to radiation and is, therefore, dependent on the temperature on this surface, on the position of this surface and on the wind conditions. With regards to wind conditions we will take the conservative assumption that wind-velocity can be neglected (so-called free convection). In these circumstances, for a surface temperature equal to 293 K , the value of α is found to be: $\alpha = 2$ to $3 \text{ W m}^{-2} \text{ K}^{-1}$. For a surface temperature from 373 to 473 K we find: $\alpha = 7 \text{ W m}^{-2} \text{ K}^{-1}$ [26]. The significance of convective heat transfer, with increasing surface temperature, strongly declines in comparison to heat transfer due to radiation, see, for example (7.1)–(7.3). Due to this we will consider, in what follows, a value of $\alpha = 7 \text{ W m}^{-2} \text{ K}^{-1}$ for damage level 1 as well as for damage level 2.

Remark

The total incident radiation intensity comes, in fact, from two sources:

- The primary radiation source
- The secondary radiation sources due to reflections and emissions of other surfaces in the surroundings.

In view of the unknown character of the surroundings of the surface under consideration subjected to radiation, the contribution of the secondary sources will be disregarded, which is further justified by the uncertainty regarding the intensity of the primary source. (Note: in this respect, an implicit condition is that the surface subjected to radiation is not partially protected).

7.3.2

Wood

As already previously indicated, it is customary for the evaluation of the damage on wood, for damage level 1, to consider a critical radiation intensity of 15 kW m^{-2} . It would be of interest, making use of the assumptions of the previous paragraph, to find out to which surface temperature this radiation intensity would correspond. We use, for this purpose the following values in (7.1):

$$\begin{aligned}
 q_i &= 15 \text{ kW m}^{-2} \\
 T_o &= 293 \text{ K} \\
 a &= 1.0 \\
 \epsilon &= 1.0 \\
 \alpha &= 7 \text{ Wm}^{-2}\text{K}^{-1}
 \end{aligned}$$

We find, then, a value of $T_{(1)} = 683 \text{ K}$ for the surface temperature. This represents, in all aspects, a reasonable answer.

For the evaluation of the damage at damage level 2 (= serious discolouration), the type of paint which is applied plays, in this respect, an important role. In the Netherlands, paints of the alkyd resin type are commonly used. This type of paint begins to discolour at temperatures higher than 343 K. Deterioration takes place for temperatures of 373 to 393 K. It would appear reasonable, in view of the foregoing, to take $\gamma = 373 \text{ K}$ as critical surface temperature for an evaluation of the damage at damage level 2.

With the help of (7.1) and with $a = 0.7$ (!) we now find the corresponding critical radiation intensity to be equal to:

$$q_{i(2)} = 2 \text{ kW} \cdot \text{m}^{-2}$$

7.3.3

Synthetic materials

Synthetic materials which are very often used on the outer faces of buildings are:

- reinforced polyester in facade panels
- PVC in window frames and small panels
- perspex in synthetic windows

The behaviour in fire conditions of synthetic materials displays a strong variation and is dependent on both the nature of the material as well as its composition. As a reasonable average assumption it can be considered that combustion or serious disintegration of the above mentioned synthetic materials occurs in circumstances comparable to the ones which are required to set wood on fire [26]. It follows, from this, that for the critical radiation intensity for damage level 1 the value $q_{i(1)} = 15 \text{ kW} \cdot \text{m}^{-2}$ can be retained.

Discolouration and, for thermoplastic materials, deterioration, take place at about 373 K. In addition, for some synthetic materials, already at 343 K degradation (= physical aging) seems to occur. Since this last phenomenon manifests itself only after a long lasting exposure, we will not take it here into consideration. The critical temperature for synthetic materials, with regards to a damage evaluation at damage level 2, can consequently, be taken equal to $T = 373 \text{ K}$, the same as in the case of painted wood. With the help of (7.1) this gives again a value of $\approx 2 \text{ kW} \cdot \text{m}^{-2}$ for the critical radiation intensity.

7.3.4

Glass

It will be sufficient, for glass, to make a damage evaluation only for damage level 1 (= breakage). It is clear that there is no necessity to consider the case of discolouration of glass, since possible soot formation can easily be removed.

The cracking of glass under the influence of heat radiation is provoked by a non homogenous temperature distribution in the glass. As the subsequent deformations are partially or totally prevented, this gives rise to stresses within the glass. In particular the tensile stresses at the locations of the runways are, in this respect, important, since at these locations the glass is protected from radiation and, consequently, the temperature there is lower.

On the basis of theory and tests it seems that a temperature difference of 100 K leads to crack formation [28]. If we assume that the temperature of the glass near the runways does not increase at all above the initial temperature equal to 293 K, it then follows that the critical temperature, for damage level 1, will

be equal to $T = 393$ K. With the help of (7.2) we can now calculate the critical radiation intensity, taking for the absorption coefficient of glass $a = 1$. We find:

$$q_{i(1)} = 4 \text{ kWm}^{-2}$$

7.3.5

Steel

For the evaluation of structural steel elements both damage level 1 as damage level 2 are of importance.

Failure or collapse of structural steel elements under the influence of heat radiation take place, practically speaking, in elements with a load bearing function. The failure temperature is dependent on the load and, for a conventionally dimensioned steel element, its value lies between 673 and 873 K. For a global average value a figure of 773 K can be retained [29]. With the help of (7.3) and for $a = 1.0$ we can now calculate the corresponding critical radiation intensity. This, in turn, is dependent on the ratio s_i/s_u , with s_i and s_u as defined in Paragraph 7.3.1 The relationship referred to is represented in Figure 7.3.

Damage level 2 occurs when the paint system provided on a structural steel element is damaged to such an extent that re-painting becomes necessary. Enamel layers are often used on steel. Discolouration or deterioration of such layers takes place at a temperature of about 473 K. With this limit value, and with $a = 0.7$, we can now calculate the critical radiation intensity $q_{i(2)}$, again with the help of (7.3). The relationship between $q_{i(2)}$ and the ratio s_i/s_u , found in this manner, is also given in Figure 7.3.

For a proper understanding of Figure 7.3 it is necessary to develop some notion with regard to the values of the ratio s_i/s_u which appear in practice. Consider, for this, Figure 7.4a. For profiles for which the height ($= h$) is equal to the width ($= b$), such as HEA and HEB profiles commonly used for columns, with cross sectional dimensions smaller than 300 mm, and, also, for profiles with a square cross section, we find: $s_i/s_u = 0.25$ in the case of one-sided radiation. For profiles in which the ratio width height is not equal to 1.0 the orientation of the radiation versus the one of the profile is of importance. This is applicable to IPE profiles, very often used in practice, with a height smaller than ≈ 400 mm, for which: $h/b \approx 2$. If the radiation acts on the body (web) of such a profile, we find (see Figure 7.4b):

$$\frac{s_i}{s_u} = \frac{2}{6} = 0.33$$

If the radiation is oriented on one of the flanges, we find (see Figure 7.4c).

$$\frac{s_i}{s_u} = \frac{1}{6} = 0.17$$

It is proposed to take, as a global average value for steel profiles the ratio: $s_i/s_u = 0.25$. We find, with this, respectively for damage level 1 and damage level 2 the following (see Figure 7.3):

$$q_{i(1)} = 100 \text{ kWm}^{-2}$$

$$q_{i(2)} = 25 \text{ kWm}^{-2}$$

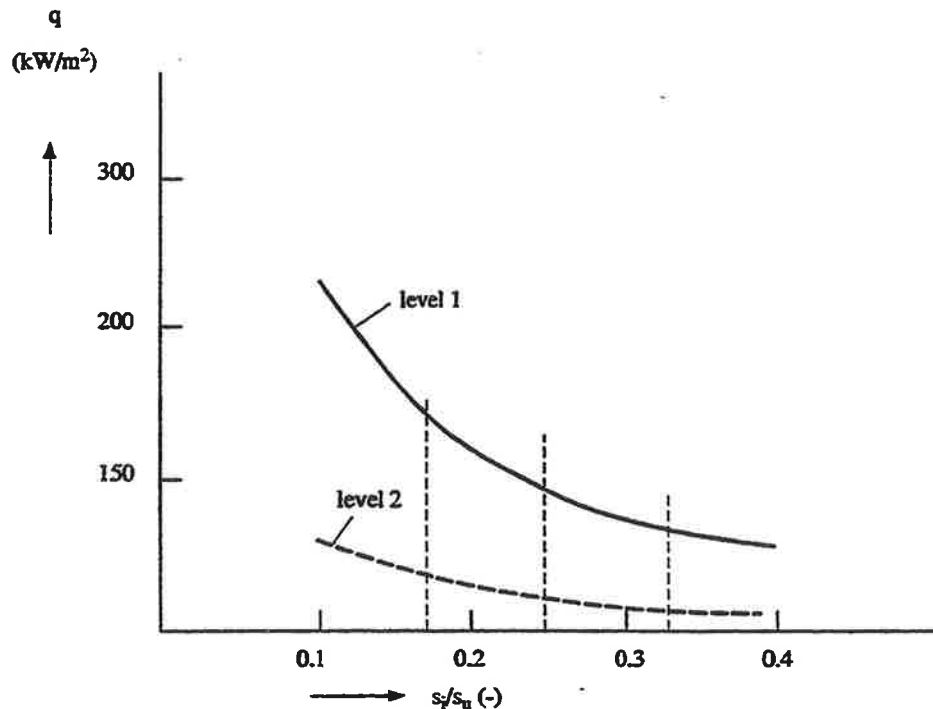


Fig. 7.3 Critical radiation intensity for steel for damage evaluation at levels 1 and 2, as function of the factor s_i/s_u

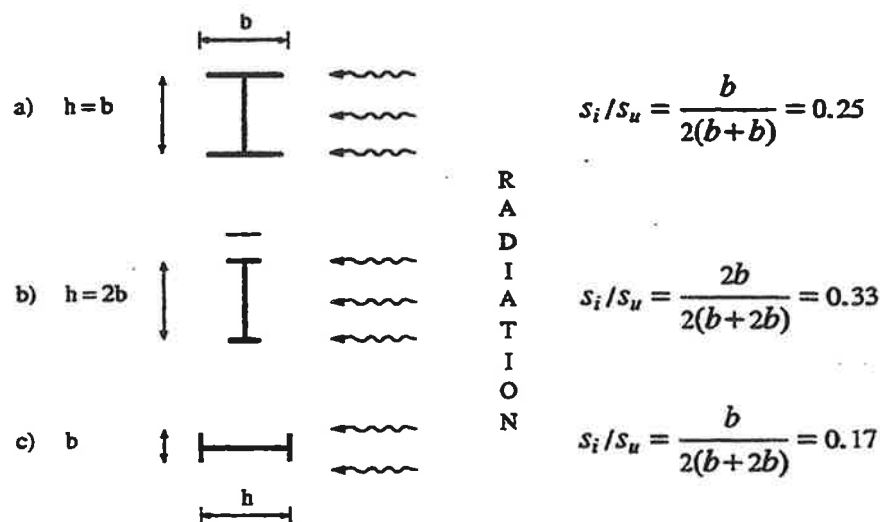


Fig. 7.4 Effect of the orientation of the radiation versus the one of the steel profile on the value of the factor s_i/s_u

7.3.6

Evaluation

In the preceding paragraphs, values for the critical radiation intensity of wood, synthetic materials, glass and steel have been established. In agreement with the definition given in Paragraph 7.2 of the concept "critical radiation intensity" it is assumed, thereby, that the radiation holds for an undetermined long time, so that on the surface of the material a stationary heat flux establishes itself. Particular for materials with good heat conducting properties such as glass and steel, a relatively important heat transfer to the surroundings will take place. Because of this, a certain amount of time will pass before the steady state is reached. As an illustration, the warming up behaviour of a glass panel and of two steel profiles is given in Appendix C. Representative situations have been chosen for these examples. It would appear that for glass exposed to a (critical) radiation intensity of $4 \text{ kW} \cdot \text{m}^{-2}$, already after about 10 minutes 90% of the (critical) final temperature of 393 K has been reached. See Figure C.1.

For a damage level 1 evaluation for steel, considering practical cases, for a critical temperature of 773 K and a radiation intensity of 100 kW m^{-2} , this 90% limit is reached after about 20 minutes. See Figure C.2. For a damage level 2, an evaluation of an IPE 200 profile (radiation intensity of 25 kW m^{-2} , critical temperature of 473 K) indicates that already after about 15 minutes the temperature of the steel has reached 90% of its end value. For heavier profiles, however, this time span can increase significantly. For an HE-B200 profile, under the same conditions, the time was found to be 50 minutes. See Figure C.3.

A fully developed fire will in general last for more than half an hour. The concept "critical radiation intensity", as worked out in this report, appears useful, for providing a first, global idea. In case of relatively short exposure durations a more refined evaluation may be necessary, taking into account the geometry of the structural element and its orientation versus the radiation. This is especially valid for a damage level 2 evaluation in steel construction.

As a guideline, finally, an overview is given, in Table 7.2, of the maximum heat radiation (= sun radiation) that occurs in the Netherlands [25]. This appears to have a maximum value of 0.9 kW m^{-2} , which means smaller, by a factor of about 2, than the smallest of the critical radiation intensities which we found in the situations discussed in this report.

Table 7.2 Maximum heat radiations from the sun, per month, in the Netherlands [25]

Month	Max. radiation [W/m^2]
january	261
february	420
march	595
april	767
may	865
june	895
july	876
august	799
september	666
october	489
november	311
december	221

Considerations regarding the results

In the calculation of the extend of the damage due to a calamity, the various ways in which people can be injured are considered separately. In the case of injuries due to a fire, the causes for the injuries fall in two categories:

1. Injuries due to direct flame contact within the dimensions of the (pool) fire.
2. Injuries due to heat radiation.

It is accepted, as a likely probability, that people within the dimension of the fire will die due to direct flame contact (see also Paragraph 6: damage due to a flash fire). Considering a realistic average exposure of 10 s (see Appendix B), a heat radiation level, as given in formula (3.5): 17 kW/m^2 , would account for 1% lethality among the people exposed to it. Personal injury, in case of the absence of protection provided by clothing, can already be incurred, for a long term exposure, for a radiation intensity of about 1 kW/m^2 .

According to the "Yellow Book" [1], the radiation level at the surface of the flame is in the range of 100 kW/m^2 (LPG pool fire). In the case of a fire-ball, this radiation level can reach much higher values, up to a maximum of about 200 kW/m^2 . The area in which at least 1% of fatal injuries due to radiation can take place, consequently, from the boundary of the flame to the distance where the view-factor is about $1/6$ (for a pool-fire), and about $1/12$ (for a fireball).

Clothing can provide a protective effect in case it does not ignite due to either auto-ignition or sparks (see Paragraph 4.4). Its protective effect is expressed by a reduction of the skin-area affected by burns and the corresponding mortality (see Paragraph 4.2, Table 2.1). If the clothing catches fire, the lethal probability can be considered as 100%.

For the calculation of the exposure duration (Δt) no fixed guidelines can be given. Factors which influence the value of Δt are, among others (see Chapter 5 and Appendix B):

- Sheltering possibilities: For a density built-up area we can consider a value of Δt of 10 seconds.
- Escape possibilities: For an area which is not built-up (open escape routes), escape will account for a decrease of the dose. This is expressed in terms of an "effective exposure duration" which is smaller than Δt .
- Composition of the group: People in treatment, old people, children and vacationers, among others, represent an extra vulnerable group. People familiar with the consequences of an accident are less vulnerable. This is expressed by either an increase or, respectively, a decrease of the value of Δt .

In the calculation of material damage due to heat radiation difference is made between two damage levels:

- **Damage level 1:** The catching of fire by surfaces of materials exposed to heat radiation as well as the rupture or other type of failure (collapse) of structural elements.
- **Damage level 2:** damage caused by serious discolouration of the surface of materials, peeling-off of paint and/or substantial deformation of structural elements.

For the following materials: wood, synthetic materials, glass and uncoated steel, global values of radiation intensity are indicated, whereby, for materials commonly used on the outer faces of buildings

and installations, damage must be considered. Hereby the concept of "critical radiation intensity" is introduced, which is to be understood as the value of the radiation intensity for which, by a long term exposure, damage is initiated.

Qualitative Appraisal of Final Results

Considering as basis the probit-function for a fatal injury due to heat radiation according to formula (3.5) and a 100% fatal injury inside a fireball, then (by a homogeneous distributed population) the number of victims outside of the fireball will be about five times as large as the number of victims inside of the fireball, see Appendix A. For a pool fire, the number of victims outside the pool will be about twice as large as the number of victims inside the pool.

The calculated results presented in Appendix A are strongly dependent on the heat radiation intensity and on the exposure duration. The values chosen are representative of both fire situations.

The calculations show that personal injuries due to heat radiation are more important, in case of a fireball, than for other types of fires. In case of a flash fire the injury outside the vapour cloud will be relatively minor (see Paragraph 4.6).

The values of critical radiation intensities which have been obtained are presented in Table 8.1. The results show that glass, on the basis of a damage level 1 evaluation, is the most critical of all: ($q_{i(1)} = 4 \text{ kW/m}^2$). The critical values for wood and synthetic materials and steel, respectively 15 and 100 kW/m^2 , are significantly higher.

Considering damages at damage level 2, the results show that wood and synthetic materials are the most vulnerable ($q_{i(2)} = 2 \text{ kW/m}^2$). The critical radiation intensities obtained for steel are one order of magnitude higher ($\approx 25 \text{ kW/m}^2$). An evaluation at damage level 2 for glass is not considered as relevant.

The values shown in Table 8.1 must be interpreted as global indications, valid for exposure durations which are not too short, for example more than 30 minutes. For fires of shorter duration, a more refined approach is necessary, in which the geometry of the structural element and its orientation versus the radiation must be taken into account. See Appendix C. This can be particularly of importance for an evaluation of the damages to steel structures at damage level 2.

Table 8.1 Global values of the critical radiation intensity for the materials considered.

Material	Critical radiation intensity [KW/m^2]	
	Damage level 1	Damage level 2
wood	15	2
synthetic materials	15	2
glass	4	-
steel	100	25

References

- [1] Methoden voor het berekenen van de fysische effecten van het incidenteel vrijkomen van gevaarlijke stoffen (vloeistoffen en gassen) "Yellow Book", CPR 14.
Rapport van de Commissie Preventie van Rampen door gevaarlijke stoffen. Uitgave van het DGA, Voorburg, 1979.
- [2] Revision of [1], CPR 14, 1988.
- [3] Eisenberg, N.A., C.J. Lynch, R.J. Breeding.
Vulnerability Model: A simulation System for Assessing Damage Resulting from marine Spills (VMI).
US Coast Guard, AD/A-015 245, NTIS report no. CG-D-137-75, 1975.
- [4] Brandwonden.
Philips-Duphar Nederland B.V., Amsterdam, 1979.
- [5] J.P. Bull.
Revised analysis of mortality due to burns.
Medical Research Council Industrial Injuries and Burns Unit, Birmingham Accident Hospital, Birmingham, The Lancet, November 20, 1971, 1133-1134.
- [6] A.M. Stoll.
Heat transfer in biotechnology, in Advances in Heat Transfer, Vol, 4 Academic Press, New York, 1967, pp. 67-141.
- [7] Hardee, H.C., D.J. Lee.
A Simple Conduction Model for skin Burns Resulting from Exposure to Chemical Fireballs.
Fire Research, 1, 1977/78, 199-205.
- [8] J.B. Perkins, H. E. Pearse and H.D. Kingsley.
Studies of flash burns: the relation of time and intensity of applied thermal energy to the severity of burns.
The University of Rochester, UR-317, Dec. 1952.
- [9] A.M. Stoll and M.A. Chianta.
Method and rating system for evaluation of thermal protection.
Aerosp. Med., 40 (11), 1969, 1232-1238.
- [10] Hymes, I.
The physiological and pathological effects of thermal radiation. U.K. Atomic Energy Authority, Safety and Reliability Directorate, Culchetch, Warrington, SRD R 275, 1983.
- [11] Finney, D.L.
Probit analysis, London, Cambridge University Press, 1971.
- [12] Glasstone, S., editor.
The effects of nuclear weapons.
U AEC, april 1962, p. 571.

- [13] Tsao, C.K., W.W. Perry.
Modifications to the Vulnerability Model: A Simulation System for Assessing Damage Resulting from Marine Spills (VM4).
US Coast Guard, AD/A-075231, NTIS report no. CG-D-38-79, 1979.
- [14] Hilado, C.J., Murphy, R.M.
Ignition and Flash-fire Studies of Cellulosic Materials.
Fire and Materials, vol. 2, no. 4, 1978, 173-176.
- [15] Wulff, W.
Fabric ignition, Tex. res. J., October 1973.
- [16] Rausch, A.H., N.A. Eisenberg, C.J. Lynch.
Continuing development of the Vulnerability model (VM2).
Department of Transportation United States Coast Guard,
Washington D.C., Report no. CG-D-53-77, Feb. 1977.
- [17] LPG-Integraalstudie. Vergelijkende risico-analyse van de opslag, de overslag, het vervoer en het gebruik van LPG en benzine.
MT-TNO, May 1983.
- [18] Pietersen, C.M.
Analysis of the LPG-incident in San Juan IXHUATEPEC, Mexico City, 19 November 1984.
MT-TNO, ref. 85-0222, May 1985.
- [19] EFFECTS, the TNO software package for calculation of the physical effects of the escape of hazardous material.
Product of MT-TNO dept. of Industrial Safety, Apeldoorn,
The Netherlands.
- [20] Ermak, D.L., H.C. Goldwire, W.J. Hogan, e.a.
Results of 40 m³ LNG spills onto water.
Paper presented at the second symposium on Heavy Gases and Risk Assessment.
Battelle-Institute e. V., Frankfurt, FRG, May 25-26, 1982.
- [21] Puttock, J.S., G.W. Colenbrander, D.R. Blackmore.
Maplin Sands experiments 1980: Dispersion results from continuous releases of refrigerated liquid propane.
Paper presented at the second Symposium on Heavy gases and risk analysis, Frankfurt, May 1982.
- [22] Twilt, L.
Beoordelingsmethode voor brandbeschermende bekleding op staalconstructies onder verschillende brandomstandigheden.
TNO-IBBC-reportno. B-85-541, november 1985.
- [23] Lie, T.T.
Brandoverslag door straling.
Polytechnische Tijdschrift, uitg. A, 12e jaargang nr. 11-12, 1957.
- [24] Lie, T.T.
Fire in Buildings.
Applied Science Publishers Ltd, London, 1972.
- [25] NEN 5067: Ontwerpberekening Koellast.
Nederlands Normalisatie Instituut, Delft.

- [26] Zorgman, H.
Brandgedrag van kunststoffen.
Plastica 31, nr. 6, juni 1979.
- [27] Verhoeff, G.
Het mogelijke temperatuurverloop van een LPG-tank in het ruim van een binnenvaartschip betrokken bij brand.
TNO-IBBC-rapportnr. B-85-361.
- [28] Dekker, J.
Gedrag van glas bij brand.
De Brandweer, juni 1972.
- [29] Twilt, L. en J. Witteveen.
Brandveiligheid Staalconstructies.
Staalbouwkunding Genootschap, 2e druk, september 1985
- [30] Rausch, A.H., C.K. Tsao, R.R. Rowley.
Third-stage Development of the Vulnerability Model: A Simulation System for Assessing Damage Resulting from Marine Spills (VM3).
US Coast Guard, NTIS report no. CG-D-5-78, 1978.
- [31] Kreyszig, E.
Advanced Engineering Mathematics.
Wiley and Sons, New York, 1967
- [32] Mitchell, H.H.
A general approach to the problem of estimating personnel damage on atom bombed targets.
Raud Report, RM-1149, Oct. 12, 1953.
- [33] Lie, T.T.
Eigenschappen van warmtebeschermende Kleding en Keuringsmethoden.
Brand, 1963.
- [34] Haffmans, L., P.J. van het Westeinde.
TTO-IBBC, rapport B-81-545.
- [35] Van Aken, J.A.
Beproevingmethode voor op laboratoriumschaal beoordelen van de thermische isolatie van beschermende kleding.
TNO-IBBC-rapportnr. B-84-483, april 1984.
- [36] Buttner, K.
Effects of extreme heat and cold on human skin.
I. Analysis of temperature changes caused by different kinds of heat application.
II. Surface temperature, pain and heat conductivity in experiments with radiant heat.
J. Appl. Phys., Vol 3 (12) (1951), pp. 691-702, 703-713.
- [37] Zeeuwen, J.P., C.J.M. van wingerden, R.H. Dauwe.
Experimental investigation into the blast effect produced by unconfined vapour cloud explosions.
4th International Symposium on Loss Prevention and Safety Promotion in the Process Industries.
(1983).
- [38] Schaplowsky, A.F. Bulletin of the New York Academy of Medicine, 43, no. 8, August 1967.

Appendix A

Fatal Injury outside of a Fireball or a Pool Fire due to Heat Radiation

The probit function P_r for fatal injury without the influence of the protective effect of clothing is (see 3.5):

$$P_r = -36.38 + 2.56 \ln (t * q^{4/3}) \quad (\text{A.1})$$

with

t : exposure duration (f.i. 10 s)

q : radiation level [W/m^2]

Neglecting the damping of the heat radiation due to water vapour in the air, we find q from:

$$Q = q_o * 4\pi R^2 \quad (\text{A.2})$$

$$q = \frac{Q}{4\pi r^2}$$

$$q = \left(\frac{R}{r}\right)^2 * q_o$$

with

q_o : the surface radiation level (f.i. $190 \text{ kW}/\text{m}^2$)

R : the radius of the fireball [m]

r : the distance [m]

If the number of persons present is **homogeneously** distributed over the area, then the number of fatalities **inside** the fireball will be:

$$N_1 = N_o * \pi R^2 \quad (\text{A.3})$$

with

N_o : the population density [$1/\text{m}^2$]

πR^2 : ground area covered by the fireball

The number of fatalities outside of the fireball N_2 is determined by:

$\Delta N_2(r) = p(r) * N_o * \Delta A$
 p = fraction of fatalities (function of the distance)
 N_o = (homogenous) population density
 ΔA = Segment of the area of the circle at distance r

The total number of fatalities is found by integration:

$$N_2 = \int_R^{\infty} p(r) * N_o * 2\pi r dr \quad (A.4)$$

The relationship between the probit function and the percentage of fatalities (p) is given by (see also Table 3.1):

$$p = 1/2 \left[1 + \operatorname{erf} \left(\frac{Pr - 5}{\sqrt{2}} \right) \right]$$

A combination of (A.5), (A.4) and (A.1) provides a figure for the number of fatalities due to heat radiation. The combination of (A.4) with (A.3) provides a figure for the number of fatalities outside the cloud related to the number inside the cloud.

$$\Delta = \frac{N_2}{N_1} = \int_R^{\infty} p(r) * 2 \left(\frac{r}{R} \right) d \left(\frac{r}{R} \right) \quad (A.6)$$

$$\Delta = \int_1^{\infty} p(\zeta) * 2\zeta d\zeta$$

with

$$\zeta = \frac{r}{R}$$

N.B. : $p = f(q)$

$$q + q_o / \zeta^2 \text{ (see A.2)}$$

Thus, the parameter ζ in p is simplified by the substitution of the factor $\frac{r}{R}$.

In Figure A.1, on the right-side of the diagram, the integrant from (A-6) is plotted versus ζ (for $q_o = 190 \text{ kW/m}^2$ and $t = 10 \text{ s}$). For this situation we have:

$$\Delta \approx 5$$

which means that outside of the fireball there will be five times more fatalities.

Due to the fact that a pool fire q_o is much smaller (f.i. 90 kW/m^2), the distance at which fatal injury can be incurred is smaller. As an example, we will consider a pool fire of (liquefied) propane with a radius of 50 m and a exposure duration of 10 s. For this situation, in the same manner as for the fireball, we find:

$$\Delta = 2$$

which means that outside of the pool there will be twice as many fatalities as inside.

- The assumptions which have been made are as follows:
- No explicit account has been taken for the protective effect of clothing.
- The fireball developed in an open space; in other words no sheltering possibilities are available.
- The density of the people is homogeneously distributed.
- Inside the fireball the lethality is 100%.

Note:

- Δ is by definition equal to the area under the curve;
- $2 * p * \zeta$ is, in fact, for every distance the relationship between the number of fatalities at this distance and the numbers of fatalities inside the fireball.

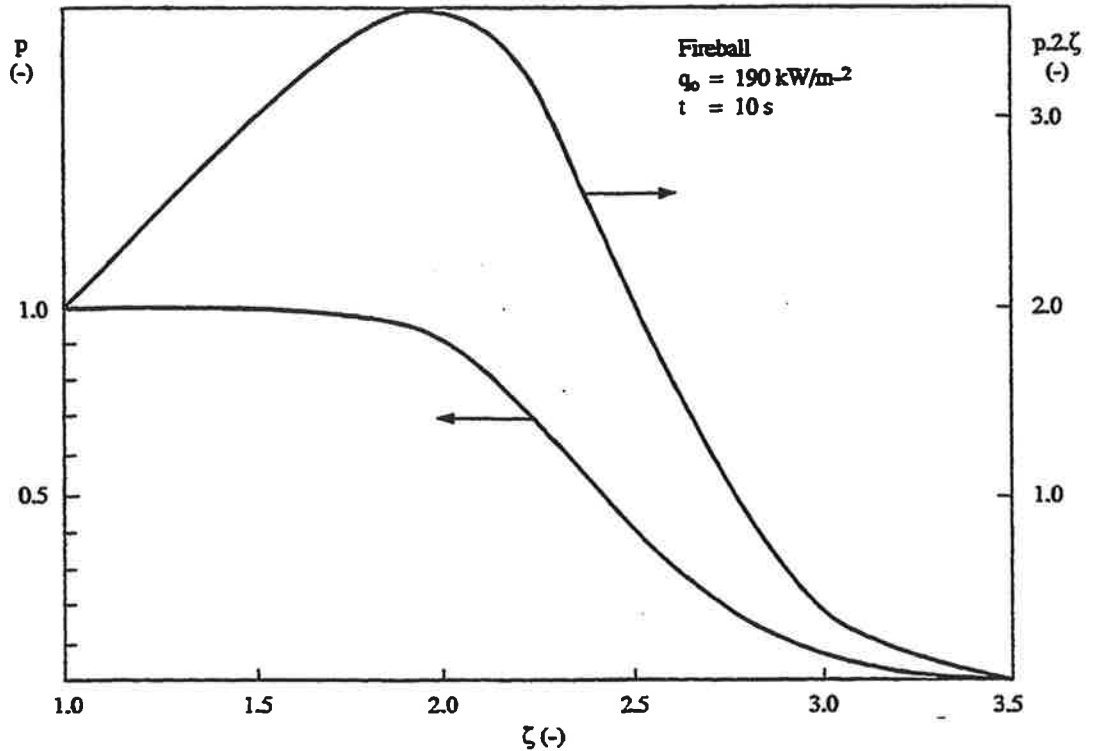


Fig. A1 Probability of fatal injury by heat radiation due to a fireball.

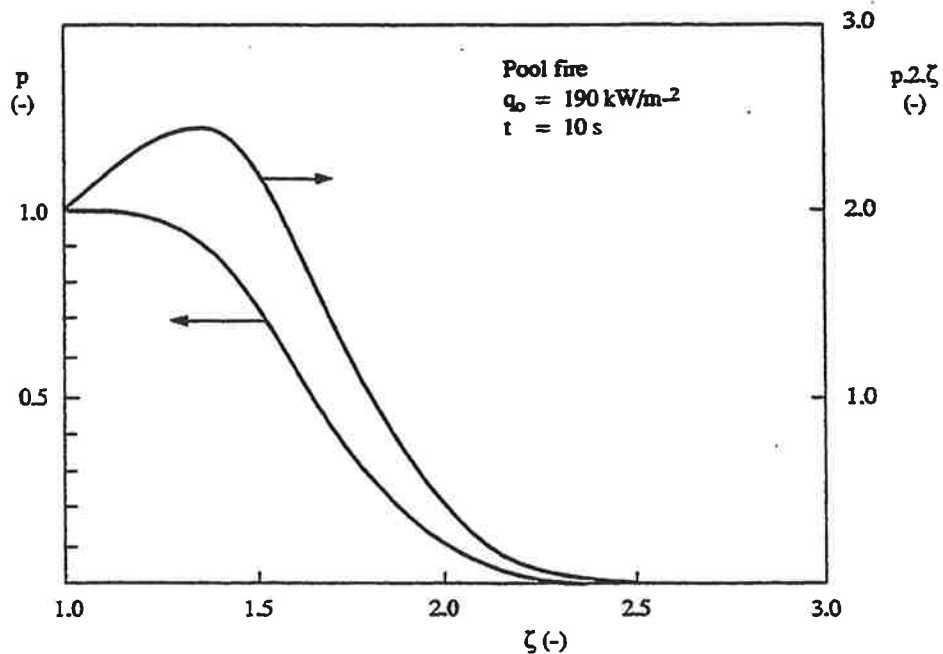


Fig. A2 Probability of fatal injury by heat radiation due to a pool fire.

Appendix B

Example of Calculation of the Exposure Duration

The results of effect calculations, with the help of "Effects" (based on models from the Yellow Book [1]), are given, in Table B.1 for a pool fire scenario.

Question: The exposure duration of a person who, at the beginning of the fire, is located at a distance of about 40 m from the center of the pool (10-15 m from the edge).

The pool had developed before initiation of the fire, due, for example, to the escape from a vessel, and it is assumed that it has a 55 m fixed dimension.

Table B.1 Results of a pool fire calculation with "Effects" [19].

CALCULATION MODEL : HEAT RADIATION — ISOBUTYLENE

AMBIENT TEMPERATURE	=	293.	(K)
DIAMETER POOL	=	55.	(M)
INTENSITY OF RADIATION	=	86.0	(KW/M^2)
RELATIVE HUMIDITY	=	90.	(%)

THE THERMAL LOAD IS CALCULATED FROM THE EDGE OF THE POOL

DISTANCE (M)	THERMAL LOAD Q(KW/M^2)		
	Q HOR.	Q VERT.	Q MAX.
3.	28.9	36.2	46.3
6.	23.3	31.2	38.9
8.	19.8	27.7	34.1
11.	17.3	25.1	30.5
14.	15.3	22.9	27.6
28.	9.4	15.9	18.4
55.	4.3	9.1	10.1
83.	2.2	5.8	6.2
110.	1.2	3.9	4.9
248.	0.2	1.0	1.0
385.	0.0	0.4	0.4
523.	0.0	0.2	0.2

At a distance of 247 m (x_s) from the edge of the pool the radiation intensity is 1 kW/m². The escape distance to be covered is $(x_s - x_o)/u = (247 \text{ m} - 11 \text{ m}) = 235 \text{ m}$. The time required for this is:

$$t_v = \frac{x_s - x_o}{u} = \frac{235 \text{ m}}{4 \text{ m/s}} \approx 80 \text{ s}$$

Taking into account a reaction time of : $t_r = 5 \text{ s}$, the total exposure duration is equal to:

$$t_c = (t_r + t_v) = 85 \text{ s}.$$

The total dose of radiation can be determined as follows: Consider a person located at a distance x_o from the center of the fire. The radiation level at this location is q_o . The radiation intensity, as a function of the distance, can be expressed as:

$$q(x) = q_o * \left(\frac{x_o}{x} \right)^2 \quad (B.3)$$

The radiation intensity which an escaping person from $x = x_o$ is subjected to, is:

$$q(t) = q_o \left(\frac{x_o}{x_o + u * (t - t_r)} \right)^2 \quad (B.4)$$

(Taking into account the reaction time: $t_r = 5$ s.)

The total dose of radiation can be expressed as:

$$D_s = D_s (\text{reaction time}) + \bar{D}_s (\text{escape time})$$

$$= q_o^{4/3} (t_r) + \int_{t_r}^{t_c} q(t)^{4/3} * dt \quad (B.5)$$

$$= q_o^{4/3} \left[t_r + \frac{3}{5} \frac{x_o}{u} \left\{ 1 - \left(1 + \frac{u}{x_o} (t_c - t_r) \right)^{-5/3} \right\} \right]$$

$$= q_o^{4/3} (t_r + t_{v,eff})$$

$$= q_o^{4/3} * t_{eff}$$

N.B. : \bar{D}_s = average dose of radiation

Filling - in the values for q_o , x_o , u , t_r and t_c gives, for this example :

$$t_{eff} = 11s$$

$$D_s = (3 * 10^4)^{4/3} * 11 * (W/m^2)^{4/3} s \cong 10^7 (w/m^2)^{4/3} * s$$

If the duration of the fire is short that the escape duration, for instance in case of a BLEVE, then this duration of the fire must be filled-in for the t_c value.

Assume that in the above example the duration of the fire is equal to 40 s:

$$t_{eff} \cong 5 + \frac{3}{5} \frac{x_o}{u} \left\{ 1 - \left(1 + \frac{u}{x_o} (40 - 5) \right)^{-5/3} \right\} = 10.5 s \quad (B.6)$$

For a fire duration of 20 s we find $t_{eff} = 9.5$ s and for 10 s, we find $t_{eff} \cong 8$ s, see Figure B.2. This example shows that the effective the exposure duration (and with it the dose of radiation) does not increase substantially if the duration of the fire $\geq 1/2$ of the calculated escape duration.

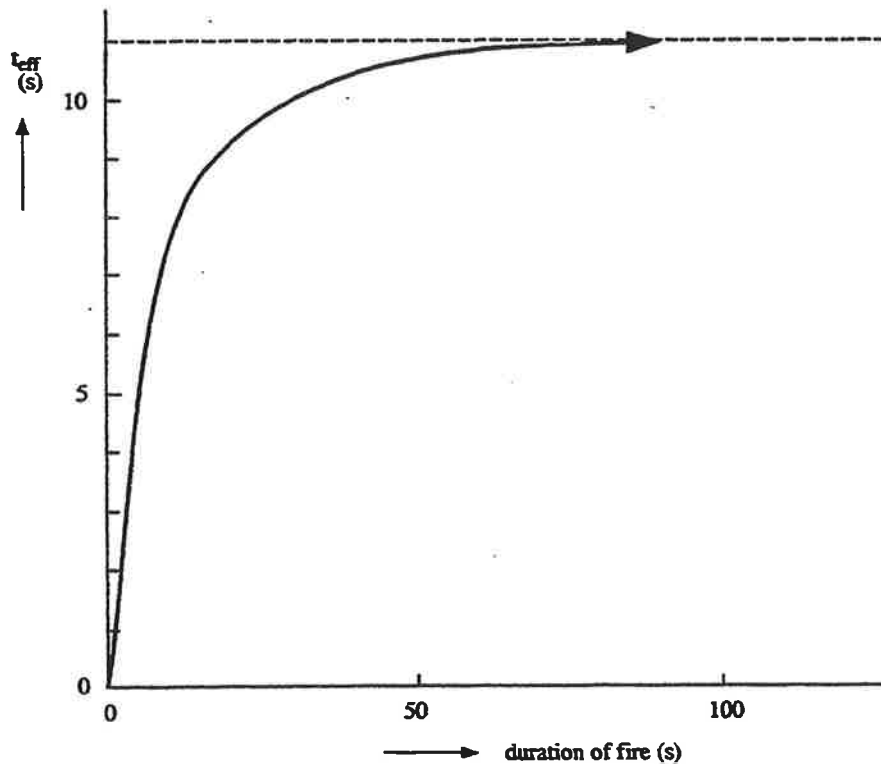


Fig. B.2 Effective exposure duration as function of the duration of the fire.

Considerations with regards to escape time (see Chapter 5).

In the so-called “urban area” with high building density, the exposure duration has been set equal to:
 $\Delta T = 10\text{s}.$

with:

$\Delta t = t_r + t_v$	t_r = reaction time
$t_v = \frac{x_v}{u}$	t_v = escape time
$t_r = 5\text{ s}$	x_v = safe distance
$u = 4\text{ m/s}$	u = (pessimistic) escape rate

This means that the sheltering possibilities are located, on the average, at a distance of some 20 meters from the potential victim. Since this is a relatively small distance, it can be considered that the radiation intensity, during the escape, does not vary significantly. In the same time, however, we cannot consider that the shelters which can be found are all located in the direction of the flame. Consequently, the average radiation intensity does not have a constant value in all directions.

In the case of a free escape route, in a so-called “open-area”, sheltering possibilities are not a consideration and people escape, then, always away from the flame.

During the escape to a sufficiently large and (safe) distance from the center of the flame, the radiation intensity will be decreasing. This decrease, in turn, can be discounted from the exposure duration:

$$D_s = q_o^{4/3} * (t_r + t_{v,eff})$$

$$= q_o^{4/3} * t_{eff},$$

For the so-called “built-up area” the situation is not as simple as for the other two areas which represent, in fact, the two limiting situations.

Those treated must always decide, on their own, whether it is preferable to run from the flame or seek shelter.

In order to be able to estimate the number of victims, we must first have an idea regarding the average distances between buildings; a distance of 50 meters may, in this respect, represent offhand a reasonable choice.

This gives, then:

$$t_v \approx \frac{50}{U} \approx 13 \text{ s}$$

which, inclusive of the reaction time (t_r) of 5 seconds, gives a total exposure duration (t_c) of 18 seconds.

In an area where buildings are fairly well separated from each other, the natural tendency of people, is to try and move away from the flame. It is then logical, in view of the foregoing, to calculate the effective time of exposure based on the time of exposure for the selected distance between buildings.

$$\begin{aligned} D_s &= D_s(t_r) + \bar{D}_s(t_v) & (t_v &= t_c - t_r) \\ &= q_o^{4/3} * t_{eff} \end{aligned}$$

$$= q_o^{4/3} * \left(t_r + \frac{3}{5} * \frac{x_o}{u} \left\{ 1 - \left(1 + \frac{u}{x_o} (t_c - t_r) \right) \right\} \right)$$

with

$$u = 4 \text{ m/s}, \quad t_c = 18 \text{ sec and } t_r = 5 \text{ sec.}$$

Appendix C

Considerations with Regard to the Non-Stationary Character of the Heat Flux

The non-stationary heat condition of a steel I profile (as per Figure 7.2), subjected to heat radiation, will now be discussed. If we consider the heat transfer which takes place over a time-span of Δt and $t + \Delta t$, we then have:

supplied to the profile: $a q_i h * \Delta t$

taken away from the profile: $\left\{ \epsilon \sigma (T)^4 + \alpha (T - T_0) \right\} (b + h) 2 * \Delta t$

stored in the profile: $\rho c A * \Delta t$

whereby:

- t : time at the beginning of the time-interval considered[s]
- Δt : time interval[s]
- T : temperature of the steel at the beginning of the time interval considered[K]
- ΔT : increase of the temperature of the steel during Δt [K]
- ρ : specific mass of steel ($= 7850 \text{ kg/m}^3$)
- c : specific heat of steel ($= 510 \text{ J/kg} * \text{K}$)
- A : contents of steel per unit-length [m^{-3}]

The assumption which is made is that the heat-flux is always perpendicular to the steel profile.

The application of the heat balance equation gives:

$$a q_i h * \Delta t - \left\{ \epsilon \sigma (T)^4 + \alpha (T - T_0) \right\} (b + h) 2 * \Delta t = \rho c A * \Delta t \quad (\text{C.1})$$

With some approximation with $s_i = h$ en $s_u = 2 (b + h)$, we find:

$$\Delta T = \frac{s_i}{\rho c A} \left[a q_i - \frac{s_u}{s_i} \left\{ \epsilon \sigma (T)^4 + \alpha (T - T_0) \right\} \right] * \Delta t \quad (\text{C.2})$$

With the help of (C.2), the variation of the steel temperature with time can be calculated. For practical reasons, this calculation should be handled with the help of a computer.

Nothing that for a glass panel subjected to a one-sided radiation we have:

$$s_u = 2 s_i$$

and

$$A/s_i = d \text{ (= panel thickness)}$$

With this (C.2) transforms into :

$$\Delta\gamma = \frac{1}{\rho c d} \left[a q_i - 2 \left\{ \epsilon \sigma (T)^4 + \alpha (T - T_0) \right\} \right] \Delta t \quad (C.3)$$

Substituting ρ and C by the values applicable to glass (respectively 2600 kg/m^3 and $840 \text{ J/kg} \cdot \text{K}$), we can now, with the help of (C.3), calculate the temperature variations in a glass panel subjected to a one-sided radiation.

Taking a realistic glass-panel thickness of $d = 5 \text{ mm}$, the temperature variation in the glass is calculated (in Figure C.1), taking as point of departure the critical radiation intensity determined in Paragraph 7.3.4 of $\approx 4 \text{ kW/m}^2$. As expected, the temperature in the glass approaches a fixed value of about 393 K . This last value is theoretically reached after an endless long time. However, the value after already 10 minutes deviates from this end value by less than 10%.

Results of similar calculations are presented in Figure C.2, in this case, however, valid for the heat radiation on steel profiles. Practical column profiles have been chosen for these calculations, (HE 200B, with radiation to its flanges) and a much used in practice IPE 120 profile, with radiation to its body. The above for the critical radiation intensity of 100 kW/m^2 , as per Paragraph 7.3.5. After about 20 minutes, the temperature in the steel deviates less than 10% from the end-value ($\approx 773 \text{ K}$).

In Figure C.3 the temperature variation is shown, for the same two profiles, for a critical radiation intensity of 25 kW/m^2 (= damage level 2). This shows that, for the relatively heavy HE 200B profile, a relatively long time is required until the temperature comes near to the value of 473 K .

Note:

For a given radiation intensity the **end-temperature**, in a steel profile, is dependent on the material which has been used. In the figures below, the theoretical end-temperature is shown for only one steel-profile.

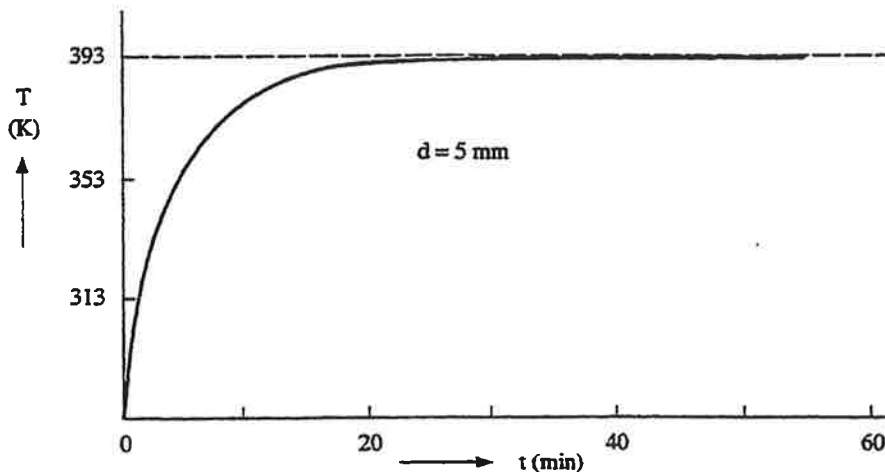


Fig. C.1 Temperature variation in a glass-panel ($q_i = 4 \text{ kW m}^{-2}$)

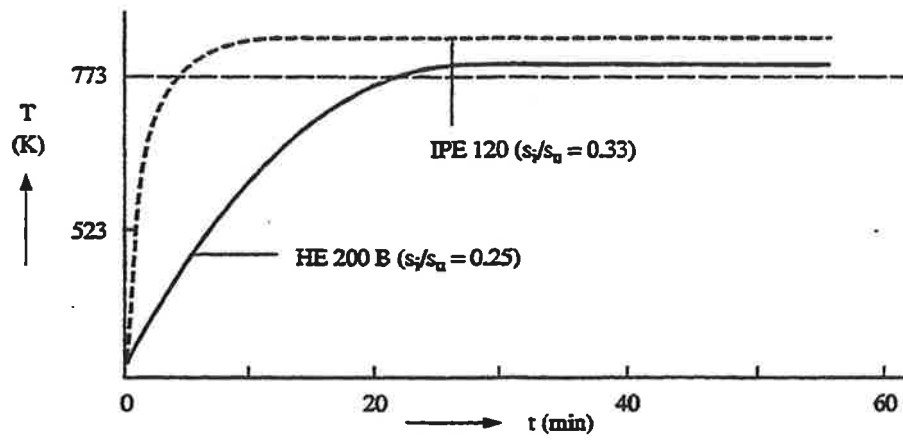


Fig. C.2 Temperature variations in two steel I-profiles ($q_i = 100 \text{ kW m}^{-2}$)

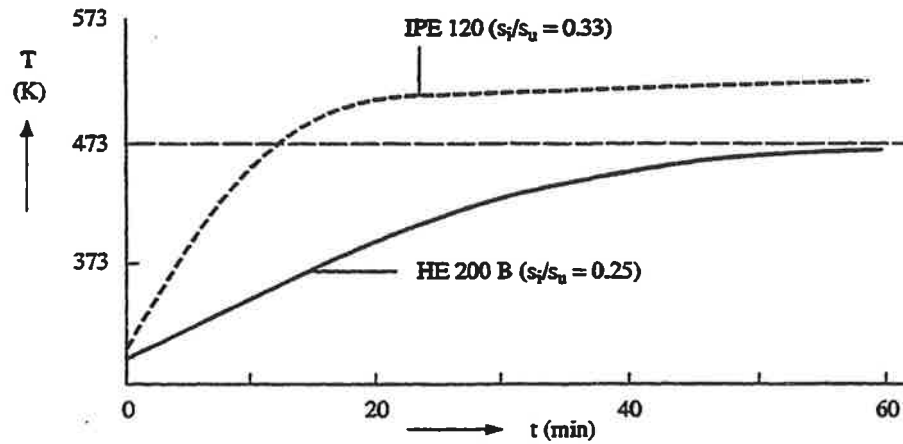


Fig. C.3 Temperature variations in two steel I-profiles ($q_i = 25 \text{ kW m}^{-2}$)

Chapter 2

The consequences of explosion effects on structures

Summary

In this report a method is given with which the effect of blast on structures can be determined. The phenomenon of blast and the interaction between blast and a structure are examined. The load on a structure is determined. Schematization of the structure to a single-degree of freedom system makes it possible to determine the dynamic response resulting from this load. If the static strength, the ductility ratio and the natural frequency of the structure are known the possible damage can be determined. Besides this analytical approach, also an empirical pressure-impulse diagram is presented with which the damage can be determined. A method to calculate the strength of window panes is presented. Probit functions are derived with which the probability of a defined damage level can be calculated. Examples are given to illustrate the determination of the parameters required.

Contents

	Page
List of symbols used	6
1. Introduction	8
1.1 Identification chart	8
2. Blast	11
3. Interaction between blast and structure	13
3.1 Reflection	14
3.2 Dynamic pressure	15
3.3 Load on a reflective surface	16
3.4 Load on a structure	17
3.5 Example	18
4. Structural response	21
4.1 Dynamic load	21
4.2 Schematic representation of a structure	22
4.2.1 Single-degree of freedom system	23
4.2.2 Natural frequency	23
4.2.3 Spring characteristic	24
4.3 Maximum displacement, dynamic load factor	25
4.4 Pressure impulse diagrams for structures	26
5. Determination of values required	30
5.1 Static strength	30
5.1.1 Safety factors	30
5.1.2 Wind load	31
5.2 Natural frequency	34
5.2.1 Empirical formulae	35
5.2.2 Raleigh method	36
5.2.3 Determination of the natural frequency from the static load	36
5.2.4 Example	37
5.3 Ductility	39
6. Glass	41
6.1 Method for determining the strength of window-panes	41
6.2 Examples	43
7. Damage criteria	45
7.1 Empirical data	45
7.2 Damage criteria and probit functions	48
7.2.1 Houses	48
7.2.2 Industrial installations	50

7.2.3	Window breakage	50
7.3	Examples	50
8.	Conclusions and recommendations	56
	References	57
	Appendix I: Single-degree of freedom system	60
	Appendix II: Raleigh method	65
	Appendix III: Comparison of Jarrett's damage criteria with real-scale experiments	68
	Appendix IV: Probit functions	70
	Appendix V: Accuracy of models for determining the explosion effects on structures	74

List of symbols used

A	: area	$[m^2]$
A_i	: internal work	$[J]$
A_k	: cross-section of column	$[m^2]$
A_1	: cross-section of girder	$[m^2]$
A_u	: external work	$[J]$
a	: dimension	$[m]$
B	: width	$[m]$
B_k	: distance between columns (column interval)	$[m]$
b	: dimension	$[m]$
C, C_1, C_2	: constants	$[-]$
C_D	: drag coefficient	$[-]$
C_p	: specific heat at constant pressure	$[J \cdot kg^{-1} \cdot K^{-1}]$
C_v	: specific heat at constant volume	$[J \cdot kg^{-1} \cdot K^{-1}]$
C_w	: wind coefficient	$[-]$
c_o	: speed of sound at atmospheric pressure	$[m \cdot s^{-1}]$
DLF	: dynamic load factor	$[-]$
D_u	: ductility	$[-]$
d	: plate thickness	$[m]$
E	: Young's modulus	$[Pa]$
E_k	: kinetic energy	$[J]$
E_p	: potential energy	$[J]$
F_b	: force	$[N]$
F_v	: spring-force	$[N]$
f	: frequency	$[Hz]$
f_t	: tensile strength	$[Pa]$
$f_o(x)$: deflection at unit load	$[m]$
g	: acceleration of gravity	$[m \cdot s^{-2}]$
H	: height	$[m]$
h	: storey height	$[m]$
I	: moment of inertia	$[m^4]$
I_k	: moment of inertia of column	$[m^4]$
i	: impulse per unit area	$[Pa \cdot s]$
i_r	: positive impulse of the reflected blast	$[Pa \cdot s]$
i_s	: positive impulse of the side-on blast	$[Pa \cdot s]$
K	: spring constant	$[N \cdot m^{-1}]$
k_i	: constant	$[Hz \cdot m^{-3/4}], [Hz \cdot m^{-1}], [Hz \cdot m^{-1/2}]$
L	: depth	$[m]$
l	: girder length	$[m]$
M	: mass	$[kg]$
M_{st}	: static absorbable moment	$[Nm \cdot m^{-1}]$
M_w	: moment due to wind load	$[Nm \cdot m^{-1}]$
m	: mass per unit-length or unit-area	$[kg \cdot m^{-1}], [kg \cdot m^{-2}]$
n	: number of storeys	$[-]$
P	: load per unit-area	$[Pa]$
Pr	: probit	$[-]$
P_r	: reflected peak overpressure	$[Pa]$

P_s	: side-on peak overpressure	[Pa]
P_{st}	: static absorbable load	[Pa]
P_{eg}	: load due to own weight	[Pa]
P_o	: atmospheric pressure	[Pa]
P_s	: absolute pressure	[Pa]
P_w	: wind load	[Pa]
Q	: load by air particles	[Pa]
Q_D	: dynamic pressure	[Pa]
q	: uniformly distributed load	[Pa]
q_w	: stagnation pressure due to wind	[Pa]
rk	: reflection coefficient	[-]
S	: total impulse	[N · s]
S	: dimension	[m]
T	: natural period of vibration	[s]
t	: time	[s]
t_p	: duration of positive phase	[s]
t_s	: running time of relieving wave	[s]
t_o, t_1	: time stages	[s]
U	: velocity of shock wave	[m · s ⁻¹]
u_s	: velocity of air particles	[m · s ⁻¹]
V	: variable	[-]
w	: deflection	[m]
x	: coordinate, displacement	[m]
x_{el}	: elastic displacement	[m]
x_r	: residual displacement	[m]
x_{st}	: static displacement	[m]
\ddot{x}	: acceleration	[m · s ⁻²]
y	: coordinate	[m]
α_i	: angle of incidence	[°]
B	: safety coefficient	[-]
γ	: ratio C_p/C_v	[-]
δ	: deflection	[m]
Σ	: summation symbol	[-]
η	: correction factor	[-]
ν	: Poisson's modulus	[-]
ρ	: specific mass	[kg · m ⁻³]
ρ_s	: air density	[kg · m ⁻³]
σ	: stress (tension)	[Pa]
ω	: angular frequency	[s ⁻¹]
ω_o	: tensile reinforcement percentage	[-]
ω_o'	: compressive reinforcement percentage	[-]

Superscripts:

\bar{x}	: scaled x
\hat{x}	: maximum value of x
x'	: limit value of x

Introduction

This report presents a method to determine the damages to structures caused by an explosion.

An explosion causes a number of effects. The explosive material or mixture converts itself, practically instantaneously, into reaction products with very high temperature and pressure. A shock or pressure wave develops in the surroundings, which is most of the times referred to as blast. This blast moves at supersonic speed through the surrounding air. At the same time, pressure is exerted on the soil, generating a ground shock, which moves through the ground. This pressure can be so high that a crater may form. If the explosion takes place inside a building, debris (fragments) will fly at high velocity. Due to their impact and due to blast, other breakages and consequent other debris will appear.

Not all of the effects may be present at every possible explosion. The blast and the flying fragments are the ones which are mainly important for the determination of the damages caused to structures. A lot of investigations have been carried out with regards to the quantification of blast and to consequences of a blast loading. Not much is known with regards to consequences of the impact of flying fragments. Investigations of the size, distribution, density of these fragments as well as of the distances they may cover, have only been initiated during the last few years. Also statistical data: registration and analysis of explosions only provide very summary data, insufficient for an accurate determination of the damages.

1.1

Identification Chart

An identification chart is given in Figure 1. With its help, the determination of damages to structures caused by an explosion are illustrated. The numbers, in the diagram, refer to the appropriate explanations.

Ad. 1 The effects which can produce damages to structures which are not located in the immediate vicinity of the explosion are blast and flying fragments. Data regarding the impact of flying fragments are so insufficient that no calculation procedure of its consequences can be provided.

Ad. 2 The blast parameters are dependent on the distance between a structure and the centre of the blast. A determination of the values of such distances is not presented in this report. The known design assumptions are: shape of the shock wave, side-on, or incident peak overpressure P_s and positive phase duration t_p (determined, for example, using [30]). A schematic representation of the blast is given in Chapter 2.

Ad. 3 Methods allowing to determine damages due to blast are indicated for different types of structures.

Ad. 4a For buildings, apart from window breakage, three other damage levels can be differentiated. Descriptions of the degrees of damage corresponding to these levels are given in Chapter 7.

Ad. 4b Data about damages which have been caused to industrial installations are very limited. A general sub-division into damage levels is not given. Industrial buildings can be placed as belonging to structures type 1 or structures type 2. A global classification into damage levels is given in Table 5 of Chapter 7.

Ad. 5 In the determination of collapse probabilities different types of buildings can be differentiated. The empirical pressure-impulse diagram given in Chapter 7 is only developed for houses lower than 4 floors.

The probability of collapse of buildings higher than 4 floors can be determined by a schematic treatment of the structure as a single-degree of freedom system. A closer look at this procedure is given in Chapter 4.

Ad. 6 Determination of the strength of glass is more closely analyzed in Chapter 6. On the one hand, global values of pressures are indicated for which windows will normally fail. On the other hand, a method is also given which allows us to determine, for a given window, the static failure load. This value of the static strength is important in the determination of the dynamic strength. A procedure for this determination is given in Chapter 4.

Ad. 7 In order to calculate the damage using a single-degree of freedom procedure, data about the loading on the structure as well as information about the structure itself must be known. In Chapter 3 a closer analysis is conducted regarding the blast-structure interaction, whereby concepts such as overpressure and reflection must be introduced. Also a quantifying procedure for the blast loading on the structure is given in Chapter 3. Determination of data (information) about the structure itself is presented in Chapter 5. The data required are: natural frequency, ductility and static strength in the direction of the blast load.

Ad. 8 When the necessary data are available, it will be then possible, using the criteria outlined in Chapter 7, to get an idea about the type of damage to be expected.

An empirical pressure-impulse diagram is presented for the determination of the following damage levels: minor damage, major structural damage and collapse. In the same time, probit functions have been derived which permit us to estimate the probability corresponding to a given damage level.

In Chapter 4, two analytically derived pressure-impulse diagrams are presented. Dependent on the shape of the blast wave (shock wave or pressure wave), one or the other will be suitable for the calculation of the dynamic resistance of structures or structural elements, such as walls and windows.

A table is given in Chapter 7, in which damages which appeared in structural elements of industrial structures are shown, for given corresponding pressures.

In order to estimate the probability of a given degree of damage probit functions have been derived. These functions are assembled in Chapter 7.

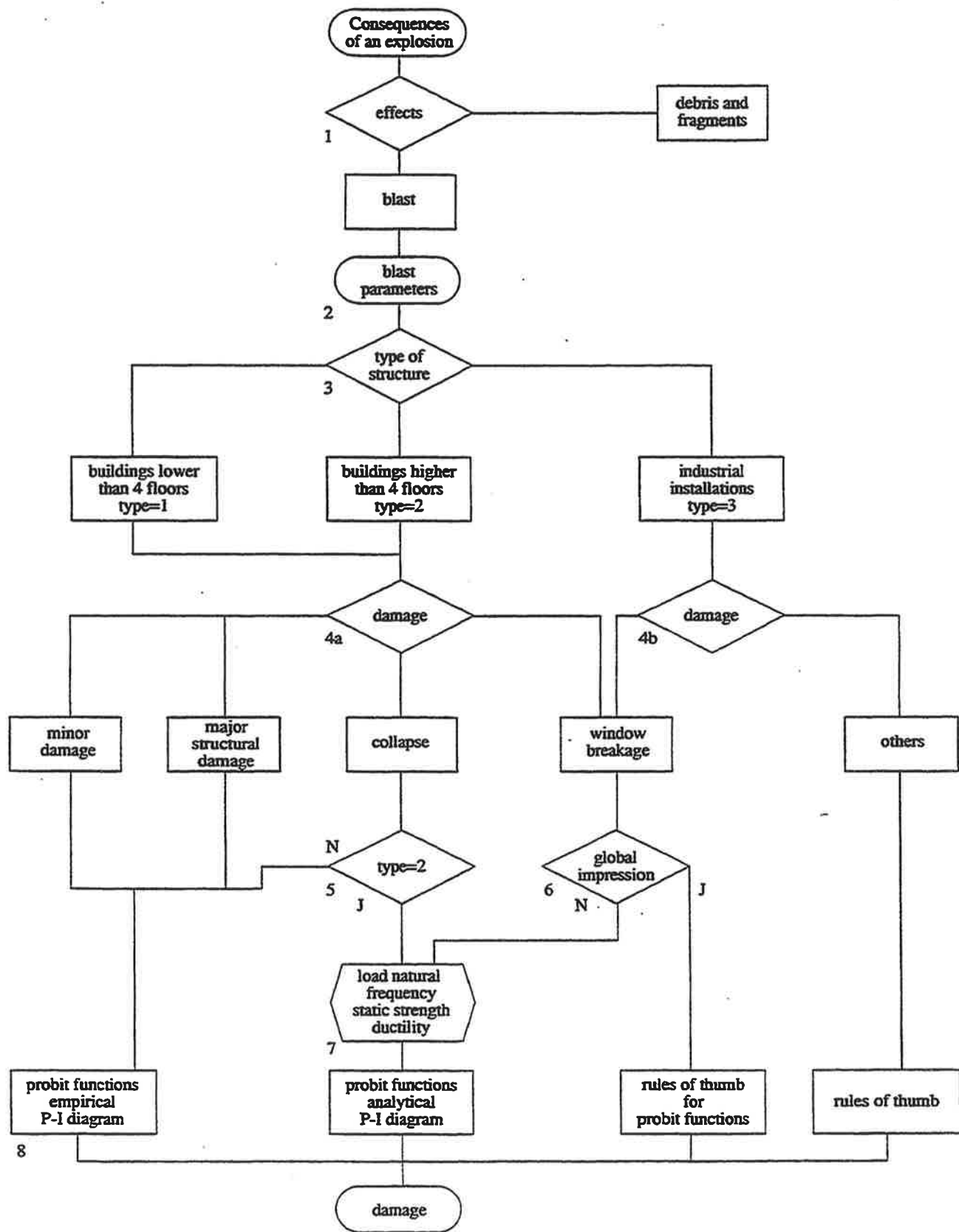


Fig. 1 Identification Chart.

2

Blast

One of the effects of an explosion is a sudden pressure rise. This pressure rise will move, in the form of a wave, from the center of the explosion. The shape of this wave depends on the magnitude of the explosion and on the distance to the center of the explosion.

Explosions are differentiated between deflagrations and detonations. In case of a gas explosion, a deflagration usually takes place. A source of ignition will provoke a flame front in the gas cloud, due to which the temperature will rise very quickly and, in view of the expansion of the gases, a pressure build-up will take place. The maximum pressure will be reached after a certain time, the so-called rise time.

The characteristic shape of the pressure build-up due to a deflagration is also called the pressure-wave. Figure 2b shows a typical example of it. The shape and rise time of the pressure wave depend on the deflagration process itself.

A detonation is mainly due to the explosion of condensed explosives, but can also develop in case of a very powerful gas explosion. The pressure rise is practically instantaneous, thus without a rise time. Figure 2a shows a typical example of the shape of the air shock following a detonation. This shape is also called the shock wave. Shock waves and pressure waves are jointly called blast.

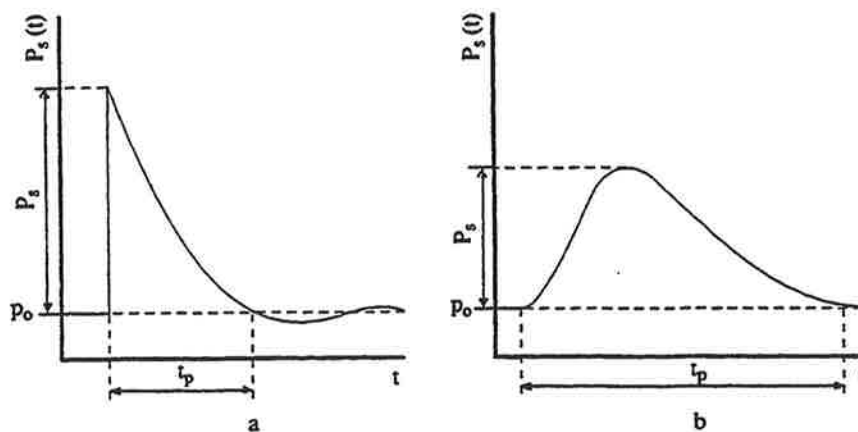


Fig. 2 Characteristic shape of the variation with time of:
a) a shock wave b) a pressure wave

By a shock or pressure wave, the maximum pressure rise, the peak overpressure P_s , will, following a determined path, decrease to zero within a given time. For a shock front this time duration is called the "positive phase duration", called t_p . After this time, a time period with negative pressure takes place. The maximum value of this negative pressure does not normally play any important role, since this negative pressure is relatively gradual and its maximum value is generally low as compared to the peak overpressure. For these reasons, this negative phase is often disregarded.

The velocity U with which the front of the shock-wave runs dependent upon the peak overpressure P_s . For small values of P_s this velocity is equal to the velocity of sound through air (± 340 m/s). As the distance to the center of the explosion increases, the peak overpressure and the velocity of the shock-front decrease.

Besides the all-sided overpressure in a shock-or pressure wave, another noticeable phenomenon is the air displacement which, for an undisturbed wave, moves in the same direction as the wave front. The velocity of the air particles u_s is also dependent on the overpressure in the blast wave.

The maximum overpressure, by a pressure wave, does not appear at the location of the wave front. The air particles behind the wave front have, thereby, a higher velocity than the particles within the front. Due to this after a certain time, the pressure wave transforms itself into a shock wave (steepening).

Apart from the peak overpressure and phase-duration, the pressure or shock waves are also characterized by the so-called positive "impulse", i_s or short way impulse. This is defined as the area under the time-pressure diagram as follows:

$$i_s = \int_{t_p} P_s(t) dt \quad (1)$$

A very common simplification of the shape of the time-pressure diagram of a shock or pressure wave consists in approximating the pressure variation by a straight line, as shown in Figure 3.

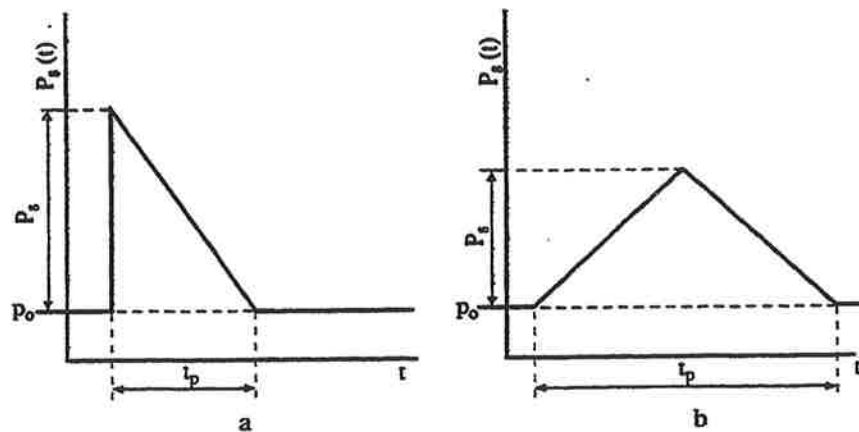


Fig. 3 Schematic representation of the pressure-time diagram
a) for a shock wave b) for a pressure wave.

The important properties, for the blast, are thus:

- The shape: shock or pressure wave
- The peak overpressure P_s
- The positive phase duration t_p
- The impulse, in both cases equal to:

$$i_s = \frac{1}{2} \cdot P_s \cdot t_p \quad (2)$$

In what follows in this report, the schematic representations of the blast shown in Figure 3 will be retained.

Interaction between blast and structure

When the blast meets a structure or, more generally, an obstacle, then is this blast locally disturbed. In view of this disturbance, the loading on the obstacle is not equal to the time-pressure path of the undisturbed blast, but takes a more complex form which is dependent on the size and the shape of the structure.

Figure 4 shows, schematically, in which way the blast load acts on a structure. Four stages are differentiated in this figure.

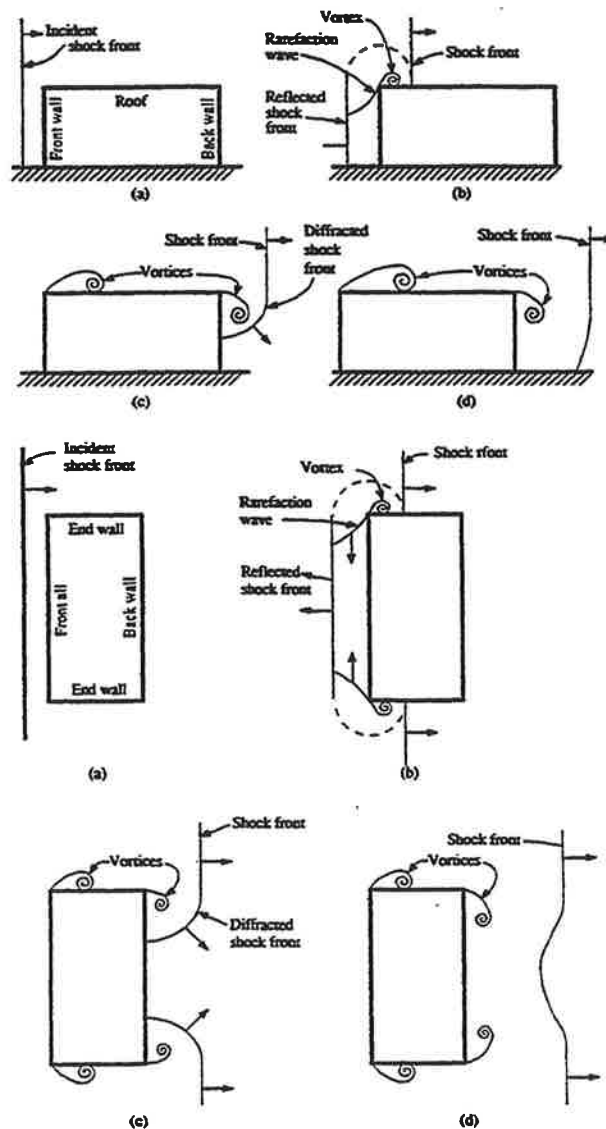


Fig. 4 Schematic representation of the disturbance of the blast caused by a structure. Taken from [18].

a: The wave front is still in front of the structure and is not yet disturbed.

b: The wave front has reached the structure. Reflection takes place and a rarefaction wave is formed.

c: The blast envelops the structure.

d: Situation whereby the wave-front has passed the structure.

The blast-wave, initially, reflects against the structure, and the reflected wave begins to move in a direction opposite to the incident wave. The surface on which the incident wave is reflected becomes loaded by an overpressure P_r of the reflected wave which is higher than the peak overpressure P_s of the incident wave.

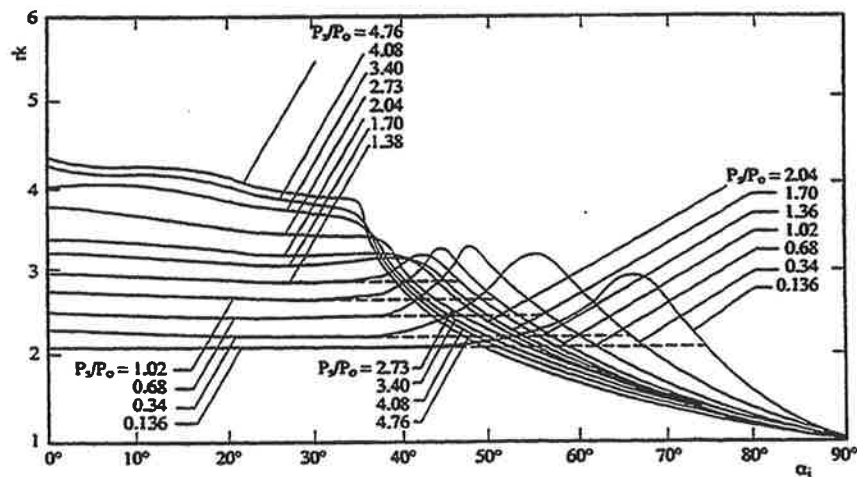
The ratio between the reflected and the incident overpressure is called the reflection coefficient:

$$rk = \frac{P_r}{P_s} \quad (3)$$

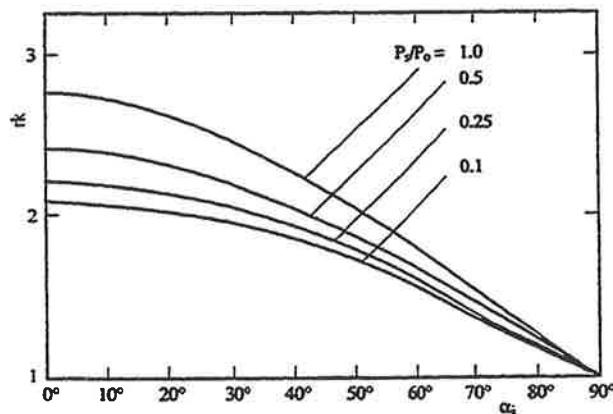
The value of this coefficient is dependent on:

- The angle of incidence α_i of the wave-front on the reflecting surface. This angle varies from 0° for a perpendicular reflection to 90° for a parallel wave.
- The overpressure. If the overpressure is low compared to the atmospheric pressure p_0 , then the reflection coefficient depends on the value of this overpressure. By increasing overpressures the reflection coefficient increases.
- The wave type. A shock wave behaves differently, from a reflection view-point, from a pressure wave.

The values of the reflection coefficients for different values of the overpressure, as functions of the angle of incidence, are given in Figure 5.



a: Shock wave



b: Pressure wave

Fig. 5 The reflection coefficient, as function of the angle of incidence α_i , for different values of P_s . Taken from [1].

The perpendicularly reflected overpressure due to a shock-wave can be expressed by the following formula:

$$P_r = 2 * P_s + \frac{(\gamma + 1) * P_s^2}{(\gamma - 1) * P_s + 2 * \gamma * p_o} \quad (4)$$

Whereby γ is the ratio between the specific heat by constant pressure C_p and the specific heat by constant volume C_v . If we retain, for air, a value of $\gamma = 1.4$, then formula (4) gives a reflection factor of two for low overpressures, while for high pressures it gives a limit value of eight.

Since by high pressures, the value of γ no longer remains constant, we cannot determine an upper limit of the reflection factor, in these cases, from formula (4).

According to [2], certain sources report maximum values up to twenty.

Considering reflection factors it would appear that, for shock waves (Figure 5a), the reflected pressure, for certain angles of incidence, is higher than for the perpendicular reflection. These higher values of the reflection factor seem to have arisen from theoretical calculations. Test results [35] and [36] do not support the existence of these theoretical peaks, and that despite attempts to find them. For the simplicity of calculations, therefore, the values shown in dotted lines in Figure 5a can be used for the determination of the reflection factors, such as also suggested in reference [37].

3.2 Dynamic Pressure

It has been mentioned in Chapter 2, that apart from a pressure rise, blast is also accompanied by an air displacement in the direction of the blast-wave. This air displacement, also sometimes called explosion wind, produces an extra loading on a reflective surface.

The pressure Q consequent to the air displacement is given by the following formula:

$$Q(t) = 1/2 * \rho_s * u_s(t)^2 \quad (5)$$

whereby:

ρ_s : the air density within the blast ($\text{kg} \cdot \text{m}^{-3}$)

and

$u_s(t)$: the velocity of the air particles ($\text{m} \cdot \text{s}^{-1}$)

This pressure Q can also simply be expressed in terms of the pressure P_s as follows:










$$Q = \frac{5}{2} * \frac{P_s^2}{7 * p_o + P_s} \quad (6)$$

The dynamic pressure Q_D on a structure is equal to :

$$Q_D = C_D * Q \quad (7)$$

Whereby C_D is the so-called "drag" coefficient, which is dependent on the shape of the structure. In Table I, values of C_D are given for various structural shapes.

Table 1. Coefficients C_D . Taken from [2]

Shape	Figure	C_D
Long Straight Cylinder		1.20
Sphere		0.47
Cylinder		0.82
Disc		1.17
Cube		1.05
Cube		0.80
Oblong Box		2.05
Oblong Box		1.55
Strip		1.98

3.3

Load on a Reflective Surface

Due to the disturbance of the incident wave caused by an obstacle, major pressure differences develop at the edges of a reflecting surface.

As a consequence, a rarefaction wave begins to progress, from the edges, on the surface on which reflection takes place (Figure 4).

Due to this rarefaction wave, the pressure on the surface of the reflected pressure decreases to a value equal to the pressure exerted, at that moment, by the incident wave at a given location plus the dynamic pressure.

The loading on a finite reflective surface can then be determined with the help of the reflection and dynamic pressure values. An example of the loading on a reflective surface due to a shock wave is given in Figure 6. The pressure decrease, for simplicity, is represented schematically by straight lines.

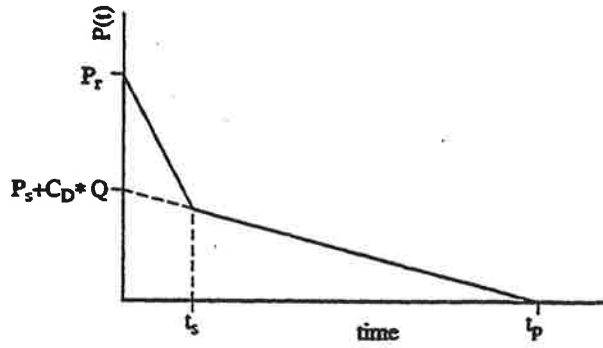


Fig. 6 Schematic representation of the time-pressure diagram for a finite reflective surface.

The time t_s at which the reflected pressure decreases to the incident plus the dynamic pressure is calculated as follows:

$$t_s = \frac{3 * S}{U} \quad (\text{from [1]}) \quad (8)$$

in which U is the velocity of the wave-front and S a characteristic dimension of the surface. The velocity U is determined by:

$$U = c_o \sqrt{1 + \frac{6 * P_s}{7 * p_o}} \quad (9)$$

in which c_o is the velocity of sound in air (± 340 m/s). For the front of a building with height H and width B , we must take, for S , the smallest of the values: H or $1/2 B$.

Equation (8) is taken from [1] and according to this reference, is in good agreement with test results.

A rarefaction wave will also develop in case of an incident pressure wave. In view of the progressive build-up of pressure corresponding to an incident pressure wave, the reflected pressure acting on a finite surface will be in fact, so much relieved that the resulting pressure will not be higher than the incident overpressure plus the dynamic pressure.

3.4

Load on a Structure

By interaction between the blast wave and a certain type of structure, we can differentiate between three extreme conditions, see Figure 7.

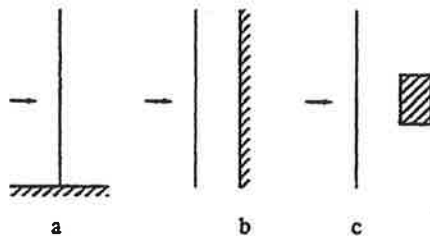


Fig. 7 Extreme loading conditions.

In case a the blast wave runs over, a large surface, without impediment and the load on this surface is then equal to the overpressure of the incident wave.

In case b the blast wave collides perpendicularly with a surface of very large dimensions, so that the rarefaction from the edges does not play any role. In this case the load on the surface is equal to the overpressure in the reflected blast wave. In case c we are dealing with an object with small dimensions. The rarefaction then, progresses so quickly that reflection does not have to be considered. Furthermore, the difference between the pressures on the front part and on the back part is so small that the load only consists of the dynamic pressure.

From a general view-point, in most structures a combination of these three cases of loading must be considered. In ref. [2, 13, 18] the determination of the loading on various types of structural shapes is discussed in detail. In this report, we will limit ourselves to the load on a closed box type structure with dimensions H , B and L , as shown on Figure 4.

The load on the front face is determined in accordance with the procedure outlined in 3.3. The load on all other faces: roof, sides and backface varies, not only as a function of time but also as a function of the location (strictly speaking, the load on the front face also varies with location, due to the rarefaction wave). In general, however, the blast passes the structure so quickly that this variation of the load with location can be disregarded. For the loading on such surfaces, consequently, we can retain the time-pressure diagram of the incident blast-wave.

For the structural framing of a building, for example, the propagation velocity of the blast wave is, on the other hand, important. During the time span $t = L/U$ required for the blast wave to reach the back face, the horizontal load exerted on the structural framing is high. After this time, an opposite load of small magnitude will be acting on the back-face. The time span required for this loading on the back face to reach its maximum is assumed to be equal to $t = 4 * S/U$. The horizontal load on a structural framework is schematically represented in Figure 8.

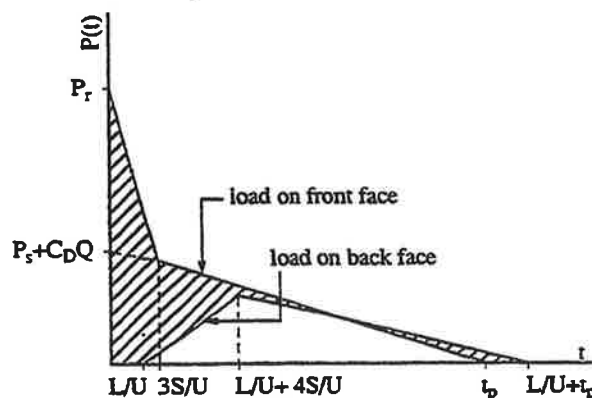


Fig. 8 Schematic representation of the horizontal load on the structural framing of a closed building.

If there is a possibility that, during the incident phase, an overpressure develops inside the structure, for instance if the outer face is partially open, this will then compensate the external pressure. If there are relatively many openings in the front wall, for instance due to the breakage of the windows, the blast can then traverse the structure and, consequently, the back wall may receive the reflected pressure loading. For spherical or cylindrical types of structures the angle of incidence of the blast wave is different in every location. The reflected peak overpressure, for every location, can then be determined with the help of Figure 5.

3.5

Example

The loading due to a shock wave, with $P_s = 0.5 * 10^5$ Pa and $t_p = 200$ ms, acting perpendicularly on the front face of a building will be calculated. The building dimensions are: $H \times B \times L = 30 \times 20 \times 10$ m.

From (4) we obtain :

$$P_r = 2 * 0.5 * 10^5 + \frac{2.4 * (0.5 * 10^5)^2}{0.4 * 0.5 * 10^5 + 1.4 * 10^5} = 1.3 * 10^5 Pa$$

From (6) :

$$Q = \frac{5}{2} * \frac{(0.5 * 10^5)^2}{7 * 10^5 + 0.5 * 10^5} = 8.3 * 10^3 Pa$$

Table I gives $C_D = 1.05$, so that, according to (7) :

$$Q_D = 1.05 * Q = 8.75 * 10^3 Pa$$

From (9) we obtain :

$$U = 340 \sqrt{1 + \frac{6 * 0.5 * 10^5}{7 * 10^5}} = 406 \text{ m/s}$$

Substituting this value in (8) :

$$t_s = \frac{3 * \frac{20}{2}}{406} = 0,074 \text{ s}$$

Time required to reach the back face :

$$L/U = \frac{10}{406} = 0,025 \text{ s}$$

Time required to reach the maximum pressure on the back face :

$$\frac{4 * S}{U} = \frac{4 * \frac{20}{2}}{406} = 0.099 \text{ s}$$

If we retain the schematic representation of Figure 8, then the loading on the structural framing of the building will be as shown in Figure 9:

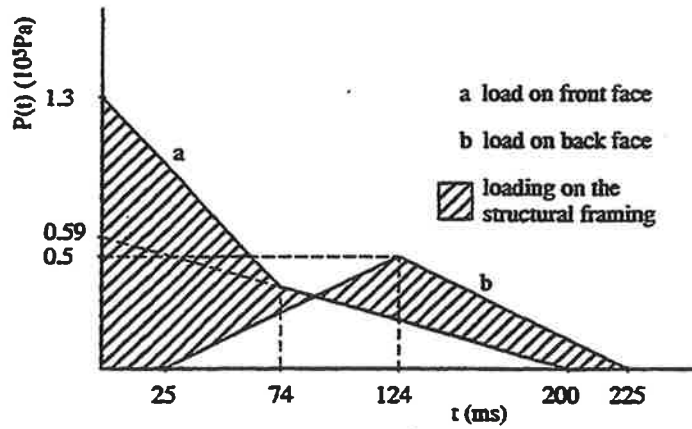


Fig. 9 Load on a building with $H \times L \times B = 30 \times 10 \times 20 \text{ m}^3$ due a shock-wave with $P_s = 0.5 \times 10^5 \text{ Pa}$ and $t_p = 200 \text{ ms}$.

Assuming that the building has a tapered roof which makes an angle of 30° with the horizontal, then the angle of incidence of the incident wave is equal to 60° . The reflected pressure on the roof is then determined from Figure 5 for:

$$\frac{P_s}{P_o} = 0.5$$

which gives $rk = 2.1$, with which $P_{r(\text{roof})} = 1.05 \times 10^5 \text{ Pa}$.

The pressure on the lee side of the roof, similarly to the back face and side faces, will be equal to the overpressure of the incident blast-wave and will have a value of $0.5 \times 10^5 \text{ Pa}$.

4

Structural response

Structures which are loaded, one way or another, deform. The manner in which these deformations take place, as well as their values, depend not only on the loading but also on the properties of the structure. These properties are determined, in turn, by the properties of the materials used for the different structural components as well as on the manner in which these components are put together.

If a structure is loaded by a transient load, it will then react to this variation of the loading by deforming differently. Structures can also vibrate, phenomenon whereby their own periods of vibration play an important role. The types of loads considered here, coming from an explosion, can be very large in comparison with the loads which the structure is calculated to withstand under normal conditions. The probability that a given structure during its life-time, will be subjected to a loading due to an explosion, is small. It is therefore often not economical to design a structure for this type of load. Consequently, it is possible to accept, in practice, a certain degree of damage, in the form of a permanently remaining deflection, when dealing with such exceptional load conditions. A property of the structure which, in this respect, plays a role is its ductility. Ductility provides a measure for this permanently remaining deflection.

In order to be able to determine the response of a structure in the form of deflections produced by external loads, a certain degree of schematization is necessary. Very simple schematizations will not require a lot of calculation work, but they will lead, in turn, to only global and limited information. Lesser degrees of schematization will probably provide more data, but they, in turn, will require the use of very advanced computational techniques.

4.1

Dynamic Load

In case a load is present during a long time without changing, or if it changes only very slowly, we are then dealing with a static load. The deflections which take place develop internal forces in the structure. These internal forces are then in equilibrium with the load which is present. However, if the load varies very quickly with time (or location), then the mass and the stiffness of the structure play a role in the distribution of the internal forces in it. The internal forces are then in balance with the load which is acting jointly with the mass inertia-forces. The latter develop due to the fact that the structure has been set into movement. In these conditions we are dealing with a dynamic load.

The following example illustrates the difference between static and dynamic loads. A mass M is loaded by a load F_b and is supported by a force F_v .

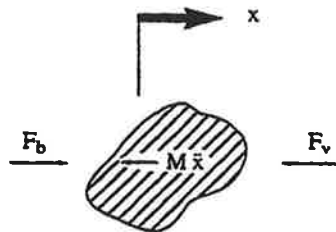


Fig. 10 Forces acting on a body.

The supporting force F_v provides the resistance required to prevent the mass M to displace. In general, for a state of equilibrium in accordance with Newton's law, we have:

$$F_b = F_v + M * \ddot{x} \quad (10)$$

whereby x represents the acceleration of the mass M . In case of a static load, eventual movements and deflections are so slow, that the acceleration is equal to zero. Consequently:

$$\text{Static : } F_b = F_v \quad (11)$$

In case of a dynamic load the acceleration no longer can be neglected and, consequently, we then have, generally:

$$\text{Dynamic : } F_b \neq F_v \quad (12)$$

There is then a dynamic equilibrium between the forces and the inertia of the mass.

4.2

Schematic Representation of a Structure

In order to be able to determine analytically the response of a structure, a schematic representation of the structure is necessary. This schematic representation consists, basically, of a system of masses concentrated at given points, coupled with springs which correspond to calculated spring factors of the structural elements. The damping of the structure can be taken into account by bringing into the model the required dampers. If a structure is split into n concentrated masses, we are then dealing with an n -mass-spring-system (n degrees of freedom system). A special case of it is a single-degree of freedom system (one mass-spring system), the simplest schematic representation of all. In such a system, the structure is represented by one concentrated mass, and one spring, sometimes a damper.

The determination of the structural response consists of setting up the equation of equilibrium for every mass. This leads to a system of n differential equations. The solution of this system of equations gives the spring forces and the displacements of all the masses.

For the determination of the response of simple geometrical systems, such as girders or floors, these systems can be represented, schematically, by beams and plates. The solution of the differential equation provides, then, continuous displacement and force diagrams. This type of schematic representation is called "continuous system".

It is also possible to split the structure into small elements with known properties. Proper connection conditions between these elements are then established. The number of equations which must be solved with this so-called procedure of finite elements can be so big that the use of computers becomes a necessity.

For the schematic representation of a structure subjected to an explosion loading, we will make use of the single-degree of freedom system. Since the duration of the loading is normally very short, the maximum response of the structure will take place during the first vibration. Damping, at that moment, does not practically play any role. A more accurate schematic representation suggests a more accurate determination of the damage. However, since this determination of the damage can only be made in a global fashion, this more accurate procedure is not justified. Continuous systems for beams and plates are summarily treated in Annex II.

4.2.1

Single-Degree of Freedom System

This schematic representation of a structure is the most simplified system of all. The structure is represented by a single mass M and a single spring with spring stiffness K . In principle, the degree of freedom x can be taken at any arbitrary point of the structure. The most obvious choice is to take the point where maximum deflection is to be expected.

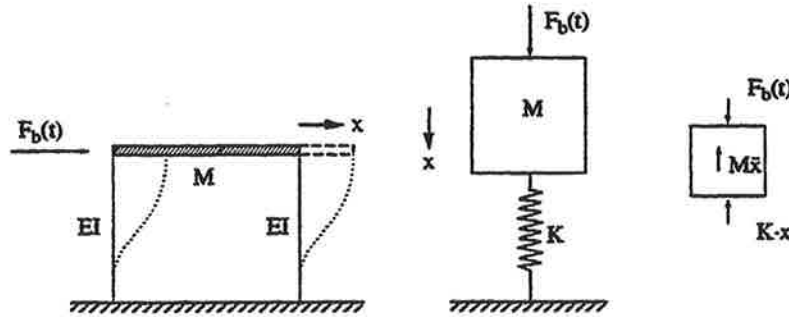


Fig. 11 Single-degree-of-freedom system.

The equation of equilibrium of a single-degree-of freedom system is identical to (10) and can be written as follows:

$$M \cdot \ddot{x} + K \cdot x = F_b(t) \quad (13)$$

The response of single-degree-of freedom systems to certain given load-time functions is given in Annex I.

4.2.2

Natural Frequency

The solution of equation (13) leads to a property of the system under consideration, namely the natural frequency. The natural frequency of a structure is the frequency with which the structure vibrates after it had been set into movement through a push (or induced displacement). In the case of such a free vibration, the load (right side of equation 13) is equal to zero.

The number of natural frequencies of a continuous system is, in principle, infinite. For a n -degree-of freedom system we have n natural frequencies. For a single-degree-of freedom system there is only one. In general, this will be the first and the lowest natural frequency.

It is shown, in Annex I, that the so-called angular velocity or, also angular frequency ω is determined by the relationship:

$$\omega = \sqrt{\frac{K}{M}} \quad (14)$$

The natural frequency f , which gives the number of vibrations per second, is related to the angular frequency as follows:

$$f = \frac{\omega}{2\pi} \quad (15)$$

The natural period of vibration T , which is the time required for the vibration to go through one complete cycle, (Figure 12) is equal to:

$$T = \frac{1}{f} \quad (16)$$

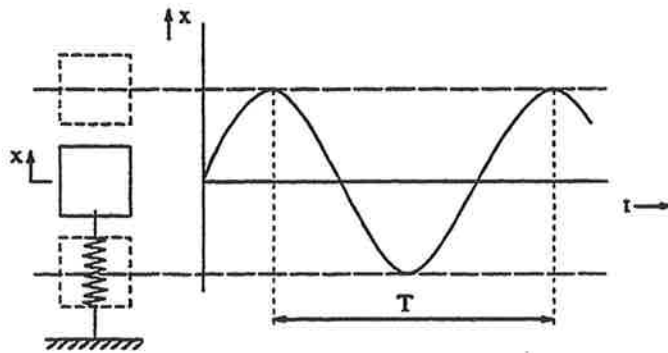


Fig. 12 Natural period of vibration.

4.2.3

Spring Properties

In the preceding paragraphs, a linear relationship was taken between the force acting on the spring F and the displacement x , according to:

$$F_v = K * x \quad (17)$$

whereby K represents the constant spring stiffness. When the load disappears, the force in the spring and the displacement become equal to zero. In such a case, we are dealing with a linear-elastic force – displacement relationship. This type, plus a few other relationships are represented in Figure 13.

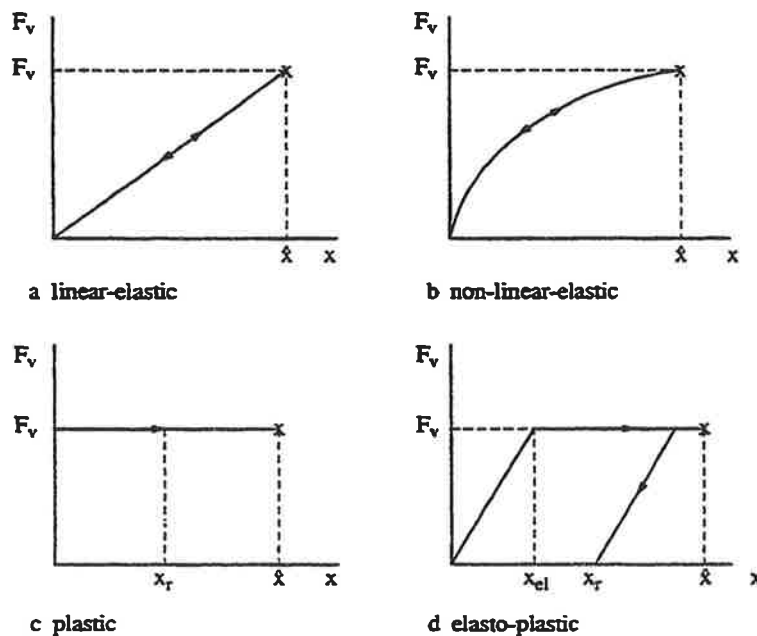


Fig. 13 Force-displacement relationships.

Displacement during plastic behaviour occurs when the force has reached its maximum value. If the loading is static, the structure fails in this condition. However, if the loading is dynamic and is of such short duration that it has disappeared before maximum displacement has been reached, the structure, then, does not fail, but retains a residual displacement x_r .

The majority of construction materials (concrete, wood, steel) exhibit a behaviour which can be idealized as elasto-plastic (Figure 13d).

Structures must also exhibit such type of behaviour. The passage from the elastic zone to the plastic zone cannot be, normally, so clearly defined as in the idealized model. In general, structures must be

designed to behave elastically under normal types of loadings such as: dead-loads, live-loads, wind-loads. Plastic displacements can be allowed only under exceptional loading conditions.

A measure of the maximum plastic displacement is the so-called ductility ratio:

$$D_u = \frac{\hat{x}}{\hat{x}_{el}} \quad (18)$$

which is the ratio between the maximum displacement and the maximum elastic displacement.

4.3

Maximum Displacement, Dynamic Load Factor

A dynamic calculation provides data about the manner in which a structure reacts to a dynamic load. Such type of calculation can easily require a lot of calculation work. Quite often, we only are interested in the values of the maximum forces and of the maximum displacements of a structure. In order to determine them in a simple fashion, the so-called "quasi-static" calculation procedure can be used. In this procedure, the maximum value of the dynamic loading is multiplied by a given factor, whereby it becomes possible to calculate the structure using statical design methods. This factor by which the maximum dynamic load must be multiplied is called the dynamic load factor (in abbreviation: DLF). The DLF is determined with the help of the dynamic response calculation of a single-degree-of-freedom system, and is primarily dependent on the duration of the dynamic loading. Values of the DLF are given in Figures 14 and 15 for a linear-elastic type of structure, for the two load schemes retained in this report: pressure wave and shock wave.

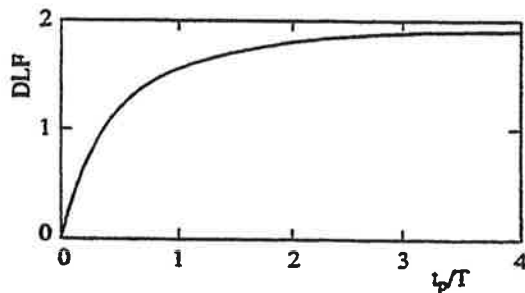


Fig. 14 Dynamic load factor for a shock wave.

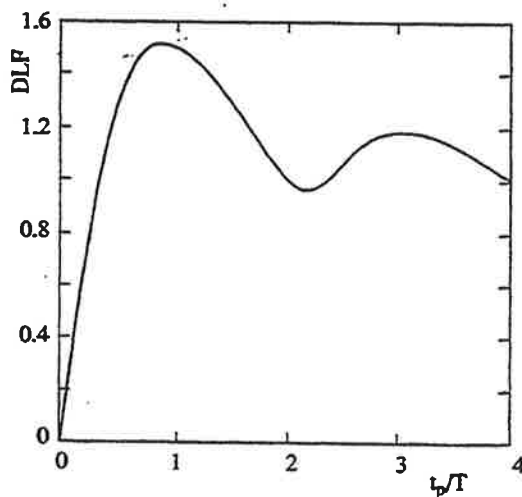


Fig. 15 Dynamic load factor for a pressure wave.

Some values of the DLF can be checked in a simple manner. For a positive phase of long duration, the shock wave transforms itself into a step function. This type of response is calculated in Annex I. The DLF, in this case, is equal to two. If the positive phase is very long by a pressure wave, the load, then, increases progressively; this loading is then static, so that the value of the DLF becomes equal to one. If the duration of the positive phase is short versus the natural period of vibration, the DLF becomes smaller than one: this means that the dynamic load the structure must withstand can be larger than the static load. For very short load durations, the form is less and less important in the determination of the response. The load, then, approaches an impulse-load.

For elasto-plastic behaviour of structures, the ductility also plays a role in the determination of the maximum displacement. In Reference [13] diagrams are given, for a number of load schemes, with which the maximum response can be determined. The diagrams for a pressure wave and for a shock wave are shown in Figures 16 and 17 taken from the above reference. These diagrams can be used in a number of different fashions:

If data about the load are known (peak overpressure and positive phase duration), we can find, from these diagrams, the required combinations of DLF and ductility which are necessary to prevent failure of a structural system.

If on the other hand, data about the structure are given (ductility, static strength), we can find, from these diagrams, what type of dynamic load the structure can withstand.

Finally, if all data are known, it permits us to obtain an impression about the safety (or lack thereof) of a given structure.

4.4

Pressure-Impulse Diagrams for Structures

The preceeding paragraphs have shown that, for the load schemes considered, two extreme cases must be differentiated: the step load and the impulse load. It is therefore logical, in the determination of the response of the structure, to also analyze the difference between these two extreme cases of load. To do this, it becomes necessary to convert the values given by Figures 16 and 17 into so-called pressure-impulse diagrams. This can be achieved using the expressions for the impulse i and the angular frequency ω .

The results are shown in Figures 18 and 19, respectively for a pressure wave and a shock wave, for values of the ductility between 1.5 and 10.

In these figures the scaled values of the impulse and the scaled values of the pressure are set-up along the axes, as follows:

$$\bar{i} = \frac{i * \omega}{P_{st}} \quad (19)$$

and

$$\bar{P} = \frac{P}{P_{st}} \quad (20)$$

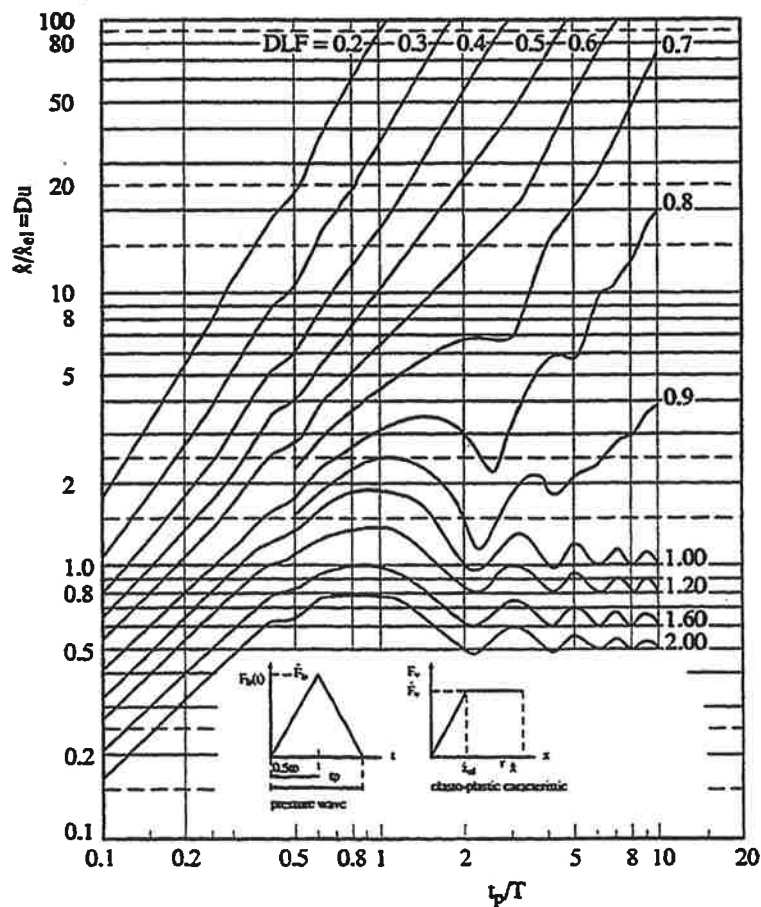


Fig. 16 Maximum response of an elasto-plastic single-degree-of freedom system for a pressure wave (from [13]).

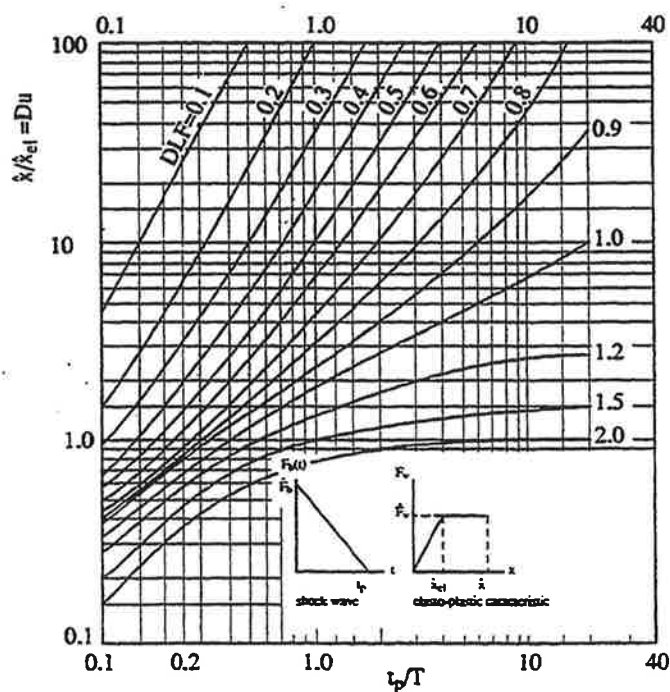


Fig. 17 Maximum response of an elasto-plastic single-degree-of freedom system for a shock wave (from [13]).

In analogy with a single-degree-of freedom system, the maximum value of the load acting on the structure must be set-in for P . For a perpendicular reflection we must have: $P = P_p$, while for a side-on wave it will be: $P = P_s$.

The static strength P_{st} is analogous to the maximum spring force in the single-degree-of freedom system, as per: $F_v = K * \hat{x}$. If the materials used for the structure and the dimensions of the structure are known, then can P_{st} , in principle, be determined. We must note that the units for i and P , respectively, are $\text{Pa} * \text{s}$ and Pa , by difference for S and F_b , for which the units are $\text{N} * \text{s}$ and N .

The extreme values in Figures 18 and 19 can be checked in a simple manner. For loads of short duration, the response to an impulse load is valid. For loads of long duration, the response to a shock wave is that of a step load, while the response to a pressure wave is that of a static load. It is calculated, in Annex I, that the impulse, in both cases, can be approximated by:

$$\bar{i}' = \sqrt{2 * Du - 1} \quad (21)$$

The pressure asymptote, for the shock-wave, has the following value:

$$\bar{p}' = \frac{Du - 1/2}{Du} \quad (22)$$

and, for the pressure wave :

$$\bar{p}' = 1 \quad (23)$$

The pressure-impulse diagrams have been derived for a single-degree-of freedom system. The question may arise: to what degree are these diagrams actually applicable to structures? In fact, structures are continuous systems with a large number of natural frequencies. By using the single-degree-of freedom system it is implicitly assumed that the response is determined by the lowest natural frequency.

An investigation of the response of continuous systems such as beams or plates [33] has shown that the internal forces, such as transverse forces and bending moments, can depart from the values obtained using the single-degree-of freedom system in case the duration of the load is smaller than 0.1 times the lowest natural period of vibration.

Consequently, the above figures can be accepted as suitable as long as $t_p/T > 0.1$ and as long as it is considered that the load is uniformly distributed over the entire surface.

It is now possible, thanks to the foregoing, to get an idea about the value of the maximum deflection of a structure subjected to a given load of short duration. Once the ductility has been established, it is possible to determine the maximum dynamic load which the structure is capable of withstanding. If it is then possible to establish a connection between the deflection which takes place and the consequent damage (or percentage), we can then use the above-mentioned diagrams in order to establish damage criteria. The data needed for this purpose are as follows:

- For the load:
 - a. shape
 - b. peak overpressure
 - c. positive phase duration
- For the structure:
 - a. static resistance
 - b. natural frequency
 - c. ductility

In the next chapter, a closer analysis will be made in order to determine the values which must be known with regards to a given structure.

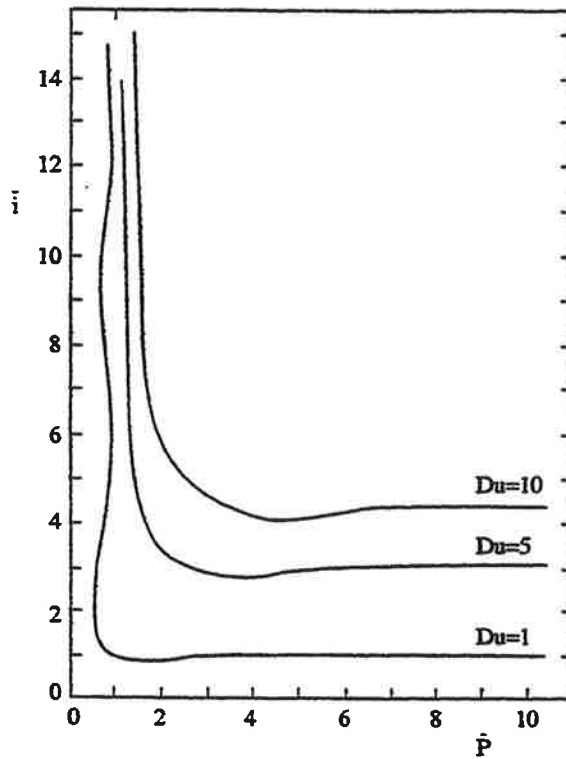


Fig. 18 Pressure-impulse diagram for a pressure wave.

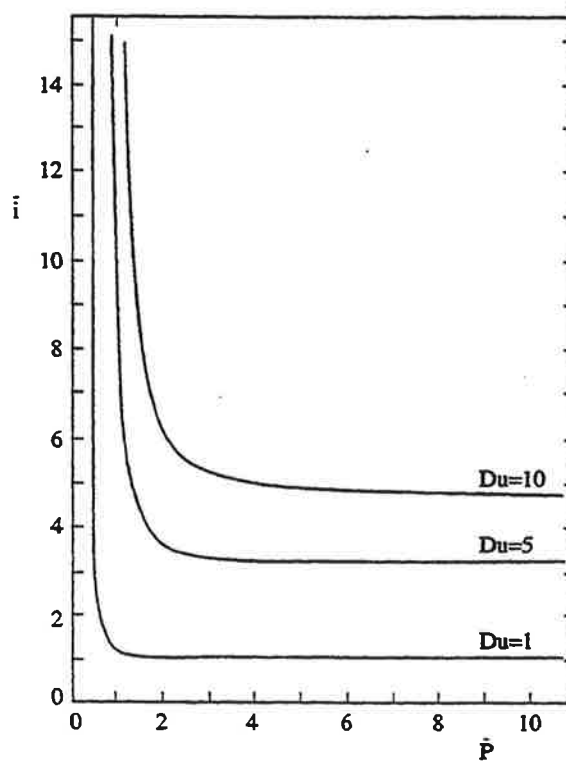


Fig. 19 Pressure-impulse diagram for a shock wave.

Determination of values required

In order to be able to make use of the diagrams presented in the preceding chapter for the determination of the response, a number of values must be known. The determination of the values regarding the blast itself has already been treated previously. In this chapter we will concentrate on values required with regard to the structure under consideration. These values are static strength, natural frequency and ductility.

5.1 Static Strength

The concept "static strength" must be interpreted as the value of a statically applied load (acting in the same direction as the eventual dynamic load) for which either the structure or the structural element, to which this static load is applied, will fail. For structural framings of buildings this statically applied load is considered to be horizontal. For structural elements such as walls, roofs, frames and panels it is considered that the uniformly distributed load acts perpendicularly to their surface.

The value of the static strength is an average value: in 50 % of the cases failure will occur.

In designs and calculations of structures, codes and design standards are normally used, in which specific requirements for the structure are given. Such requirements, among others, are: strength, stiffness, durability, insulation processability and appropriate transport conditions. All of these requirements jointly determine the dimensions and the types of materials to be used, whereby, with regards resistance, the structure can sometimes be overdesigned. In all such cases the static strength must be determined on the basis of the dimensions and materials which have already been chosen. This can lead, in many instances, to types of calculations in which many different assumptions must be made. It will become apparent, from what follows, that such types of calculations are generally not needed for the topic with which we are now dealing.

In cases where static strength is decisive in the dimensioning of the structure, the value of this static strength can easily be determined on the basis of the loads prescribed and of the allowable or characteristic strengths of the materials used. The prescribed safety factors and the ratios between allowable and average material properties, jointly, provide then a value for the average static strength.

An important load condition is the wind load. In the design rules [3] values are given for a static load corresponding to wind. The wind load, for high buildings, appears to represent a decisive factor, which means, in turn, that the determination of the static strength of such buildings can be based on these wind load requirements.

5.1.1 Safety Factors

Concrete [13, 16]:

In the calculation of concrete structures, a safety factor of 1.7 is always foreseen, a factor by which the prescribed load must be multiplied. The stresses due to this factored load must not be higher than the specified characteristic strength. This specified characteristic strength, in turn, is lower than the average strength. The factor between the two is in the order of 1.5. For loads of short duration the strength is found to be higher than for slowly applied loads. This latter increase in strength is equal to 1.2.

Multiplying all of the above factors one by another leads to a safety factor of 3.0 versus the average strength.

Steel [14]:

For steel considerations similar to concrete are applicable. A safety factor of 1.5 is retained. In this case, the load is not multiplied by this factor but, rather the factor is used to determine the value of an allowable stress in relation to the yield stress. The ratio between the average value and its lower limit is equal to 1.2, while the influence of the high speed of load is taken into account by using a factor of 1.1. Jointly, all of this leads to a safety factor of 2.0 versus the average.

Wood [25]:

In the case of wood, its bending strength is mostly taken as critical since, according to test data, this bending strength can be as low of 1/5 of the experimentally obtained values. The influence of the speed of load is not known. The safety factor versus the average, consequently, is taken equal to 5.

Glass [17]:

For glass we foresee a safety factor of 2. The average strength is equal to about 2 x the lower limit. Also the influence of the speed of load gives a factor of 2. Consequently, the safety factor versus the average is taken equal to 8.

5.1.2

Wind Load

The wind pressures to be retained for the statical calculation of buildings are given in TGB [3] as functions of the height. A difference is made between structures located along the Dutch North Sea coast and structures located more inland. The rules are given in Table 2. The limit value of the distance to the North Sea coast, by which column 1 must be used, is equal to 25 times the height of the building. For column 2 the value is 50 times the height of the building. For distances between these two limit values, the value of the wind pressure can be obtained by linear interpolation.

For the wind load on buildings the following must be applied:

$$p_w = C_w * q_w \quad (24)$$

The factor C_w is determined by the orientation of the loaded surface versus the wind direction. For a surface which forms an angle α_i with the wind direction we have:

$$C_w = + 0.4 \text{ for } 0^\circ \leq \alpha_i \leq 65^\circ$$

$$C_w = + 0.8 \text{ for } 65^\circ \leq \alpha \leq 90^\circ$$

For surfaces on the other side of the wind we must take a negative value for C_w :

$$C_w = - 0.4$$

Table 2 Wind pressure q_w according to [3].

Height above ground level in m	1 On North Sea coast in N/m ²	2 Inland N/m ²
≤ 7	970	710
8	990	730
9	1010	750
10	1020	770
15	1070	830
20	1120	880
25	1150	930
30	1190	970
35	1220	1010
40	1250	1040
45	1270	1070
50	1300	1100
55	1320	1120
60	1330	1140
65	1350	1160
70	1360	1180
75	1380	1200
80	1390	1220
85	1400	1230
90	1410	1250
95	1420	1260
100	1430	1280
110	1450	1300
120	1460	1320
130	1480	1340
140	1490	1360
150	1500	1380
160	1510	1400
170	1520	1410
180	1530	1430
190	1540	1440
200	1550	1450
250	1570	1510
300	1600	1560

Surfaces parallel to the wind direction are loaded due to friction, with $C_w = 0.04$. For rooms with openings facing the wind a pressure with $C_w = +0.8$ is considered. For openings on the other side of the wind, a negative pressure with $C_w = -0.4$ is used in the calculations. Reference [3] provides ample information regarding the values to be taken in design. Globally, we find $C_w = 1.3$. The pressure q_w , as function of the height, is given in Figure 20.

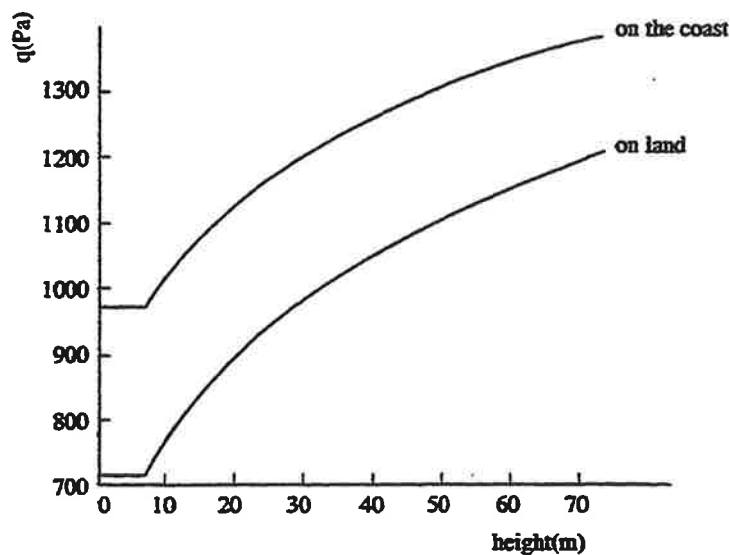


Fig. 20 Pressure q_w as function of the height (according to [14]).

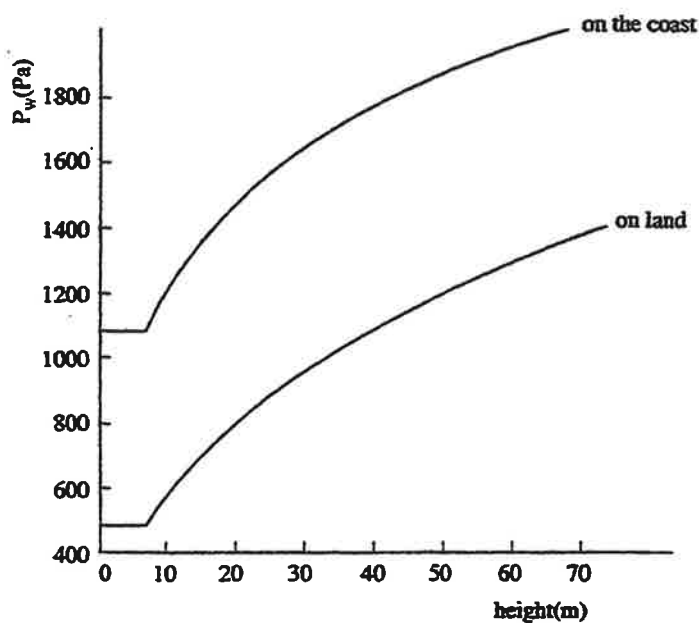


Fig. 21 Wind load on windows as function of the height (according to [17]).

A simple example will demonstrate, below, how the static strength due to wind load must be determined.

A building with a height $H = 30$ m must be designed for wind load. In order to determine the required static strength due to the wind load, the latter can be schematically represented as shown in Figure 22, in which the load varies linearly as function of the height.

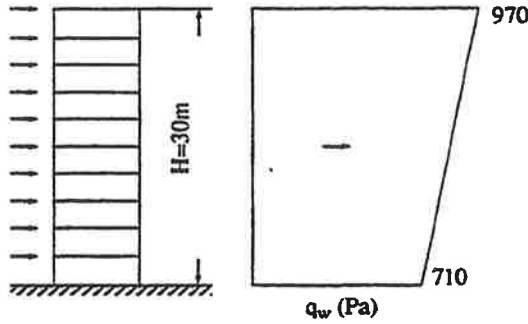


Fig. 22 Approximate wind load on a building with a height equal to: $H = 30$ m.

The wind load produces, at the base of the building, a fixed-end moment M_w per meter of width which is equal to:

$$M_w = C_w \left(\frac{1}{2} * 710 * H^2 + \frac{1}{3} * (970 - 710) * H^2 \right) \quad (25)$$

with

$C_w = 1.3$ and $H = 30$ m we find :

$$M_w = 517 \text{ kPa/m}$$

An uniformly distributed static load, which acts horizontally, produces a moment M_{st} equal to :

$$M_{st} = \frac{1}{2} * P_{st} * H^2 \quad (26)$$

Assuming that the wind load is the controlling load, we then have :

$$M_{st} = \beta * M_w \quad (27)$$

whereby β is the safety factor. If the structural framework is of concrete construction, we have seen previously that we must take $\beta = 3$. It follows then, from the above, that: $P_{st} = 3445$ Pa.

5.2

Natural Frequency

An evaluation of the dynamic behaviour of structures shows that natural frequencies play an important role. The natural frequency is directly related to the natural period of vibration. During the time required for the natural period of vibration a full vibration-cycle is completed, which means that the system twice reaches the maximum displacement from its state of equilibrium. Consequently this natural period of vibration is determinant for the speed at which the structure reacts to the variation of the load.

For loads of short duration, such as blast, the structure will vibrate with its lowest natural frequency. If the duration of the load is long versus the natural period, the maximum value of the deflection will be reached. For loads of short duration, the load is already no longer acting on the structure by the time the maximum deflection is reached.

As shown by equation [14], the natural frequency of a structure is determined by its mass and by its stiffness. The stiffness depends on the stiffness of the materials used, the shape, the dimensions and the structural concept of the structure. While it is possible to properly determine the mass, it is much more difficult, from the design, to calculate the stiffness. Due to this fact, it is often not possible to properly determine the natural frequency of the system.

However, thanks to results obtained from a large number of tests, empirical formulae have been derived which allow us to obtain, in a global fashion, the natural frequencies of buildings. These formulas will be presented in what follows. Most of the time, instead of natural frequencies, the natural periods of vibration are determined.

5.2.1

Empirical Formulae

The most important factor, for the determination of the natural period of vibration, is the height H of the building. It can be seen that the natural period of vibration increases with an increase of the height. Many of the formulae, then, are based on a linear relationship between height and natural period of vibration, as follows:

$$T = k_1 * H \quad (28)$$

A number of values for the constant k_1 are assembled in Reference [19]. For buildings of masonry construction the values of k_1 vary between 0.014 to 0.0165. For buildings with structural frameworks the k_1 values vary from 0.025 to 0.030. For high buildings a value of $k_1 = 0.029$ is quoted for steel construction and of 0.021 for other building materials. The value of k normally used in the Netherlands is 0.02. These figures lie in the middle of the above-mentioned spread of k_1 values. A very global determination of the natural period of vibration of buildings in general can then be made by substituting $k_1 = 0.02$ into formula (28).

A general formula in which, apart from the height also the depth L of the building is considered, is as follows:

$$T = k_2 \frac{H}{\sqrt{L}} \quad (29)$$

The value of L represents the depth of the building in the direction of the blast wave displacement. Only one quoted reference [21] limits the application of this formula to buildings with supporting partition-walls. The values of k_2 quoted in [19] vary from 0.087 to 0.109. A value of $k_2 = 0.091$ is mentioned as being based on a very high number of observations. This last figure is also retained in the design specifications of some countries. A choice of $k_2 = 0.09$ in formula (29) is, consequently, justified.

For buildings with a structural framework the following formula can be applied:

$$T = 0.1 * n \quad (30)$$

Hereby T is determined by the number of storeys n . A formula is also given, for this type of buildings, in Reference [21], which is:

$$T = k_3 * H^{3/4} \quad (31)$$

For steel structures the value of k_3 is given as:
 $k_3 = 0.085$, and for concrete structures: $k_3 = 0.061$.

The fact that the empirical formulae previously indicated only provide a global idea of the values of the natural periods of vibration is illustrated in Figure 23, taken from Reference [21]. The natural frequency varies from 10 Hz for low buildings to 0.10 Hz for very high buildings. The value of 10 Hz is, among others, quoted in Reference [22], in which frequency measurements are reported, mostly conducted on wooden buildings, 1 or 2 storeys high.

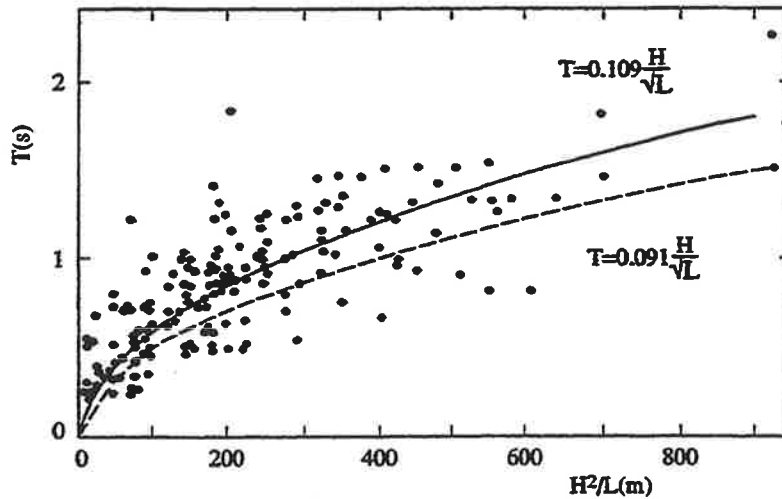


Fig. 23 Spread of measured natural periods of vibration, according to [21].

The value of 0.1 Hz is valid for very high buildings, such, for instance, as the Empire State Building in New York, which is 450 m high and has a natural frequency of 0.12 Hz.

A rough value of 5 Hz can be retained for the natural frequency of houses and buildings up to several storeys high.

5.2.2

Raleigh Method

An attractive method which permits to obtain a quick approximation of the lowest natural frequency is the Raleigh method. This method is based on an energy consideration. During the vibration of a system a continuous interchange between kinetic energy and potential energy takes place, respectively E_k and E_p . Considering that the total quantity of energy remains constant, we then have:

$$E_k + E_p = C \quad (32)$$

For continuous and multi-degree of freedom systems a choice must be made with regard to the geometric shape of the deformed system. Then, with the help of the energy balance, equation (32), for this deformed shape the exact value of the natural frequency can be determined. The method is applied, in Annex 2, to a continuous system for a girder and a plate. The application of the Raleigh method to multi-degree of freedom systems does not enter into the framework of this report. More information about the method can be found in References [13] and [24].

5.2.3

Determination of the Natural Frequency from the Static Load

It is quoted in TGB 1972 [3] that the natural frequency of a structure to a wind load can be approximated by the following formula:

$$f = \sqrt{\frac{0.25}{\delta}} \quad (33)$$

whereby δ is the largest deflection in m of the structure when the structure is loaded by its own weight and a constant load, acting horizontally in the direction of the wind. Formula (33) can be directly obtained from the natural frequency f of a linearly elastic single-degree-of freedom system.

The force F_v in the system produced by the mass M under the influence of gravity is equal to:

$$F_v = M * g \quad (34)$$

whereby g is the acceleration of gravity. The deflection of the spring is then :

$$\delta = F_v * K \quad (35)$$

substituting into [14] and [15], this gives :

$$f = \frac{1}{2\pi} * \sqrt{\frac{g}{\delta}} \quad (36)$$

which leads to (33).

The maximum deflection δ can be obtained either through calculation or by measurement.

In order to be able to obtain a more accurate determination of the natural frequency, two rather commonly used structural elements, the girder and the plate, are treated in Annex II. In this treatment a relation between the natural frequency and the static deflection is established, with the help of the Raleigh method.

It is found :

$$\text{For the girder : } T = 1.76\sqrt{\delta} \quad (37)$$

$$\text{and for the plate : } T = 1.58\sqrt{\delta} \quad (38)$$

If, for a plate or a girder, the correct values of the modulus of elasticity E and of the moment of inertia I are known, the lowest natural frequency, for freely mounted plates and girders, are then as follows

Girder :

$$f = \frac{\pi}{2 * l^2} * \sqrt{\frac{EI}{\rho * A_1}} \quad (39)$$

Plate :

$$f = \frac{\pi}{2} * \left(\frac{1}{a^2} + \frac{1}{b^2} \right) \sqrt{\frac{EI}{\rho * d * (1 - \nu^2)}} \quad (40)$$

Where l is the length of the girder, A , its cross-section, ρ its density, a, b , and d the length, width and thickness of the plate and ν its Poisson's modulus.

5.2.4

Example

The structural framing of high buildings for housing is commonly made of columns placed in the facades and in the middle of the building. The floors are considered as rigid shear panels which transfer the horizontal loading to the columns. A plan of such type of construction is shown in Figure 24.

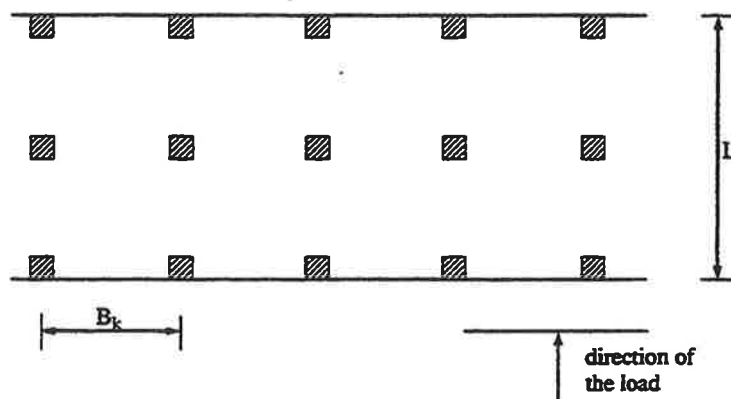


Fig. 24 Plan of structural framework.

The natural period of vibration will be calculated for a building with 10 floors (storeys), with a height of 30 m. For such type of building the static strength is computed in Paragraph 5.1.2.

Due to the horizontal load, the structure will bend. The deformation consists of two components:

- The floors can be considered as infinitely stiff in comparison with the columns. The columns bend between two adjacent floors. The deformation which takes place is comparable to that of a sheared girder.
- The structure, as a whole, acts like a bending girder, in which the columns in the facades are, respectively, in tension and in compression. The columns in the center of the building are not loaded.

Both of the bending components are shown in Figure 25.

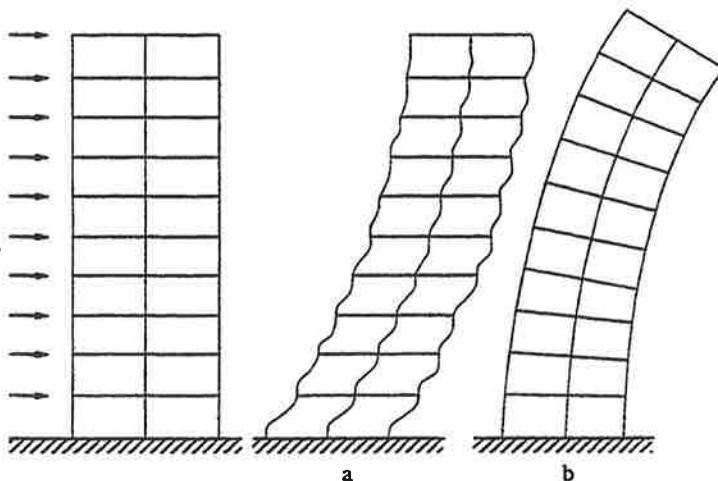


Fig. 25 Deformation shapes: a. shear,

b. bending.

The maximum displacement due to the horizontal motion of the building's own weight must now be determined. For the deformation of the sheared girder we have [12]:

$$\delta = \frac{p_{eg} * n^2 * h^2}{24 * E * \Sigma I_k} \quad (41)$$

In which ΣI_k is the summation of the moments of inertia of the columns in one line, in the direction considered (in this case: 3).

For the own weight we have:

$$P_{eg} = \rho * g * B_k * L \quad (42)$$

The deformation of the bending girder is, in this case [12] :

$$\delta = \frac{P_{eg} * n^4 * h^4}{4 * E * A_k * L^2} \quad (43)$$

in which A_k is the cross-section of one column.

For the determination of the total displacement δ , the following values are used:

Structural material concrete:	$E = 25 * 10^9 \text{ Pa}$
Specific mass of building:	$\rho = 200 \text{ kg/m}^3$
Building: 10 storeys:	$n = 10$
Dimensions:	$h = 3 \text{ m}, B_k = 4 \text{ m}, L = 10 \text{ m}$ en $A_k = 0.5 * 0.5 = 0.25 \text{ m}^2$
so that	$I_k = 1/12 * 0.5^4 = 0.0052 \text{ m}^4$

Filling-in these values into (41) and (43) gives: $\delta = 0.104 \text{ m}$. The formulae to be applied give:

$$f = \sqrt{\frac{0.25}{0.014}} = 1.55; T = \frac{1}{1.55} = 0.64 \text{ s} \quad (33)$$

$$T = 0.02 * 30 = 0.6 \text{ s} \quad (28)$$

$$T = 0.1 * 10 = 1.0 \text{ s} \quad (30)$$

$$T = 0.061 * 30 = 0.78 \text{ s} \quad (31)$$

The values obtained using the different formulae show relatively appreciable differences. The preference goes to the values obtained using (28), (31) and (33), so that, globally, the natural period of vibration of the building can be taken equal to 0.7 s.

5.3

Ductility

The term "ductility" of a structure represents a measure of the amount of energy the structure is still able to absorb after the maximum elastic deformation has taken place. For an elasto-plastic single-degree-of-freedom system the ductility is the ratio of the maximum deformation versus the elastic deformation. Data regarding the ductility of structures are very sparse.

A value of the ductility equal to 4 is normally retained for buildings which must be able to withstand seismic conditions [31]. Investigations of prestressed concrete frames [32] have also indicated values of the ductility in the order of 4. In these investigations, the maximum displacement was measured at the moment when the structure was beginning to reach a failure-mechanism form, so that a reserve was still available.

Ductilities, for a number of structural shapes, based on test data, are given in Reference [18]. These values of the ductility are given in Table 3 below.

Table 3 Ductility Factors (from [18]):

	Du
Reinforced-concrete girders	$\left\{ \frac{0.1}{\omega_o - \omega'_o} \right\}$
Steel girders, under bending stress	26.4
Steel girders, under bending and pressure stress	8.1
Welded portal frames, under vertical stress	6-16
Composite T girder	8

Unless buildings are specially designed with the purpose of withstanding very heavy loads (control buildings or industrial complexes, for example [34]) it does not appear possible, at the present time, to properly determine the ductility of a building. A global value of 4 can be retained as an average value. A maximum value of the ductility appears to be in the range of 10.

Within the framework of the subject treated in the present study, a more exact determination of the ductility anyway, does not have much sense: see for this, the Figures 18 and 19 and the Formulas (21), (22) and (23).

For the pressure asymptote of a pressure wave, the ductility, in fact, is not important.

For a shock wave, the pressure asymptote rises from 0.95 to 0.97 for an increase of ductility from 10 to 15. The impulse asymptote, for the same increase of ductility from 10 to 15, and for both types of waves, rises from 4.36 to 5.39.

6

Glass

Glass is a material commonly used in structures. If a load following an explosion breaks a window-pane, the pieces of glass which come loose, as a consequence of it, cannot only produce serious injuries but can, also, sometimes, lead to the death of people who are hit by them. When a structure is suddenly subjected to a blast pressure, the window-panes are normally the first ones to fail. Consequently, the breakage of window-panes can be considered as the lowest limit with regard to possible damages to a structure.

Whether a window-pane is capable of withstanding a given blast load can be determined by the model presented in the previous chapters. Its static strength is determined by the wind load (Figure 21). Its natural frequency is determined using Formula (40) for a plate and, due to the fact that glass is a very brittle material, the ductility factor is equal to 1.0. The necessary material properties for glass are:

$$E_{glass} = 75 \cdot 10^9 \text{ Pa}, \rho = 2,500 \text{ kg/m}^3$$

and

$$\nu = 0.25$$

The lowest limit of the peak overpressure of the blastwave which can still produce breakage of a window-pane, often retained, is 1 kPa. It is considered, as an average, that for 3 kPa 50% of all window-panes will be broken.

Developments in the building industry whereby smaller window-panes are more and more used and, in addition, are often of double-glass construction, help to render these window-panes stronger. Global values of pressures which may lead to breakages are, therefore, higher for houses built during the last 15 years. The lowest limit is then taken as 2 kPa and the average value is 5 kPa.

A lot of investigation has been carried-out with regard to the behaviour of window-panes subjected to a shock wave, experimental as well as theoretical [29]. Due to this, a method has been developed for the determination of the static strength of these panels. This calculation method is presented in what follows.

6.1

Method for Determining the Strength of Window-panes

It has already been mentioned that glass is a very brittle material. The smallest weakness in the material leads to stress concentrations which in turn, introduce possible failure areas and, thereby, weaken the strength of the material. The possible presence of scratches on the glass surface is, in this respect, important.

If we schematically represent a window-pane as a thin plate and determine its theoretical strength, we find, in practice, that this theoretical strength does not have a constant value, not even for a glass material of chosen quality. Factors which, in this respect, play a role are the thickness (thick glass is more sensitive to scratches) and the surface area (as this surface area increases, the chances of the presence of fatal scratches increases as well).

The following formula has been derived for the average bending-tensile-strength of normal glass subjected to a shock wave:

$$f_t = \frac{2 * 10^6}{A^{0.18} * d^{0.7}} \quad (44)$$

This strength has approximately a normal distribution, with a 20% standard deviation. The relationship between an external static load and the stress is strongly dependent on a membrane-type behaviour. If the bending is sufficiently large then the stresses in the corners are governing. We have, for this:

$$\sigma = 0.225 * q * \frac{a^2}{d^2} \quad (45)$$

hereby a is the smallest span (m).

This formula can only be used if the deflection δ , with relation to the thickness d , has at least a determined critical value. This value is dependent on the length-width ratio b/a ($b \geq a$):

$$\left(\frac{\delta}{d}\right)_{kr} = 6 * \left(\frac{b}{a}\right)^{1.5} \quad (46)$$

The value of $\frac{\delta}{d}$ comes from :

$$\frac{\delta}{d} = 706 * 10^{-15} * q * \frac{a^3 * b}{d^4} \quad (47)$$

If the above condition does not apply, so that :

$$\frac{\delta}{d} < \left(\frac{\delta}{d}\right)_{kr} \quad (48)$$

then a correction factor η must be introduced into the calculation, with :

$$\eta = 1 + \frac{1}{9} \left(\left(\frac{\delta}{d}\right)_{kr} - \frac{\delta}{d} \right) \quad (49)$$

The formula for the stress becomes then :

$$\sigma = \eta * 0.225 * q * \frac{a^2}{d^2} \quad (50)$$

The static failure load P_{st} can be determined with the help of the above formula, for normal glass. This P_{st} is equal to the value of q for which the resulting stress σ is equal to the tensile strength f_t .

For double glass with different pane thicknesses, the thickest pane is the one which is governing: the loading distributes itself over both panes proportionally to their stiffnesses. The strength P_{st} calculated for this thickest pane (with $d = d_1$) must then be multiplied by the following factor:

$$\frac{d_1^3 + d_2^3}{d_1^3} \quad (51)$$

If both panes have the same thickness then, in view of the doubling of the total surface area, the bending-tensile-strength calculated with Formula (44) must be decreased by about 10%.

6.2

Examples

In order to illustrate the calculation method of the "static" strength presented in the preceding paragraph, two calculation examples will now be presented.

The average static strength will be determined for a window-pane measuring $1.5 \times 1.0 \text{ m}^2$, with a 5 mm thickness.

The bending strength, according to (44) is equal to:

$$f_t = \frac{2 * 10^6}{1.5^{0.18} * 0.005^{0.7}} = 75.9 * 10^6 \text{ Pa}$$

The static strength is calculated using (45) :

$$75.9 * 10^6 = 0.225 * P_{st} * \frac{1}{0.005^2} \rightarrow P_{st} = 8.43 * 10^3 \text{ Pa}$$

A check of the deflection gives :

$$\left(\frac{\delta}{d}\right)_{kr} = 6 * 1.5^{1.5} = 11.02$$

$$\text{and: } \frac{\delta}{d} = 706.10^{-15} * 8.43.10^{-3} * \frac{1.5}{0.005^4} = 14.28$$

$$\frac{\delta}{d} > \left(\frac{\delta}{d}\right)_{kr}$$

the answer is valid, thus

$$P_{st} = 8.43 * 10^3 \text{ Pa}$$

The use of the correction factor will be shown in the example which follows. A window-pane measuring $1 \times 1.5 \text{ m}^2$ is now assumed to have a thickness of 6 mm. The determination of the average static strength proceeds as follows:

$$f_t = \frac{2 * 10^6}{1.5^{0.18} * 0.006^{0.7}} = 66.8 * 10^6 \text{ Pa}$$

$$P_{st} = 10.69 * 10^3 \text{ Pa}$$

A check of the deflection gives :

$$\frac{\delta}{d} = 8.74$$

which is smaller than the critical deflection :

$$\left(\frac{\delta}{d}\right)_{kr} = 11.02$$

The factor η is equal to :

$$1 + \frac{1}{9}(11.02 - 8.74) = 1.25$$

The corrected static load is then :

$$P_{st} = \frac{10.69 * 10^3}{1.25} = 8.53 * 10^3 \text{ Pa}$$

A new check of the deflection gives :

$$\frac{\delta}{d} = 6.97$$

which means that a new correction is necessary. After a number of iteration procedures we find:

$\eta = 1.63$ and $P_{st} = 6.57 * 10^3 \text{ Pa}$. The deflection now corresponds to the applied load. The increased thickening of the window-pane results in the consequence that the window-pane becomes stiffer and its deflection becomes smaller. Due to this, membrane stresses are not generated and the window-pane fails in bending.

Damage criteria

A method has been presented, in the preceding chapters, which allows us to obtain a global idea about the dynamic load which structures are able to withstand. Some remarks must be added, when dealing with the above method, to emphasize its global character.

A schematic representation of a structure by a single-degree-of-freedom system and the subsequent calculation of its static strength, ductility and natural frequency could lead to a situation whereby the determination of the dynamic strength, obtained in this manner, may give values which depart from the true values.

Another procedure to determine the strength of structures can be conducted in an empirical approach. Practical "rules of thumb" can be found in literature which provide values of overpressures corresponding to a given degree of damage. A drawback of such rules comes from the fact that the types of structures and damage levels described in them are presented in very general terms. Furthermore, only overpressures are mentioned, while it has been shown, in the preceding chapters, that impulse is also important.

A closer examination of these empirical rules shows that many of them come from Reference [2] and apply to nuclear explosions. A blast load consequent to such an explosion leads to positive phase durations which are sufficiently long so that the impulse never actually governs. It is clear that values obtained in such approach can only be very global.

In order to come to more adequate damage criteria, we will first make a review of the known empirical rules whereby in combination with the method previously analysed, the damage criteria chosen will be presented.

7.1

Empirical Data

Empirical data about pressures which produce a given damage generally quote overpressures within the incident shock wave. It has clearly been established, in the foregoing, that the pressures exerted on a structure are generally not equal to these overpressures, but are dependent on the presence of reflections. In order to get an idea of the damage as function of the distance to an explosion a classification is made of 4 different zones (9), (Table 4).

Table 4. Damage Levels.

Zone	Levels	psi	kPa
A	Total destruction	>12	>83
B	Heavy damage	> 5	>35
C	Moderate damage	> 2.5	>17
D	Minor damage	> 0.5	> 3.5

The values quoted in the above table represent peak overpressures in the incident wave.

Total destruction, for buildings, must be understood as such a level of damage that these buildings can no longer be restored. A completely new building must be built. By heavy damage, a number of load-bearing structural elements have failed and the structure has partially collapsed. Walls which have not collapsed are majorly damaged and cracked. The remaining part, on the whole, must be demolished. In the case of moderate damage the building may, indeed, still be useable, but the walls, however, will be badly cracked and will not be reliable, the load-bearing structural elements will be damaged and twisted or buckled, and the inner walls as well as the roof and wall coverings, will also be damaged. In case of a minor damage it is considered that windows and doors will fail, and that a light crack-formation will appear in the walls and in the carrying structural elements. Also wall panelling and roof covering will be partially destroyed.

In the review which is presented below a number of pressure levels are shown, as well the degrees of damage corresponding to these pressure levels. These figures relate to typical brick-built English houses.

- 70 kPa : More than 75% of all outer walls have collapsed.
- 35 kPa : The damage is not repairable; 50% to 75% of all outer walls are lightly to heavily damaged.
The remaining walls are unreliable.
- 7-15 kPa : Not habitable without very major repair works. Partial roof failures, 25% of all walls have failed, serious damages to the remaining carrying elements. Damages to window-frames and doors.
- 3 kPa : Habitable after relatively easy repairs. Minor structural damage.
- 1-1.5 kPa : Damages to roofs, ceilings, minor crackformation in plastering, more than 1% damage to glass-panels.

For typical American-style houses the following applies:

- 70 kPa : Total collapse.
- 30 kPa : Serious damage. Collapse of some walls.
- 15 kPa : Moderate to minor damage. Deformed walls and doors; failure of joints. Doors and windowframes have failed. Wall covering has fallen down.
- 7-10 kPa : Minor damage. Comparable to a damage due to a storm; wooden walls fail, breakage of windows.

An overview is given, in Table 5, from data available in literature, showing pressure levels and corresponding damages, such as have been established from tests or actual accidental explosions.

The data quoted in Table 5 provide only a small sample on information available from various sources. A closer study shows that the greatest part leads us back to information taken out of Reference [2], in which primarily the consequences of nuclear explosions have been investigated. The damages shown in Table 5 correspond to the pressures given in this table. Nothing proves, however, that the same levels of damage could not have been caused by lower pressures. In fact, seeing the high values of some of the pressures shown, this should certainly be the case. Thus it is only possible, from these data, to obtain a rough idea about the damages which could be expected.

The most reliable known data appear to be the data given by Jarret [11], [25]. A great number of very properly described explosions and records about damages to housing due to bombing are presented in these references. Thanks to this information it becomes possible to establish a relationship between the quantity of explosives and the distance to the center of the explosion at which a given degree of damage has taken place. Since the parameters of a shock wave: peak overpressure and positive phase duration or impulse are, at a certain distance, determined by this quantity of explosives, it is then possible to establish a connection between these parameters and a given degree of damage. The results, in this

manner, are of more general application. Such a study has been performed by Baker in [1], and its results are shown in Figure 26. In the so-called pressure-impulse diagram three iso-damage lines are shown in this figure. These lines provide the lowest limit of the shockwave parameters corresponding to a given degree of damage.

Table 5. Damages to structures.

Description of Damage	P_s (kPa)
Connections between steel or aluminium ondulated plates have failed	7-14
Walls made of concrete blocks have collapsed	15-20
Brickstone walls, 20 - 30 cm, have collapsed	50
Minor damage to steel frames	8-10
Collapse of steel frames and displacement of foundation	20
Industrial steel self-framing structure collapsed	20-30
Cladding of light industry building ripped-off	30
The roof of a storage tank has collapsed	7
The supporting structure of a round storage tank has collapsed	100
Cracking in empty oil-storage tanks	20-30
Displacement of a cylindrical storage tank, failure of connecting pipes	50-100
Damage to a fractioning column	35-80
Slight deformations of a pipe-bridge	20-30
Displacement of a pipe-bridge, breakage of piping	35-40
Collapse of a pipe-bridge	40-55
Plating of cars and trucks pressed inwards	35
Breakage of wooden telephone poles	35
Loaded train carriages turned-over	50
Large trees have fallen down	20-40

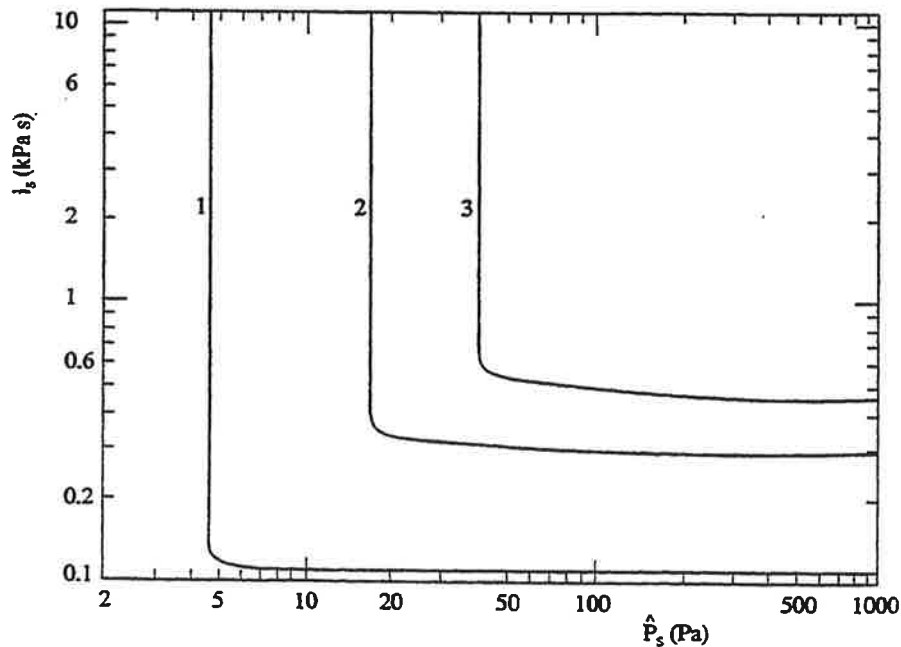


Fig. 26 P-i diagram for masonry building damage.

- 1 Threshold for minor structural damage. Wrenched joints and portions.
- 2 Threshold for major structural damage. Some load bearing girders fail.
- 3 Threshold for partial demolition. 50 to 75% of walls destroyed or unsafe.

Reference [7] provides a possibility to cross-check the results given in Figure 26. Tests are described in this reference whereby true-scale houses had been submitted to explosive loads. For four different types of houses it is determined what the degree of damage is for a given pressure or impulse. This degree of damage is expressed in the form of a percentage of the construction cost. The results compare reasonably well with the ones given in Figure 26. Applicable data are assembled in Annex III.

7.2 Damage Criteria and Probit Functions

The preceding paragraphs show that only scarce empirical data are known for the determination of the damages to structures due to an explosive load. For typical structural concepts in the Netherlands, such as cavity-walls, no data are available.

In the foregoing chapters an analytical model has been presented which also permits obtaining an idea about the degree of damage to be expected. Suitable damage criteria must also then be put together by combining the two approaches. In order to calculate analytically the probability of a given degree of damage, so-called probit functions are also given. These probit functions are derived in Annex IV. Jointly with the Table IV-1 from this Annex a percentage can be calculated which indicates the probability of a given event.

7.2.1

Houses

Even if the Jarrett damage criteria for houses (according to Figure 26) have not been developed for conditions prevailing in the Netherlands, we will retain these criteria for dutch conditions. Three damage levels are differentiated:

- 1 Minor damage: breakage of window-panes, displacements of doors and window-frames, damages to roofs.
- 2 Major structural damage: next to the above-mentioned damages also cracks in walls, collapse of some walls.
- 3 Collapse: the damage is so extensive that the house has totally collapsed.

In the Netherlands we have, apart from separate houses, also terraced houses and apartment-buildings. The number of storeys in apartment-buildings is generally higher than nine or lower than five. Few apartment-buildings can be found in which the number of storeys is between four and ten.

The structural framing of high apartment-buildings is calculated for the wind load, which means that its static strength to horizontal loads is therefore known. It is then obvious that the model presented in the foregoing chapters for high buildings must be used, instead of the third criterium of Jarrett.

For houses or apartment-buildings up to four storeys we can use Figure 26. For higher apartment-buildings we are dealing with the first two damage levels. For a possible collapse of the structural framing, dependent on the shape of the blastwave, Figures 18 or 19 are to be used.

The derivation of the probit functions for different types of buildings is given in Annex IV. Here only the results are given.

The probit functions for houses or apartment-buildings up to 4 storeys are as follows:

1. Minor damage :

$$P_r = 5 - 0.26 * \ln V \quad (52)$$

with

$$V = \left(\frac{4600}{P_s} \right)^{3.9} + \left(\frac{110}{\bar{i}_s} \right)^{5.0} \quad (53)$$

2. Major structural damage :

$$P_r = 5 - 0.26 * \ln V \quad (54)$$

with

$$V = \left(\frac{17500}{P_s} \right)^{8.4} + \left(\frac{290}{\bar{i}_s} \right)^{9.3} \quad (55)$$

3. Collapse :

$$P_r = 5 - 0.22 * \ln V \quad (56)$$

with

$$V = \left(\frac{40000}{P_s} \right)^{7.4} + \left(\frac{460}{\bar{i}_s} \right)^{11.3} \quad (57)$$

For apartment buildings higher than four storeys the probit functions for light or structural damage are identical to (52) and (54). The probability of collapse is determined by the following probit functions:

– Shock wave

$$P_r = 5 - 2.92 * \ln V \quad (58)$$

with

$$V = \left(\frac{0.9}{\bar{P}} \right)^{1.4} + \left(\frac{3}{\bar{i}} \right)^{2.7} \quad (59)$$

– Pressure wave

$$P_r = 5 - 2.14 * \ln V \quad (60)$$

with

$$V = \left(\frac{1.25}{\bar{P}} \right)^{1.9} + \left(\frac{3}{\bar{i}} \right)^{2.5} \quad (61)$$

For the scaled units \bar{P} and \bar{i} , the scaled values for the reflected or incident pressure and impulse must be filled in, as per formulas (19) and (20), dependent on the type of load.

7.2.2

Industrial installations

For industrial buildings which are not specially designed for a blast load, we can retain the criteria and probit functions of the preceding paragraph. In cases when the wind load is not determinant for the static strength to a horizontal load, such static strength must then be determined by calculation. Blast resistant structures, such as control buildings are normally designed to withstand a given overpressure and impulse. The following guide-lines can be indicated for control buildings: the walls subjected to possible reflection must be calculated for an overpressure of 30 kPa; the roof must withstand 20 kPa. In both these cases the positive phase duration is taken equal to 100 ms. Apart from the above pressure wave, control buildings must also be able to withstand a shock wave with a reflected peak overpressure of 300 kPa for the walls and a peak overpressure of 200 kPa for the roof. The positive phase duration, in these cases, is taken equal to 15 ms [26].

Data for industrial installations other than buildings are scarce and insufficient. Use can be made of the values given in Table 5.

7.2.3

Breakage of window-panes

The lowest limit of the static strength is obtained from Figure 21 for wind load. A more accurate calculation of the average static strength can be made using the procedure given in Paragraph 6.1. The dynamic strength is determined with the help of diagrams 18 and 19, whereby a ductility factor $D_u = 1.0$ must be used.

A global idea of the dynamic strength is obtainable for the pressures indicated in Chapter 6 and with the help of the following probit functions:

– window - panes in old buildings (before 1975)

$$P_r = -11.97 + 2.12 * \ln P_s \quad (62)$$

– window - panes in newer buildings (after 1975)

$$P_r = -16.58 + 2.53 * \ln P_s \quad (63)$$

7.3

Examples

Example 1:

An apartment building with the following dimensions: $L \times H \times B = 10 \times 30 \times 20 \text{ m}^3$, 10 storeys high, is loaded on the long facade, by a shock wave with: $P_s = 0.5 * 10^5 \text{ Pa}$ and $t_p = 200 \text{ ms}$. What damage to the building can be expected?

The load on such a building has already been determined in Paragraph 3.5. The load on its structural framing is again reproduced in Figure 27.

The static strength is calculated using the example given in Paragraph 5.1.2. Its value is:

$P_{st} = 3445 \text{ Pa}$. The natural frequency has been determined in Paragraph 5.2.4. We found: $T = 0.7 \text{ s}$.

For the determination of the damage to the structural framing we must use the single-degree-of-freedom-system. For a triangular pulse load Figures 18 and 19 furnish a solution. The shape of the load in this case is not such that one or the other of these two figures can simply be applied.

The load on the structural framing consists of a positive phase with a $1.2 * 10^5 \text{ Pa}$ peak overpressure and an 89 ms. duration, and a negative phase with a $0.28 * 10^5 \text{ Pa}$ overpressure and a 136 ms duration (Figure 27).

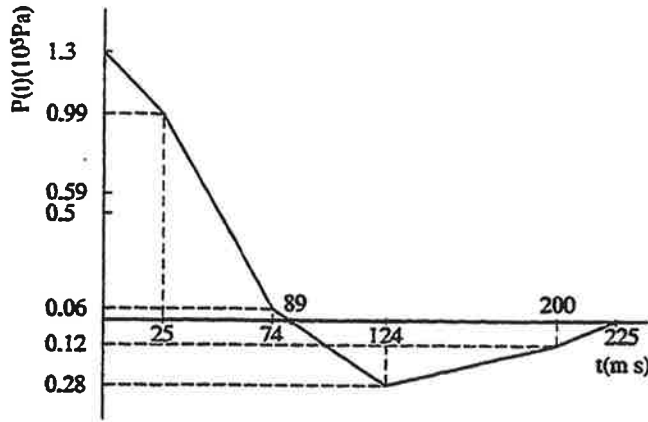


Fig. 27 Horizontal load on structural framing.

The total duration of the load is so short versus the natural period of vibration that this load can be interpreted as an impulse. If we evaluate the structure as a single-degree-of-freedom-system we can, then, using the response to an impulse load (Annex I), determine whether plastic deformation will take place. The impulse acting on the structure is approximately equal to (2):

$$i = \frac{1}{2} * 1.3 * 10^5 * 0.089 - \frac{1}{2} * 0.28 * 10^5 * (0.225 - 0.089) = 3881 \text{ Pa} * s$$

The maximum dynamic deflection for a linear-elastic single-degree-of freedom-system is determined by:

$$\hat{x} = \frac{i}{m * \omega} \quad (\text{I-12})$$

The mass-density of buildings is in the order of 200 kg/m^3 . The depth of the building, in this example, is equal to 10 m , so that: $m = 2000 \text{ kg/m}^2$. The natural period of vibration is 0.7 s , whereby the angular frequency is equal to: $\omega = 2\pi/0.7 = 8.98 \text{ s}^{-1}$. The maximum deflection is then equal to (I-12):

$$\hat{x} = 3881 / (2000 * 8.98) = 0.22 \text{ m}$$

The static deflection, according to (17), is equal to :

$$\hat{x}_{st} = \frac{P}{K}$$

The stiffness K must be determined from ω .

We have : $\omega^2 = K/m$ (14) so that :

$$K = 2000 * 8.98^2 = 1.61 * 10^5 \text{ N/m}^3.$$

The static deflection is then equal to :

$$\hat{x} = 1.2 * 10^5 / 1.61 * 10^5 = 0.75 \text{ m}$$

The dynamic load factor is then equal to :

$$DLF = \frac{0.22}{0.75} = 0.293$$

The quasi-static load which the structural framing must be able to withstand is, according to Chapter 4.3:

$$0.293 * 1.2 \times 10^5 = 35200 \text{ Pa}$$

The static strength is equal to 3445 Pa. This static strength is exceeded by a very wide range: consequently, there will be a plastic deformation.

The ductility required to be able to absorb the impulse is calculated using (21):

$$i = \frac{P_{st}}{\omega} \sqrt{2 * Du - 1}$$

which, filling in the values gives :

$$Du = \left(\left(\frac{8.98 * 3881}{3445} \right)^2 + 1 \right) * 0.5 = 51.7$$

This value of the ductility can also be determined with the help of Figures 16 and 17.

If the load is interpreted as a shock wave, with $P = 1.2 * 10^5$ and $i = 3881 \text{ Pa} * \text{s}$, we then find: $t_p = 0.065 \text{ s}$. We need, in order to use Figure 17:

$$t_p / T = 0.065 / 0.7 = 0.09 \quad DLF = 3445 / 1.2 * 10^5 = 0.03$$

Both values do not actually appear in the figure. However, an extrapolation gives an approximate value of: $Du = 50$.

This value of the ductility is much bigger than the value acceptable for buildings. An average value $D_u = 5$ has been indicated in Paragraph 5.3. Consequently, the structural framing, in this example, will collapse.

In order to be able to apply Figure 19, only the positive phase of the load will be considered. Such a procedure is somewhat on a conservative side. We require, for this, the values of P and i , according to (20) and (19):

$$\tilde{P} = \frac{1.2 * 10^5}{3445} = 34.8$$

and

$$\tilde{i} = 0.5 * 1.3 * 10^5 * 0.089 * 8.98 / 3445 = 15.1$$

We can see, from Figure 19, that this combination is far above the lines for constant ductility, which means that the structure collapses.

The probit function for shock waves gives with (58) and (59):

$$V = \left(\frac{0.9}{34.8} \right)^{1.4} + \left(\frac{3}{15.1} \right)^{2.7} = 0.019$$

$$Pr = 5 - 2.92 * \ln 0.019 = 16.6$$

We can see, using Table IV-1, that the probability of collapse of the structural framing is higher than 99.9%.

Example 2:

A gas explosion in an industrial installation produces a pressure wave in a housing area located at a few hundred meters distance. The peak overpressure in the pressure wave, at the location of the housing area, is equal to 5 kPa, and its duration is 500 ms. The housing area is composed of: individual houses, apartment-buildings up to 4 storeys and a few high apartment-buildings with dimensions similar to the ones of the previous example. What damage can be expected and what is the probability of a given damage level. In order to be able to use figure 26 we also need, apart from the peak overpressure $P_s = 5$ kPa, also the impulse: $i = 0.5 * 5000 * 0.5 = 1250$ Pa · s. The combination pressure and impulse is close to line 1 in Figure 26. The damage will be minor.

Apart from the breakage of window-panes, the roofs will be damaged and minor cracking will take place in walls and ceilings. The probability of a minor damage is to be determined from (52) and (53):

$$V = \left(\frac{4600}{5000} \right)^{3.9} + \left(\frac{110}{1250} \right)^{5.0} = 0.72$$

$$Pr = 5 - 0.26 * \ln 0.72 = 5.08$$

From Table IV-1 we find that this probability is equal to 53%.

The probability of a major structural damage is to be determined from (54) and (55):

$$V = \left(\frac{17500}{5000} \right)^{8.4} + \left(\frac{290}{1250} \right)^{9.3} = 3.7 * 10^4$$

$$Pr = 5 - 0.26 * \ln 3.7 * 10^4 = 2.26$$

From Table IV-1 we find that this probability is smaller than 1%.

The probability of collapse is nil. The probability of breakage of window-panes, in old houses, is equal to [according to (62)]:

$$Pr = -4.39 + 1.17 * \ln 5000 = 5.58; \text{ probability} = 72\%$$

The probability of breakage of window-panes, in new houses, is equal to [according to (63)]:

$$Pr = -6.85 + 1.39 * \ln 5000 = 4.99; \text{ probability} = 50\%$$

The load on the structural framing of high apartment-buildings is obtained from Figure 28.

According to (6), the following is determined:

$$Q = \frac{5}{2} * \frac{5000^2}{7 * 10^5 + 5000} = 89 \text{ Pa}$$

and, according to (9) :

$$U = 340 * \sqrt{1 + \frac{6 * 5000}{7 * 10^5}} = 347 \text{ m/s}$$

while :

$$L/U = \frac{10}{347} = 0.030 \text{ s}$$

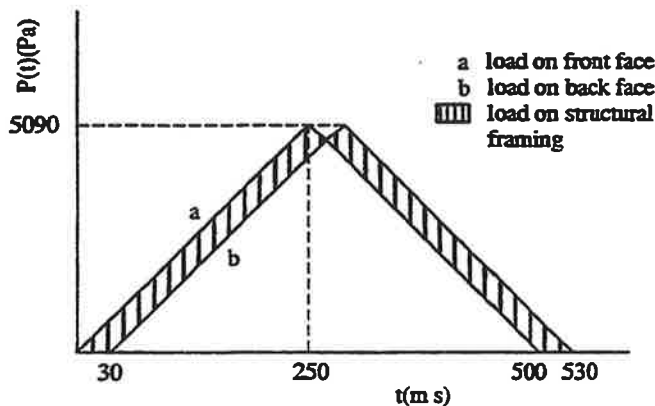


Fig. 28 Horizontal load on a structural framing of an apartment-building consequent to a pressure-wave.

The resulting horizontal load on the structural framing is low, maximum 610 Pa. This structural framing, consequently, is not damaged. The load on front, back and side facades and on the roof has a maximum of 5000 Pa. Therefore, local damages, for these elements, are possible.

Example 3

A window-pane with dimensions $1.5 \times 1.0 \text{ m}^2$, and a thickness of 5 mm has an average static strength of $8.43 \times 10^3 \text{ Pa}$ (See example 6.2.). Can this panel withstand the pressure wave of the previous example?

The following is known about the load:

- the shape: pressure wave
- the peak overpressure: $P_s = 5000 \text{ Pa}$
- the impulse: $i_s = 1/2 * 5000 * 0.5 = 1250 \text{ Pa} * \text{s}$

For the window-pane the following is known:

- the ductility: $Du = 1.0$
- the static strength: $P_{st} = 8.43 \times 10^3 \text{ Pa}$

We must further determine the natural frequency.

With $E = 75 * 10^9 \text{ Pa}$, $\rho = 2500 \text{ kg/m}^3$ and $\nu = 0.25$, we find, from (40):

$$f = \frac{\pi}{2} \left(\frac{1}{1.5^2} + \frac{1}{1.0^2} \right) \sqrt{\frac{75 * 10^9 * \frac{1}{12} * 0.005^3}{2500 * 0.005 (1 - 0.25^2)}} = 12.6 \text{ Hz}$$

$$\omega = 2 * \pi * f = 2 * \pi * 12.6 = 79 \text{ s}^{-1}$$

$$\bar{P} = \frac{P_s}{P_{sr}} = 0.59 \text{ and } \bar{i} = \frac{i * \omega}{P_{sr}} = \frac{1250 * 79}{8.43 * 10^3} = 11.7$$

This P - i combination, in Figure 18, is under the line $Du = 1.0$. Consequently, the window-pane remains intact.

Conclusions and recommendations

It has appeared possible, with the help of a combination of empirical data with a simple analytical model, to obtain a global idea about the effect of blast on structures. For houses: apartment houses up to four storeys and similar types of structures, use can be made of an empirically determined pressure-impulse diagram. For the structural framing of higher buildings the pressure-impulse diagram is determined by representing the structure, schematically, by a single-degree-of-freedom system. The accuracy of this analytical model depends on the input data, which, in general, can only be determined in a global approach.

The application of the analytical model provides the possibility to appreciate the interaction between the blast and a given structure, as well as the dynamic response of the structure.

Data about damages to structures caused by explosions are generally scarce; certainly for explosions the strength of which is known, so that the damage which took place can be properly related to it. The data are also scarce for conditions prevailing in the Netherlands. Empirical rules which permit us to appreciate the damages are either based on data available from World-War II, or on data coming from tests in which the pressure-time pulse was such that the test results can only be used for a cautious evaluation.

With regard to fragments and debris, their effect on structures is to such a degree unknown that this subject is not treated in this report.

In order to obtain more reliable data about damages to structures due to explosions in the Netherlands, the damages which take place during an actual explosion must be properly registered and the information must be properly assembled and centralized. It is especially important, in this respect, to pay attention to damages to buildings in the surroundings of the accident. Present investigations are primarily directed towards the establishment of the causes of the explosions.

Registration of the damages must be so conducted by experts that none of the relevant information could possibly be lost: this means, at the same time, that all records must be registered as quickly as possible after the explosion.

The strength of window-panes, with the help of the method given in this report, can be determined with more accuracy. In comparison with the static strength of window-panes, calculated for wind load, the strength of these window-panes appears to be on the high side. It is possible that the static strength determined for wind load gives values which are too low. A closer investigation of the strength of structures against horizontal loads and, also, of the ductility of the structures, is necessary.

It appears, finally, that the natural frequency of structures can be determined with a sufficient degree of accuracy.

References

- [1] Baker W.E., Cox P.A., Westine P.S. et al.
Explosions hazards and evaluation.
Elseviers Scientific Publishing Company (1983).
- [2] Glasstone S.
The effects of nuclear weapons.
United States Atomic Energy Commission (1967)
- [3] Technische grondslagen voor de berekening van bouwkonstrukties-TGB 1972
NEN 3850 (1972)
- [4] Dragosavic e.a.
Schade aan gebouwen ten gevolge van de explosie van een gaswolk.
IBBC-TNO (1976)
- [5] Uniform Building Code, vol.1
International conference of building officials.
Pasadena, California (1970).
- [6] Clough R.W., Penzien J.
Dynamics of structures
McGraw-Hill (1975)
- [7] Wilton C., Gabrielsen B.
House damage assessment.
14th Annual Explosives Safety Seminar (1972)
- [8] Pickering E., Bockholt J.L.
Probabilistic air blast failure criteria for urban structures.
Stanford Research Institute (1971).
- [9] Stephens M.M.
Minimizing damage to refineries from nuclear attack, natural and other disasters.
The office of oil and gas, Department of the Interior, USA (1970).
- [10] Schwanecke R.
Sicherheitsanforderungen an Messwarten Wasser.
Luft und Betrieb 13 (1969) Nr. 6.
- [11] Giesbrecht H., Hemmex G. et al.
Analysis of explosion hazards on spontaneous release of inflammable gases into the atmosphere.
Ger. Chemical Engineer 4 (1981).
- [12] Harmanny A.
De respons van gebouwen op een explosiebelasting PML-TNO, 1982.

- [13] Biggs J.M.
Introduction to structural dynamics.
- [14] Technische grondslagen voor de berekening van bouwkonstrukties
TGB 1972 - Staal.
Staalkonstrukties NEN 3851 (1974)
- [15] Technische grondslagen voor de berekening van bouwkonstrukties
TGB 1972 - Hout.
Houtkonstrukties NEN 3852 (1974).
- [16] Voorschriften Beton VB 1974.
Deel A: Gemeenschappelijk gedeelte, NEN 3861 (1977).
- [17] Diktebepaling van ruiten van vensterglas en spiegelglas.
NEN 2608 (1968).
- [18] Norris C.H. et al.
Structural design for dynamic loads.
McGraw-Hill (1959).
- [19] Steffens R.J.
Structural vibration and damage.
Department of the Environment, Building Research Establishment, London (1974).
- [20] Blevins R.D.
Formulas for natural frequency and mode shape.
Van Nostrand Reinhold (1979).
- [21] Adeli H.
Approximate formulae for period of vibrations of building systems.
Civil Engineering for practicing and design engineers, vol.4. (1985).
- [22] Dowding C.H.
Dynamic properties of residential structures subjected to blast load.
Journal of the Hydraulics Division.
ASCE, vol. 107, ST7 (1981).
- [23] Design and siting of buildings to resist explosions and fire.
Oyer Publishing Limited, London (1980).
- [24] Timoshenko et al.
Vibration problems in Engineering.
John Wiley and Sons (1974).
- [25] Jarrett D.E.
Derivation of the British explosives safety distances.
Annals of the New York Academy of Sciences, vol. 152 (1968).
- [26] Veiligheid van gebouwen in de procesindustrie.
Directoraat Generaal van de Arbeid (concept, 1987).
- [27] Edwards A.T.
Experimental studies of the effects of blasting on structures.
The Engineer (1960).

- [28] Fletcher E.R., Richmond D.R.
Glass fragment hazard from windows broken by air blast.
Lovelance Biomedical and Environmental Research Institute.
Albuquerque New Mexico (1980).

- [29] Nowee J., Harmanny A.
De invloed van het glaskozijn op de dynamische bezwijkbelasting van ruiten.
PML-TNO (1983).

- [30] Methoden voor het berekenen van de fysische effecten van het incidenteel vrijkomen van
gevaarlijke stoffen, CPR 14.
Directoraat-Generaal van de Arbeid, Voorburg (1979).

- [31] Pekan O.A., Gocevski V.
Elasto-plastic analysis of coupled shear walls.
Eng. Struct. (1981) vol.e.

- [32] Muguruma H.
Study on hysteretic behaviour of statically indeterminate prestressed concrete frame structure subjected
to reversed cyclic lateral load.
Structural concrete under seismic ations, vol.3. Proceedings 1979.

- [33] Karthaus W., Leussink J.W.
Dynamic load: more than just a dynamic load factor.
Proceedings of the First Symposium on the Interaction of non-nuclear munitions with structures.
Colorado (1983).

- [34] Schiebroek C.J.M., Nelissen M.G.P.
Ontwerp voor een explosiebestendig controlegebouw op Rozenburg / Rotterdam.
Cement (1979), nr.6.

- [35] Kingerey C.N., Coulter G.A.
Reflected overpressure impulse on a finite structure.
ARBRL-TR-02 537. 1983.

- [36] Dewey J.M., Heilig W., Reichenbach W.
Height of burst results from small scale explosions.
Proceedings MABS 9, 1985.

- [37] Newmark N.M. et al.
Principles and practises for design of hardened structures.
U.S. Department of Commerce, AB-295 408, 1962.

Annex I

Single-degree-of-freedom system

In this annex the response of a single-degree-of-freedom system to certain types of load will be determined. The differential equation of motion of a single-degree-of-freedom system, with a linear spring characteristic, is as follows:

$$M \ddot{x} + K \cdot x = F_b(t) \quad (I-1)$$

(See Figure 11 and Equation (13)).

The solution of the homogeneous equation :

$$\ddot{x} + \omega^2 \cdot x = 0 \quad (I-2)$$

with

$$\omega^2 = \frac{K}{M} \quad (I-3)$$

is given by :

$$x(t) = C_1 \cdot \sin \omega t + C_2 \cdot \cos \omega t \quad (I-4)$$

The constants C_1 and C_2 are determined by the initial conditions. For example, if for $t = 0$ there is a displacement $x(0) = x_0$ and an initial velocity $\dot{x}(0) = \dot{x}_0$, we then have:

$$x(t) = \frac{\dot{x}_0}{\omega} \cdot \sin \omega t + x_0 \cdot \cos \omega t \quad (I-5)$$

The full solution of (I-1) can be found by adding a particular solution to (I-4).

For the explosive load which is here under consideration, two extreme cases must be differentiated. In the first case, the positive phase duration t_p is big versus the natural period of vibration T :

$$t_p \gg T \quad (I-6)$$

and, in the second case, the positive phase duration is small versus the natural period of vibration T :

$$t_p \ll T \quad (I-7)$$

Furthermore, for an explosive load, we must differentiate between a shock wave and a pressure wave. If we are dealing with a shock wave and a condition for which (I-6) is valid, the load is then represented by a so-called "step" load, as shown in Figure I-1.

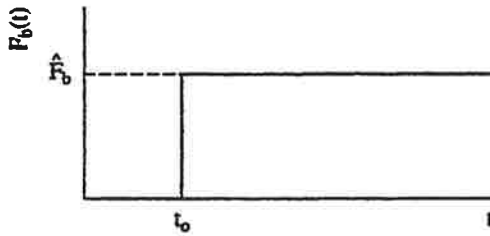


Fig. I-1 "Step" load.

For a pressure wave for each $t_p \gg T$, the progress of the load is to such a slow degree that for every moment, we are practically dealing with a static load. If $t_p \ll T$, then the load, for either a shock wave or a pressure wave can be represented by an impulse load, as shown in Figure I-2.

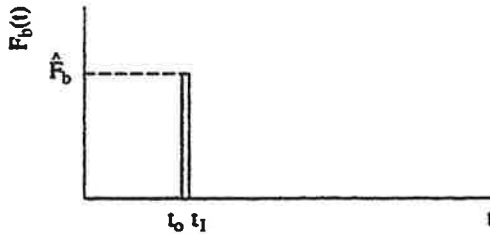


Fig. I-2 Impulse load.

The total impulse S is important for the response to either a shock wave or to a pressure wave.

The particular solution for a step load (figure I-1), acting when $t = t_0 = 0$ is equal to:

$$x = \frac{F_b}{K} \quad (I-8)$$

The initial conditions are : $x(0) = 0$ and $\dot{x}(0) = 0$, which gives :

$$C_1 = 0$$

and

$$C_2 = -\frac{\hat{F}_b}{K}$$

so that the final solution is :

$$x = -\frac{\hat{F}_b}{K} (1 - \cos \omega x) \quad (I-10)$$

The solution for an impulse load at $t = 0$ is given by the solution of the homogeneous equation, since for $t > 0$ there is no longer any external load present.

The initial velocity \dot{x}_0 is to be determined from the impulse equilibrium condition.

$$M * \dot{x}_0 = S \quad (I-11)$$

in which S represents the total impulse, so that the initial conditions are:

$$\dot{x}(0) = 0 = \frac{S}{M}$$

The solution is then :

$$x(t) = \frac{S}{M * \omega} * \sin \omega t \quad (I-12)$$

The dynamic load factor (DLF) is found by dividing the maximum dynamic displacement by the static displacement:

$$\hat{x}_{st} = \frac{\hat{F}_b}{K}$$

For a step load we find, simply DLF = 2.

The DLF for an impulse load is dependent on the shape of the load. For a shock wave we have $S = F_b * t_p$, so that:

$$DLF = \frac{\hat{F}_b * t_p}{M * \omega} * \frac{K}{\hat{F}_b} = \omega * t_p \quad (I-13)$$

For a pressure wave, we have :

$$S = \frac{1}{2} * \hat{F}_b * t_p$$

so that

$$DLF = \frac{\hat{F}_b * t_p}{2 * M * \omega} * \frac{K}{\hat{F}_b} = \frac{1}{2} * \omega * t_p \quad (I-14)$$

The variation of the DLF, as function of the ratio t_p/T , is given in Figures (14) and (15), respectively for a shock wave and for a pressure wave. With $T = 2\pi/\omega$, the values of the DLF's derived above can easily be traced back for the extreme conditions.

These values of the DLF for the extreme load conditions can also be obtained with the help of an energy consideration.

– Step load, linear elastic.

The external work A_u is equal to:

$$A_u = \hat{F}_b * x \quad (I-15)$$

The inner work A_i is equal to :

$$A_i = \frac{1}{2} * \hat{F}_v * x \quad (I-16)$$

(see Figure 13a).

with $A_i = A_u$, we simply have :

$$DLF = \frac{\hat{F}_v}{\hat{F}_b} = 2$$

– Impulse load, linear elastic

The energy transmitted by the impulse S is:

$$A_u = \frac{S^2}{2 * M} \quad (I-17)$$

For the shock wave and, respectively, for the pressure wave, we have:

$$S = \hat{F}_b * t_p \text{ resp } S = \frac{1}{2} * \hat{F}_b * t_p$$

so that (I-17) combining with (I-16) gives:

Shock wave: $DLF = \omega * t_p$

Pressure wave: $DLF = 1/2 * \omega * t_p$

For an elasto-plastic behaviour, the extreme values can be determined in an identical way. Apart from (I-15) and (I-17) we now have (Figure 13d):

$$A_i = \hat{F}_v * (x - 1/2 * \hat{x}_{el}) \quad (x > \hat{x}_{el}) \quad (I-18)$$

so that for the step load we obtain :

$$DLF = 1 - \frac{\hat{x}_{el}}{2 * x} \quad (I-19)$$

for the impulse load we can derive :

$$S = \frac{F_v}{\omega} * 2 * \frac{x}{\hat{x}_{el}} - 1 \quad (I-20)$$

so that for the shock wave we obtain :

$$DLF = \omega * t_p * \sqrt{\frac{1}{\frac{2 * x}{\hat{x}_{el}} - 1}} \quad (I-21)$$

and for the pressure wave :

$$DLF = \frac{1}{2} * \omega * t_p * \sqrt{\frac{1}{\frac{2 * x}{\hat{x}_{el}} - 1}} \quad (I-22)$$

The extreme values of the maximum load which can be absorbed, the pressure - and impulse asymptote such as defined in paragraph 4.4 (21), (22) and (23), can now be obtained from (I-19) and (I-20) with the help of

$$\frac{i}{P_{st}} = \frac{S}{F_v} \quad (I-23)$$

and

$$Du = \frac{\hat{x}}{\hat{x}_{el}} \quad (I-24)$$

Annex II

Raleigh method

The Raleigh method will be applied for the determination of the natural frequency for a freely mounted girder and a freely mounted plate.

The vibration of a girder can be expressed as follows:

$$w(x, t) = P * f_o(x) * \sin \omega t \quad (\text{II-1})$$

where

$w(x, t)$: the deflection, as function of location and time

$f_o(x)$: the deflection due to a unit load

p : the magnitude of the load

At time $t = 0$ the displacement is zero and the kinetic energy is at a maximum:

$$E_k = \frac{1}{2} * m * \int_0^1 \left(\frac{\partial w(x, t)}{\partial t} \right)^2 dx \quad (\text{II-2})$$

where: m = the mass of the girder per unit length

l = the length (span) of the girder

The equation can also be written as:

$$E_k = \frac{1}{2} * m * P^2 * \omega^2 * \int_0^1 f_o(x)^2 dx \quad (\text{II-3})$$

At the time

$$t = \frac{\pi}{2}$$

the velocity is zero and all of kinetic energy is connected into potential energy E_p .

The potential energy is described by:

$$E_p = \frac{1}{2} * P * \int_0^1 w(x, t) dx \quad (\text{II-4})$$

or, otherwise written :

$$E_p = \frac{1}{2} * P^2 * \int_0^1 f_o(x) dx \quad (\text{II-5})$$

Since we have $E_p = E_k$ we obtain :

$$\omega^2 = \frac{\int_0^1 f_o(x) dx}{m * \int_0^1 f_o^2(x) dx} \quad (\text{II-6})$$

If now a bulge form is chosen, the associated natural frequency can be determined. An obvious choice is:

$$f_o(x) = f_o * \sin\left(\frac{\pi * x}{1}\right) \quad (\text{II-7})$$

in which f_o is the maximum deflection.

Substituting (II-7) into (II-6) gives:

$$\omega^2 = \frac{4}{m * f_o * \pi} \quad (\text{II-8})$$

For the maximum deflection δ by the own weight in g we have :

$$\delta = m * g * f_o \quad (\text{II-9})$$

Substitution into (II-8) gives :

$$\omega^2 = \frac{4 * g}{\pi * \delta} \quad (\text{II-10})$$

and with

$$T = \frac{2\pi}{\omega} \quad (\text{II-11})$$

follows

$$T = 1.76 * \sqrt{\delta} \quad (\text{II-12})$$

For a plate with dimensions a and b, the expression for the natural frequency becomes:

$$\omega^2 = \frac{\int_0^a \int_0^b f_o(x, y) dx dy}{m * \int_0^a \int_0^b f_o^2(x, y) dx dy} \quad (\text{II-13})$$

in which m now represents the mass per unit area.

Choosing for the bulge form:

$$f_o(x,y) = f_o * \sin \frac{\pi x}{a} * \sin \frac{\pi y}{b} \quad (\text{II - 14})$$

and substituting into (II - 13), jointly with (II - 11), we find :

$$T = 1.58 * \sqrt{\delta} \quad (\text{II - 15})$$

Annex III

Comparison of Jarrett's Damage Criteria with Real-Scale Experiments

Experiments are described in reference [7] in which four different types of houses are subjected to an explosive load. Even though primarily typical American houses have been tested, some tests are also performed for European-type houses. Typical cavity-walled houses in the Netherlands have not been tested. An overview is given in Table III-1.

Table III-1 Types of houses tested.

Type 1:	Two-storey wooden house with a ground area of $10 \times 7,5 \text{ m}^2$, with cellars extending under the whole house. The house has a saddle-type roof.
Type 2:	Two-storey brick house, 1-brick supporting walls. Ground-area $10 \times 7,5 \text{ m}^2$. Cellar extending under the whole house; saddle-type roof.
Type 3:	One-storey wooden house with a concrete floor. The bathroom was built with 20 cm thick reinforced concrete walls.
Type 4:	Two-storey brick house with supporting walls. Ground area $12 \times 9 \text{ m}^2$; height 11 m. Sloping roof. No windows in the side walls.

For the determination of the percentage of damage, the following procedure was used: the total construction costs were broken down into costs of specific structural components, such as: roof, walls, floors, doors, windows, etc. After the tests, the percentage of damage was established for each component so that, using the cost distribution, a single percentage indicates the total damage. An overview of the percentages of damage is given in Table III-2, such as they had been ascertained for different pressure and impulse levels.

These test results can be compared with Jarrett's damage criteria shown in Figure 26, even though, in fact, such a comparison only holds good for brick houses. The test results and the criteria are combined in Figure III-1.

The test results all lie within the pressure zone of the diagram. For damage percentages in the range of 10% the damages consisted primarily the following: breakages of windows, caved-in doors and slight roof damage.

In the cost distribution, the foundation, represents about 20%. For damage percentages in the range of 80% the foundations had been only slightly damaged. Accordingly, the dwelling can be regarded as collapsed.

Even though only a few brick houses have been tested, the agreement between test results and criteria is good.

Table III-2 Test results.

Type	Pressure P_s (kPa)	Impulse i_s (Pas)	Damage (%)
1	12.4	6.200	13.7
	34.0	12.000	81.6
	27.6	11.000	35.6
	17.9	7.900	17.7
	0.9	324	5.2
	0.8	300	6.5
	0.76	1.276	5.6
	11.0	1.110	10.8
	18.6	2.340	25.2
2	11.7	5.790	10.9
	35.2	12.760	81.4
3	13.1	5.790	11.7
	35.2	12.800	81.6
4	24.8	3.585	23
	59.3	6.340	53

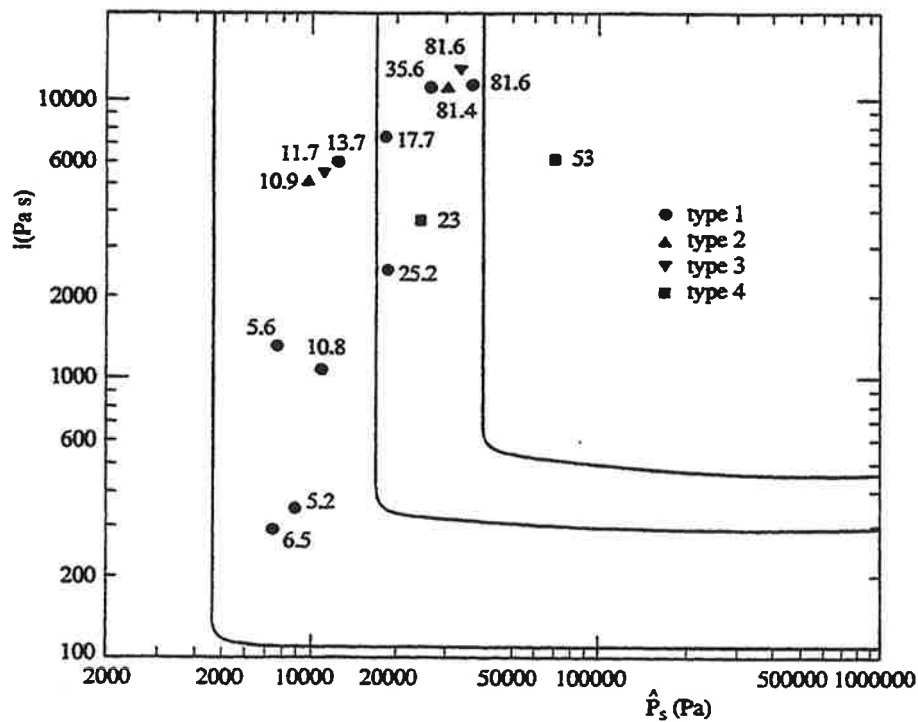


Fig. III-1 Comparison of criteria and test results.

Annex IV

Probit functions

With the help of probit functions,

$$\text{where } Pr = C_1 + C_2 * \ln V \quad (IV-1)$$

Pr = the probit
 C_1 and C_2 : constants
 V : a variable

Depending on the value of the variable V , it is possible to determine a percentage indicating the probability of a defined occurrence.

The percentage corresponding to a defined value of the probit Pr is given in Table IV-1:

Table IV-1 Relationship between probabilities and probits.

%	0	1	2	3	4	5	6	7	8	9
0	—	2.67	2.95	3.12	3.25	3.36	3.45	3.52	3.59	3.66
10	3.72	3.77	3.82	3.897	3.92	3.96	4.01	4.05	4.08	4.12
20	4.16	4.19	4.23	4.26	4.29	4.33	4.36	4.39	4.42	4.45
30	4.48	4.50	4.53	4.56	4.59	4.61	4.64	4.67	4.69	4.72
40	4.75	4.77	4.80	4.82	4.85	4.87	4.90	4.92	4.95	4.97
50	5.00	5.03	5.05	5.08	5.10	5.13	5.15	5.18	5.20	5.23
60	5.25	5.28	5.31	5.33	5.36	5.39	5.41	5.44	5.47	5.50
70	5.52	5.55	5.58	5.61	5.64	5.67	5.71	5.74	5.77	5.81
80	5.84	5.88	5.92	5.95	5.99	6.04	6.08	6.13	6.18	6.23
90	6.28	6.34	6.41	6.48	6.55	6.64	6.75	6.88	7.05	7.33
—	0.0	0.1	0.3	0.3	0.4	0.5	0.6	0.7	0.8	0.9
99	7.33	7.37	7.41	7.46	7.51	7.58	7.65	7.75	7.88	8.09

In the following chapters probit functions are derived for different damage criteria.

IV-1. Jarrett's Damage Criteria

We make use of Figure 26. V is determined by:

$$V = \left(\frac{P'_s}{P_s} \right)^{\alpha_1} + \left(\frac{i'_s}{i_s} \right)^{\alpha_2} \quad (IV-2)$$

where α_1 and α_2 are constants to be more closely defined, and P'_s and i'_s are limit values to be chosen for P_s and i_s .

The limit values for the criteria given in Figure 26 are shown in Table IV-2.

Table IV-2. Limit values.

	P_s' (Pa)	i_s' (Pa s)
Slight damage	4600	110
Structural damage	17500	290
Collapse	40000	460

The probit function for slight damage is determined by assuming that a 50% probability of slight damage exists with the criterium for slight damage and a probability of 90% exists with the criterium for structural damage.

The following is selected:

$$V = \left(\frac{4600}{P_s} \right)^{\alpha_1} + \left(\frac{110}{i_s} \right)^{\alpha_2} \quad (\text{IV-3})$$

The constants α_1 and α_2 are defined such that for the line for slight damage from Figure 26 the value $V = 1$ is approximated to as closely as possible.

This gives: $\alpha_1 = 3.9$ and $\alpha_2 = 5.0$.

The average value of V determined, with these data, for the 90% line is $V = 0.0068$. With Table IV-1 we have:

$$\begin{aligned} 50\%: 5.00 &= A + B \ln 1, \text{ and} \\ 90\%: 6.28 &= A + B \ln 0.0068 \end{aligned}$$

from which A and B can be determined.

The probit function for slight damage is, thus:

$$Pr = 5 - 0.26 * \ln V \quad (\text{IV-4})$$

with

$$V = \left(\frac{4600}{P_s} \right)^{3.9} + \left(\frac{110}{i_s} \right)^{5.0} \quad (\text{IV-5})$$

For the determination of the probit function for structural damage it is assumed that a 50% probability exists with the criterium for structural damage and a probability of 90% with the collapse criterium. Using a procedure identical to the one for the determination of the probit function for slight damage, we find:

$$Pr = 5 - 0.26 * \ln V \quad (\text{IV-6})$$

with

$$V = \left(\frac{17500}{P_s} \right)^{8.4} + \left(\frac{290}{i_s} \right)^{9.2} \quad (\text{IV-7})$$

The probit function for collapse is determined by assuming that a 10% probability exists with the criterium for structural damage and a 50% probability with the collapse criterium. The probit function is determined in the same manner as previously.

$$Pr = 5 - 0.22 * \ln V \quad (IV - 8)$$

with

$$V = \left(\frac{40.000}{P_s} \right)^{7.4} + \left(\frac{460}{\bar{i}_s} \right)^{11.3} \quad (IV - 9)$$

IV-2. Probit function for collapse of tall apartment-buildings

Depending on the shape of the blast wave, the probit function is determined for, respectively, a shock wave and a pressure wave. It is assumed that a 50% probability of collapse exists if the pressure-impulse combination requires a ductility $Du = 5$; a 10% probability of collapse arises for $Du = 1$ and a 90% probability of collapse for $Du = 10$.

The limit values, for a shock wave, of P and i are assembled in Table IV-3 (see Figure 19):

Table IV-3 Limit values in relation to a shock wave.

Probability	\bar{p}	\bar{i}
10%	0.5	1
50%	0.9	3
90%	0.95	4.36

Assuming that for a 50% probability the value of V must approach 1, it is determined that:

$$V = \left(\frac{0.9}{\bar{P}} \right)^{1.4} + \left(\frac{3}{\bar{i}} \right)^{2.7} \quad (IV - 10)$$

The average value of V in respect of a 90% probability amounts to:

$V = 0.65$, so that

$5.0 = A + B * \ln 1$, and

$6.28 = A + B * \ln 0.65$, it leads to:

$$Pr = 5 - 2.92 * \ln V \quad (IV - 11)$$

The limit values for a pressure wave are assembled in Table IV-4 (See Figure 18):

Table IV-4 Limit values by a pressure wave.

Probability	\bar{p}	\bar{i}
10%	1	1
50%	1	3
90%	1	4.36

Since the limit values for \bar{P} all approach 1 it is not easily possible to determine a probit function. For this reason, for the limit values those values are arbitrarily taken which are associated with a scaled impulse $\bar{i} = 12$. Adopted are:

Probability 10%: $\bar{p} = 1$

Probability 50%: $\bar{p} = 1.25$

Probability 90%: $\bar{p} = 1.5$

In the same manner as above it can be determined that:

$$V = \left(\frac{1.25^{1.9}}{\bar{P}} \right) + \left(\frac{3}{\bar{i}} \right)^{2.5} \quad (\text{IV - 12})$$

and

$$Pr = 5 - 2.14 * \ln V \quad (\text{IV - 13})$$

IV-3. Window breakage

A distinction is drawn between windows in relatively old buildings and windows in more modern buildings.

It can be assumed that for windows in older buildings a 1% probability of breakage exists at a pressure of $P_s = 1$ kPa, and a probability of 50% at a pressure of $P_s = 3$ kPa. The constants A and B can be easily determined. This gives:

$$Pr = -11.97 + 2.12 * \ln P_s \quad (\text{IV - 14})$$

In newer buildings the 1% probability exists at a pressure of $P_s = 2$ kPa and the 50% probability at a pressure of $P_s = 5$ kPa. This gives:

$$Pr = -16.58 + 2.53 * \ln P_s \quad (\text{IV - 15})$$

Annex V

Accuracy of models for determining the explosion effects on structures

A. Damage to buildings less than four storeys high

Three probit functions have been established for damages to houses less than four storeys high ((52) to (57) incl.).

The probability of a defined occurrence is determined solely by the parameters of the undisturbed blast wave at the site of the construction under consideration. In principle, the parameters can assume any value, depending on the distance to the explosion and the nature and force of the explosion. In reality, however, the blast wave will not remain undisturbed: reflections and reliefs will occur. In the determination of the probit functions, the type of house is not taken into account. Also, consequently, these functions are only applicable to, for instance, an entire housing estate and certainly not to the case in which only one house is considered.

For all possible P-i combinations zones should be indicated, in which either the pressure P, or the impulse i is determinant. In the review which follows we will take a closer look at this.

1. Slight damage

The pressure determines the damage where the impulse is greater than about $290 \text{ Pa} \cdot \text{s}$.

Probability (%)	P_s (kPa)
10	1.3
50	4.6
90	17.5

If the pressure is greater than 17.5 kPa then the impulse determines the damage:

Probability (%)	i (Pa * s)
10	40
50	110
90	290

2. Structural damage

Pressure zone ($i > 460 \text{ Pa} \cdot \text{s}$)

Probability (%)	P_s (kPa)
10	10
50	17.5
90	40

Impulse zone ($P_s > 40$ kPa)

Probability (%)	i (Pa * s)
10	170
50	290
90	460

3. Collapse

Pressure zone ($i > 770$ Pa * s)

Probability (%)	P_s (kPa)
10	17.5
50	40
90	85

Impulse zone ($P_s > 85$ kPa)

Probability (%)	i (Pa * s)
10	290
50	460
90	770

For the remaining combinations of pressure and impulse, both quantities determine the damage.

B. Damage to buildings more than four storeys high

For damages to buildings more than four storeys high, the functions for slight and structural damage are identical to the ones for low buildings. For the collapse probabilities of tall buildings two functions are given. The choice between the two is dependent on the shape of the blast ((58) to (61) incl.).

The influence of the diagrammatic representation of the blast by a triangular pattern can be examined by substituting the actual form of the pressure pattern into the single-degree-of-freedom system. This influence will probably be greater in the case of a pressure wave originating from a gas explosion, where a large scale of pressure patterns can occur. What the shape of a pressure wave form in the event of an explosion will be is difficult to predict. Therefore, the question will always remain: which precise form must be taken into consideration?

The probability of a defined quantity of damage, for both types of wave shapes, is determined by a scaled pressure, a scaled impulse and by the ductility of the structure under consideration.

1. Influence of ductility

Very little is known about the ductility of buildings. In the determination of probabilities we have assumed that an average value of 5 can be adopted for the ductility of buildings, so that for a pressure-impulse combination which requires a ductility of 5 in order to prevent collapse still a 50% collapse will nevertheless occur. We have also assumed that if a ductility equal to 1.0 is required, there is still a 10% collapse possibility, and a 90% collapse possibility for a ductility equal to 10. The influence of ductility is of importance within the impulse zone of a shock or pressure wave (Figures 18 and 19). If the ductility of a specific structure is equal to 10 instead of 5, then, for a pressure-impulse combination of under concern, the probability of collapse will, for instance, reduce from 90% to 50%.

2. Influence of pressure and impulse

The pressure and impulse zones, for a shock wave, according to the probit functions (58) and (59) are:

Pressure zone ($\bar{i} > 10$)

Probability (%)	\bar{P}
10	0.65
50	0.9
90	1.2

Impulse zone ($\bar{P} > 4$)

Probability (%)	\bar{i}
10	2.6
50	3
90	3.5

In the case of a pressure wave, there is no real pressure zone to distinguish. For all values of the ductility (and thus probability) the scaled pressure is close to 1. The effect, then, is determined by the scaled impulse in the case where the scaled pressure is greater than about 3 (impulse zone).

The scaled pressure and impulse are determined by the parameters of the blast (pressure and impulse) and by the static strength and natural frequency of the structure.

The difficulty in determining the blast parameters has already been discussed in the introduction. We will now take a closer look at the influence of the parameters of the structure itself.

3. Influence of Natural Frequency

A formula which allows us to determine the natural frequency on an overall basis is given in (29). Figure 23 gives us an idea about the spread of the values: a 50% deviation from the average can easily occur. Other formulae, however, are also available for specific types of structures. It can be expected, consequently, that a lesser spread will occur then.

The natural frequency is only of importance in relation to the scaled impulse and, as a consequence, the influence of a variation of the natural frequency is greatest within the impulse zone. If, within the impulse zone, there is a 50% collapse probability, then, in turn, a 50% variation in the natural frequency can decrease this probability to less than 10% or, to the contrary, increase it to more than 90%.

We must note that the probit functions represent approximations of Figures 18 and 19. In the example which has been presented of the use of these figures a 50% change of the natural frequency can, in turn, modify the collapse probability to values varying from 10% to 90%.

Generally, however, the pressure-impulse combinations originating from a gas cloud explosion will lie within the pressure zone, so that the influence of the natural frequency, in these conditions, will be substantially less pronounced.

4. Influence of Static Strength

A parameter which we also must consider is the static strength of the structure. This static strength has an influence on the scaled impulse and also on the scaled pressure. Due to the fact that the influence on scaled impulse is as great as that of the natural frequency (see (19)), this static strength can be of major importance with regard to collapse probabilities, for all pressure-impulse combinations.

The spread in the values of the static strength is due to the spread of the values of the strength of the materials. An estimation of the latter gives 10% to 25%. We will now examine the influence of a 25% variation of the static strength on collapse probabilities for a pressure-impulse combination which does not lay within the pressure or impulse region. Such a combination is $\bar{P} = 2$ and $\bar{i} = 3$ (Figure 18). The collapse probability is 20%. For $\bar{P} = 2.5$ and $\bar{i} = 3.75$ the probability is 76%, and for $\bar{P} = 1.5$ and $\bar{i} = 2.25$ the probability is less than 1%.

Chapter 3

The consequences of Explosion effects on humans

Summary

In this report the effects on humans submitted to the phenomena of an explosion are investigated.

For the phenomena blast and whole-body displacement, pressure-impulse graphs are given to determine the probability of survival.

The effects of fragments and debris are given in such a way that one is able to determine whether a fragment will cause severe injuries depending on the mass, velocity and shape of the fragments or piece of debris.

The effects of the collapse of a building are given in some broad figures about the amount of the death and injuries.

For all the phenomena, except for the last one, probit functions are presented with which one is able to determine survival probabilities.

Contents

	Page
LIST OF SYMBOLS USED	5
1. Introduction	6
1.1 Introduction	6
1.2 Identification chart	7
2. Blast effects	10
2.1 Lung Damage	11
2.1.1 Pressure-Time graph	11
2.1.2 Pressure-Impulse graph	14
2.2 Damage to Hearing	16
3. Effects of whole-body displacement phenomena	18
3.1 Criteria	18
3.2 Pressure-Impulse graphs	19
4. Effects of fragments and debris	23
4.1 Fragments	23
4.2 Debris	25
4.3 Injury Criteria	26
4.4 Glass fragments	27
5. Collapse of buildings	29
5.1 Consequences for humans	29
6. Examples	30
6.1 Example 1	30
6.2 Example 2	32
6.3 Example 3	32
7. Conclusions	33
References	34
Appendix I: Probit Functions	36
Appendix II: Accuracy of the Models for the Determination of the Effects of Explosions on humans	41

List of symbols used

A	: Surface area	[m ²]
a	: constant	[-]
b	: constant	[-]
C	: viscous drag coefficient	[Pa.s.m ⁻¹]
DLF	: dynamic load factor	[-]
f	: viscous drag of skin	[Pa]
f ₀	: constant viscous drag	[Pa]
i	: scaled impulse i	[Pa ^{1/2} .s.kg ^{-1/3}]
i _m	: impulse of the whole-body displaced person	[Pa.s]
i _s	: impulse of the incident pressure or shock wave	[Pa.s]
k	: shape factor of a fragment	[kg.m ⁻³]
m	: mass	[kg]
P	: peak overpressure exerted in the person or structure	[Pa]
P _r	: reflected peak overpressure	[Pa]
Pr	: probit	[-]
P _s	: peak overpressure in the incident pressure or shock wave	[Pa]
P _{st}	: static strength of the window pane	[Pa]
P ₀	: atmospheric pressure	[Pa]
Q	: dynamic pressure or thrust pressure	[Pa]
S	: variable	[-]
t	: time	[s]
t _p	: positive phase duration	[s]
u	: velocity of particles	[m.s ⁻¹]
V	: variable	[-]
v	: velocity	[m.s ⁻¹]
V _m	: velocity of whole-body displacement	[m.s ⁻¹]
V ₀	: impact velocity of a fragment or piece of debris	[m.s ⁻¹]
v ₅₀	: impact velocity whereby 50% of the fragments penetrate	[m.s ⁻¹]
x	: maximum penetration depth	[m]
ρ ₀	: air density at atmospheric pressure	[kg.m ⁻³]
ρ ₁	: air density in the shock or pressure wave	[kg.m ⁻³]

Superscripts

\bar{x}	: scaled x
x'	: limit value of x

1

Introduction

The consequences of an explosion represent a potential danger to man. In order to be able to assess to what extent these consequences are acceptable and, any consequences to man can be limited, it is necessary to obtain a good idea about the explosion effects on man.

In this chapter the consequences to man of the following effects occurring in an explosion will be investigated: blast, whole-body displacement (persons displaced), fragments and debris and collapse of buildings. The effects of heat radiation will be dealt with in a separate chapter.

1.1 Introduction

It is usual to divide the explosion effects into a number of categories. A main division consists in differentiating direct and indirect effects.

a) Direct or primary effects

The pressure change caused by the blast can cause injury to the sensitive human organs.

b) Indirect effects

The indirect effects are always, sub-divided into secondary and tertiary effects.

– Secondary effects

Consequences due to fragments and debris represent this term. These fragments can originate directly from the source of the explosion, but they can also come from objects located in the surroundings of the source of the explosion which, due to the blast wave, are thrown away.

– Tertiary effects

As consequence of the blast and associated explosion wind, people may undergo whole-body displacement and collide with stationary objects or structures (total body impact).

An injury which can occur as a result of this impact belongs to the category of tertiary effects.

One of the reasons for the distinction between direct and indirect effects is that, for direct effects, it is assured that a human being will be subjected to the pressure increase. By indirect effects, on the other hand, there is only a possibility that a person might be hit by fragments or debris, or that a person who undergoes a whole-body displacement may collide with an obstacle.

An effect which falls outside of the usual classification, but must certainly be considered, is the possible injury to people inside a building when, the building either partially or completely collapses as a result of an explosion.

Identification Chart

The consequences of an explosion to man can be determined with the help of the identification chart presented in Figure 1. The numbers on the chart refer to the explanation below. The section used to determine the data in question is indicated between brackets.

re 1

The position of the person for whom the consequences must be determined is important. A distinction must be made between people located inside a building and people located in the open air.

re 2

For people in the open air there are three effects of which, the influence on people, must be determined. The effect of heat radiation will not be discussed here, since this subject will be dealt with in a separate chapter. For the consequences of a sudden pressure increase, the blast, it will be assumed that the time-pressure pulse of a shock or pressure wave is known, so that the peak overpressure, the positive phase duration and the impulse can be determined at arbitrary distances from the center of the explosion (to be determined with [17])

re 3

For the determination of the direct blast effects, the orientation of the person in question in relation to the direction propagation of the increase in pressure is important. The pressure exerted on a person is influenced by this orientation (2.1.1).

re 4

In two out of three possible orientations, reflection and flow around, the exerted pressure is not equal to the incident pressure of the blast. The exerted pressure can be calculated with the help of the formulae given in this report (2.1.1 formula (3) to (7) incl.).

re 5

From data taken from literature the probability of survival can be determined for the so-called direct effects of the blast: [lung injury: (8),(9) and Figure 7 from 2.1.1 or probit functions (10) and (11). Injury to the ears: Figure 8 and probit function (12)].

re 6

If the orientation of the person exposed is such that flow around him takes place, total body-impact by the explosion wind can occur. The probability of survival, after the collision of the body with a rigid obstacle, can be determined with the help of: [3.2 Figures 10 and 11, or probit functions (17) and (19)].

These so-called tertiary effects must be combined with the primary effects (Example 1).

re 7

The effects of fragments and debris, the so-called secondary effects, must be determined on the basis of their mass, velocity and shape. These quantities are assumed to be known in this chapter (to be determined for example with [17]).

The probability whether a person will or will not be hit by a fragment or piece of debris is not examined.

It will be shown which mass and velocity of a fragment or debris can be critical in the sense that serious injuries with fatal consequences will occur (fragments: 4.1, Formula (25) and Figure 14. Debris: 4.2 Table IV.]. Assuming that a person has been hit by a fragment or a piece of debris, the probability of survival, can be estimated (4.3 probit functions (26), (27), (29), and figure 15).

re 8

Based on a comparison with buildings which collapsed due to earthquakes, it will be possible to give broad percentages for the number of deaths (section 5).

re 9

For an estimate of the probability of survival of people hit by glass fragments a separate probit function has been given (4.4).

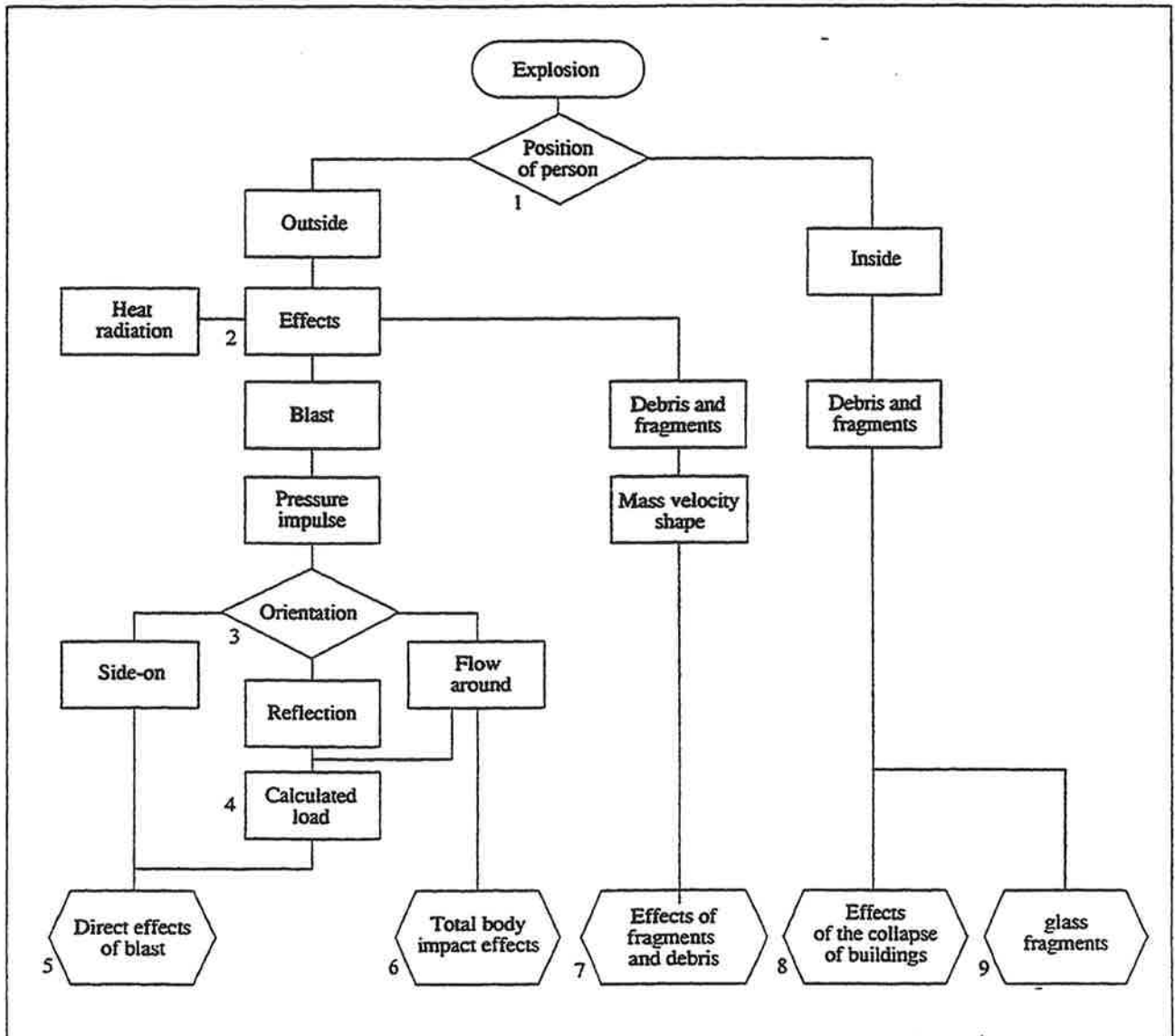


Fig. 1: Identification Chart.

Blast effects

One of the effects of an explosion is blast. This blast consists of a rapid increase in pressure which moves away from the center of the explosion at a specific velocity. Depending on the time required to reach the maximum overpressure, the blast is called either a shock wave or a pressure wave. If the pressure increase is instantaneous we are dealing with a shock wave. If, on the other hand, a certain rise time is required before peak overpressure is reached, we are dealing with a pressure wave. After the overpressure has reached its peak value, it begins to decrease again to zero and even becomes negative for some time. The magnitude of the underpressure is generally slight in comparison with the peak overpressure, and can generally be neglected.

The pressure-time curve of a shock wave or of a pressure wave is often simplified, schematically, to a triangle (Figure 2).

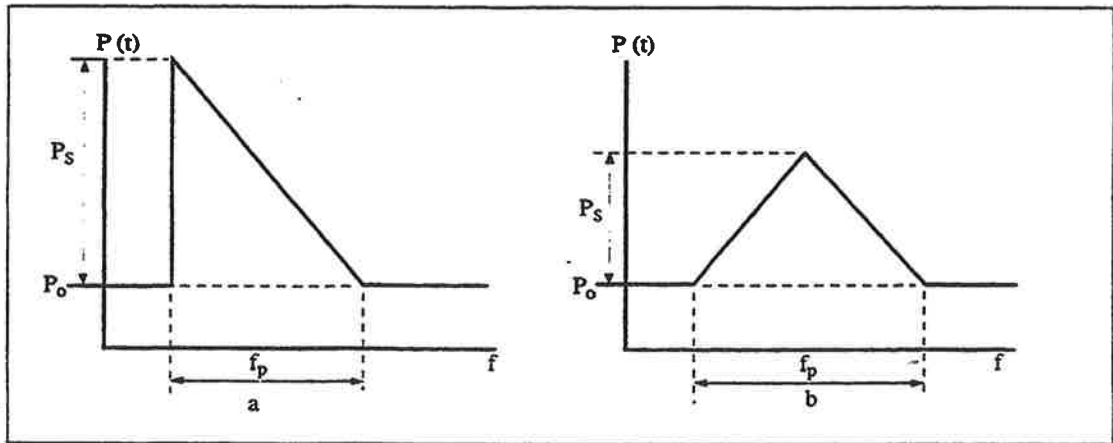


Fig. 2: Schematic simplified pressure-time curve:

a: for a shock wave

b: for a pressure wave.

The most important characteristics of a shock or pressure wave are: the peak overpressure P_s , the positive phase duration t_p (time period in which a pressure rise occurs), and the impulse. The impulse is equal to:

$$i_s = \int_{t_p} (p_s(t) - p_o) dt \quad (1)$$

Using the schematic simplified pressure-time curve, the impulse, for both shock wave or pressure wave, is then equal to:

$$i_s = \frac{1}{2} * P_s * t_p \quad (2)$$

The human body is easily capable of adapting to large changes in pressure. The condition for it is, however, that this pressure change must take place gradually, so that it can be compensated by a pressure change in the organs in which is air. If this change is sudden, a pressure difference arises which can lead to the damage of these organs.

The most vital organs which contain air are the lungs. In the available literature most attention is given to lung damages, since lung damage can provoke death. A less vital organ, however most sensitive to pressure changes, is the ear.

2.1 Lung Damage

When a pressure difference arises between the inside and the outside of the lungs, the outer pressure is generally higher, than the inner pressure in the case of an explosion. Due to this, the thorax is pressed inwards, which can lead to lung damage. Since this "pressing inwards" process requires some time, apart from the value of the overpressure, the duration of the load is also significant.

Experiments on animals have shown that for a long term load only the magnitude of the overpressure is important, while for a short term load only the total impulse is important [4]. This is in agreement with the behaviour of structures subjected to a shock wave, whereby we are also dealing with pressure and impulse asymptotes.

This agreement has led some researchers to attempt to simplify the thorax and lungs to a mechanical system of masses coupled by springs and viscous dampers [4], [13]. It is then possible, in this manner, to select the correct parameters, whereby the results obtained with animals can be scaled for application to human.

Many criteria can be found in literature with regard to lung damage. It would appear that most publications derive their data from reference [1] or other publications by the same author.

2.1.1 Pressure-Time Graph

In Reference [1] a number of graphs is given with which the probability of survival can be determined, dependent on the maximum overpressure and the phase duration of the shock wave. These graphs are applicable to humans weighing 70 kg and at an atmospheric pressure of 100 kPa. The choice of the correct graph is determined by the position of the person versus the direction of propagation of the shock wave. The latter is necessary since the overpressure exerted on a person by a shock wave as a result of reflection and flow around him, can become greater than the maximum incident overpressure in the shock wave.

Once the actual overpressure on a person is determined, then the associated probability of survival is no longer dependent on the position of the person.

The variation in the probability of survival, in relation to the actual peak overpressure which is exerted on a person and the phase duration of the shock wave, is shown in Figure 3.

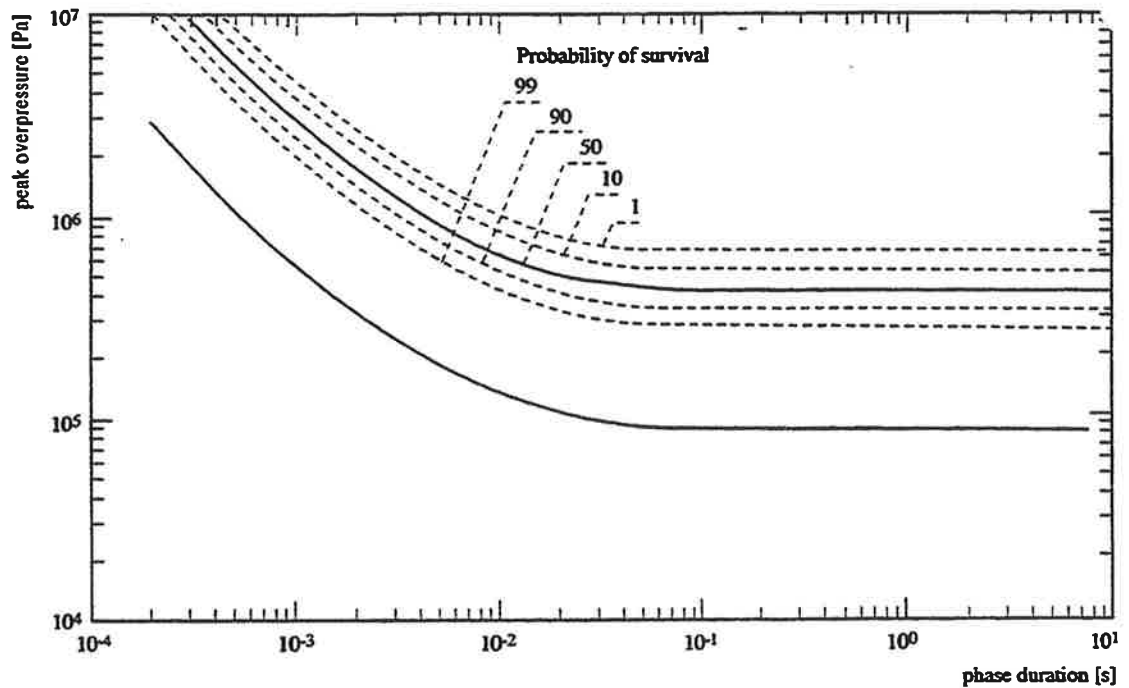


Fig. 3: Probability of survival in the case of lung damage for a person weighing 70 kg at 100 kPa atmospheric pressure [1].

Dependent on the position of the person, the peak overpressure P_s of the shock wave can be translated into the overpressure P actually exerting on this person.

Three different positions, in this respect, can be differentiated:

- a) The shock wave runs past the person without any obstruction (Figure 4). In this case, the longitudinal axis of the body lies in the direction of the shock wave.



Fig. 4: No obstruction of shock or pressure wave due to the human body.

In this case, the peak overpressure on the person is equal, to the incoming peak overpressure of the shock wave.

$$P = P_s \quad (3)$$

- b) The shock wave flows around the person (Figure 5). The longitudinal axis of the body is perpendicular to the direction of the shock wave.

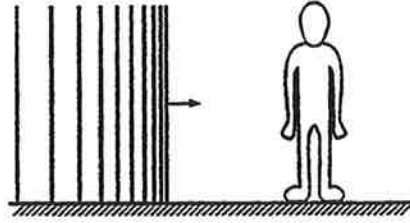


Fig. 5: Flow around the human body of a shock or pressure wave.

As a result of this flow an additional force is exerted on the person, which is called dynamic pressure or thrust pressure Q . The total overpressure exerted in this case is then:

$$P = P_s + Q \quad (4)$$

This dynamic pressure Q can be determined by the following formula [2]:

$$Q = \frac{5 * P_s^2}{2 * P_s + 14 * 10^5} \quad (5)$$

in which Q and P_s are expressed in Pascals.

c) The person is at any arbitrary position directly in front of a surface on which the shock wave reflects (Figure 6).

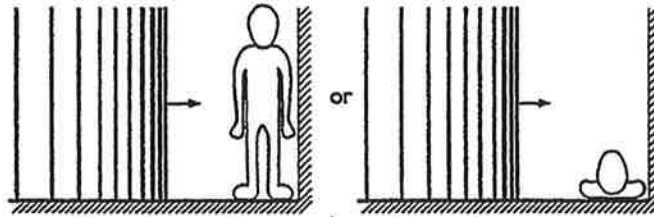


Fig. 6: Reflection of a pressure or shock wave against a surface in the immediate surroundings of a person.

The reflected pressure P_r now prevails in the area in front of the surface, hence:

$$P = P_r \quad (6)$$

This reflected pressure can be determined with [2]:

$$P_r = \frac{8 * P_s^2 + 14 * P_s * 10^5}{P_s + 7 * 10^5} \quad (7)$$

[2]

in which P_r and P_s are expressed in Pascals.

It has previously been mentioned that, instead of pressure and phase duration, often pressure and impulse are taken as parameters for damage evaluation. The results of a shock wave load are then often presented in the form of the so-called pressure-impulse graphs (P-I graphs).

Such a P-I graph is shown in Reference [2], for the case in which flow around the person takes place.

This graph is compiled using the graphs mentioned earlier from Reference [1]. A pressure-impulse graph can also be composed from the general time-pressure graph, shown in Figure 3, in a similar manner.

In Reference [2] scaling laws are derived with which it is possible to determine the probability of survival for other bodyweights and atmospheric pressures than, respectively, 70 kg and 100 kPa.

The P-I graph is shown in Figure 7.

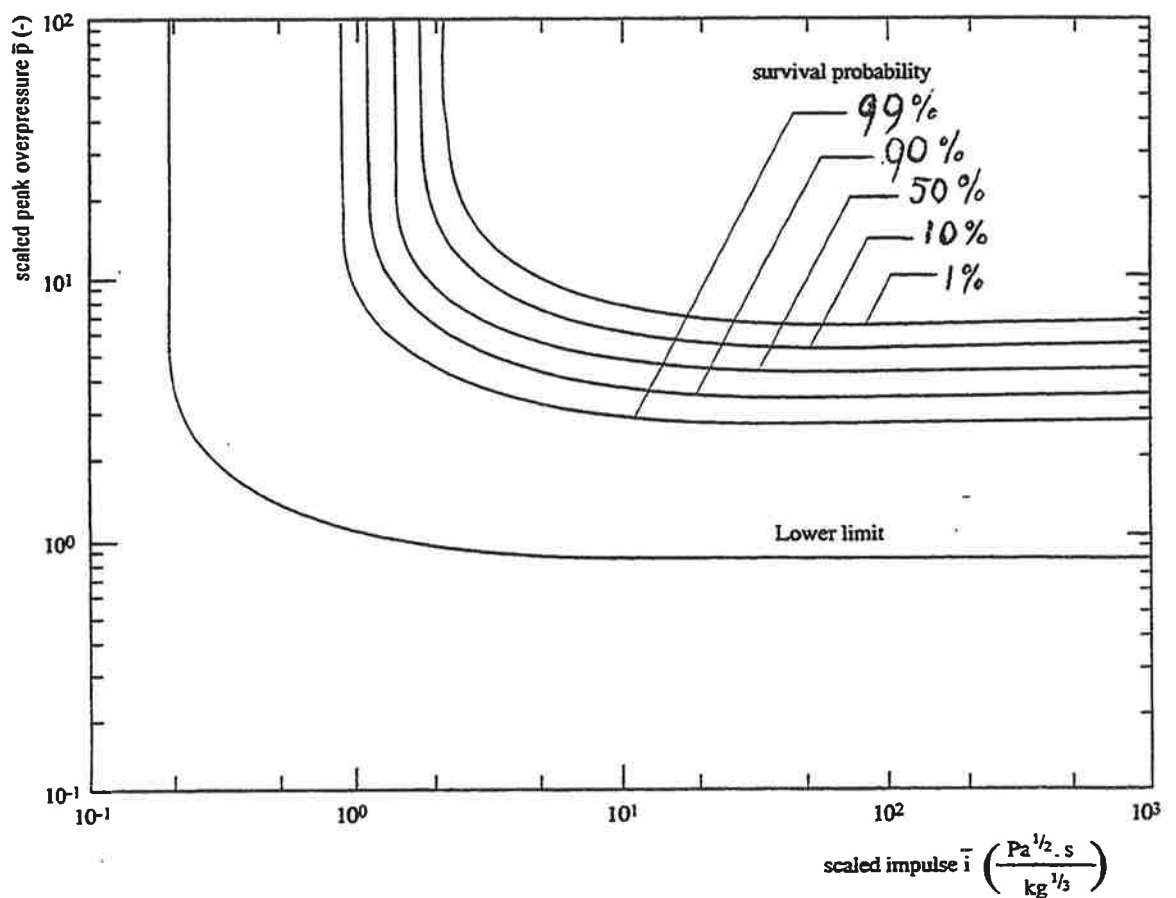


Fig. 7: Pressure-impulse graph for lung damage (processed according to [1]).

The scaled pressure \bar{P} and impulse \bar{i} are plotted in the figure as follows:

$$\bar{P} = \frac{P}{P_0} \quad (8)$$

and

$$\bar{i} = \frac{i}{p_o^{\frac{1}{2}} * m^{\frac{1}{3}}} \quad (9)$$

In which p_o is the atmospheric pressure, P the pressure exerted on a the body, m the mass of the body and i the impulse of the shock wave.

The following values of the mass are recommended in [2]:

- 5 kg for baby's
- 25 kg for small children
- 55 kg for adult women
- 75 kg for adult men

In order to be able to calculate the probability of survival analytically, Figure 7 will be approximated by a so-called probit function. With the help of the probit function a probit Pr is determined with wich, jointly with table I-1 of annex I, the probability of survival can be determined. This probability of survival is equal to 100 minus the death probability.

The probit function for lung damage is equal to:

$$Pr = 5.0 - 5.74 * \ln S \quad (10)$$

where

$$S = \frac{4.2}{\bar{p}} + \frac{1.3}{\bar{i}} \quad (11)$$

Equations (10) and (11) are derived in Annex I. The method to determine the lung damage due to a sudden overpressure can be summarized as follows:

- Determine, the peak overpressure P_s and the impulse i_s of the shock wave at the spot where the person is located.
- Determine the actual pressure exerted on the person, dependent on the position of this person.
- Determine, the scaled overpressure \bar{P} and the scaled impulse \bar{i} , dependent on the atmospheric pressure and the body weight.
- Determine the position in the P-I graph, or the probit Pr , with which the probability of survival is to be determined.

Note:

The P-I graph is applicable to shock waves. The consequences of an explosion whereby a pressure wave arises are less dangerous (4). However, no literature is known which permits us to evaluate to what extent this probability of survival is improved. Consequently, when we use Figure 7 for cases when people are exposed to a pressure wave, the probability of survival found, with this use, represents an underestimate.

The ear is a sensitive organ which reacts to very small pressure variations.

A study, described in Reference [3], shows that rupture of the ear-drum is decisive for the damage to hearing. On the basis of data from other sources, Reference [3] gives the probability of rupture of the ear-drum at a particular peak overpressure (see Figure 8).

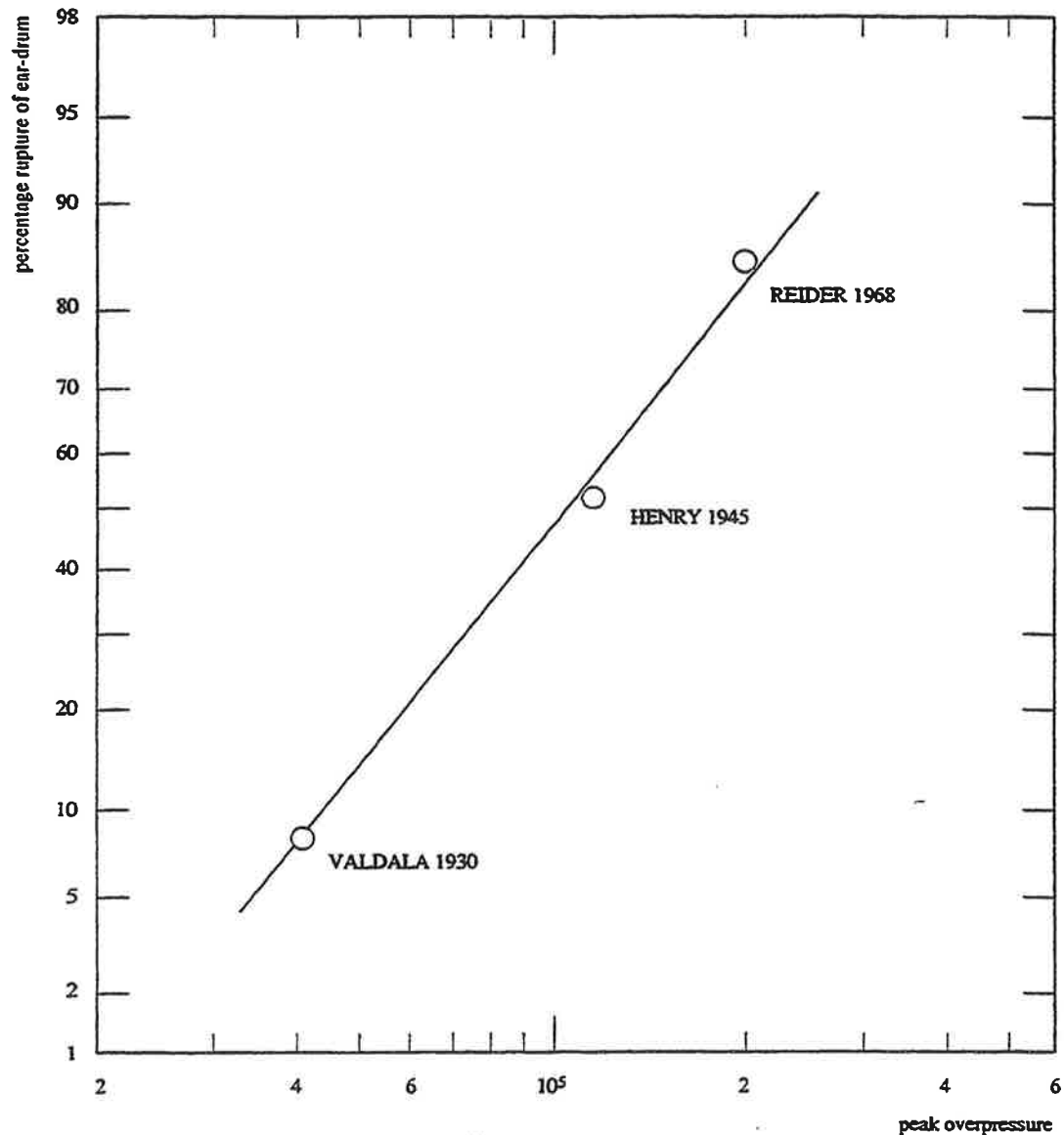


Fig. 8: Rupture ear-drum as function of the overpressure, ref. [3].

No reference data give information about the influence of the duration of the overpressure on the percentage rupture of the ear-drum. It might be expected that a pressure and impulse asymptote are also involved here.

The ear is capable to register signals with frequencies in the order of 10 kHz, which means a time duration of 0.1 ms. It therefore appears likely that a shock or pressure wave is always in the pressure range.

Also nothing is quoted in literature about the influence of flow around and reflection. However, it does appear, likely that some reflection against the body will always take place, with a short time duration. Consequently, the pressure actually exerted on the ear is the reflected pressure. Because of this, it is not necessary to adjust the values given in Figure 8 to the orientation of the person.

The probit function by which the probability of rupture of the ear-drum can be determined is:

$$Pr = -12.6 + 1.524 \ln P_s \quad (12)$$

For the derivation of Formula (12) see Annex L

Effects of whole-body displacement phenomena

The air particles behind the shock or pressure wave have a specific velocity in the same direction as the blast. As consequence of this so-called explosion wind a person can be picked up and displaced over a particular distance. Primarily, such whole-body displacement will occur if the person is standing upright, this in a position as shown in Figure 5.

During such a displacement, tumbling and sliding over a the surface can lead to injuries. There is also the possibility that, during this displacement, collision with a rigid object may take place. Any fatal consequences of the whole-body displacement are primarily caused by such collisions. The extend of these consequences majorily depends on the velocity of the impact, the hardness and shape of the object or obstacle and on the part of the human body involved in the impact.

3.1

Criteria

It is generally accepted that, in case of a collision, the skull is the most vulnerable part of the body. Due to this, criteria are given in literature whereby the probability of survival is to be determined when the skull strikes a rigid and hard obstacle. In Table I (from Reference [2]) critical impact velocities are shown which correspond to a particular probability of fracture of the base of the skull.

Table I: Probability of a skull-base fracture.

Impact Velocity (m/s)	Criterion
3.0	Safe
4.0	Threshold
5.5	50 %
7.0	Almost 100 %

The velocities quoted have been derived from the results of tests with animals.

Next to the criteria regarding impact velocities for the skull, criteria are also given for the determination of the probability of survival in the case when the entire body collides with a stiff obstacle. By these latter criteria no special part of the body is taken into consideration. (Table II from [2].

Table II: Probability of death in case of impact of the whole-body.

Collision Velocity (m/s)	Criteria
3.0	Safe
6.5	Threshold
16.5	50 %
42.0	Almost 100 %

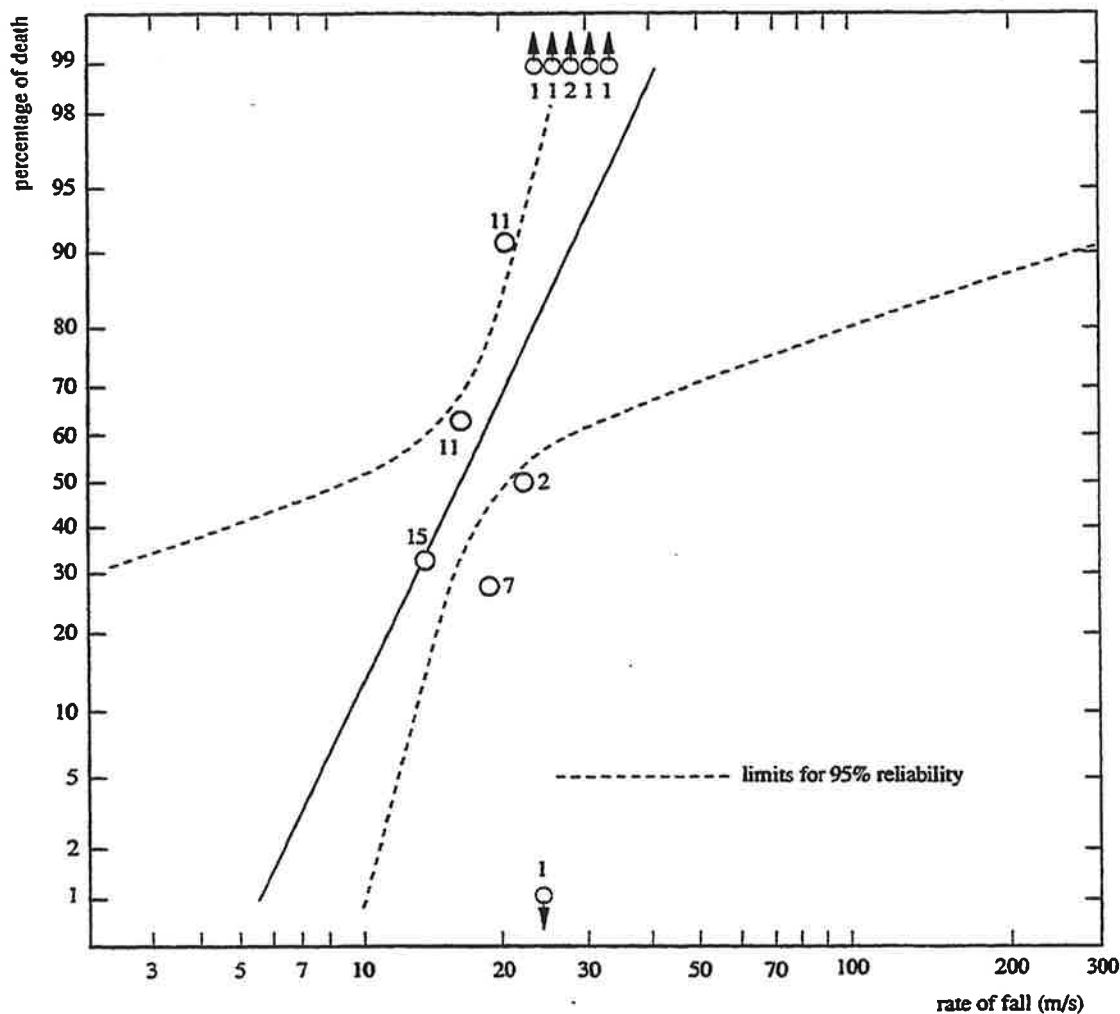


Fig. 9: Percentage deaths among persons falling on to concrete.

The figures in this graph give the number of associated cases.

It is of interest to note, that Tables I and II, both give an equal value for the impact velocity which is regarded as safe. Since the skull is more vulnerable than the rest of the body, this explains why the other velocities, in Table II, are higher than the ones in Table I. The probability, that by a collision of the whole body only the skull will be involved is smaller than one, due to which an equal effect will only take place by a higher velocity.

3.2

Pressure-Impulse Graphs

The thrust or dynamic pressure Q which is exerted by the explosion wind on a stationary object or person is equal to:

$$Q = \frac{1}{2} * C_D * \rho_1 * u^2 \quad (13)$$

where:

- C_D : the "drag" coefficient
- ρ_1 : the air density behind the blast wave, and
- u : the velocity of the particles in the wave

The acceleration \dot{v}_m with an object (or person) is subjected to, can be determined from:

$$m * \dot{v}_m = \frac{1}{2} * C_d * A * \rho_1 (u - v_m)^2 \quad (14)$$

where:

m: the mass of the displaced object (or person)

A: the surface-area perpendicular to the direction of propagation of the blast wave

The velocity of the particles u and the density ρ_1 are dependent on the atmospheric pressure p_o , the pressure P_s and the air density ρ_o of the air in front of the blast wave, according to the formulae below (see Ref. 2):

$$\rho_1(t) = \frac{7P_o + 6 * P_s * (t)}{7 * P_o + P_s * (t)} * \rho_o \quad (15)$$

and

$$u(t) = P_s(t) \sqrt{\frac{5}{\rho_o * (7 * P_o + P_s(t))}} \quad (16)$$

The maximum whole-body displacement velocity can be determined by solving the differential equation (14), after substituting (15) and (16).

The P_s and i_s combinations which correspond to the values of the whole-body displacement velocities given in Tables I and II are determined in Figures 10 and 11. The following assumptions are made in order to be able to compose these figures:

It was assumed that we are dealing with a person with a mass $m = 70$ kg, a density of 1 kg/dm^3 and a length-width ratio of 7. If we simplify the human body to a cylinder, hit surface area of a person standing upright is equal to: $A = 0.382 \text{ m}^2$.

It was further assumed that during the duration of the whole-body displacement this surface area A does not change.

The pattern of a shock wave, simplified to a triangle, is adopted for the pattern of the blast wave according to:

$$P_s(t) = P_s * \left(1 - \frac{t}{t_p}\right) \quad (17)$$

The overpressures given in Figures 10 and 11 are limited to a value of 10^6 Pa , because at higher overpressures and the impulses associated with the particular whole-body displacement velocities the model is no longer valid.

If whole-body displacement is involved the maximum whole-body displacement velocity can be determined in relation to the peak overpressure and impulse. If we further assume that a collision with a rigid object takes place at this velocity, we can also determine, the probability of lethality.

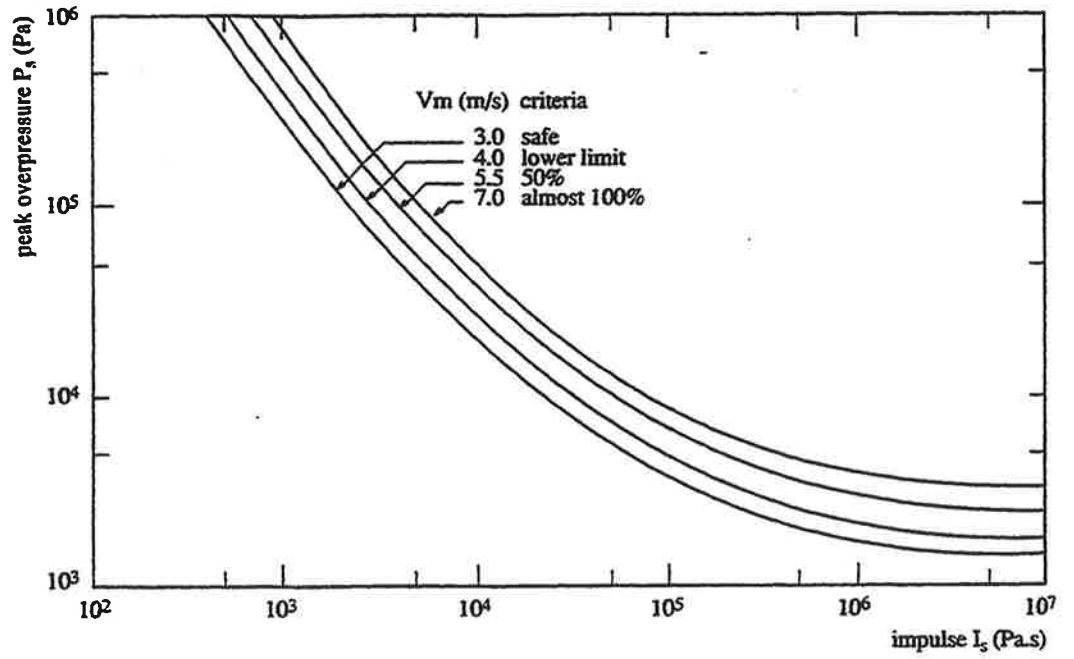


Fig. 10: P-I graph for a skull-base fracture.

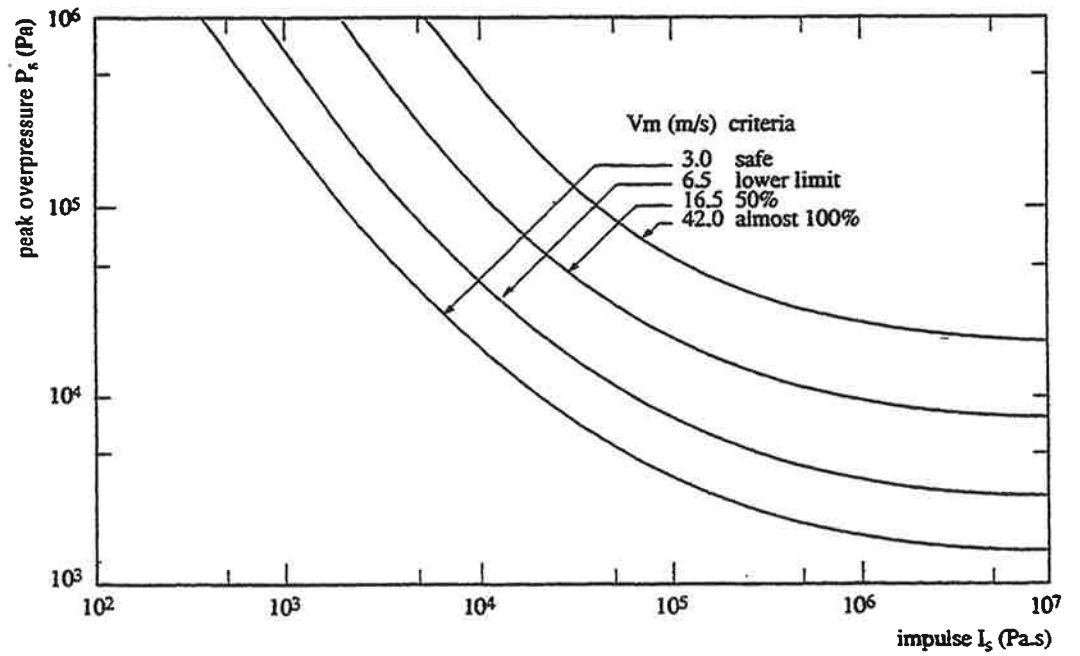


Fig. 11: P-I graph for impact of the whole body.

The probit function for the determination of the probability of survival after impact of the head is:

$$Pr = 5.0 - 8.49 \ln S \quad (17)$$

where

$$S = \frac{2.43 \cdot 10^3}{P_s} + \frac{4 \cdot 10^8}{P_s \cdot I_s} \quad (18)$$

The probit function for the determination of the probability of survival after impact with the whole body is:

$$Pr = 5.0 - 2.44 * \ln S \quad (19)$$

where

$$S = \frac{7.38 * 10^3}{P_s} + \frac{1.3 * 10^9}{P_s * i_s} \quad (20)$$

Both probit functions (17) and (19) are applicable for overpressures P_s which are lower than 0.4 to $0.5 \cdot 10^6$ Pa.

Effects of fragments of debris

An explosion can give rise to fragments which are accelerated, and which can be dangerous to people who are hit by them. These fragments can originate directly from the explosion source, but can also come from objects in the surroundings of the explosion, when such objects are subjected to the blast wave.

In discussing the effects of fragments on a human body it is mostly customary to split them into two categories: cutting and non-cutting fragments. Cutting fragments penetrate through the skin; this category is usually classified as fragments. The non-cutting fragments produce injuries due to contact pressure; this category is usually referred to as debris.

4.1 Fragments

The penetration of fragments is often determined by considering a theoretical model in which the skin is treated as an ideal rigid-viscous medium. The resistance f of such a medium, as function of the fragments velocity v , is shown in Figure 12.

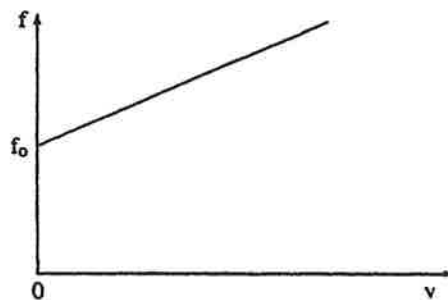


Fig. 12: Characteristics of the penetration resistance of an ideal rigid-viscous medium.

The resistance, expressed by a formula, is equal to:

$$f = f_0 + C * v \quad (21)$$

For a fragment with surface area A of the cross-section perpendicular to the direction of displacement, and a mass m , the following relationship between the penetration depth x and the impact velocity can

$$V_0 = x * C \frac{A}{m} + \frac{f_0}{C} \quad (22)$$

be used:

A review of test results conducted by several investigators is given in Reference [2]. These results are compared with the theoretical formula derived by Sperrazza and Kokinakis (Figure 13):

$$v_{50} = 1247.1 * \frac{A}{m} + 22.03 \quad (23)$$

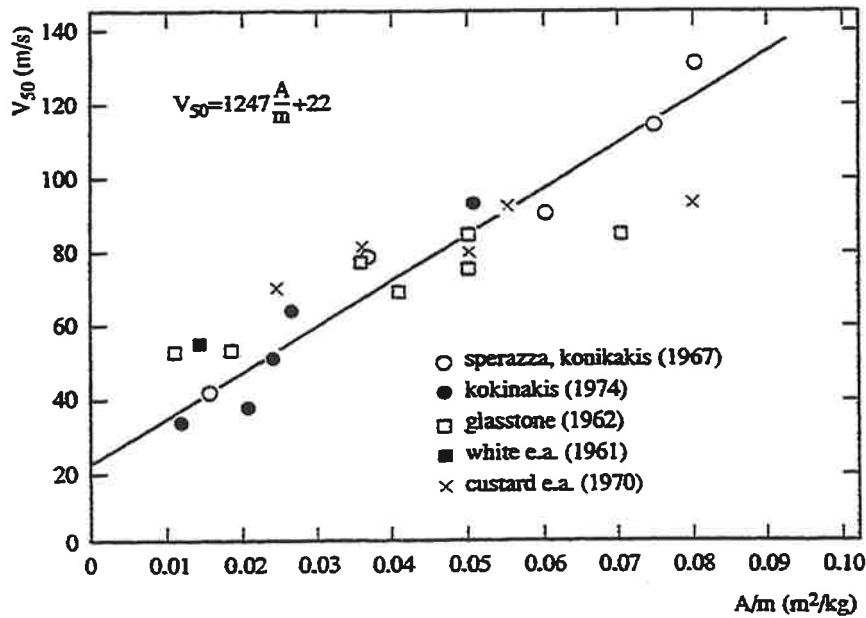


Fig. 13: Impact velocity at which 50% penetration occurs, as function of surface area-mass ratio [2].

The velocity v_{50} is defined as the impact velocity of the fragments whereby 50% of the fragments which hit the body penetrate through the skin. It is assumed that the residual velocity of the fragment which has penetrated is sufficiently high to cause severe injuries.

It is stated, in Reference [6], that serious injuries will be produced if the fragments penetrate 1 cm or more or are stopped by a bone.

The results reproduced in Figure 13 represent averages of a large number of comparable test results.

In order to characterize the shape of a projectile, the ratio A/m is not suitable, since it does not remain constant on geometric scaling.

A commonly used shape factor k , is defined as follows:

$$k = \frac{m}{A^{\frac{3}{2}}} \quad (24)$$

This shape factor is, among others, used in Reference [7]. Formula (12) can then be written as:

$$v_{50} = 1247 * \frac{1}{(k^2 * m)^{\frac{1}{3}}} + 22.03 \quad (25)$$

Some values of k are also given in Reference [7]. For naturally shaped fragments coming from bombs and projectiles k is taken equal to 2370 kg/m³, and for the most effective fragments it is taken equal to 4740 kg/m³.

Critical impact velocities of glass fragments are determined in reference [6], based on tests on animals with covered and uncovered skin. These results are presented in Figure 14.

The same reference, also gives values for v_{50} in cases when glass fragments which hit the head cause skull fracture. These values are shown in Table III, in relation to the angle of incidence and the mass m of the glass fragment.

Table III: v_{50} values for skull fracture by to glass fragments.

Mass (Kg)	Angle of Incidence (°)	v_{50} (m/s)
0.001	45	39.9 ± 3.7
0.01	180	36.3 ± 1.0
0.01	90	14.7 ± 1.2
0.01	45	10.8 ± 0.9
0.1	90	4.7 ± 0.6
0.1	45	2.7 ± 0.4

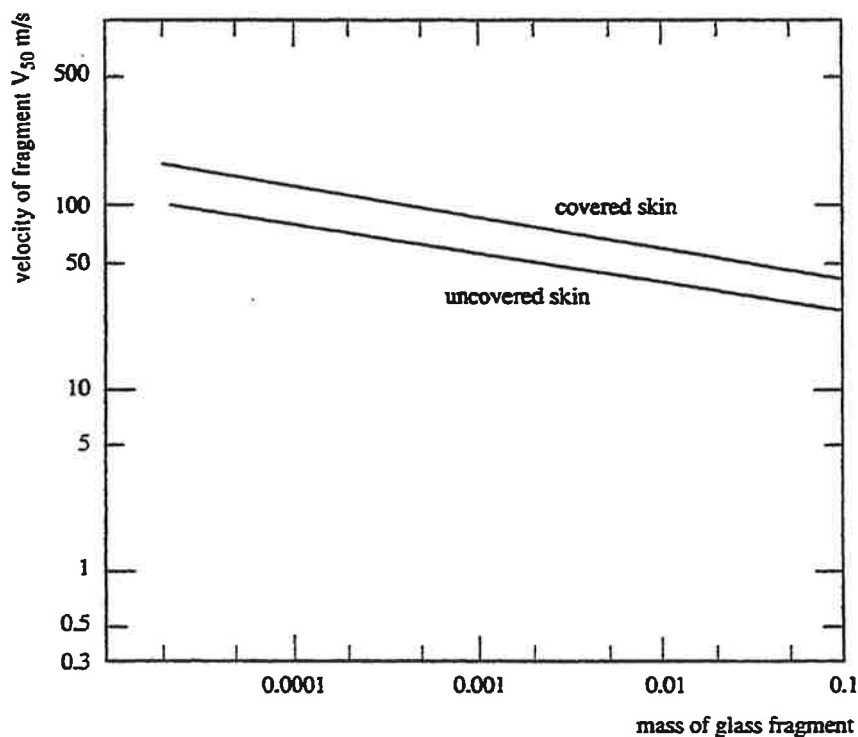


Fig. 14: Impact velocity of fragment whereby a 50% penetration occurs, as a function of the fragment mass.

4.2

Debris

Debris, causes high compressive stresses and deformations in the body when it collides with it. High stresses can lead to fractures of stiff brittle parts: the bones. Large deformations can also lead to damages of all sorts of organs, with consequent internal bleeding etc.

Since a human body represents a very complex structure, it is virtually impossible to predict, theoretically, which quantities are decisive for the injuries which will occur. Furthermore, the occurrence of an injury may, or may not, be strongly dependent on the part of the body which has been hit.

Consequently, only very general criteria can be found in literature regarding possibilities of injury due to the impact of debris on human bodies.

According to explosion safety criteria in the U.S.A., a piece of debris can be considered as dangerous if its kinetic energy is equal to 79 joules (or higher). See, for instance, Reference [7].

In a study of industrial helmets [10] it is quoted that serious injuries to the forehead can occur on the impact of fragments which have a kinetic energy between 40 and 60 joules.

In literature (also in [2]) velocities are given, for a piece of debris weighing 4.5 kg, with respect to skull-base fractures (Table IV).

Table IV: Critical velocity for the impact of a piece of debris weighing 4.5 kg against the skull.

Impact Velocity (m/s)	Criteria
3.0	Safe
4.5	Lower limit
7.0	Almost 100 %

It is interesting to note that the same velocities also result in fracture of the base of the skull in the case of a whole-body displacement in which the skull collides with a rigid object (see Table I). A 4.5 kg mass approximately coincides with the mass of the human head.

It appears then likely that the above criteria are based on the assumption that the impact of a relatively large piece of debris with the head is identical to the impact of the head against a rigid mass. Such a comparison, however, can only be made if the mass of the fragment is 4.5 kg or more. However this conclusion is not encountered anywhere in the relevant literature.

4.3

Injury Criterion

From scarce and insufficient data which are available, it is difficult to develop a clear injury criterion. The criteria previously described in Paragraphs 4.1 and 4.2 are put together in Figure 15. The impact velocity and the mass of fragments and debris are the respective coordinates in this figure. Despite the lack of adequate information, Figure 15 permits us to obtain an idea which fragments or debris may cause injuries. For fragments less than 0.1 kg the fragment criterion is decisive.

For masses between 0.1 and 4.5 kg the energy criterion governs. For masses of more than 4.5 kg the probability of skull-base fracture is predominant.

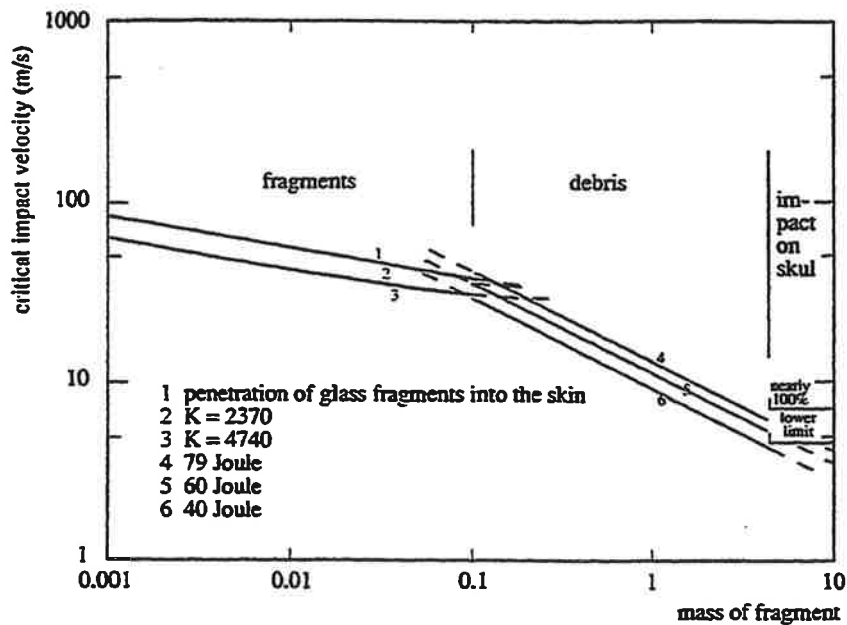


Fig. 15: Injury criterion for fragments and debris.

The probit functions for the determination of the probability of survival, for secondary effects, are as follows:

For fragment masses greater than 4.5 kg:

$$Pr = -13.19 + 10.54 \ln v_o \quad (26)$$

For fragments masses between 0.1 and 4.5 kg:

$$Pr = -17.56 + 5.30 \ln S \quad (27)$$

with

$$S = \frac{1}{2} m v_o^2 \quad (28)$$

For fragment masses between 0.001 and 0.1 kg:

$$Pr = -29.15 + 2.10 \ln S \quad (29)$$

with

$$S = m v_o^{5.115} \quad (30)$$

4.4

Glass Fragments

At a greater distance from an explosion, damages to buildings are mostly restricted to broken window panes due to the low overpressure. However, the mass and velocity of glass fragments may be sufficiently high to be able to produce injuries to people who are behind the window panes during the explosion. Consequently, injuries due to glass fragments can be incurred even at great distances from the center of the explosion. The latter is a sufficiently important reason to justify deriving a separate probit function for the effect of these glass fragments.

The initial velocity and the mass of glass fragments coming from a failing window pane depend on the dimensions of the pane (length, width, thickness) and the load on the pane. If the load is a number of

times higher than the failure load of the pane, more dangerous fragments will occur than in the case when this load is slightly greater than the failure load. A person standing right behind the pane can be hit by fragments of higher velocity than a person standing further away from it. Also the position of the person versus the pane has an influence.

Test results [6], [10] have shown that there is a wide spread in the mass and velocity of glass fragments in the window panes which were tested. Still, it would appear from an investigation carried out by PML – TNO (also [18]) that, in spite of a load equal to twice the failure load of the window pane, the velocity-mass distribution was such that this lays above the v_{50} for skull fracture. With the help of data from Reference [18] it can be determined that the probability of skull fracture in this case (twice the failure load) is equal to 94%. The velocity-mass distribution is determined at 1.75 m distance behind the window pane, with $1.68 \times 1.13 \text{ m}^2$ pane dimensions.

It was also shown that the spatial spread of the fragments remains limited; the major part of them was found right behind the pane.

For someone behind the pane there is a high probability that this person's head will be hit. Consequently, the probability of lethality can also be evaluated on the basis of skull fracture caused by glass fragments. The profit function, for this probability of lethality due to glass fragments is derived in Annex I. It gives:

$$Pr = 2.67 + 5.62 \ln \frac{DLF * P}{P_{st}} \quad (31)$$

in which P_{st} and DLF are dependent on the dimensions of the window pane and the dynamic load. The latter can be determined using data from the section on "Consequences of explosion effects on structures".

Collapse of buildings

Buildings can collapse, due to blast, by load which are far lower than the ones required to produce direct damage to human beings. If people are present inside a collapsing building, they may suffer serious injuries or even be killed due to this collapse. However, when a building collapses, arches often form (two walls hanging against each other etc.), this offers a certain degree of protection. It is, certainly, not the case that all people present will always be killed.

5.1 Consequences for Humans

Data about the number of deaths and injuries due to the collapse of buildings caused by explosions are scarce. In this respect, we can use, data about collapse of buildings due to earthquakes. Both occurrences, explosion and earthquake, will take place at an unexpected moment, so that people who are present cannot previously be warned and be able to find a safe place.

Glass and other investigators [7] have found that the number of deaths caused by the collapse of a building is dependent on the age of the people in question. It was found that young children and old people, in houses, had a lower probability of survival. It also appears that in almost all age categories more women than men were seriously or fatally injured.

With regard to the size of the building, more serious or deadly injuries were noticed in larger houses (seven or more persons) than in smaller houses. Also the age of the building is of importance. More seriously or deadly injuries were registered in old houses (8 years or older) than in more modern houses.

Reference [15] quotes that a complete collapse of a building due to an earthquake will produce a 100% of victims, whereby 50% dead and 50% injured. In a revised report [16] these figures were changed to 20% dead and 80% injured.

Blume, in Reference [11] assumes that 50% of the people will die as result of the collapse of a building due to an earthquake.

Reference [14] quotes the collapse of an apartment building due to an explosion caused by explosive substances. In this case, 40% of the people in the building were killed.

It can be concluded, from the foregoing data, that when a building collapses due to an earthquake, between 20% and 50% of the people present will die. We assume that in case of a collapse caused by an explosion, the percentages will be the same as for an earthquake.

6

Examples

6.1 Example 1

A person weighing 70 kg is exposed to a shock wave with a peak overpressure $P_s = 3 \cdot 10^5 \text{ Pa}$ and a positive phase duration $t_p = 0.05 \text{ s}$. The atmospheric pressure p_0 is equal to $1 \cdot 10^5 \text{ Pa}$. What is the probability of survival of this person, dependent on his orientation, for primary and tertiary effects?

The probability of survival will be determined with the help of previously given graphs and probit functions.

Solution:

The impulse i_s of the shock wave is equal to:

$$i_s = 0.5 \cdot 3 \cdot 10^5 \cdot 0.05 = 7.5 \cdot 10^3 \text{ Pa} \cdot \text{s}$$

1) The person is in a laying position.

The overpressure exerted on the person is equal to:

$$P = P_s = 3 \cdot 10^5 \text{ Pa}$$

The probability of survival can now be determined using Figure 7.

The scaled peak overpressure \bar{P} is equal to:

$$\bar{P} = 3 \cdot 10^5 / 1 \cdot 10^5 = 3.$$

The scaled impulse is equal to:

$$\bar{i} = 7.5 \cdot 10^3 / ((1 \cdot 10^5)^{1/2} \cdot 70^{1/3}) = 5.75 \text{ Pa}^{1/2} \cdot \text{s} \cdot \text{kg}^{-1/3}$$

The probability of survival, from Figure 7, is found to be 99%. With the help of probit functions (10) and (11) we find:

$$S = 4.2/3 + 1.3/5.75 = 1.63; \text{Pr} = 2.20 \text{ and the probability of survival: } (100 - 1)\% = 99\%.$$

2) The person is close to a surface against which the shock wave is reflected.

The peak overpressure acting on the person, P_r , can be determined by Equation (7):

$$P = P_r = \frac{8 \cdot (3 \cdot 10^5)^2 + 14.3 \cdot 10^5 \cdot 10^5}{3 \cdot 10^5 + 7 \cdot 10^5} = 11.4 \cdot 10^5 \text{ Pa}$$

So that \bar{i} is equal to: $0.5 \cdot 11.4 \cdot 10^5 \cdot 0.05 = 2.85 \cdot 10^4 \text{ Pa}\cdot\text{s}$

From here follows $P = 11.4$. With $i = 21.87$ we find, from Figure 7, that the probability of survival is less than 1%.

For the probit function (10) we have: $S = 0.43$; $Pr = 9.87$. The probability of lethality is thus greater than 99%. Therefore, the probability of survival, as previously, is less than 1%.

3) The person stands in a upright position, but not near a surface on which reflection can take place. In this case flow around the person will take place. The associated dynamic pressure can be determined using Equation (5):

$$Q = \frac{5 \cdot (3 \cdot 10^5)^2}{2.3 \cdot 10^5 + 4 \cdot 10^5} = 2.25 \cdot 10^5 \text{ Pa}$$

The total peak overpressure exerted on the person will then be:

$$P = P_s + Q = 2.25 \cdot 10^5 + 3 \cdot 10^5 = 5.25 \cdot 10^5 \text{ Pa}$$

It follows from this that:

$$\bar{i} = 0.5 \cdot 5.25 \cdot 10^5 \cdot 0.05 = 1.31 \cdot 10^4 \text{ Pa}\cdot\text{s}$$

With a scaled peak overpressure $\bar{P} = 5.25$ and a scaled impulse $\bar{i} = 41.0$ we find, from Figure 7, a probability of survival of about 15%.

The probit function gives a probability of survival of $(100-86)\% = 14\%$, with $S = 0.83$ and $Pr = 6.07$.

A whole-body displacement occurs in this case. If we use Figure 11 we find a maximum whole-body displacement velocity of about 25m/s and an estimated probability of survival of 25%.

If we try to determine the probability of survival using the probit function (19), then we have:

$$S = \frac{7.28 \cdot 10^5}{3 \cdot 10^5} + \frac{1.3 \cdot 10^9}{3 \cdot 10^5 \cdot 7.5 \cdot 10^3} = 0.60$$

and

$$Pr = 5 - 2.44 \ln 0.60 = 6.25$$

With this result the probability of survival is $(100-89)\% = 11\%$.

It must be noted that the difference between the probability of survival of 25% obtained from Figure 11 and the 11% obtained above can be explained by the fact that the profit function represents an approximation of the figure.

If the person standing in a upright position is displaced after being hit by the shock wave and collides with a rigid object at maximum velocity, then the probability of survival of that person will be equal to: $(0,15,0,11) \cdot 100\% = 2\%$.

6.2

Example 2

What is the probability, for the person from Example 1, to suffer an ear-drum rupture, depending on the person's orientation?

In the determination of the damage to hearing only the peak overpressure of the incident wave is of importance.

This peak overpressure is equal to $3 \cdot 10^5$ Pa. We see, from Figure 8, that the probability of ear-drum rupture is equal to 94%.

If this probability is calculated with the probit function (12), we find 95%.

6.3

Example 3

Three fragments with respective masses of 0.01 , 0.10 and 10 kg and an equal velocity of 30 m/s hit a person. What is the probability of survival of this person?

From Figure 15 we can see that the fragment with a mass equal to 0.01 kg will not cause any injury. The probability of an injury caused by the 0.10 kg fragment is quite low. The person will not survive the impact of a 10 kg fragment on the skull.

The probability of survival can also be determined with the help of probit functions (26), (27) and (29) and equations (28) and (30).

For the 0.01 kg fragment we have:

$$S = 0.01 \cdot 30^{5.115} = 3.59 \cdot 10^5$$

$$Pr = -29.15 + 2.10 \cdot \ln 3.59 \cdot 10^5 = 2.29$$

and the probability of survival is greater than 99%.

For the 0.1 kg fragment we have:

$$S = 0.5 \cdot 0.1 \cdot 30^2 = 45.0$$

$$Pr = -17.56 + 5.30 \ln 45 = 2.62$$

which shows that the probability of survival is greater than 99%.

For the 10 kg fragment we have:

$$S = 30$$

$$Pr = -13.19 + 10.54 \ln 30 = 22.7$$

a probability of survival which is less than 1%.

Conclusions

It was found possible, most of the effects of the explosion on people handled on this chapter, to formulate criteria with which the probabilities of survival can be estimated. This can be done either with the help of figures which are given or with the probit functions derived for this purpose.

The consequences of the direct effects of the blast have mostly been investigated; however, these consequences will only be of influence for high peak overpressures.

With regard to the secondary effects, the impact of fragments and debris, despite the broad data, it has still been possible to evaluate whether such fragments are to be considered dangerous, dependent on their velocity and mass. The determination of the distribution of mass and velocity of a fragment from the parameters of the blast does not form part of this chapter.

The consequences of the tertiary effects are determined on the basis of the assumption that a person will be displaced and will collide with a rigid object at maximum displacement velocity. This assumption represents an overestimate of this effect. A simple model is presented for the determination of the maximum velocity of whole-body displacement from the blast parameters. This model, however, is not valid for a combination of high values for the peak overpressures and small values for the impulses.

For the determination of the consequences of the collapse of buildings due to an explosion only very broad data can be found in literature.

References

- [1] Bowen J.G., Fletcher E.R., Richmond D.R.
Estimate of man's tolerance to the direct effects of air blast.
Lovelace Foundation for Medical Education and Research,
Albuquerque, New Mexico, 1968. DASA-2113.
- [2] Baker W.E., Cox P.A., Westine P.S., e.a.
Explosion hazards and evaluation.
Elseviers scientific publishing company, 1983.
- [3] Hirsch F.G.
Effects of overpressure on the ear – a review.
Annals of the New York Academy of Sciences, 1968.
- [4] White C.S., Jones R.K., Damon E.G.
The biodynamics of airblast.
Lovelace Foundation for Medical Education and Research.
Albuquerque, New Mexico, 1971. DNA 2738T.
- [5] Lewis W.S., e.a.
Jumpers Syndrom – The trauma of high, free-fall as seen at Harlem Hospital.
J. Trauma, 5: 812 – 818, 1965.
- [6] Fletcher E.R., Richmond D.R., Yelverton J.T.
Glass fragment hazard from windows broken by airblast.
Lovelace Biomedical and Environmental Research Institute, Albuquerque, New Mexico, 1980.
DNA 5593T.
- [7] Zaker T.A.
Fragment and debris hazards.
Department of Defense Explosive Safety Board, Washington D.C., 1975. DDESB TP12.
- [8] Merz H.A.
Letalitätskriterien für explosionen mit konventionellen Sprengstoff.
Forschungsinstitut für militärischen bautechnik, Zurich,
1976. FMB 76-10.
Lethality criteria for explosions involving conventional explosive.
- [9] Fegulso L.E., Rathmann C.E.
Effect of earth cover on far-field fragment
distributions
Department of Defense Explosive Safety Board, Washington
D.C., 1973.
Minutes, 15th DDESB seminar.

- [10] Proctor T.D.
A review of research relating to industrial helmet design
Journal of Occupational Accidents, 3: 259-272, 1982.
- [11] Blume J.A.
Civil structures and earthquake safety.
Interim report of the special subcommittee of the San Fernando earthquake study, 1971.
- [12] Glass R.J. e.a.
Earthquake injuries related to housing in a Guatemalan village.
Science, volume 197: 638-643, 1977.
- [13] Clemedson C.J., Jönsson A.
Effects of the frequency content in a complex air shockwaves on lunginjuries in rabbits.
Aviation, Space and Environmental Medicine: 1143-1152,
November 1976.
- [14] Somes N.F.
Abnormal loading on buildings and progressive collapse building practices for disaster mitigation.
- [15] Scenarios of buildings in given earthquake damage states.
U.S. Department of Commerce, National Technical
Information Service PB 80/150949, 1972.
- [16] Scenarios of buildings in given earthquake damage states,
Revision I
U.S. Department of Commerce, National Technical Information Service PB 80/106156, 1973.
- [17] Methoden voor het berekenen van de fysische effecten van het incidenteel vrijkomen van
gevaarlijke stoffen.
Directoraat Generaal van de Arbeid, 1979.

Methods for the calculation of physical effects
Resulting from releases of hazardous materials (liquids and gases).
The Director-General of Labour, 1979.
- [18] Nowee J.
Dynamische bezwijkbelasting en scherfwerking van thermisch geharde glazen ruiten
PML 1985-C-103.
Dynamic failure load and fragment effects of thermally hardened glass panes

Appendix 1

Probit Functions

With the help of the probit function:

$$P_r = a + b \ln V \quad (I-1)$$

where:

Pr: the probit

a and b: constants

V: a variable

we can, dependent on the value of the variable V, determine a percentage which gives us the probability of particular event.

In this report this event which is generally death as a result of one of the effects of an explosion.

The percentage which corresponds to a particular value of the probit Pr is given in Table I-1:

Table I: Relationship between probabilities and probits.

%	0	1	2	3	4	5	6	7	8	9
0	—	2.67	2.95	3.12	3.25	3.36	3.45	3.52	3.59	3.66
10	3.72	3.77	3.82	3.897	3.92	3.96	4.01	4.05	4.08	4.12
20	4.16	4.19	4.23	4.26	4.29	4.33	4.36	4.39	4.42	4.45
30	4.48	4.50	4.53	4.56	4.59	4.61	4.64	4.67	4.69	4.72
40	4.75	4.77	4.80	4.82	4.85	4.87	4.90	4.92	4.95	4.97
50	5.00	5.03	5.05	5.08	5.10	5.13	5.15	5.18	5.20	5.23
60	5.25	5.28	5.31	5.33	5.36	5.39	5.41	5.44	5.47	5.50
70	5.52	5.55	5.58	5.61	5.64	5.67	5.71	5.74	5.77	5.81
80	5.84	5.88	5.92	5.95	5.99	6.04	6.08	6.13	6.18	6.23
90	6.28	6.34	6.41	6.48	6.55	6.64	6.75	6.88	7.05	7.33
—	0.0	0.1	0.3	0.3	0.4	0.5	0.6	0.7	0.8	0.9
99	7.33	7.37	7.41	7.46	7.51	7.58	7.65	7.75	7.88	8.09

i-1

Damage to Hearing

The probit function for the determination of the probability of ear-drum rupture:

$$P_r = \lambda 12.6 + 1.524 * \ln P_s \quad (I-2)$$

is determined with the help of the values given in Table I-2.

Table I-2: Probability of ear-drum rupture.

Probability	P_s (N/m ²)
1%	$21.5 \cdot 10^3$
10%	$42.8 \cdot 10^3$
50%	$103.8 \cdot 10^3$
90%	$240.4 \cdot 10^3$

The constants a and b are determined with the pressures associated with the 50% and 90% probabilities.

I-2

Lung Damage

For the determination of the probit function for lung damage we will use Figure 7. In order to make it possible to reproduce Figure 7 by a probit function according to (I-1), an additional variable S is introduced. For each line in Figure 7 which indicates a particular probability of survival S is determined by:

$$S = \frac{\bar{p}'}{\bar{p}} + \frac{\bar{i}'}{\bar{i}} \quad (I-3)$$

In this formula \bar{p}' and \bar{i}' represent the limit values of respectively, the scaled peak overpressure which is reached by an increasing impulse and of the scaled impulse which is reached by an increasing pressure.

The values of \bar{p}' and \bar{i}' , for various probability of death, are given in Table I-3:

Table I-3: Limit values for P and i.

probability of Death	\bar{p}'	\bar{i}'
Lower limit	0.8	0.2
1%	2.7	0.9
10%	3.4	1.1
50%	4.2	1.3
90%	5.4	1.7
99%	6.5	2.1

For the incorporation of S into the probit function, the values P and i to be used correspond to a probability of death equal to 50%, so that:

$$S = \frac{4.2}{\bar{p}} + \frac{1.3}{\bar{i}} \quad (I-4)$$

Different values of S are associated with the various combinations of P and i (Table I-4).

Table I-4: Damage number S.

probability of Death	S
Lower limit	5.25
1%	1.56
10%	1.25
50%	1
90%	0.8
99%	0.64

The constants a and b, from Formula (I-1), are in turn determined with the 50% and 90% values for S, so that the probit function for lung damage is given by:

$$Pr = 5 - 5.74 * \ln S \quad (I-5)$$

with S determined according to formula (I-4).

I-3 Whole-body Displacement Effects

The determination of these effects is made with the help of the maximum velocity with which a person can be displaced by an explosion wind.

A difference is made, in this respect, between an impact on the head and an impact of the whole body against a rigid obstacle. A probit function is derived for both cases. Use is made, of the graphs from Figures 10 and 11 and of the numbers given in Tables I and II, taking into account the following criterion: the "almost 100% probability of death" means 99%, and the criterion "limit" means a 1% probability.

Impact of the whole body.

We assume that the line for a 50% probability of death corresponds to an impact velocity of 16.5 m/s. For very high values of the impulse i_s the pressure P_s approaches $7.28 \cdot 10^3$ Pa.

For low values of the impulse i_s and pressures P_s of less than 0.9 to $0.5 \cdot 10^6$ Pa, the line can be approximated by: $P_s \cdot i_s = 1.3 \cdot 10^9 \text{ Pa}^2 \cdot \text{s}$.

Using again a variable S, the latter is determined by:

$$S = \frac{7.28 \cdot 10^3}{P_s} + \frac{1.3 \cdot 10^9}{P_s \cdot i_s} \quad (I-6)$$

For the probability of survival equal to 1%, 50% and 99%, the average values for S are, respectively, 2.57, 1.0, and 0.38. With these data the constants a and b, for this probit function, can be determined.

We then have:

$$Pr = 5 - 2.44 \ln S \quad (I-7)$$

with S determined according to (I-6) and applicable to pressures P_s of less than 0.4 to $0.5 \cdot 10^6$ Pa.

Impact with the head.

For very high values of the impulse i_s , the pressure P_s associated with an impact velocity of 5.5 m/s approaches the value of $2.43 \cdot 10^3$ Pa. For low impulses and pressures of less than 0.4 to $0.5 \cdot 10^6$ Pa, the value of $P_s \cdot i_s$ is equal to approximately $4 \cdot 10^8$ Pa²·s, so that S can be determined by:

$$S = \frac{2.43 \cdot 10^3}{P_s} + \frac{4 \cdot 10^8}{P_s \cdot i_s} \quad (I-8)$$

The average values for S for the 1% and 99% probabilities, respectively, are 1.45 and 0.80. This gives:

$$Pr = 5 - 8.49 \cdot \ln S \quad (I-9)$$

with S according to (I-8) and applicable to pressures P_s of less than 0.4 to $0.5 \cdot 10^6$ Pa.

I-4

Fragments and Debris

Figure 15 is used for the determination of the probit function. It does not appear possible to arrive at a generalized probit function for the consequences of the impact of fragments and debris. For this reason, for each of the three ranges of the mass of the fragment where a criterion is decisive, a separate probit function will be determined. On the basis of the criterion of "skull-base fracture", the probit functions will be determined in such a manner that they connect one to the other.

$m > 4.5$ kg.

For the impact of a piece of debris against a human head we retain, for the variable V in (I-1), the impact velocity v_o .

The impact velocity v_o whereby there is a 1% probability of a skull-base fracture is equal to 4.5 m/s. To a 99% probability of death belongs a velocity v_o equal to 7.0 m/s.

The probit function for fragments with a mass greater than 4.5 kg is then determined by:

$$Pr = -13.19 + 10.54 \ln v_o \quad (I-10)$$

$0.1 < m < 4.5$ kg.

The criterion for the impact is determined by the kinetic energy. It is then appropriate to use the kinetic energy equal to $\frac{1}{2} \cdot m \cdot v_o^2$ for the determination of the variable V . In order to connect with the probit function for a skull-base fracture for a fragment of 4.5 kg we must retain, for the probabilities of death equal to 1%, 50% and 99%, respectively, values of the kinetic energy equal to 46, 71, and 110 J. These values agree in a satisfactory manner with the criteria given for debris. Consequently, for fragments with $0.1 < m < 4.5$ kg the following probit function is determined:

$$Pr = -17.56 + 5.30 \ln \left(\frac{1}{2} m v_o^2 \right) \quad (I-11)$$

$m < 0.1$ kg.

The lines given in Figure 15 for fragments all belong to a velocity whereby 50% of the specific fragment penetrates. In order to connect with the 50% value for debris, the fragment velocity, for a 0.1 kg mass, must be equal to 37.7 m/s. The v_{50} for a fragment with mass $m = 0.01$ kg and $k = 2370$ is equal to 37.1 m/s. These values appear to be in good agreement.

A line parallel to the criteria for fragments with a mass between 0.001 and 0.1 kg is given by:

$$S = m * v_o^{5.115} \quad (I-12)$$

For the 1%, 50% and 99% values, the values of S , respectively, are $S=3.78*10^6$; $11.55*10^6$ and $35.32*10^6$.

The probit function determined with the above is:

$$Pr = 38.83 - 2.08 \ln S \quad (I-13)$$

and this function is applicable for masses of fragments between 0.001 kg and 0.1 kg.

I-5

Glass Fragments

From tests in which the reflected peak overpressure of the shock wave was equal to twice the dynamic failure load of the tested window panes it appeared that, at a distance of 1.75 m behind the pane, there was a 94% probability of skull fracture [18]. The static failure load P_{st} of the pane can be calculated from the pane dimensions. The dynamic load factor (DLF) can be calculated from the ratio of the phase duration of the load and the natural period of vibration of the pane (Both P_{st} and DLF are to be calculated with the help of data out of: "Consequences of explosion effects on structures"). The dynamic failure load is then equal to: P_{st}/DLF .

The load P exerted on the pane is also determined with the help of data out of: "Consequences of explosion effects on structures". The 94% probability of skull fracture, from [18], will be for:

$$\frac{P}{P_{st}/DLF} = 2$$

If we assume that 1% skull fracture occurs at:

$$\frac{P}{P_{st}/DLF} = 1$$

and assuming further that the person will die as consequence of a skull fracture, this leads to the following probit function:

$$Pr = 2.67 + 5.62 \ln \frac{DLF * P}{P_{st}} \quad (I-14)$$

with which the probability of survival can be determined for a person located 1.75 m behind the pane and is hit on the head by a glass fragment.

Appendix II

Accuracy of the Models for the Determination of the Effects of Explosions on Man

Probit functions have been established, for the effects of explosions on man, in order to determine the probability of lethality as consequence of

- 1 – Lung damage (10) and (11).
- 2 – Impact of the head (17) and (18).
- 3 – Impact of the whole body (19) and (20).
- 4 – Impact of fragments and debris (26) to (30) incl.

A probit function has also been established for the determination of the damage to hearing.

1 – Lung damage

The parameters of the probit function are, firstly the pressure and impulse exerted on the body by the blast and, secondly, the mass of the body.

In the values of pressure and impulse to be considered in the calculation reflection and flow around are already included.

The accuracy with which the pressure and impulse are determined with regard to the position of an object (structure or person) is difficult to determine. Ideal situations were assumed whereby the blast wave propagates undisturbed. Even in such a case substantial variations of the predictions are foreseeable. Various diagrams are known for the explosion of explosive substances with which the pressure at a given distance can be determined. Mutual differences of 50% may occur.

The pressure-impulse diagram for lung damage (Figure 7) is established with the help of tests with animals. Variation of the test results is not known.

Within the possible pressure-impulse combinations a difference must be made between a pressure range, in which the pressure is decisive for the consequences, and an impulse range, in which the impulse is decisive. The impulse range is limited by $P > 20$ and the pressure range is limited by:

$$\bar{i} > 10 \frac{Pa^{\frac{1}{2}} s}{kg^{\frac{1}{3}}}$$

The pressure dependency of the probability of survival in the pressure range, is given by:

Probability %	\bar{P}
10	3.4
50	4.2
90	5.4

The impulse dependency on the probability of survival in the impulse range, is given by:

Probability %	\bar{i}
10	1.1
50	1.3
90	1.7

The mass of the body only has an influence on the scaled impulse, and the influence is therefore greatest in the impulse range. A variation of the mass by 10kg with respect to 70 kg results in a variation of the scaled impulse of 5%. The scaled impulse for a 50% damage then varies between 1.24 and 1.37, whereby the probability of lethality varies from 39 to 62%. It must be noted, in this respect, that this criterion has been derived for shock waves. By gas explosions pressure waves arise and the effects will be less.

2 – Impact of the Head

Dependent on peak overpressures and impulse of an undisturbed blast wave, a maximum velocity has been established at which the head impacts against an obstacle. The unknown factors in the variation of pressure and impulse have been discussed above. The degree of accuracy of the

determination of the velocity is not known. Nor is the variation in the test results known.

No pressure or impulse ranges are to be indicated in the probit function. In order to evaluate the variation of pressure and impulse, we take a value of $5 \cdot 10^4$ Pa for the overpressure and of $8 \cdot 10^3$ Pa*s for the impulse. The probability of death is then 35%. For a 25% variation of the pressure this probability varies between 1% and 56%. For a 25% variation of the impulse it varies between 1% and 92%.

3 – Impact of the whole Body

The uncertainties of the preceding paragraph are also applicable to this case. Figure 9 provides an indication of only the variation of the probability of death at a particular impact velocity. This variation is found to be great.

The combination of a pressure $5 \cdot 10^4$ Pa and of an impulse $2 \cdot 10^4$ Pa*s gives a probability of death equal to 18%. For a 25% variation of the pressure this probability varies between 5% and 37%. For a 25% variation of the impulse it varies between 6% and 34%.

4 – Impact of Fragments and Debris

Three probit functions (26 to 30 incl.) have been derived for the consequences of the impact of fragments and debris against the body. The probability of death, is dependent on the mass and velocity

of the debris. The spread in the test results is only known for the effect of fragments (Figure 13). The spread in the v_{50} values appears to be in the range of 10% to 15%. The table which follows gives an example of the influence of a 15% spread in the impact velocity for the probit function for masses between 0.001 and 0.1 kg (29) and (30).

m(kg)	v(m/s)	probability (%)
0.01	60	50
	69	95
	51	6
0.05	45	67
	52	98
	38	9

For the two remaining probit functions very little can be reported regarding the sensitivity of the test results, since these tests were based on very general criteria. Nevertheless, in order to still obtain an idea about this sensitivity we will consider a 15% spread in the impact velocity. There is a 50% probability of death after the impact of a 1 kg fragment, if this fragment has a velocity of 11.9 m/s. For a 15% variation of this velocity the probability varies between 5% and 93%.

A 15% variation of the velocity for fragments with $m > 4.5$ kg has the following influence: There is a 50% probability of death for a velocity of 5.6 m/s. This probability rises to 99% for a velocity of 6.5 m/s. and decreases to 4% for a velocity of 4.8 m/s.

5 – Damage to Hearing

The probability of an ear-drum rupture depends only on the overpressure (Figure 8). No spread is indicated in this figure. There is a 50% probability for a pressure about 10^5 Pa. If we double this value or take half of it, the probability will vary from 84% to 13%.

Chapter 4

Survey study of the products which can be released during a fire

Contents

	Page
Abbreviations used	4
1. Introduction	5
2. The formation of toxic combustion products	6
3. The extent to which toxic combustion products may be formed	9
4. Evaluation	16
5. Calculation example	17
6. References	19
Table 1	
Overview of Combustion Tests with Chlorine containing Polymers	21
Annex I	
Identification Chart for the Quantifying of the Formation of Toxic Combustion Products	22

Review of abbreviations used and of formulas of chemicals

CO	carbon monoxide	NPK	nitrogen, phosphorus, potassium
CO ₂	carbon dioxide		(the chemical composition of synthetic fertilizers)
Cl ₂	chlorine	PCDD	polychloro dibenzodioxins
CCl ₄	carbon tetrachloride	PCDF	polychloro dibenzofurans
C ₂ Cl ₄	tetrachloro ethylene	P ₂ O ₅	phosphorus pentoxide
C ₂ Cl ₆	hexachloro ethane	HF	hydrogen fluoride
CHCl ₃	chloroform	H ₂ O	water
C ₂ HCl ₃	trichloro ethylene	H ₂ S	hydrogen sulphide
C ₂ HCl ₅	pentachloro ethane		
C ₂ H ₂ Cl ₄	tetrachloro ethane	NH ₃	ammonia
C ₂ H ₄ Cl ₂	dichloro ethane	NO _x , NO ₂	nitrogen oxides
COCl ₂	phosgene		nitrogen dioxide
COS	carbonyl sulphide	PVC	polyvinyl chloride
HCl	hydrogen chloride	SO ₂	sulphur dioxide
HCN	hydrogen cyanide	TCDD	tetrachloro dibenzodioxins

1

Introduction

In this chapter of the "Green Book" on damages we will enter into the details of the extent of formation of toxic products in cases of fires.

Our purpose is to indicate which data, with regard to the formation of toxic combustion products, from a qualitative as well as quantitative view points, are presently available.

Knowledge regarding the formation of toxic combustion products is important in order to be able to evaluate the potential dangers of fires during: storage, transportation and handling of the relevant substances.

These relevant substances are, among others, synthetic materials, pesticides, synthetic fertilizers and similar.

With the exception of the majority of synthetic fertilizers, the greatest part of the relevant substances consists on organic materials. Every organic substance, in principle, burns completely as long as a sufficient amount of oxygen is present. If the substance is composed of carbon, hydrogen and oxygen, the relatively non-dangerous combustion products CO_2 and H_2O are formed. However, if the substance also contains hetero-atoms (such as chlorine, sulphur and similar) then also toxic combustion products are formed. The formation of a specific combustion product not only depends on the type of hetero-atom, but also on the chemical structure. Polychlorine aromats can, for instance, by incomplete combustion, produce chlorine dioxins.

In order to establish some type of structure within the great number of substances, which if subjected to a fire, can generate toxic combustion products, the following division is proposed:

- synthetic materials
- pesticides
- synthetic fertilizers
- others, not previously mentioned hydrocarbons, sub-divided into aromatic and aliphatic hydrocarbons.

The following will be, in succession, handled in this report: the mechanism of formation of toxic combustion products (paragraph 2) and the toxic combustion products themselves, the extend to which the different combustion products are generated (paragraph 3) and an evaluation (paragraph 4) of the survey.

Finally, in paragraph 5, an example will illustrate how the formation of different combustion products can be calculated.

The formation of toxic combustion products

General

Before entering into the subject of the possible formation of toxic combustion products, a short qualitative description will first be given of the phenomena involved in a fire.

A number of physical and chemical processes take place during a fire. The physical processes are, among others:

- heating and
- evaporation of the substance

The chemical processes are, among others:

- combustion
- pyrolysis
- decomposition, and
- reactions between combustion products.

As consequence of the heat load of a substance evaporation takes place. Dependent on a number of factors such as temperature, extent of the fire, temperature distribution, different chemical processes can develop.

By combustion of the substance a difference must be made between complete and incomplete combustion.

By a complete combustion, the temperature and the oxygen concentration are sufficiently high to fully oxidize the substance. Substances containing carbon and hydrogen burn down, then, to CO_2 and H_2O .

By incomplete combustion a non-complete oxidizing takes place and next to CO , CO_2 and H_2O other products are also generated. These products are also called secondary combustion products and are built up from broken pieces of the original substance.

Another phenomenon of incomplete combustion is the formation of smoke.

Pyrolysis takes place in case the substance is heated without supply of oxygen. By a pyrolysis such a large number of compounds can arise that it is not possible to determine, beforehand, which compounds or types of compounds can be produced.

Apart from pyrolysis a product can also, as consequence of combustion, decompose. This means that it will separate into products which are simpler than the original substance.

Next to the previously mentioned processes, it can also occur that in the heart of a fire and in its surroundings mutual reactions will take place between the different combustion products. As consequence of this type of reactions a whole series of other substances can be formed, composed of cracked and reactive products out of the original substance.

In dealing with the subject of formation of toxic combustion products, we must realize that fire is certainly a very complex phenomenon. Many different reactions can simultaneously develop.

We will indicate, in this study, which combustion products can mainly be expected.

Due to lack of data it will not be possible to provide a complete picture of the combustion products which can be formed and we will, consequently, be obliged to have recourse to estimations.

Whenever added information will make it possible, the above estimations will be complemented by test data.

Possible Toxic Combustion Products

The combustion products which can theoretically appear are mainly determined by the chemical composition of the substance.

For instance, substances which only contain carbon and hydrogen will generate CO, CO₂ and H₂O. If, besides C and H also hetero-atoms are present, for instance chlorine, sulphur and similar, then next to CO, CO₂ and H₂O also Cl₂, HCl, COCl₂, SO₂ and COS will appear.

Besides these so-called primary combustion products also secondary combustion products will be generated.

The meaning "secondary combustion products" refers to compounds which arise, during the combustion process, due to mutual reactions between the combustion products which are formed.

Generally with regard to the formation of this type of products, neither data are available nor is it normally possible to make estimates.

One type of compound, however, represents, up to now, an exception.

It is known that by the combustion of polychlorinated aromats polychlorodibenzo-p-dioxins and polychlorodibenzofurans (respectively PCDD's and PCDF's) can be formed.

Examples of polychlorinated aromats are:

- dichlorobenzene
 - trichlorophenol
 - fenoprop
 - dicamba
- } pesticides

On the basis of the chemical composition of the substance a number of combustion products which can be expected can be differentiated. These are summarized in the table below.

Group	Combustion Product
Halogen containing substances (in particular chlorine containing substances)	<u>HCl</u> , Cl ₂ , COCl ₂ , HF
Nitrogen containing substances	<u>NO_x</u> , HCN
Sulphur containing substances	<u>SO₂</u> , H ₂ S, COS
Cyanide group containing substances (i.e. isocyanates)	HCN, <u>NO_x</u> , NH ₃
Polychloro - aromats	<u>PCDD's</u> , PCDF's
Polychloro - biphenyls	<u>PCDD's</u> , PCDF's

The combustion products which are underlined must be considered as combustion products which, in general, will appear mainly.

The combustion products named in the above table can be formed during a fire. For the determination of the extent to which this formation takes place several approaches are possible.

- The product burns completely, which means that 100% of the substance is consumed, whereby the relevant combustion products are formed.
- We can assume that a quantitative conversion of an hetero-atom into a typical combustion product takes place. For example, by a quantitative conversion of chlorine into HCl it is assumed that *all of the chlorine* converts into HCl.
- Apart from a quantitative conversion, also a partial conversion can be assumed possible, for instance, besides HCl also into COCl_2 .
- In addition to the toxic combustion products named in the above table, there always will be, as consequence of an incomplete combustion, formation of CO in higher or lower proportions.

During the combustion of polychloro aromats or polychloro biphenyls, PCDD's and PCDF's will be formed as secondary reaction products due to the incomplete combustion.

We will come back, later on, to the formation of these products.

As consequence of a fire, also part of the substance, due to the evaporation, can be emitted without having burned. Even though, strictly speaking, such a substance cannot be considered as a combustion product, it still is a substance which is released as consequence of fire.

The spreading of the non-burned part of the substance is, however, only of importance for substances with a high degree of toxicity (for instance pesticides).

3

The extent to which toxic combustion products may be formed

General

The extent to which toxic combustion products may be formed depends on:

- the evaporation rate of the burning substance,
- the area of the fire,
- the degree of conversion (quantitative, non-quantitative),
- the composition, percentage-wise, of the substance.

The so-called source-strength density (= rate of evaporation, per unit area), is known only in a very global fashion.

For instance, for synthetic materials, it is known that this value varies between 0.005 and 0.025 kg.m⁻².s⁻¹ [1].

For liquids, reference [1] gives a maximum source-strength density of about 0.1 kg.m⁻².s⁻¹.

For powders such, for instance, as fertilizers and (often) pesticides, no specific values are known.

According to [2], for pesticides, the rate of evaporation per unit area lays in the range of 0.02 kg.m⁻².s⁻¹.

The above-mentioned global values are checked on the basis of the evaporation formula from the yellow book [3].

This evaporation formula is:

$$\dot{m} = \frac{10^{-3} * h_c}{C_p * \Delta T + h_v}$$

in which

\dot{m}	= source strength density	[kg m ⁻² .s ⁻¹]
C_p	= specific heat	[J/kg.K]
h_c	= heat of combustion	[J/kg]
h_v	= heat of evaporation	[J/kg]
ΔT	= temperature rise of the substance to be burned up to the boiling point	[K]

Filling in the average values for organic substances:

$h_c = 4 \cdot 10^7$ J/kg, $h_v = 4 \cdot 10^5$ J/kg, $C_p = 1.6 \cdot 10^2$ J/kg.K and $\Delta T = 400$ K gives a value for \dot{m} equal to:

$$\dot{m} = 4 \cdot 10^{-2} \text{ kg.m}^{-2}.\text{s}^{-1}$$

For substances with high chlorine contents the heat of combustion is lower. For hexachloro benzene, f.i.: $0.75 \cdot 10^7$ J/kg. This results in $\dot{m} = 7 \cdot 10^{-3}$ kg.m⁻².s⁻¹.

In this case, the variation of the heat of combustion is determinant for the change of the value of the evaporation rate.

On the basis of the above data and , also, analogy with several other studies, for instance ref. [1] and [4], it is assumed that a value of 0.025 kg.m⁻².s⁻¹ represents a reasonable estimate.

Nevertheless, if the values of h_v , h_c , C_p and ΔT can properly be established for a given substance then the source-strength density valid for this substance can be estimated on the basis of the evaporation formula.

In what follows, we will take a closer look, for each group of substances, at the extent to which combustion products can be formed. Whenever, in this respect, test data described in literature will be available, these data will always be used.

Synthetic Materials

There are so many types of synthetic materials, that a complete survey of them all is not possible.

Considering the purpose of this study, the only relevant synthetical materials are those in which hetero-atoms are present in their composition.

On the basis of the presence of different hetero-atoms, five categories of synthetic materials are differentiated.

- a. The materials containing chlorine
- b. The materials containing nitrogen
- c. The materials containing a cyanide group
- d. The materials containing fluor
- e. Other synthetic materials

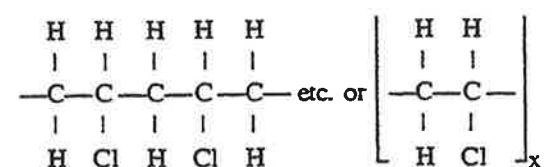
Group a.

Out of chlorine containing polymers, the most commonly used one is polyvinylchloride. For this substance also relatively many test data are available with regard to the formation of combustion products (see Table 1).

Considering these values it would appear that, at combustion of PVC, practically all of the chlorine is converted into HCl, which, consequently, represents the decisive damage factor. Only if the phosgene formation is higher than 3.4% of the total available quantity of chlorine, then this substance is determinant for the damage distance [1]. This limit is established on the basis of the difference in toxicity of HCl and phosgene. To which extent phosgene can be formed is not known. The formation of chlorine, in this latter case, is such that the chlorine cannot appreciably influence the damage which may take place.

The calculation procedure is explained with the help of an example: combustion of PVC.

The formula for the structure of PVC is as follows:



The molecular weight is 62.5 x.

By a quantitative conversion into HCl, the amount which develops, per kg PVC, is:

$$\frac{1000}{62.5} \times 36.5 = 584 \text{ gram of HCl}$$

The calculation procedure shown above is suitable for all chlorine containing synthetic materials, since it is always assumed that, at combustion, the chlorine converts into HCl.

Groups b. and c.

For synthetic materials containing nitrogen as well as products from the cyanide group, only very few test results are known. From tests described in References [8] and [9] it appears that for both types of synthetic materials only a very small quantity of HCN is formed, namely a few grams per kg of consumed product.

It is assumed that mainly NO_x (expressed as NO₂) will be formed. It should further be remarked that the toxicities of HCN and NO₂ are comparable, so that, with regard to the effect, it is not significant whether either NO₂ or HCN are going to appear.

In case of combustion of an N-containing synthetic material, due to the above reason, it can be assumed that all of the N will convert into NO₂.

Groups d. and e.

No test results are known for either of these two groups.

By the combustion of fluor-containing synthetic materials, we can also then assume a quantitative conversion, whereby all the fluor will convert into HF.

For the group of other synthetic materials, we can assume a quantitative conversion of the hetero-atom in the material under consideration.

Pesticides

General

Pesticides, can be differentiated in a number of specific products.

- insecticides (protection against insects)
- herbicides (protection against weeds)
- fungicides (protection against mould)
- etc.

In this report, in which the specific application of these various products does not play any role, we will use, in what follows, the term "pesticides".

The pesticides which are used in agriculture and in gardens, mainly consist of organic compounds. Seen from a chemical view-point, they represent a very heterogeneous group.

Within the framework of this chapter, the following most essential characteristics of pesticides can be mentioned:

- the toxicity of the product for a human-being and an animal, and
- the high percentage of products which contain hetero-atoms.

Taking into account the fact that the products themselves are toxic, in case of a fire in which pesticides are involved, not only the toxic combustion products are important, but also the non-burning pure substance which spreads to the surroundings.

During a fire, a small portion of the non-burned substance will, in fact, disperse to the surroundings. Estimations of this quantity of non-burned substance differ. For substances with a high boiling-point it is evaluated that 1 to 2% of the product will disperse non-burned. For substances with a low boiling-point this percentage is estimated to be maximum about 10% [1]. Substances with a low boiling-point, in this respect, are those with a flash point $< 100^{\circ}\text{C}$.

In the establishment of the quantity of the combustion products which are formed and of the quantity of non-burned spreading product, the composition of the substance is important. The majority of the products, by far, contain only a small percentage of the active substance, complemented, most of the time, by a non-toxic carrier material.

The Combustion Products

If the pesticide is completely consumed, then the combustion products which, in principle, are formed, are the same as described for synthetic materials.

No data can be found in literature which would allow us to deduct, for specific substances, either the types of combustion products or the extent to which they might be formed.

Only for about 30 substances, the combustion products which appear are indicated. However, to which extent they are formed is also not known.

The results show, however, that for chlorine-containing products, as much chlorine as HCl is formed.

It is interesting to note that nitrogen containing combinations not only show the appearance of NH_3 , but NO and NO_2 are also present. According to Reference [1], for nitrogen containing compounds the chance of forming of NO_x - NH_3 - HCN decreases in that order.

The toxicity of these 3 substances, however, is not very different from one to the other, so that the eventual extent of damage which they may produce is also almost identical for either of these three products.

The Forming of PCDD's and PCDF's

Chlorinated hydrocarbons, and especially chlorinated aromats, are relatively often used as active substances in pesticides.

It is known that by combustion of this type of compounds polychlorodibenzo-p-dioxins can be formed (PCDD's) as secondary combustion products. This occurs if the benzene ring contains a minimum of 2 chlorine atoms.

In order to estimate the quantity of PCDD formed during a fire data about the combustion of household waste is used.

Combustion of household waste has been chosen because many measurements have been taken during the combustion of waste containing polychloro aromats. In this manner, the extent of formation of PCDD and PCDF can be evaluated.

It is established that during combustion of household waste PCDD's are formed, under which the most toxic isomer, the 2, 3, 7, 8 TCDD (the "Seveso dioxin").

On the basis of available data from Ref.[10] and [11] it is estimated that the amount of PCDD's formed out of household waste contains about 500 mg/kg of polychloro aromats. Next to it, out of this information, it has been deducted, that the quantity of 2, 3, 7, 8 TCDD in the PCDD's is equal to about 0.1 - 0.2% ($\approx 0.5 - 1 \text{ mg/kg}^{-1}$ 2,3,7,8 TCDD).

The other PCDD isomers which are formed are less toxic than 2,3,7,8 TCDD.

Speaking in general terms, however, it must be recognized that the conditions during a fire in which pesticides are involved can deviate appreciably from the conditions prevailing in a waste combustion installation.

It is known from literature that low temperatures, such as is the case during a smouldering process, benefit the formation of PCDD's (and consequently, also the formation of the 2,3,7,8, isomer).

From tests in which pentachloro phenol was burned at a relatively low temperature (between 620 and 760°C) it appears that the formation of 2, 3, 7, 8 TCDD was lesser than 20 mg/kg of pentachloro phenol [12].

On the basis of the above data, and in view of the fact that some other PCDD isomers also have a high degree of toxicity, it is estimated that per kg of burned polychloro aromats a few milligrams of products equivalent to 2,3,7,8 TCDD will be formed.

Even though the uncertainties are relatively high, it is estimated, based on the above figures, that the source-strength can contain 1-10 mg of 2,3,7,8 TCDD - equivalents per kg. of burned product. This for uncontrolled fires of chlorinated aromats with a minimum of 2 chlorine atoms.

If more is known about the composition, the emission of PCDD isomers can be converted into an equivalent emission of 2,3,7,8, TCDD using the procedure shown below.

This conversion is made on the basis of the difference in toxicity of the various isomers. The toxicity factor of these various isomers is established as follows [5]:

PCDD ISOMER		TOXICITY FACTOR	PCDF ISOMER		TOXICITY FACTOR
2,3,7,8	- Tetra CDD	1	2,3,7,8	- Tetra CDF	0.1
1,2,3,7,8	- Penta CDD	0.5	1,2,3,7,8	- Penta CDF	0.05
			2,3,4,7,8	- Penta CDF	0.5
1,2,3,4,7,8	- Hexa CDD	0.1	1,2,3,4,7,8	- Hexa CDF	0.1
1,2,3,6,7,8	- Hexa CDD	0.1	1,2,3,6,7,8	- Hexa CDF	0.1
1,2,3,7,8,9	- Hexa CDD	0.1	1,2,3,7,8,9	- Hexa CDF	0.1
			2,3,4,6,7,8	- Hexa CDF	0.1
1,2,3,4,6,7,8	-Hepta CDD	0.01	1,2,3,4,6,7,8	- Hepta CDF	0.01
			1,2,3,4,7,8,9	- Hepta CDF	0.01
1,2,3,4,6,7,8,9	- Octa CDD	0.001	1,2,3,4,6,7,8,9	- Octa CDF	0.001

On the basis of the emission of various PCDD – and PCDF – isomers in a mixture we can, with the help of the above toxicity factors, express this emission in terms of an amount of weight of 2,3,7,8 TCDD equivalents.

The calculation procedure, with the help of an example, is illustrated in paragraph 5.

Synthetic Fertilizers

General

Synthetic fertilizers are often composed of mixtures of various anorganic products such as calcium, phosphorus, potassium and anorganic nitrogen in the form of, for instance, ammonium nitrate.

In case of a fire involving synthetic fertilizers, the combustion products are also determined by the composition of the fertilizer.

The majority of fertilizers, by far, are the so-called mixfertilizers which are mainly composed of ammonium nitrate, ammonium phosphate and potassium chloride.

But also mix-fertilizers with magnesium oxide, ammonium sulphate and P_2O_5 can be found.

The name given to these mix-fertilizers is related to the main substances entering in their composition. For instance a NPK-10-15-20 mix contains 10% nitrogen, 15% phosphorus and 20% potassium.

The evaporation rate of $0.025 \text{ kg.m}^{-2}.\text{s}^{-1}$, which has been suggested in this study, is perhaps too high for synthetic fertilizers. The reason for this is the normally inert character of the substances entering into their composition. However, the mix-fertilizers which contain ammonium nitrate are, in this respect, an exception.

Since relevant data for fertilizers, on this point, are not available, the above value of the evaporation rate, even it is perhaps a pessimistic value, is nevertheless also retained for synthetic fertilizers in general.

The Combustion Products

In case of a fire involving synthetic fertilizers, dependent on the composition of the mix, the following products can be formed.

Element	Combustion product
ammonium nitrate	NO_2
ammonium phosphate	NO_2 and P_2O_5
ammonium sulphate	NO_2 and SO_2
potassium chloride	HCl

It is thus assumed that at combustion, all of the nitrogen will convert into NO_2 .

The extent to which these different combustion products are formed depends, among others, on the specific composition.

No known data are to be found in literature regarding combustion tests with synthetic fertilizers.

For an estimation of the extent to which the different combustion products are formed, it is assumed that complete combustion of the product takes place and that *all* nitrogen, sulphur, etc. are converted into corresponding combustion products.

Other Hydrocarbons

Aliphates

During combustion of aliphates only toxic combustion products are formed, if we are dealing with an hetero-atoms are involved.

In the establishment of the types of combustion products which are formed, it is assumed (unless other information is available) that complete combustion takes place. The combustion products which can

then be expected are dependent on the hetero-atom, and equal to those mentioned in paragraph 2.

Data are available for about 8 substances, taken from combustion and heating tests [13].

These results are summarized in the table below.

SUBSTANCE	COMBUSTION PRODUCTS [g/g] ¹			
	Open flame		Red-hot charcoal	
	HCl	COCl ₂	COCl ₂	HCl
carbon tetrachloride	0.199 ²	0.008 ²	0.014	0.525
chloroform	0.138	0.006	0.011	0.554
trichloro ethylene	0.266	0.001	0.014	0.437
tetrachloro ethylene	0.238	0.007	0.002	0.321
dichloro ethane	0.240	0	0	0.389
tetrachloro ethane	0.326	0.003	0.007	0.442
pentachloro ethane	0.332	0.002	0.006	0.400
hexachloro ethane	not determined	not determined	0.006	0.465

1) Average values out of 2 observations

2) Average out of 3 observations

It appears from the tests that at combustion in an open flame, as well as by incomplete combustion, mainly HCl is formed.

Considering the fact that, in case of fire, both situations can develop, it is considered prudent to use the most pessimistic condition, thus the incomplete combustion.

Aromats

Same as for all other organic substances, it is also valid, for aromats, that only toxic combustion products will be formed; that is if hetero-atoms are present.

No test data can be found in literature. The only exception are the polychloro aromats.

In case of an incomplete combustion of polychloro aromats PCDD's are formed. The situation is then similar to the one of pesticides, previously described, in both the qualitative as the quantitative senses. Per kg. of burned product, thus, 1-10 mg of 2,3,7,8, TCDD equivalents will be formed.

In case of a complete combustion of polychloro aromats CO₂, H₂O are formed, and/or Cl₂, HCl, COCl₂. To which extent these various products appear is not known. For an estimate of the quantities of formed products we can use the results of combustion of aliphates as a point of departure.

Also then, for the combustion of aromatic substances, we can assume that formation of phosgene takes place besides hydrochloric acid while the formation of PCDD'S must also be taken into consideration. For the combustion products of aromats with other heteroatoms than chlorine, we refer to the previously given table in paragraph 2.

Evaluation

An inventory of data presently available in literature regarding combustion products shows that information regarding the extent of their formation as well as the types of formed products is scarce (see also [14]). For further sources of information reference is made to [15], [16] and [17].

Only for a limited number of substances qualitative as well as quantitative data are known.

For these reasons, the formation of combustion products estimated in this study is primarily based on a theoretical approach. Whenever possible, the assumptions can be complemented by data out of practice.

The knowledge presently available is unified, so that for specific applications it can be used as a point of departure for estimates of emissions. The previously mentioned values and guidelines for the evaluation of the extent of formation of combustion products can, therefore, be considered as indications containing a relatively high degree of uncertainty. Consequently, in the application of the values obtained this uncertainty must always be taken into consideration.

In order to clarify the method to be followed, an identification chart is presented in Annex I, in which a short description of the various steps is given.

Calculation example

Three examples are presented in this chapter, in order to help making it clearer in which manner the formation of combustion products can be quantified.

Two of these examples are related to the formation of PCDD's, whereby in one case data about the isomer structure are known. The third example deals with the formation of HCl by the combustion of lindane.

Formation of PCDD's

a. The PCDD mixture is not known

In the case where the composition of the combustible gases is not known it is assumed that the emission contains 1-10 mg TCDD - equivalents per kilogram of burned product (see heading "the forming of PCDD's and PCDF's").

It is further recommended to estimate a source-strength density of $0.025 \text{ kg.m}^{-2}.\text{s}^{-1}$, that is in case this cannot be calculated using the previously given evaporation formula (for instance if sufficient data are not available). We will use the above value in this example.

On the basis of the above we can calculate the emission in case of a fire.

This value varies, per m^2 of fire area, between:

$$1 \cdot 10^{-6} \times 0.025 = 2.5 \cdot 10^{-8} \text{ kg.m}^{-2}.\text{s}^{-1}, \text{ and}$$

$$10 \cdot 10^{-6} \times 0.025 = 2.5 \cdot 10^{-7} \text{ kg.m}^{-2}.\text{s}^{-1}$$

b. The PCDD mixture is known

We assume that $50 \text{ mg.m}^{-2}.\text{s}^{-1}$ of PCDD mixture are formed. The composition is given in the table below.

COMPOSITION (% of weight)	ISOMER	TOXICITY FACTOR [-]
0.1	2,3,7,8	1
20	1,2,3,7,8	0.5
70	1,2,3,7,8,9	0.1
9.9	1,2,3,4,7,8,9	0.01

On the basis of the composition and of the toxicity factor the conversion into 2,3,7,8 TCDD equivalents is as follows:

$$0.001 \times 50 \times 1 = 0.05$$

$$0.20 \times 50 \times 0.5 = 5.00$$

$$0.70 \times 50 \times 0.1 = 3.50$$

$$0.099 \times 50 \times 0.01 = 0.050$$

$$\text{Total} \quad 8.60 \text{ mg.m}^{-2}.\text{s}^{-1} \text{ 2,3,7,8 equivalents}$$

The result is consequently, an emission of $8.60 \text{ mg.m}^{-2}.\text{s}^{-1}$ 2,3,7,8, TCDD equivalents.

Formation of HCl

For the quantification of the extent to which HCl is formed out of lindane we will assume that the product subjected to the fire contains 10% of lindane. The fire area is equal to 100 m², the calculation, then, proceeds as follows:

Assuming an evaporation rate, during the fire, of 0.025 kg. m⁻².s⁻¹, (see paragraph 3 'general') the formation of the combustion product out of 1 kg of the burned substance can be calculated as follows:

$$M_v = \frac{1}{M_1} * n * M_2 * g * 0.025$$

M_v = source-strength density of the formed combustion product [kg.m⁻².s⁻¹]

M_1 = molecular weight of the burned substance [kg.Kmol.⁻¹]

n = number of hetero-atoms in the molecule of the burned substance [-]

M_2 = molecular weight of the combustion product [Kg.Kmol.⁻¹]

g = percentage of weight of the burned substance in the product [weight %]

Applicable to this example:

Formula for lindane	: C ₆ H ₆ Cl ₆
Molecular weight	: 290.8
Number of Cl atoms	: 6
Combustion product	: HCl
Molecular weight of HCl	: 36.5
Weight percentage of lindane	: 10

$$M_v = \frac{1}{290.8} * 6 * 36.5 * 0.10 * 0.025$$

$$M_v = 1.88 * 10^{-3} \text{ kg.m}^{-2}.\text{s}^{-1} \text{ HCl}$$

The following is formed for a 100 m² fire surface:

$$100 \times 1.88 * 10^{-3} = 0.188 \text{ kg.s}^{-1} \text{ HCl}$$

References

- [1] Onderzoek naar de gevaren van de opslag van bestrijdingsmiddelen, BIV-TNO, dossiernr. 8713-3534, mei 1980.
- [2] Jonge de, S.L.
Brandveiligheid van de opslag voor gewasbeschermingsmiddelen. rapportnr. 2-79-8100 VM 01, februari 1979.
- [3] Methoden voor het berekenen van de fysische effecten van het incidenteel vrijkomen van gevaarlijke stoffen (vloeistoffen en gassen) CPR-14.
Directoraat Generaal van de Arbeid, 1979.
- [4] Duiser, J.A.; Hoftijzer G.W.
Onderzoek naar de mogelijke gevaren van de opslag van bestrijdingsmiddelen bij Aagrunol. MT-TNO. ref.nr. 80-0285, mei 1980
- [5] Voorstel tot een methode voor de beoordeling van de toxiciteit van mengsels van gehalogeneerde dibenzo-p-dioxines en dibenzofuranen.
Werkgroep toxiciteitsequivalentie, maart 1988.
- [6] Naas, Leonard, I.: ed.
Encyclopedia of PVC, Vol.3
Marcel Dekker Inc.
- [7] Coleman E.H., Thomas C.H.,
The products of combustion of chlorinated plastics,
Journal of applied chemistry, 4 July 1954.
- [8] De vorming van al dan niet voor de gezondheid schadelijke ontledingsprodukten door brandende of smeulende kunststoffen,
Verzameling bouwstudies nor. 14.
Uitgave Bouwcentrum Weena 700. Rotterdam, Juni 1966.
- [9] Dr. Rennoch Detlef,
Physikalisch-chemische analyse sowie toxische Beurteilung der beim thermischen Zerfall organischchemischer Baustoffe entstehenden Brandgasse. Literaturstudie (Teil I und II),
Bundesanstalt für Materialprüfung (BAM),
Berlin, 1978/1979.
- [10] Ir. Kiers A. Ir. Bartelds H., Ing. Brem G.,
Verbranding van fracties huishoudelijk afval in een wervelbedvuurhaard,
MT-TNO. dossiernr. 8727-50081, april 1985.
- [11] Meinema Dr. H.A.,
Polychloordibenzo-p-dioxines en polychloordibenzofuranen in verbrandingsprodukten van huisvuilverbrandingsinstallaties, december 1979.

- [12] Janssen B. and Sundström G.,
Formation of polychlorinated dibenzo-p-dioxins during combustion of chlorophenol formulations,
The science of the total environment.
10 (1978) 209-217
- [13] Sjöberg. B.,
Thermal decomposition of chlorinated hydrocarbons,
Svensk Kemisk Tidskrift vol. 64, pp. 63-79, 1952.
- [14] Finnecy, E.E. Krol, A.A.;
Hazardous combustion products.
Environmental Safety Centre Harwell Laboratory,
United Kingdom Atomic Energy Authority,
Health and Safety Executive.
June 1988. HSE/SRD/047/NP3 AERE - R12817
- [15] Klimisch, H.J. e.a.
Bioassay procedures for fire effluents: basic principles, criteria and methodology.
Journal of fire sciences, vol. 5, March/April 1987.
- [16] Draft for development: code of practice for the assessment of toxic hazards in fire buildings and transport.
BSI standards. Document 88/43550. September 1988.
- [17] Doe, J.E.
The combustion toxicology of polyvinylchloride revisited.
Journal of fire sciences vol. 5, July/August 1987.

Table I

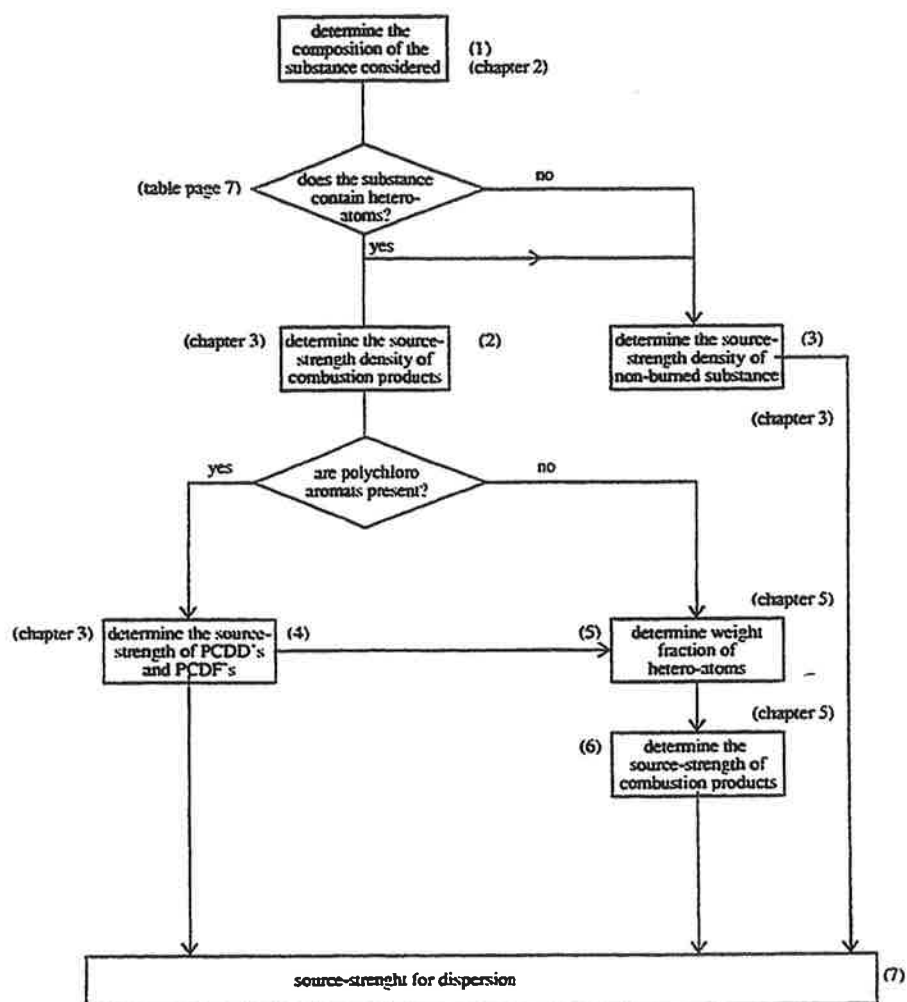
Overview of combustion tests with chlorine containing polymers.

SUBSTANCE	gram/kg of burned product			SOURCE
	HCl	CL ₂	COCL ₂	
PVC (56% Cl)	583	0	0	[6]
idem	535	0	0	[6]
idem	580	0	0	[6]
Chlorinated polymethyl metacrylate (27% Cl)	147	0	0.120	[7]
PVC (57% Cl) (not stabilized)	480	0	0.105	[7]
Vinyl-and-vinylidene chloride (copol.) 61% Cl	545	0	0.455 ¹	[7]
PVC-stabilized 33% Cl	220	0.011	0.500	[7]
PVC-stabilized 31% Cl	235	0.011	0.500	[7]

¹⁾ Average value of results for 3 combustion temperatures, namely about 300, about 600 and about 900°C.

Annex I

Identification chart for the quantifying of the formation of toxic combustion products



Explanations for the identification chart

ad 1. The composition of the chemical substance determines the combustion products which can be formed.

See Chapter 2 for further description.

ad 2. The source-strength density gives the *total* evaporated, and so the burning, amount of the substance. These data constitute a point of departure for the calculation of the extent to which toxic combustion products will be formed.

See Chapter 3 for a detailed description.

ad 3. Dependent on the value of the boiling point, a certain degree of emission of the non-burned product is assumed to take place. This is namely important for substances with high toxicity.

See Chapter 3 for further description.

ad 4. By combustion of chloro aromats (with at least 2 Cl-atoms in the molecule) dioxins and furans can be formed.

It is explained, in Chapter 5, in which manner the amount of formation of the so-called 2,3,7,8 TCDD equivalents is determined.

ad 5. and ad 6.

Based on the weight fraction of the hetero-atom or atoms in the molecule and of the (quantitative) conversion of it into a combustion product, jointly with the source-strength density (see ad 2), the extent of emission of the combustion product can be determined.

With the help of an example (Chapter 5), the calculation of this extent of emission is explained.

ad 7. When the extent of emission of combustion products has been determined, the concentration in the surroundings can be calculated using the appropriate dispersion models.

Chapter 5

Damage caused by acute intoxication

Contents

	Page
Explanation of terms and abbreviations	4
Summary	6
1. Introduction	7
2. Scope	8
3. Selection of substances	9
4. Inventory of data on toxicity	10
4.1 General	10
4.2 Inventory	10
5. Adaptation of data on toxicity	11
5.1 Extrapolation of acute inhalation toxicity data from animal to human being	11
5.1.1 Introduction	11
5.1.2 Methodology	11
5.2 Calculation of probit constants	14
5.2.1 Probit analysis	14
5.2.2 Estimate of human probit constants	16
6. Discussions and conclusions	20
7. References	22
Annex 1	
Selection of substances	25
Annex 2	
Inventory of data on toxicity	27
Annex 3	
Data on animals and the LC ₅₀ values for human beings calculated from it	35

Explanations of terms and abbreviations

Acute	Of short duration; minutes to (max 24) hours
Averaging time	Time duration within which the concentration differences over the width of a plume of released substance are averaged
Casuistry	Practice, in this study: past accidents
Concentration	Fraction of a given substance in a medium (air, water, ground, another substance)
Dermal	Through the skin
Dispersion	Spreading in the medium in which the substance has been released and mixing with this medium
Dose	1. The total quantity of absorbed substance 2. Function of concentration and exposure duration
Effect model	Description of physical effects (which take place during an accident)
EPEL	One-time population exposure limit; concentration to which the population, on the basis of present knowledge, can be exposed one-time in a life-time for a short duration ($1/2$ to 2 hours), with, as maximum consequence, a reversible sickness phenomenon
Ground roughness	Measure of the effect of ground conditions on dispersion
Human	Applicable to human beings
Inhalation	Through the respiratory system
Interspecies differences	Differences of one type versus another species
Intraspecies differences	Differences between individuals of one and the same type (intra = inner)
LC	Lethal concentration; a concentration by which a given percentage of the exposed population will be fatally injured (this percentage is given as an index).
LD	Lethal dose (analogous to LC)
Lethal	Deadly, mortal
Linear regression	Statistical technique, whereby, based on a number of observations (x_i, y_i) the parameters a and b of the function $y = a + bx$ are determined.
Oral	Via the alimentary canal
Pasquill-class	Weather (stability) class, based on time of day, the magnitude of the clouds, the wind velocity and the season
Probability model	Description of probabilities related to the occurrence of effects and damage
Probit	Quantity; obtained by a statistical transformation of a percentage; very sensitive in the range around 50%, and with little sensitivity in ranges near 0 and 100%
Probit analysis	Statistical technique, with which the relationship between response and stimulus (i.e. exposure to toxic substances) is presented
(-constant,-function)	
Release rate	Amount of released substance per unit of time
Reliability interval	Interval round the calculated value of a quantity, within which a certain percentage of observations (for instance 95%) will be located
Response fraction	Part (i.e. of exposed population) which exhibits a given response (in our cases incurs a given type of injury)
Response percentage	Response fraction x 100%
RTECS	Registry of Toxic Effects of Chemical Substances
Sample	Sample from population
Species	(Animal) type

Standard deviation	Measure for the spread in the observations
STEL	Short Term Exposure Limit; average concentration over 15 minutes, the exceeding of which (even only once during a working day) is considered unacceptable
TC	Toxic Concentration; lowest measured concentration by which a degree of toxic effect is still possible .
TD	Toxic dose (analogous to TC)
Toxic	Poisonous
Vulnerability model	Relationship between response fraction and dose, for a given type of injury

Summary

Within the framework of the 'Green Book', making use of a new methodology, we will establish, for a number of substances, acute toxicity data, which are applicable for the inhalation by human beings. For this purpose, some 25 substances have been selected on the basis of toxicity, volatility and frequency of presence (stored/used quantities). The selection was made with the help of discussions with companies and authorities and, also, on the basis of data out of FACTS, the accident database of TNO. An inventory of data available in open literature, for these substances, was made of their acute toxic consequences for inhalation. On the basis of these data (mostly from animals), with the help of a specially developed extrapolation model, a 30 minutes LC₅₀ value for the human being has been derived. Further-on, making use of these LC₅₀ values, vulnerability models applicable to humans have been established for use in risk analysis. These models are presented in the form of probit functions, for which the necessary parameters have been derived.

The methodology used in this study to derive probit functions is primarily directed towards substances for which (too) little toxicity data are available. Whenever a user intend to offer a better backed-up probit function, based on sufficient toxicity data, this will be judged by a forum of experts (to be set-up). The exact procedure, will be established by the Committee for the prevention of Disasters.

1

Introduction

In this chapter of the 'Green Book' consideration is given to damage to people due to exposure to toxic substances¹. We differentiate, hereby, between exposure duration and way of exposure, as well as the degree of toxicity. We limit ourselves, in this study, to the problem of lethal injury due to acute inhalation exposure. The subject is further described in Paragraph 2.

A number of substances have been selected for the purpose of the present study. This selection was made, on one side, on the basis of indications given by industry regarding quantities of products used and stored, and, on the other side, on the basis of the toxicity of the substances as well as of their volatility (which represents a measure of the possible spreading of the substance in the atmosphere). The selection is further explained in Paragraph 3 and in Annex 1.

In Paragraph 4 results of an inventory of toxicity data are given for the selected substances, taken over from information which was available. In the same time, it is also indicated to what extent these results can be used in order to estimate the acute toxicity for people. Finally, in Paragraph 5, attention is given to the applicability of data obtained with animals to humans. Also, in Paragraph 5, relationships are established between toxicity data of different types of injuries.

¹ For an explanation of terms and abbreviations, see the list given in page 4.

2

Scope

In the evaluation of exposure to toxic substances we must differentiate between the way of exposure and the time of exposure.

The way of exposure means the way in which a given individual comes into contact with the toxic substance. In this respect, we can differentiate between exposure through the alimentary canal (oral), through the respiratory system (inhalation), through the skin (dermal), etc.

For the time of exposure we must differentiate between chronical and acute exposure. Chronical exposure can stretch for periods between days to years, while for acute exposure minutes up to some hours (max. 24 hours) are considered.

At the same time, the toxicity of the substance is important. This toxicity manifests itself in the degree of injury due to a given type of exposure. We orient ourselves, in this study, towards lethal (deadly) injury and, in particular, on short-term consequences of the release of toxic gases and/or vapours. The intoxication, then, results from breathing-in the toxic substance. We are dealing here, consequently, with acute inhalation intoxication.

The release of a toxic substance represents a potential danger for the surroundings whenever a given number of people can be subjected to the consequences of toxicity. The danger, on one side, is dependent on the possible spreading of the substance and, on the other side, it is also dependent on the concentration for which the substance is still toxic, as well as on the duration of the exposure. For most of the substances considered in this study, the quantity of released substance dangerous to people is such that only substances stored and/or transported in relatively large quantities are of importance. This, in practice, applies to products normally used in the industry.

Selection of substances

Since it is not practically feasible to establish damage criteria for all toxic products used by the industry, we have selected those products for which an inventory of their toxicity data is considered necessary. The criteria applicable to such a selection are:

- a. specific toxicity
- b. volatility (of liquids)
- c. frequency (how often it is encountered in practice)

The extent to which a toxic substance can produce damage to the surroundings is determined by the dispersion and by the toxicity of the substance. The dispersion is dependent on the release rate, the weather conditions and (for liquids) on the volatility of the substance. A liquid, for instance, with a low vapour pressure will evaporate slowly when released, so that the distance at which a toxic concentration may still be present is generally small. This leads to a given variation of the concentration as function of the distance. Duizer [14] established a risk index, a quantity, in which the above-mentioned factors are combined. The risk index RI is the ratio of the concentration which is reached at a given distance to the source versus the concentration above which a given degree of injury may be incurred. This risk index has been calculated for a substantial number of substances.

The risk index is used as a quantity for the selection of the substances for which the probit-function is relevant. This selection procedure is described in Annex 1. The substances selected are indicated in Table 3.1.

Table 3.1 Selected substances.

UN-nr	Substance	UN-nr	Substance
1092	Acrolein	1051	Hydrogen cyanide
1093	Acrylonitrile	1052	Hydrogen fluoride
1098	Allyl alcohol	1053	Hydrogen sulphide
1005	Ammonia	1062	Methyl bromide
-	Azinphosmethyl	2480	Methyl isocyanate
1744	Bromine	1067	Nitrogen dioxide
1131	Carbon disulphide	1668	Parathion
1016	Carbon monoxide	1076	Phosgene
1017	Chlorine	-	Phosphamidon
1040	Ethylene oxide	2199	Phosphine
1198/	Formaldehyde	1079	Sulphur dioxide
2209		1829	Sulphur trioxide
1050	Hydrogen chloride	-	Tetraethyllead

Inventory of data on toxicity

4.1 General

For the inhalation exposure the following data on toxicity must be differentiated:

a. EPEL values

The EPEL (One-time population exposure limit) is a criterium which is applied as a limit value for a light irritation².

The EPEL value is defined as the concentration to which the population, on the basis of present knowledge, can be exposed for a short duration ($\frac{1}{2}$ to 2 hours). It is thereby considered that a benign and reversible (curable) sickness phenomenon is acceptable.

b. LC values

An LC value is the concentration at which a given percentage of the exposed population will die. The injury percentage is given as an index.

c. Vulnerability models.

The vulnerability model gives a percentage of response (or of the quantity derived for it, the probit) as function of the concentration and of the exposure duration.

The inventory indicates that not for all of the selected substances one of the above-mentioned values is available. In order to still be able to get an idea about the toxicity of such substances, the LD value (lethal dose) is given for them (to the degree to which it is known).

4.2 Inventory

Data out of open literature are used for the establishment of the inventory of the data on toxicity for the selected substances.

The following basic points have been chosen for the selection:

- exposure duration < about 4 hours
- inhalation exposure
- exposure duration known
- data regarding the animal species subjected to the test
- data based on accidents (human data)

For each of the selected substances it has been carefully checked which (recent) information about their toxicity is available. An important part of the data available for this purpose has been taken out of the automated database of RTECS [1].

Annex 2 contains an overview of the inventory.

² The Health-Council has advised that EPEL should no longer be applied in the jurisdiction for external safety [19].

Adaptation of data on toxicity

With information assembled as described in the previous chapter, several adaptations have been made for the purpose of establishing vulnerability models applicable to human beings.

The methodology presented in this study is based on hypotheses referred to n and b, and a calculation of a with the help of an LC_{50} value applicable to a human being. This type of extrapolation will be handled in the forthcoming paragraph, while the calculation of the probit constants will be presented in Paragraph 5.2.

5.1 Extrapolation of acute inhalation toxicity data from animal to human

5.1.1 Introduction

Up to now, there is no generalized method allowing us, from acute toxicity data obtained from tests with animals, to calculate the number of human victims (for a given population) resulting from a short term exposure to a certain degree of concentration of a substance. The purpose of a 'Green Book', however, requires a method permitting us to calculate the lethality for humans, in case of a calamity.

Due to the absence of relevant data regarding acute toxicity for humans, it does not appear possible, on the basis of present knowledge of toxicology, to develop a general method or a calculation procedure allowing us to determine the percentage of fatalities caused by a given accident.

However, in view of the urgent necessity of such a calculation and extrapolation model, we will present a method in what follows. The method presented, if we properly take into consideration its limitations, appears to be applicable.

5.1.2 Methodology

Substances which can enter the lungs can be differentiated between locally acting substances and systemically acting substances. The locally acting substances exert their effect on the organ in which they penetrate; since, in this study, we are dealing with the inhalation exposure, the locally acting substances will be the ones which produce damage to the respiratory channels.

The systemically acting substances are the ones absorbed by the lungs and transported by blood, which means that their effect can manifest itself somewhere in the body. Hereby, pharmaco-kinetics and pharmaco-dynamics play an important role. They can be strongly species dependent.

5.1.2.1 Locally acting substances

The damage which a substance can cause to the respiratory channels is dependent on: the toxicity of the substance, the sensitivity of the species, the total quantity of breathed-in substance (breathed-in dose) and on the area of the lungs (the quantity of tissue) over which the substance has spread; for the same breathed-in dose the damage will be smaller for a large area versus a smaller area. The breathed-in dose per unit-area of the lungs, D'' [mg/m^2], can consequently be considered as a measure of the damage caused by locally acting substances. This is given by:

$$D'' = D/A \text{ [mg/m}^2\text{]} \quad (1)$$

with D - breathed-in dose [mg]
 A - area of the lungs [m^2]

The breathed-in dose is dependent on the quantity of breathed-in air (a product of the exposure duration and of the breathing-minute-volume) and on the concentration of the substance in the air. This is given by:

$$D = (V_a/1000)C \cdot t \quad (2)$$

with V_a - breathing-minute-volume [l/min]

C - concentration [mg/m³]

t - exposure duration [min]

Assuming that all of the breathed-in substance turns up in the lungs (passing-by the possibilities that substances can be reabsorbed or discharged via the lung clearance), the breathed-in dose per unit lung area is equal to:

$$D'' = C \cdot t (V_a/1000)/A \quad (3)$$

It appears possible to derive the lung area and the breathing-minute-volume from the weight of the body, according to empirically determined formulas [30].

$$V_a = u \cdot W^{0.70} \quad (4)$$

$$A = v \cdot W^{0.92} \quad (5)$$

with W - weight of the body

u, v - regression coefficient

If we fill-in results (4) and (5) into (3), the breathed-in dose becomes proportional to the weight of the body, according to the following relationship:

$$D'' = (u/v) \cdot W^{-0.22} \quad (6)$$

The ratio between the loads exerted on animal and human, for the same concentration, is then equal to the ratio of the corresponding breathed-in doses; this ratio can then be calculated by substituting, in (6), the weights of the bodies of the animal and of the human-being, respectively, and then divide the two results by each other. For a rat weighing 300 g and a human weighing 70 kg, the load on the rat is equal to 3.3 times the load on the human; for a mouse weighing 30 g the loading is equal to 5.5 times the load on the human.

The ratios mentioned above are only valid for a condition of rest, for either human or animal.

In assuming that all of the substance will turn-up in the lungs, we have disregarded the fact that in the front air channels a portion of the substance will already have been caught and that, consequently, this portion will not come into the lungs. The absorption efficiency of the nose of a test animal is much larger than that of the human. In addition, the human breathes a lot through the mouth, which has a minor absorption efficiency. The majority of test animals, on the other hand, are obligated nose breathers. Due to this, more substance will penetrate, proportionally, into the lungs of a human being than into the lungs of the animal. Furthermore, it is not known if the same dose of substance per unit area has the same effects by the animal as by the human. In order to cover these possible differences between species, an arbitrarily chosen safety factor of 5 is applied.

On the basis of formula (6) and of the above-mentioned safety factor of 5, the extrapolation factor f_d has been determined for a number of animal species (see Table 5.1).

5.1.2.2

Systemically acting substances

The systemically acting substances penetrate into the blood-circuit and distribute in the body, leading

thereby to damages. The differences between a human and an animal are related, on one side, to the way in which the substance is taken by the blood, and, on the other side, to the pharmaco-kinetics and the pharmaco-dynamics, which determine the consequences of the toxicity.

A measure of the absorbed quantity, in this case, is the dose per unit body weight D' ; similarly to (1) this can be calculated as:

$$D' = D/W \quad (7)$$

For systemically acting substances the quantity of absorbed substance is more proportional to the oxygen consumption than to the breathing-minute-volume; the oxygen consumption, in turn, is also dependent on the body weight, approximately similar to equation (4). Filling-in values (2) and (4) into (7) gives:

$$D' = u \cdot W^{-0.3} \quad (8)$$

We can calculate, with the above, that the load on a rat (300 g) and, respectively a mouse (30 g), is equal to 5.1 times and 10.2 times, respectively, the load on a human (70 kg).

The pharmaco-kinetics and pharmaco-dynamics, as well as metabolism, are important for the toxicity of systemically acting substances. Large differences could arise, in this case, between the different animal species and the human-being, even though it is assumed that, generally, these differences will not be all that large.

Admittedly, in this respect, data are known for only a very limited number of substances which can be inhaled.

All of this means that, under a condition of rest, and by identical kinetics, dynamics, metabolism and sensitivity, the LC_{50} values for the human will be much higher than those for the mouse and higher than those for the rat.

It could, however, be expected that, in as much as the substances will be taken-in slower by the human than by a small animal, the elimination of the substances will also be generally slower. Since major differences in metabolism, pharmaco-kinetics and pharmaco-dynamics between animal species and humans cannot be excluded, the degree of uncertainty, in this case, will be higher than for locally acting substances. For this reason, a safety factor of 10 is foreseen for systemically acting substances, twice as large as for the locally acting substances.

For systemically acting substances the extrapolation factor f_d , determined for a number of animal species, is presented in table 5.1.

5.1.2.3

Complementary considerations

Basing ourselves on the above-mentioned assumptions, it can be established that, as far as the end result is concerned, there really will not be any differences between locally acting substances and systemically acting substances. Consequently, with regard to the extrapolation from animal to human being, there is actually no need to differentiate between the two.

The application of the previously named safety factor to a large number of substances will, on the average, lead to an appreciable overestimate of the lethality to a human-being. If this extrapolation, for purposes of risk analysis, is applied to individual substances, then its application without this safety factor could easily lead, in turn, to an underestimate of the risk of lethality. For this reason, such an application (without safety factor) would not be considered as responsible.

In all of the above considerations no account has been taken, yet, of differences in bodily activities of the individuals in question. In an LC_{50} experiment the animal encounters itself in a condition of rest. As consequence of stress, it could happen that the breathing-minute volume could be somewhat higher.

Also, for individuals located indoors during a calamity a similar effect, due to stress, could take place. A person located outdoors will try to escape, and then his breathing-minute-volume could increase by about 5 times. On the average, however, more people will be located indoors than outdoors. We will assume, consequently, that the average breathing-minute-volume of an exposed population will increase to twice the value of the rest condition. This means that the safety factor will, in fact, again be multiplied by 2 (the LC_{50} values for the human will be divided by 2).

*Table 5.1 Extrapolation factor f_d for the calculation of LC_{50} (human)
(30 minutes LC_{50} (human) = $f_d \times 30$ minutes LC_{50} (animal)).*

Animal (d)	Substance	<u>Load animal</u> Load human	Safety factor	Extrapolation factor f_d
Rat (1)	Local	3.3	5 x 2	0.33
	Systemical	5.1	10 x 2	0.26
				} 0.25
Mouse (2)	Local	5.5	5 x 2	0.55
	Systemical	10.2	10 x 2	0.51
				} 0.5
Guinea pig (3)	Local	2.6	5 x 2	0.26
	Systemical	3.8	10 x 2	0.19
				} 0.2
Hamster (4)	Local	3.6	5 x 2	0.36
	Systemical	5.8	10 x 2	0.29
				} 0.3
Others (5)				Estimate per substance

5.2

Calculation of Probit Constants

5.2.1

Probit Analysis

It is possible, with probit functions, to determine a relationship between response and dose (function of concentration and exposure duration), for every arbitrarily chosen concentration. This by difference, for instance, with LC values, which only give one combination of concentration, exposure duration and response. In the same time, a probit function indicates how the contributions of concentration and duration relate to each other.

A vulnerability model for acute inhalation toxicity, for purposes of risk analysis, is thus generally given in the form of a probit function.

The probit function, in the most elementary form, is equal to:

$$Pr = a + b_1 \ln C + b_2 \ln t \quad (5.3)$$

in which Pr is a quantity derived, via a statistical transformation, from the response fraction R as follows:

$$R = \int_{-\infty}^{Pr-5} \exp\left(-\frac{1}{2}u^2\right) du \quad (5.4)$$

A graphical reproduction of the relationship between $\ln D$ (D = dose) and the response percentage, respectively the probit, clearly shows the difference. In Figure 5.1 the response percentage left, and the

probit right, are set-up linearly: the S-forming curve belongs by the left axis and the straight line by the right-axis.

Table 5.2 Relation between percentages and probits (Ref.: [16]).

%	0	1	2	3	4	5	6	7	8	9
0	-	2.67	2.95	3.12	3.25	3.36	3.45	3.52	3.59	3.66
10	3.72	3.77	3.82	3.87	3.92	3.96	4.01	4.05	4.08	4.12
20	4.16	4.19	4.23	4.26	4.29	4.33	4.36	4.39	4.42	4.45
30	4.48	4.50	4.53	4.56	4.59	4.61	4.64	4.67	4.69	4.72
40	4.75	4.77	4.80	4.82	4.85	4.87	4.90	4.92	4.95	4.97
50	5.00	5.03	5.05	5.08	5.10	5.13	5.15	5.18	5.20	5.23
60	5.25	5.28	5.31	5.33	5.36	5.39	5.41	5.44	5.47	5.50
70	5.52	5.55	5.58	5.61	5.64	5.67	5.71	5.74	5.77	5.81
80	5.84	5.88	5.92	5.95	5.99	6.04	6.08	6.13	6.18	6.23
90	6.28	6.34	6.41	6.48	6.55	6.64	6.75	6.88	7.05	7.33
-	0.0	0.1	0.2	0.3	0.4	0.5	0.6	0.7	0.8	0.9
99	7.33	7.37	7.41	7.46	7.51	7.58	7.65	7.75	7.88	8.09

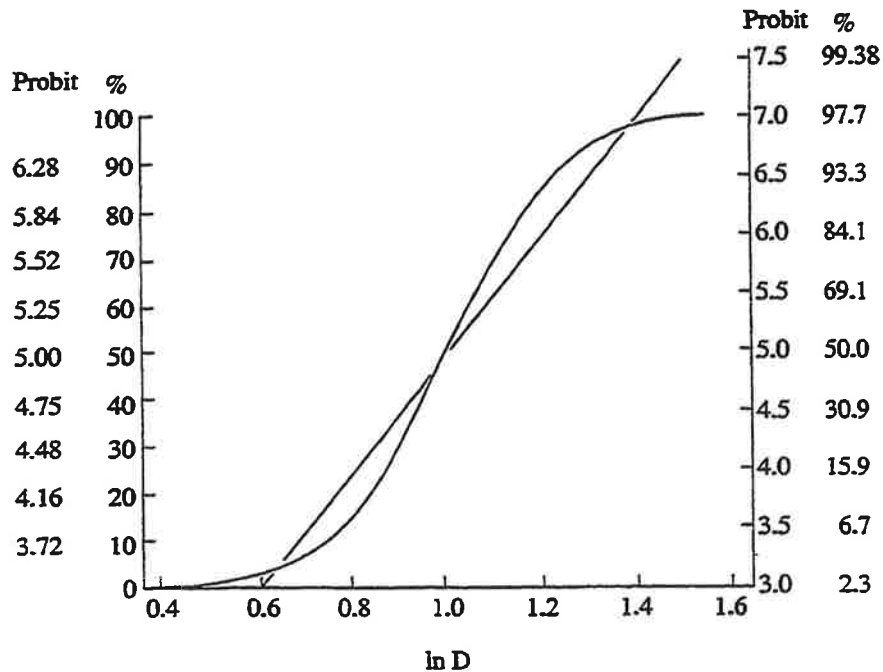


Fig. 5.1 Effect of a probit transformation. The S-curve changes into a straight line when the percentage is no longer set-up linearly on the vertical axis, but the probits are given linearly (Ref.: [16]).

In practice, Table 5.2 is used for the conversion of percentages into response or vice-versa.

Most of the times, instead of equation 5.3, equation 5.5 (below) is used. Hereby: $b = b_2$ and $n = b_1/b_2$.

$$\text{Pr} = a + b \ln(C^n) \quad (5.5)$$

Even though many attempts have been made, in the past, to establish a-values for injuries other than lethal injury, it is not possible, within present knowledge of acute toxicity and of probit-analysis, to determine a-values for other injuries which would be equally reliable to the ones for lethal injury. Even the probit constants for lethal injury presented here are, in great part, based on assumptions and estimates.

5.2.2

Estimate of Human Probit Functions

In order to arrive at an estimate of human probit functions as responsible as obtainable, the following hypotheses are made:

Inter-species differences

The reasons for the differences in response between various species have been discussed in the preceding paragraph. It has been shown that the difference in sensitivity is one of the important reasons. This difference in sensitivity can be expressed as a factor which influences the concentration C (or the exposure duration); the same applies to the other reasons. Such a factor, from a calculation view-point, always appears in the a-term. This means that a difference in sensitivity between human-being and animal does not influence the b-term (and, consequently, also not the n-term), but only the a-term.

Intra-species differences

The response differences within a given species are the consequences of variations of the vulnerability of individuals. This variation expresses itself in the steepness of the probit function.

A measure for the steepness of the probit function is the ratio of the doses (C^{nt}) corresponding to response percentages of, for example, 95% and 5%. This ratio is:

$$D_{95}/D_5 = \exp (Pr_{95} - Pr_5)/b$$

The ratio is smaller for higher values of b. The value of b is known for a number of substances; it seems to vary between 1.1 and 6.1 (see Table 5.3). If we take $b = 1.0$, the above ratio is equal to about 27. Since, in practice, the ratio of concentrations corresponding to the lowest and highest response percentages is often < 10 , (although 20 has also been observed), this means that the assumption $b = 1.0$, if the concentration is lower than the LC_{50} concentration, is generally a conservative assumption. With this we take into account the greater spreading in sensitivity for a human population, as compared to a group of young and healthy animals used for toxicity tests. For concentrations higher than the LC_{50} value however such an approach is unsafe.

However, in practice, the concentrations to which a group of population will be exposed are most of the time lower than the LC_{50} values, for which $b = 1.0$ is justified.

Concentration and exposure duration

The relative contribution of concentration and exposure duration to the toxic load is not equal for all substances. In the probit function, this relation is expressed by the factor n. Not much is known, up to now, about the variation of n between species and within species; due to this, it will be assumed in this study that the value of n such as it is known for animals is also applicable to humans. If several values are available, then an average will be taken. Generally, this value of n is in the range of 2; for substances for which n is not known, this value of 2 will then also be retained.

Calculation procedure

The final calculation procedure for the probit constants is reproduced in Figure 5.1. The first step, if required, is to convert the LC_{50} values to a 30 minute period, under the assumption $C^{nt} = \text{constant}$. If the value of n is not known, it will be taken equal to 2. In the next step, the LC_{50} (human) is calculated, using the extrapolation factors out of table 5.1. If toxicologically relevant data about several animal species are known, the LC_{50} (human) will be set equal to 2 x the average of the animal values. Finally, with the LC_{50} values determined in this manner, the a-values can be obtained.

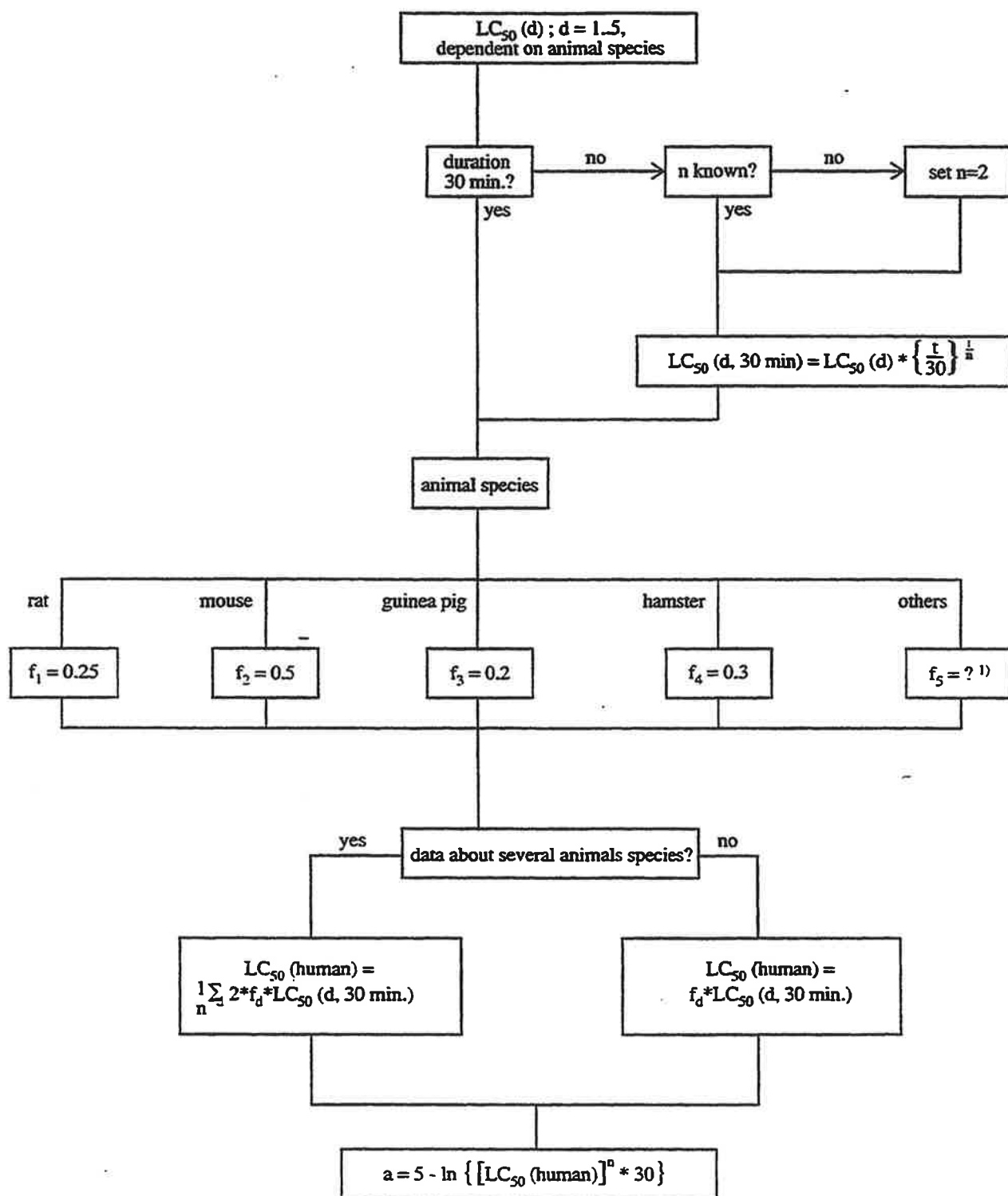


Fig. 5.1 Calculation procedure for the probit constants.

1) Estimate per substance.

The hypotheses and results of the calculation of the probit constants are given in Table 5.3.

Table 5.3 Probit constants for humans calculated on the basis of extrapolated LC₅₀ values, and according to the method, developed for substances for which little (insufficient) toxicity data are available (concentration in mg/m³, duration in minutes).

Substance	30 min-LC ₅₀ mg/m ³	n	b	a
Acrolein	304	1.0	1	- 4.1
Acrylonitrile	2533	1.3	1	- 8.6
Allyl alcohol	779	1.0 ¹⁾	1	- 5.1
		2.0 ²⁾	1	-11.7
Ammonia	6164	2.0	1	-15.8
Azinphosmethyl	25	1.0 ¹⁾	1	- 1.6
		2.0 ²⁾	1	- 4.8
Bromine	1075	2.0	1	-12.4
Carbon monoxide	7949	1.0	1	- 7.4
Chlorine	1017	2.3	1	-14.3
Ethylene oxide	4443	1.0	1	- 6.8
Hydrogen chloride	3940	1.0	1	- 6.7
Hydrogen cyanide	114	2.4	1	- 9.8
Hydrogen fluoride	802	1.5	1	- 8.4
Hydrogen sulphide	987	1.9	1	-11.5
Methylbromide	3135	1.1	1	- 7.3
Methylisocyanate	57	0.7	1	- 1.2
Nitrogen dioxide	235	3.7	1	-18.6
Parathion	59	1.0 ¹⁾	1	- 2.5
		2.0 ²⁾	1	- 6.6
Phosgene	14	0.9	1	- 0.8
Phosphamidon	568	0.7	1	- 2.8
Phosphine	67	1.0 ¹⁾	1	- 2.6
		2.0 ²⁾	1	- 6.8
Sulphur dioxide	5784	2.4	1	-19.2
Tetraethyllead	300	1.0 ¹⁾	1	- 4.1
		2.0 ²⁾	1	- 9.8

1) = no "n" value available; calculated on the basis of n = 1

2) = no "n" value available; calculated on the basis of n = 2

Use of Probit Functions

With the probit constants given in Table 5.3 the following can be determined:

a. given: concentration C [mg/m³], exposure duration t (min)
determine: the response percentage

Procedure

1. Find (from Table 5.3) the probit constants a,b,n;
2. Calculate the probit $Pr = a + b \ln(C^nt)$;
3. From Table 5.2 find the response percentage corresponding to the value of the probit.

Note:

This is the response percentage for a **lethal injury**; for other types of injury other probit functions must be used.

b. given: response percentage, exposure duration
determine: the concentration

Procedure

1. Find, in Table 5.2 the probit value corresponding to the response percentage;
2. Find, in Table 5.3 the probit constants a, b, n ;
3. Calculate the concentration with:

$$C = \{[\exp ((Pr - a)/b)]/t\}^{1/n}$$

c. given: response percentage, concentration
determine: the exposure duration

Procedure

1. Find, in Table 5.2, the probit value corresponding to the response percentage;
2. Find, in Table 5.3, the probit constants a, b, n ;
3. Calculate the exposure duration with:

$$t = [\exp ((Pr - a)/b)] C^n$$

In order to obtain the correct percentage from Table 5.2, we must look for the appropriate combination of the ten-numbers (row) and singular numbers (column); for instance $16\% = 10\% + 6\%$. The number at the crossing of row and column gives the corresponding probit.

The other way around, for a given probit, the corresponding percentage can be found by adding the ten-number to the singular number.

Discussion and conclusions

The establishment of the vulnerability models applicable to the human-being requires two steps: the determination of the $LC_{50}(\text{human})$ and the calculation of the probit constants.

The calculation of the $LC_{50}(\text{human})$ is based on the known $LC_{50}(\text{animal})$ values. The latter, when necessary, are converted to values corresponding to a 30 minute exposure duration. Thereafter, the extrapolation is made with the help of the extrapolation factor. This factor has been estimated for, on one side, the locally acting substances and, on the other side, the systemically acting ones.

For locally acting substances, the differences between animal and human in breathing-minute-volume and lung area are taken into account. Influences such as: eventual differences in the way of breathing (through the nose or not), the sensitivity of the lung-tissue, the affectation of the lungs to the rest of the organism, are all taken into consideration by providing an (estimated) safety factor.

For systemically acting substances, the breathing-minute-volume plays a role as well. Also for these substances a safety factor has been established, in which, in this case, the differences in pharmacokinetics and pharmacodynamics are considered. Further-on, for both types of substances, a difference in activity is taken into account: for the animal in the test(condition of rest) and, for a human in accidental conditions (possible escape behaviour).

Finally, dependent on the number of animal species for which data are known, the extrapolation factor is adjusted (or not) in the direction of a less conservative estimate.

An extrapolation method is developed, in which the measurable differences (such as breathing-minute-volume, lung area) are quantified as well as possible, while for values for which less is known an estimated safety factor is provided. This leads to an extrapolation factor with as much back-up data as possibly obtainable.

The methodology used for the calculation of the probit constants is based on the LC_{50} because, for these values, the most and most accurate data from tests with animals are available. By setting the value of b equal to 1.0, a conservative assumption is made for concentrations $< LC_{50}$, which is appropriate for the spreading in vulnerability of the exposed population at a calamity.

The calculation of the probit constant a proceeds, then, in a known fashion, using the extrapolated $LC_{50}(\text{human})$ and $b = 1.0$.

The methodology used in this study to derive the probit functions is primarily meant for substances for which (too) little toxicity data are available. Whenever a user intends to offer a better backed-up probit function, based on sufficient toxicity data, this will be judged by a forum of experts (to be set-up). The exact procedure, will be established by the Committee for the Prevention of Disasters.

The vulnerability models (probit functions and toxicity criteria) presented here are meant as a start on the way to more reliable dose-effect relationships. The probit functions are (still), for the greater part, obtained from data on animals. For the parameter a , which reflects the difference in sensitivity between animal and human-being, an attempt has been made to arrive at the best founded estimate.

The parameter a is valid for lethal injury. Within the extent of present knowledge, proper values of this parameter for other types of injuries cannot be responsibly provided. It could be recommended, for future research on acute toxicity, to try and obtain better definitions for, among others, these other types

of injuries. In this respect, occurrences such as: a 50% lung damage, respiratory system and alimentary canal disturbances lasting a certain period of time, are worth considering. However, reliable toxicity data for these other types of injuries can only be established when this field is clearer defined.

Despite the proper foundation behind the results, the probit constants for human beings represent no more than an indication. A lot of research is still necessary to arrive at really reliable dose-effect relationships. However, the vulnerability models presented in this study are, in the first place, for use in the so-called quantitative risk analysis. The uncertainties in these vulnerability models must therefore be considered within the framework of other, sometimes relatively large uncertainties, which also play a role in the risk analysis. We can mention, in this respect: effect models, probability models, population data, etc.

Within such a type of framework, the vulnerability models presented here can still properly contribute to the calculation of risks of a given activity, mainly in a relative sense (reduction of risk, comparison between various activities). Furthermore, the present study also provides a good overview of acute toxicity data for the most important substances. These data make it possible for the reader to also obtain an insight, in a different manner, with regard to the properties of the substances which are related to acute inhalation toxicity.

7

References

- [1] Registry of Toxic Effects of Chemical Substances.
National Institute of Occupational Safety and Health (1983).
- [2] a. N.A. Eisenberg, C.J. Lynch and R.J. Breeding.
Vulnerability Model. A simulation system for assessing damage resulting from marine spills,
CG-D-136-75, US Coast Guard, Washington DC, June 1975.
b. A.H. Rausch, N.A. Eisenberg, C.J. Lynch.
Continuing development of the Vulnerability Model,
CG-D-53-77, US Coast Guard, Washington DC, February 1977.
c. W.W. Perry and W.J. Articola,
Study to modify the vulnerability model of the risk management system.
CG-D-22-80, US Coast Guard, Washington DC, February 1980.
- [3] W.F. ten Berge, A. Zwart, L.M. Appelman
Concentration-time mortality response relationships of irritant and systemically acting vapours and
gases.
Journal of Hazardous Materials 13 (1986) 301-309.
- [4] M.M. Verberk
De Eenmalige Populatie Expositie Limiet (EPEL)
De Ingenieur, 87 (1975) 878-880.
- [5] Threshold Limit Values for chemical substances in the work environment adopted by ACGIH
with intended changes for 1985-1986.
American Conference of Governmental Industrial Hygienists
ISBN 0-936712-61-9.
- [6] W.F. ten Berge
The toxicity of methylisocyanate for rats.
Journal of Hazardous Materials, 12 (1985) 309-311.
- [7] Canvey - an investigation of potential hazards from operations in the Canvey Island/Thurrock
area. Health and Safety Executive HMSO, London 1978.
- [8] Risk analysis of six potentially hazardous industrial objects in the Rijnmond area. A pilot study.
Reidel Publishing Company. Dordrecht, Holland. 1982.
- [9] Study into the risks from transportation of liquid chlorine and ammonia in the Rijnmond area.
Technica Ltd, July 1985.
- [10] R.M.J. Withers, F.D. Lees
The assessment of major hazards: the lethal toxicity of chlorine (part 1 and 2).
Journal of Hazardous Materials 12 (1985) 231-302.
- [11] W.F. ten Berge, M. Vis van Heemst
Validity and accuracy of a commonly used toxicity assessment model in risk analysis.
4th Int. Symp. Loss Prevention, Harrogate (1983).

- [12] L.M. Appelman, W.F. ten Berge, P.G.J. Reuzel
Acute inhalation toxicity of ammonia in rats with variable exposure periods
American Industrial Hygiene Journal, 43 (1982) 662.
- [13] Provinciale Waterstaat Groningen, private communication.
- [14] J.A. Duiser,
Letselecriteria voor toxische stoffen,
TNO-rapport ref.nr. 85-06564, Apeldoorn 1985.
- [15] R.M.J. Withers, F.D. Lees
The assessment of major hazards: the lethal toxicity of bromine.
Journal of Hazardous Materials, 13 (1986) 279-299.
- [16] D.J. Finney
Probit Analysis
Cambridge University Press, Cambridge, 1980 (3rd ed.).
- [17] R.L. Zielhuis, F.W. van der Kreek
International Archives of Occupational and Environmental Health, 42 (1979) 191-201.
- [18] Methoden voor het berekenen van de fysische effecten van het incidenteel vrijkomen van
gevaarlijke stoffen (vloeistoffen en gassen) ("Yellow Book").
Rapport van de Commissie Preventie van Rampen door gevaarlijke stoffen. Uitgave van het DGA,
Voorburg, 1979.
- [19] Gezondheidsraad.
Advies inzake de EPEL-waarden
Den Haag, 1982.
- [20] J.H.E. Arts
Acute (1-hour) inhalation toxicity study of acrolein in rats
CIVO Report No. 87.181.
- [21] A. Zwart and R.A. Woutersen
Acute inhalation toxicity study of chlorine in rats and mice; time-concentration-mortality relationship
and effects on respiration.
Journal of Hazardous Materials (in press).
- [22] A. Zwart
Acute (1-hour) inhalation toxicity study of ethylene oxide in rats
CIVO Report No. V 86.548.
- [23] J.H.E. Arts
Acute (1-hour) inhalation toxicity study of phosphine in rats
CIVO Report No. V 87.234.
- [24] A. Zwart
Acute (1-hour) inhalation toxicity study of phosgene in rats
CIVO Report No. V 87.029
- [25] J.H.E. Arts
Acute (1-hour) inhalation toxicity study of carbon disulphide in rats
CIVO Report No. V 87.182.

- [26] A. Zwart
Acute (1-hour) inhalation toxicity study of methyl bromide in rats
CIVO Report No. V 87.127.
- [27] J.H.E. Arts
Acute (1-hour) inhalation toxicity study of hydrogen cyanide in rats
CIVO Report No. V 87.284.
- [28] A. Zwart
Acute (1-hour) inhalation toxicity study of hydrogen sulphide in rats
CIVO Report No. V 87.027.
- [29] A. Zwart
Acute (1-hour) inhalation toxicity study of sulphur dioxide in rats
CIVO Report No. V 87.543
- [30] W.F. ten Berge en C.P. Guldemon.
Required knowledge for the evaluation of health hazards from acute inhalatory exposure of humans.
Paper presented at the meeting of the International Process Safety Group, Cannes 14-15 September, 1986.
- [31] D. Henschler, W. Laux.
Zur Spezifität einer Toleranzsteigerung bei wiederholter Einatmung von Lungenoedem erzeugenden Gasen
Naunyn - Schmiedbergs Arch. Exp. Pathol. Pharmacol.
239 (1960) 433-441.

Annex 1

Selection of substances

The following hypotheses have been made in the establishment of the concentration at a given distance:

- neutral weather (Pasquill class D)
- wind speed 4 m/s
- ground roughness 1 m (residential area with densely located but low buildings)
- average time 15 minutes

In these conditions, the concentration at a 500 m distance downwind from the source is considered as representative; its value is given by [18]:

$$c = 6.74 \times 10^{-5} \dot{m} \quad (3.1)$$

with \dot{m} = release rate [kg/s]

Since the toxicity criteria, for the above considered applications, is mostly given in mg (or kg)/m³, the concentration given above will be converted to a release rate of 1 m³/s; this gives:

$$c = 2.80 \times 10^{-6} M \times p_r \quad (3.2)$$

with M = molecular weight

$$p_r = \frac{\text{saturation pressure}}{\text{atmospheric pressure}} \quad (3.2)$$

The STEL value is chosen as injury criterium; this is the limit value below which, by inhalation during a short time (< 15 min), no irritation, tissue damage or stupor will take place.

The ratio of the two concentrations gives the risk index:

$$RI = \frac{2.80M \times P_r}{STEL} \quad (3.3)$$

(STEL in mg/m³)

In the selection of the substances, first the results obtained from contacts with industry and authorities were considered. Further-on, an inventory was made of past accidents with toxic substances in which victims fell or evacuation of the surroundings either took place or had been considered. This inventory was made using the TNO database FACTS.

Practically all of the substances selected in this way have an RI > 1.0 (see Table 3.1), which means that the STEL value, under the above conditions, will still be reached at a 500 m distance downwind from the source. We can also see that for substances with a higher risk index the potential damage distance will be larger.

Consequently, practically all of the selected substances (in a general way) satisfy a criterion which can be formulated as follows: "the substance will, under neutral conditions, at a distance downwind from the source of 500 m and a exposure duration equal to 15 minutes, produce irritations or serious injuries".

Substances which do not satisfy the above criterion and still mentioned in the selected group. This is done due to the established need to develop vulnerability models for humans also for these substances. Namely the pesticides (such as azinphosmethyl and phosphamidon) represent a regular subject of (safety) studies. Discussions with industry and authorities have further shown that, due to the necessity of a better quantifying of the toxicity of allyl alcohol and tetraethyllead, the selection of these substances is therefore further justified.

Table B1.1 Selected substances with risk index (RI).

UN nr	Substance	RI	UN nr	Substance	RI
1092	Acrolein	60	1051	Hydrogen cyanide	6
1093	Acrylonitrile	1	1052	Hydrogen fluoride	11
1098	Allyl alcohol	0.4	1053	Hydrogen sulphide	80
1005	Ammonia	15	1076	Methyl bromide	8
-	Azinphosmethyl	<<0.01	-	Methyl isocyanate	450
1744	Bromine	54	2199	Nitrogen dioxide	12
1131	Carbon disulphide	1	1062	Parathion	14
1016	Carbon monoxide	18	2480	Phosgene	330
1017	Chlorine	148	1067	Phosphamidon	-
1040	Ethylene oxide	31	1668	Phosphine	2800
1198/ 2209	Formaldehyde	129	1079	Sulphur dioxide	59
			1829	Sulphur trioxide	30
1050	Hydrogen chloride	620	-	Tetraethyllead	0.6

Annex 2

Inventory of data on toxicity

An overview of the toxicity data of the selected substances is given in this annex, such as it can be found in open literature.

Values of TC, LC and STEL are given in Table B2.1; the values are from reference [1], unless otherwise noted.

In Table B2.2 we find the probit constants a, b and n for the application in a vulnerability model (see Paragraph 4.1). These constants belong to the following relationship:

$$Pr = a + b \ln(C^n \cdot t) \quad (1)$$

Equation (1) represents the probit function in the most commonly used form. Pr is a statistical transformation of the response fraction R (as per equation 2):

$$R = \int_{-\infty}^{Pr-5} \exp\left(-\frac{1}{2}u^2\right) du \quad (2)$$

Response percentage = R x 100%

For details with reference to the techniques of probit analysis, see Reference [16]. The constants given in Table B2.2 are applicable for concentrations expressed in mg/m³ and duration expressed in minutes.

Table B2.1 Toxicity data for the selected substances.

Substance	Duration	Criterium	Species	Value
Acrolein	-	TC ₁₀	human	1 ppm
	10 min.	LC ₁₀	human	153 ppm
	2 hours	TC ₁₀	child	300 ppb
	4 hours	LC ₁₀	rat	8 ppm
	6 hours	LC ₅₀	mouse	66 ppm
	8 hours	LC ₁₀	cat	1570 mg.m ⁻³
	6 hours	LC ₁₀	rabbit	24 mg.m ⁻³
	6 hours	LC ₁₀	guinea pig	24 mg.m ⁻³
	< 15 min.	STEL	human	0.8 mg.m ⁻³ [5]
	1 hours	LC ₅₀	rat	110 mg.m ⁻³ [20]
Acrylonitrile	20 min.	TC ₁₀	man	16 ppm
	1 hour	LC ₁₀	man	1 g.m ⁻³
	4 hours	LC ₁₀	rat	500 ppm
	1 hour	LC ₁₀	mouse	900 mg.m ⁻³
	4 hours	LC ₁₀	dog	110 ppm
	4 hours	LC ₁₀	cat	600 ppm

Table B2.1 *contd.*

Substance	Duration	Criterion	Species	Value
Acrylonitrile (contd.)	4 hours	LC ₁₀	rabbit	258 ppm
	4 hours	LC ₅₀	guinea pig	576 ppm
Allyl alcohol	4 hours	LC ₅₀	rat	165 ppm
	2 hours	LC ₅₀	mouse	500 mg.m ⁻³
	4 hours	LC ₁₀	ape	1000 ppm
	-	LC ₁₀	rabbit	1000 ppm
	< 15 min.	STEL	human	10 mg.m ⁻³ [5]
Ammonia	-	TC ₁₀	man	20 ppm
	5 min.	LC ₁₀	man	5000 ppm
	4 hours	LC ₁₀	rat	2000 ppm
	1 hour	LC ₅₀	mouse	4230 ppm
	1 hour	LC ₁₀	cat	7000 ppm
	1 hour	LC ₁₀	rabbit	7000 ppm
	40 min.	LC ₅₀	rat	14170 ppm [12]
Azinphosmethyl	1 hour	LC ₅₀	rat	69 mg.m ⁻³
Bromine	-	LC ₁₀	man	1000 ppm
	9 min.	LC ₅₀	mouse	750 ppm
	7 hours	LC ₁₀	cat	140 ppm
	6½ hours	LC ₁₀	rabbit	180 ppm
	7 hours	LC ₁₀	guinea pig	140 ppm
	< 15 min.	STEL	human	2 mg.m ⁻³ [5]
Carbon disulphide	30 min.	LC ₁₀	man	4000 ppm
	5 min.	LC ₁₀	man	2000 ppm
	oral	LD ₅₀	rat	3188 mg.kg ⁻¹
	oral	LD ₅₀	mouse	2780 mg.kg ⁻¹
	oral	LD ₅₀	rabbit	2550 mg.kg ⁻¹
	1 hour	LC ₁₀	rat	20500 mg.m ⁻³ [25]
Carbon monoxide	30 min.	LC ₁₀	man	4000 ppm
	45 min.	TC ₁₀	man	650 ppm
	5 min.	LC ₁₀	man	5000 ppm
	4 hours	LC ₅₀	rat	1807 ppm
	4 hours	LC ₅₀	mouse	2444 ppm
	46 min.	LC ₁₀	dog	4000 ppm
	-	LC ₁₀	rabbit	4000 ppm
	4 hours	LC ₅₀	guinea pig	5718 ppm
	< 15 min.	STEL	human	440 mg.m ⁻³ [5]
Chlorine	30 min.	LC ₅₀	mouse	1500 mg.m ⁻³ [21]
	30 min.	LC ₅₀	rat	2000 mg.m ⁻³ [21]
	30 min.	LC ₁₀	man	873 ppm
	5 min.	LC ₁₀	man	500 ppm
	1 hour	LC ₅₀	rat	293 ppm
	1 hour	LC ₅₀	mouse	137 ppm
	30 min.	LC ₁₀	dog	800 ppm
	4 hours	LC ₁₀	cat	660 ppm

Table B2.1 *contd.*

Substance	Duration	Criterion	Species	Value
Chlorine (contd.)	7 hours	LC ₁₀	guinea pig	330 ppm
	< 15 min.	STEL	human	9 mg.m ⁻³ [5]
Ethylene oxide	10 sec.	TC	man	12500 ppm
	2 min.	TC ₁₀	woman	500 ppm
	4 hours	LC ₅₀	rat	1460 ppm
	4 hours	LC ₅₀	mouse	836 ppm
	4 hours	LC ₅₀	dog	960 ppm
	4 hours	LC ₅₀	guinea pig	1500 mg.m ⁻³
	1 hour	LC ₅₀	rat	10950 mg.m ⁻³ [22]
Formaldehyde	-	TC ₁₀	man	8 ppm
	30 min.	TC ₁₀	man	17 mg.m ⁻³
	10 min.	TC ₁₀	man	0.3 mg.m ⁻³
	-	LC ₅₀	rat	590 mg.m ⁻³
	2 hours	LC ₁₀	mouse	900 mg.m ⁻³
	8 hours	LC ₁₀	cat	820 mg.m ⁻³
	< 15 min.	STEL	human	3 mg.m ⁻³ [5]
Hydrogen chloride	30 min.	LC ₁₀	man	1300 ppm
	5 min.	LC ₁₀	man	3000 ppm
	30 min.	LC ₅₀	rat	4701 ppm
	1 hour	LC ₅₀	rat	3124 ppm
	30 min.	LC ₅₀	mouse	2644 ppm
	1 hour	LC ₅₀	mouse	1108 ppm
	30 min.	LC ₁₀	rabbit	4416 ppm
	30 min.	LC ₁₀	guinea pig	4416 ppm
	30 min.	LC ₅₀	rat	5666 ppm
aerosol	30 min.	LC ₅₀	mouse	2142 ppm
Hydrogen cyanide	5 min.	LC ₁₀	human	200 ppm
	1 hour	LC ₁₀	human	120 mg.m ⁻³
	10 min.	LC ₁₀	human	200 mg.m ⁻³
	2 min.	LC ₁₀	human	400 mg.m ⁻³
	5 min.	LC ₅₀	rat	484 ppm
	5 min.	LC ₅₀	mouse	323 ppm
	1 min.	LC ₅₀	dog	616 mg.m ⁻³
	1 min.	LC ₅₀	ape	1616 mg.m ⁻³
	1 min.	LC ₅₀	cat	1226 mg.m ⁻³
	1 min.	LC ₅₀	rabbit	980 mg.m ⁻³
	1 min.	LC ₅₀	piglet	1740 mg.m ⁻³
	1 min.	LC ₅₀	guinea pig	2112 mg.m ⁻³
	1 hour	LC ₅₀	rat	163 mg.m ⁻³ [27]
Hydrogen fluoride	30 min.	LC ₁₀	human	50 ppm
	1 hour	LC ₅₀	rat	1276 ppm
	1 hour	LC ₅₀	mouse	342 ppm
	1 hour	LC ₅₀	ape	1774 ppm
	7 hours	LC ₁₀	rabbit	260 mg.m ⁻³
	15 min.	LC ₅₀	guinea pig	4327 ppm
	<15 min.	STEL	human	5 mg.m ⁻³ [5]

Table B2.1 contd.

Substance	Duration	Criterium	Species	Value
Hydrogen sulphide	30 min.	LC ₁₀	human	600 ppm
	-	LC ₁₀	human	5.7 mg.kg ⁻¹
	5 min.	LC ₁₀	human	800 ppm
	-	LC ₅₀	rat	444 ppm
	1 hour	LC ₅₀	mouse	673 ppm
	8 hours	LC ₁₀	guinea pig	1 mg.m ⁻³
	1/2, 1, 2 hours	EPEL	human	1-2 ppm [4]
	60 min.	LC ₅₀	rat	900 mg.m ⁻³ [28]
Methylbromide	30 min.	LC ₅₀	rat	12900 mg.m ⁻³
	8 hours	LC ₅₀	rat	1208 mg.m ⁻³
Methylisocyanate	-	TC ₁₀	human	2 ppm
	4 hours	LC ₅₀	rat	5 ppm
	1 hour	LC ₁₀	mouse	37 mg.m ⁻³
	1 hour	LC ₁₀	guinea pig	37 mg.m ⁻³
Nitrogen dioxide	1 min.	LC ₁₀	human	200 ppm
	40 min.	TL ₁₀	human	90 ppm
	4 hours	LC ₅₀	rat	80 ppm
	11 min.	LC ₅₀	mouse	1000 ppm
	-	LC ₅₀	dog	123 mg.m ⁻³
	15 min.	LC ₅₀	rabbit	315 ppm
	1 hour	LC ₅₀	guinea pig	30 ppm
	48 hours	LC ₅₀	hamster	36 ppm
	< 15 min.	STEL	human	10 mg.m ⁻³
	30 min.	LC ₅₀	dog	300 mg.m ⁻³
	30 min.	LC ₅₀	rabbit	435 mg.m ⁻³
	30 min.	LC ₅₀	rat	258 mg.m ⁻³
	30 min.	LC ₅₀	guinea pig	179 mg.m ⁻³
	30 min.	LC ₅₀	mouse	215 mg.m ⁻³
Parathion	4 hours	LC ₅₀	rat	84 mg.m ⁻³
	-	LC ₁₀	mouse	15 mg.m ⁻³
	2 hours	LC ₁₀	rabbit	50 mg.m ⁻³
	2 hours	LC ₁₀	guinea pig	14 mg.m ⁻³
Phosgene	5 min.	LC ₁₀	man	50 ppm
	-	LC ₅₀	man	3200 mg.m ⁻³
	30 min.	LC ₁₀	man	360 mg.m ⁻³
	30 min.	TL ₁₀	man	25 ppm
	30 min.	LC ₁₀	rat	50 ppm
	30 min.	LC ₁₀	dog	80 ppm
	15 min.	LC ₁₀	cat	190 mg.m ⁻³
	15 min.	LC ₁₀	rabbit	720 mg.m ⁻³
	20 min.	LC ₅₀	rat	25 ppm [31]
	20 min.	LC ₁₀	guinea pig	31 mg.m ⁻³
	21 hours	LC ₅₀	rat	38 mg.m ⁻³
Phosphamidon	4 hours	LC ₅₀	rat	135 mg.m ⁻³
	1 hour	LC ₅₀	mouse	30 mg.m ⁻³

Table B2.1 *contd.*

Substance	Duration	Criterion	Species	Value
Phosphamidon (<i>contd.</i>)	4 hours	LC ₅₀	guinea pig	1300 mg.m ⁻³
Phosphine	-	LC ₁₀	man	1000 ppm
	5 min.	LC ₁₀	man	1000 ppm
	4 hours	LC ₅₀	rat	11 ppm
	140 min.	LC ₁₀	mouse	380 mg.m ⁻³
	105 min.	LC ₁₀	cat	70 mg.m ⁻³
	20 min.	LC ₁₀	rabbit	2500 ppm
	4 hours	LC ₁₀	guinea pig	140 mg.m ⁻³
	< 15 min.	STEL	human	1 mg.m ⁻³ [5]
	1 hour	LC ₅₀	rat	361 mg.m ⁻³ [23]
Sulphur dioxide	10 min.	LC ₁₀	human	1000 ppm
	1 min.	TC ₁₀	human	4 ppm
	5 min.	LC ₁₀	human	3000 ppm
	-	LC ₁₀	rat	1000 ppm
	30 min.	LC ₅₀	mouse	3000 ppm
	<15 min.	STEL	human	10 mg.m ⁻³ [5]
	1 hour	LC ₅₀	rat	5140 mg.m ⁻³ [29]
Sulphur trioxide	-	TC ₁₀	human	30 mg.m ⁻³
	6 hours	LC ₁₀	guinea pig	30 mg.m ⁻³
Tetra ethyllead	1 hour	LC ₅₀	rat	850 mg.m ⁻³
	7 hours	LC ₁₀	mouse	650 mg.m ⁻³
	oral	LD ₅₀	rat	109 mg.kg ⁻¹
	oral	LD ₁₀	rabbit	24 mg.kg ⁻¹

Table B2.2 Probit constants for the selected substances ($[C] = \text{mg/m}^3$, $[t] = \text{min}$).

Substance	n	a (Lethal)	b	Ref.	Remark
Acrolein	1.0	- 11.67	2.05	2c	human
Acrylonitrile	1.02	- 42.1	3.74	3	rat
	1.33	- 165	11.4	3	rat
	1.43	32.8	3.01	2	human
Allylcohol	-	-	-		
Ammonia	2.02	- 80.03	2.30	3	rat male/female
	1.93	- 125.68	3.71	3	" "
	2.14	- 103.41	2.76	3	" "
	2.06	- 95.64	2.89	3	mouse
	1.36	- 27.26	2.27	2c	"
	2.75	- 49.030	2.205	7	
	2.75	- 16.00	0.782		
	2.0	- 34.58	1.91	8	rat
	2.02	- 47.8	2.30	12	
	2.75	- 29.26	1.375		
Azinphosmethyl	-	-	-		
Bromine	2.17	- 24.7	1.44	3	mouse
	2.0	- 13.81	0.92	15	average population, rest condition
	2.0	- 12.53	0.92	15	average population, standard activity
	2.0	- 12.12	0.92	15	vulnerable population, rest condition
	2.0	- 10.85	0.92	15	vulnerable population, standard activity
Carbon disulphide	1.0	- 51.4	4.2	13	
Carbon monoxide	1.0	- 38.8	3.7	13	
	1.0	- 32.57	2.16	26 in [14]	rat
Chlorine	2.75	- 18.90	1.69	2a	
	2.64	- 39.66	3.13	2c	
	3.47	- 23.2	1.10	3	mouse
	2.75	- 5.3	0.5	9	
	2.75	- 12.28	0.82	8	
	2.0	- 10.28	0.92	10	average population, rest condition
	2.0	- 9.00	0.92	10	average population, standard activity
	2.0	- 8.59	0.92	10	vulnerable population, rest condition
	2.0	- 7.32	0.92	10	vulnerable population,

Table B2.2 contd.

Substance	n	a (Lethal)	b	Ref.	Remark
Chlorine (contd.)				standard activity	
	2.75	- 6.5	0.5	11	
	1.0	- 26.84	2.78	21	rat
	1.45	- 33.74	2.72	21	mouse
Ethylene oxide	1.0	- 23.33	3.05	14	rat
Formaldehyde	1.0	- 19.91	2.18	14	mouse
Hydrogen chloride	1.0	- 17.68	2.0	2	
	1.0	- 22.86	2.65	2a	
	0.83	- 47.7	4.90	3	rat
	1.21	- 10.5	1.16	3	mouse
	1.03	- 29.1	2.68	3	rat, aerosol
	1.14	- 22.8	2.21	3	mouse, aerosol
Hydrogen cyanide	2.23	- 27.3	2.02	3	goat
	1.88	- 6.78	0.835	3	ape
	4.33	- 15.6	0.744	3	rabbit
	1.64	- 3.27	0.701	3	rat
	2.82	- 8.26	0.741	3	cat
	3.12	- 1.30	0.327	3	dog
	2.0	- 81.5	6.7	1a	
	1.43	- 59.14	4.30	2b	
Hydrogen fluoride	1.0	- 25.25	3.36	2c	
	1.94	- 7.35	0.701	3	rabbit, guinea pig
Hydrogen sulphide	1.43	- 32.92	3.01	2c	
	2.17	- 42.6	2.36	3	Lehmann, 1982
	2.0	- 44.7	2.9	13	cat, rabbit
Methylbromide	1.0	- 62.83	5.16		
	1.0	- 64.26	5.27	2c	
	1.0	- 26.95	5.13	2b	
	1.2	- 44.0	7.5	26	rat
Methyl isocyanate	0.653	- 6.64	1.64	6	rat
Nitrogen dioxide	3.49	- 15.2	0.885	3	Hine 1979 ; rat
	4.9	- 10.5	0.537	3	" ; guinea pig
	4.32	- 5.43	0.352	3	" ; rabbit
	3.29	- 38.7	1.97	3	" ; dog
	3.65	- 35.6	1.76	3	" ; mouse
Parathion	-	-	-		
Phosgene	1.0	- 24.49	3.69	2	
	0.8	- 32.87	5.44	24	rat

Table B2.2 contd.

Substance	n	a (Lethal)	b	Ref.	Remark
Phosphamidon	-	-	-		
Phosphine	-	-	-		
Sulphur dioxide	1.0	- 17.73	2.1	2	
	3.7	- 27.9	1.14	13	
Sulphur trioxide	-	-	-		
Tetraethyllead	-	-	-	-	
Tetramethyllead	-	-	-	-	

Annex 3

Data on animals and the LC₅₀ values for humans calculated from it

Table B3.1

Substance	Species	Duration/LC ₅₀ in mg/m ³	n	30 min LC ₅₀ in mg/m ³		
				animal	human I ¹	II ²
Acrolein	rat	1 hour/ 110	2	156	39	304
	mouse	6 hours/ 156	2	527	264	
Acrylonitrile	guinea pig	4 hours/ 1267	2	3584	716	2533
	rat 1 ³		1.02	8540		
	rat 2 ³		1.33	5998		
	rat, average			7269	1817	
Allyl alcohol	rat	4 hours/ 395	2	1117	279	779
	mouse	2 hours/ 500	2	1000	500	
Ammonia	mouse	1 hour/ 2971	2.06	4159	2080	6164
	rat	1 hour/ 11590	2.02	16335	4084	
Azinphosmethyl	rat	1 hour/ 69	2	98	25	25
Bromine	mouse	9 min/ 4959	1.44	2149	1075	1075
Carbon disulphide	insufficient data in order to calculate a probit function LC ₅₀ > 20.5 g.m ⁻³ (1 hour).					
Carbon monoxide	rat	4 hours/ 2091	1.0	16726	4182	7949
	mouse	4 hours/ 2827	2	7996	3998	
	guinea pig	4 hours/ 6616	2	18713	3743	
Chlorine	mouse	30 min/ 1500	1.5	1500		1017
	mouse	1 hour/ 419	3.47	512		
	mouse, average			1006	503	
	rat	30 min/ 2000	1	2000	500	
Ethylene oxide	rat	4 hours/ 2655	1.0	21240		

Table B3.1 *contd.*

Substance	Species	Duration/LC ₅₀ in mg/m ³	n	30 min LC ₅₀ in mg/m ³ animal	human I ¹	II ²
Ethylene oxide (<i>contd.</i>)	rat	1 hour/ 10950	1.0	21900		
	rat, average			21570	5393	
	mouse	4 hours/ 1520	2	4299	2150	
	dog	4 hours/ 1745	2	4936	494	
	guinea pig	4 hours/ 1500	2	4243	849	
						4443
Formaldehyde	insufficient data					
Hydrogen chloride (<i>vapour</i>)	rat	30 min/ 6993	0.83	6983		
	rat	1 hour/ 4647	0.83	10712		
	rat, average			8848	2212	
	mouse	30 min/ 3933	1.21	3933	1967	
	(<i>aerosol</i>) rat	30 min/ 8429	1.03	8429	2107	
	mouse	30 min/ 3186	1.14	3186	1593	
						3940
Hydrogen cyanide	rat	1 hour/ 163	1.64	250		
	rat	5 min/ 540	1.64	181		
	rat, average			216	54	
	mouse	5 min/ 360	1.64	121	60	
						114
Hydrogen fluoride	rat	1 hour/ 1055	1	2109	527	
	mouse	1 hour/ 283	1	565	283	
	guinea pig	15 min/ 3576	1.94	2502	500	
	ape	1 hour/ 1466	1	2932	293	
						802
Hydrogen sulphide	mouse	1 hour/ 946	2	1338	669	
	rat	1 hour/ 900	2	1273	318	
						987
Methyl bromide	rat	30 min/ 12900	1.2	12900	3225	
	rat	8 hours/ 1208	1.2	12176	3044	
						3135
Methyl isocyanate	rat	4 hours/ 12	0.7	226	57	
						57
Nitrogen oxide	rat	4 hours/ 152	3.49	294		
	rat	30 min/ 258	3.49	258		
	rat, average			276	69	
	mouse	11 min/ 1900	3.65	1443		
	mouse	30 min/ 215	3.49	215		
	mouse, average			829	415	
	rabbit	15 min/ 599	4.32	553		
	rabbit	30 min/ 435	3.49	435		
	rabbit, average			494	49	
	guinea pig	1 hour/ 57	4.9	65		

Table B3.1 contd.

Substance	Species	Duration/LC ₅₀ in mg/m ³	n	30 min LC ₅₀ in mg/m ³		II ²
				animal	human I ¹	
Nitrogen oxide (contd.)	guinea pig	30 min/ 179	3.49	179		
	guinea pig, average			122	25	
	dog	30 min/ 300	3.49	300	30	235
Parathion	rat	4 hours/ 84	2	238	59	59
Phosgene	rat	1 hour/ 38	0.9	54	14	
	rat	20 min. 102	0.9	58	14	
						14
Phosphamidon	rat	4 hours/ 135	2	382	96	
	mouse	1 hour/ 30	2	42	21	
	guinea pig	4 hours/ 1300	2	3677	735	568
Phosphine	rat	4 hours/ 8	2	23		
	rat	1 hour/ 361	2	510		
	rat, average			267	67	67
sulphur dioxide	mouse	30 min/ 7934	2	7934	3967	
	rat	1 hour/ 5140	2	7269	1817	5784
sulphur trioxide	no relevant data available					
Tetraethyllead	rat	1 hour/ 850	2	1199	300	300

1 - human I¹ = 30 minutes LC₅₀ calculated from every animal species

2 - human II² = final value for 30 minutes LC₅₀ calculated from one or several animal species

3 - calculated from the probit values as given in table B2.2

Chapter 6

Protection against toxic substances by remaining indoors

Summary

Within the framework of the "Green Book", the chapter "Protection from outdoor pollution by being indoors" has been written, based on earlier work carried out by PML-TNO and IMG-TNO, and a study of literature. For the extent of protection from being indoors for passive pollution of outdoor origin a mathematical model is given to calculate the reduction of the indoor concentration and dose. Because ventilation rates in homes and buildings play a major role in the extent of protection, some literature based ventilation parameters are given.

Contents

	Page
Summary	3
Contents	4
1. Introduction	5
2. Identification diagram	6
3. Ventilation and absorption	7
3.1 Ventilation dependent on meteorological conditions	7
3.2 Ventilation in housing	8
3.3 Ventilation in public buildings and industrial spaces	9
3.4 Intentional ventilation	10
3.5 Absorption of gases by materials present indoors	10
3.6 Reduction of the background concentration	11
4. Concentration indoors	12
4.1 Mathematical model for the penetration of a gas cloud into a residence	12
4.2 The concentration indoors as consequence of an external continuous source	13
4.3 The concentration indoors as consequence of an external temporary source	15
4.4 The concentration indoors as consequence of an external instantaneous source	18
4.5 Calculation examples for paragraphs 4.3 and 4.4	21
4.6 Passage time of a cloud originating from an instantaneous source	24
4.7 Fraction of protected area and critical ventilation-factor	25
4.8 Calculation example for paragraph 4.7	28
5. Protection and protective measures	29
6. Density effects	30
7. Accuracy of the models for the determination of the indoors protection against toxic substances	31
8. Conclusions	33
List of symbols	34
References	35
Diagrams	38
Annexes	60

1

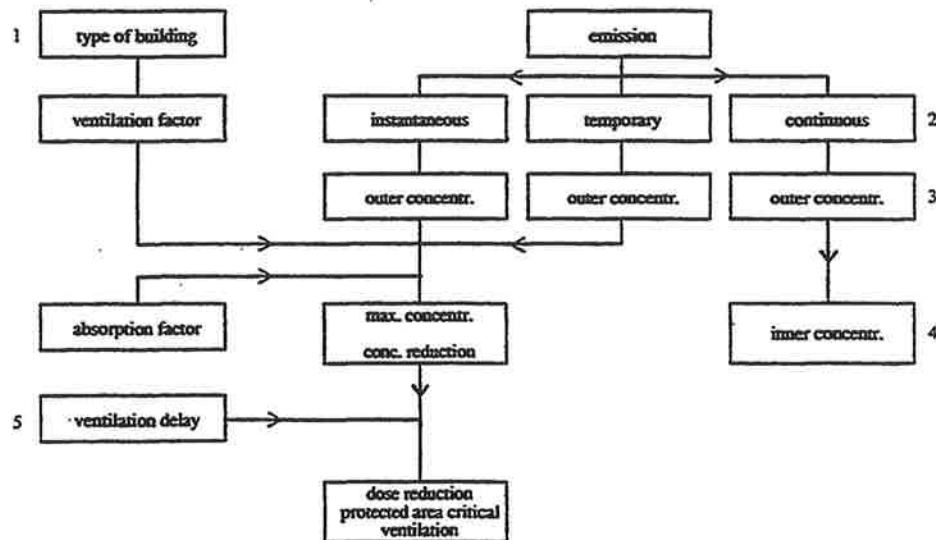
Introduction

In case of an accidental release of toxic or flammable gases or aerosols, these are carried by the wind, spread and diluted. The extent of spreading and dilution of a cloud can be determined with the help of a dispersion model. If such a cloud reaches a residential house or another type of building, the concentration inside, in case the doors and windows are closed, will fall behind the concentration outside. If, after a certain time, the cloud will pass the building, the concentration inside will generally not reach the value of the one outside. It can thus be expected that, by the passage of a toxic cloud, the fact of remaining indoors will offer a certain degree of protection. This type of protection strongly depends on the extent to which the air inside is refreshed by the outer air, thus the ventilation. Also deposits and absorption phenomena can influence the concentration indoors. Finally, at the same time, the density of the gas also influences the possibilities of penetration of the gas into the building. We will analyze, in what follows, how much protection the fact of remaining indoors can provide. We will use, for this purpose, the previously performed investigations by IMG-TNO and PML-TNO, and the references [3], [4] and [5], complemented by other data from literature.

Besides the concentration on the outside, the ventilation represents the next most determinant factor for the value of the concentration inside. For this reason, some measured ventilation parameters have been assembled in Paragraph 3. Further-on, a suggestion is made for an evaluation of such parameters. In Paragraph 4 a mathematical model is derived for the calculation of the concentration indoors for a neutral gas of about the same density as air. This model is then applied to several external sources. The degree of possible protection and the eventual measures to be applied are discussed in Paragraph 5.

Finally, in Paragraph 6, some aspects of the density of a toxic gas are analyzed. The spreading of a heavy gas proceeds differently from that of a neutral gas. No model is presented in this report, however, for a heavy gas. Tests have shown that a heavy gas inside a building generally spreads to all of the space available, due to convective currents.

Identification diagram



Explanation of the identification diagram

ad 1. A choice is made, with the help of Paragraph 3, dependent on the type of building and on the average ventilation rate.

ad 2. The emission of contaminating substances, in the model, is considered either an instantaneous or constant (lasting a certain time – temporary source). An emission for which the distance to the source divided by the wind speed and the source duration is larger than 18 can be considered as instantaneous – see, for this, ref. [1].

ad 3. The concentration on the outside of the building (or house) is calculated with the help of a dispersion model. The eventual influence of deposit losses and/or of plume rise can also be taken into account in this calculation. (See, for instance [1], revised edition).

ad 4. The maximum indoors concentration can now be calculated for either a temporary or an instantaneous source.

ad 5. The period between time “1”, at which, after passage of the cloud, the outer concentration has become lower than the inner concentration, and time “2”, at which complete ventilation has been achieved, is called the ventilation delay. If the value of this ventilation delay is known, as well as the relationship between dose load and concentration, it is then possible to calculate the dose and also the dose reduction. At the same time, the values of the fraction of the protected area and of the critical ventilation rate can be obtained from the corresponding tables.

Ventilation rate and absorption

A complete protection against contaminating substances in the outer air is achieved, during the passage of the cloud, by remaining inside a completely sealed space. However, in such a space, after a while, lack of oxygen and a surplus of carbon dioxide could manifest themselves. The latter is specially important. A CO₂ concentration of 0.10% (which is 0.07% higher than the average CO₂ concentration in the open air) can already lead to headaches or dizziness, while a 7% concentration can be lethal [6]. If we consider, from a hygienic view-point, an allowable concentration of 0.15% [6], then the maximum time one person can remain inside a 30 m³ space sealed from the outer air is only equal to 2 hours. It is consequently necessary to ventilate houses or buildings.

The extent to which the ventilation takes place is expressed by the ventilation rate. This factor is a number which shows how many times per hour the entire contents of a room will be provided with fresh air. The ventilation rate is one of the determinant parameters for the calculation of the concentration indoors, and is expressed in h⁻¹. Another commonly used measure of ventilation is the quantity of fresh air which must be brought-in per person and per hour; this is expressed in m³/h/person.

The ventilation in a building is differentiated as follows:

– **Natural ventilation**

The air in the building is refreshed, in this case, by passage through seams and joints (through which draft penetrates). At the same time, the inner air also leaves through these openings.

– **Mechanical ventilation**

The ventilation is improved, in this condition, by one or several ventilators. This can be a simple window ventilator, a suction system for (open) kitchens or sanitary rooms, and up to a complete air climatization controlling system.

– **Intentional ventilation**

The ventilation is hereby provided by open windows and/or doors.

3.1

Ventilation dependent on general meteorological conditions

The natural ventilation in a building, above all, is dependent on external meteorological conditions. A high wind speed provides a high degree of ventilation. A low temperature leads to a higher difference between the outside and the inside, so that the ventilation increases. Humidity also influences the ventilation. Dependent on humidity, runways and window frames may expand or contract, influencing thereby the openings in the joints.

The natural ventilation is provoked and maintained by:

- a. the wind
- b. the temperature difference between the outside and inside.

a. Ventilation Consequent to Wind Speed

When a horizontal flow of air is brought to a stop by the vertical walls of a building, the velocity pressure is then totally converted into a static pressure. This produces a difference of pressures between

the front side and the lee side of the building, and also between the outside and inside of it. The value of this pressure difference is dependent, apart from the wind speed, on the shape of the building and on the angle of incidence of the flow. This relatively small pressure difference (1-50 Pa)[4] is sufficient to maintain the ventilation. The pressure difference between the outside and the inside increases with an increasing wind speed and, consequently, the ventilation rate also increases. Measured ventilation rates, dependent on the wind speed outside, are published in references [5,7,9 and 10] (fig.1).

It can be seen, in Figure 1, that a positive relationship exists between the ventilation rate and the wind speed. This relationship is dependent on the type of house, on the configuration of the joints and on the angle of incidence of the wind. Due to all this, it is not possible to express it in a single formula. Furthermore, measurements performed before the 1973 oil crisis appear to have shown significantly higher ventilation rates than observed later-on.

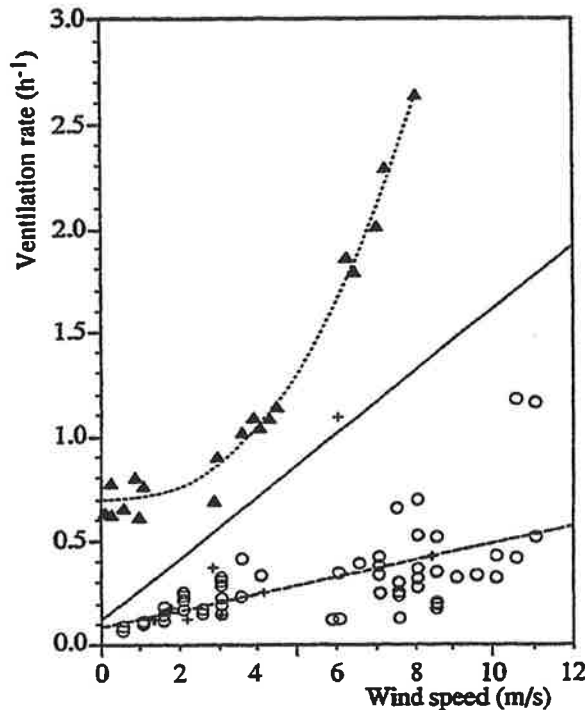


Fig.1 Relationship between the ventilation rate and the wind speed.

Δ American measurements from [7] - 1950

○ IMG-TNO measurements - Apartment building - from [9] - 1977

◇ IMG-TNO measurements - One-family house - from [10] - 1979

+ PML-TNO measurements - Maisonnette, front side - from [5] - 1978

+ PML-TNO measurements - Maisonnette, lee side - from [5] - 1978

b. Ventilation Consequent to a Temperature Difference

A temperature difference between the inner and the outer air produces, at the same time, a pressure difference. Due to this, the speed of infiltration of air increases by a higher inner temperature and, consequently, also the ventilation rate. In this manner, specially in high buildings, the ventilation is regulated via the stair cases and the air intake channels.

3.2 ventilation rate in housing

After the oil crisis in 1973, in many houses and buildings measures were taken to reduce the heat-losses due to ventilation. However, a minimum amount of ventilation is necessary for health reasons.

Reference [11] concludes that in order to obtain a proper living environment, considering a minimum amount of heat loss through ventilation, a ventilation rate of 0.5 to 1.0 h⁻¹ is necessary. A few measured ventilation rates (measured after 1973) are presented in Table I.

Table I ventilation rates for housing

Type of housing	Ventilation rate (h ⁻¹)	Year	Country	Ref.
Apartment houses	0.1 - 0.7	1977	Netherlands	9
Maisonnettes	0.1 - 0.5	1978	Netherlands	5
One-family houses	0.9 - 1.7	1979	Netherlands	10
Houses with good glass insulation	0.3 - 0.8	1983	Germany	11
For 80% of the number of houses tested	0.2 - 1.1	1983	Germany	13

Based on the measured values, reproduced in Table I and fig.1., it can be established that, in properly insulated modern houses with closed windows and doors, the ventilation rate varies from 0.3 to 0.7 h⁻¹ for high buildings and from 0.5 to 2.0 h⁻¹ for low buildings. The dependence of the ventilation rate on wind speed can be approximated by the following empirical formulas:

high buildings: ventilation rate = $0.1 + 0.04 \cdot u \cdot h^{-1}$

low buildings: ventilation rate = $0.1 + 0.14 \cdot u \cdot h^{-1}$

3.3

ventilation rate in public buildings and industrial spaces

Ventilation must be sufficient to meet minimum requirements. There is, however, a limit to a maximum amount of ventilation. ventilation rates of 7 to 8 h⁻¹ are felt like a draft. At the same time, a limitation of ventilation minimizes the heat losses. In spaces in which several people may be staying the ventilation rate must be accommodated to the number of people present. According to reference [6], a minimum amount of fresh air equal to 20 m³/hr must be supplied for an available space of 5 m³ per person, and 8 m³/hr for a space of 30 m³ per person. In public buildings and, generally, in buildings in which more than 10 people may be staying, a mechanical ventilation must be provided in most cases. Commonly used ventilation rates in public buildings and industrial buildings are presented in table II, from data out of reference [12]. For industrial buildings in which emissions of toxic or flammable gases take place, different norms must naturally be applied.

Table II ventilation rates for buildings designed for the presence of a numerous amount of people

Space type	ventilation rate (h ⁻¹)	Fresh air supply m ³ /h per person
Restaurants	8 - 12	50 - 70
Theatres		30 - 50
Shops	4 - 8	
Warehouses	6 - 8	
Public Offices	(3) - 6 - (10)	60 - 80
Hospitals	5 - 10	40 - 100
Covered swimming-pools	1 - 2	
Offices spaces	5 - 7	40 - 60
Workshops	3 - 8	
Schools	(3) - 5 - 8	30 - 50
Trains	15 - 40	

Intentional ventilation

When the windows and/or doors are open, the fact of remaining indoors provides little protection against contaminating substances outside. However, this type of ventilation is important after the passage of the toxic cloud, in order to lower the inner concentration as quickly as possible. The table below, taken from ref. [6], gives values of the ventilation rate which appear in case of an intentional ventilation.

Table III Relationship between ventilation rates and the condition of windows and doors

Windows/doors - condition	ventilation rate (h^{-1})
Windows and doors closed	0 - 0.5
Windows ajar	0.8 - 4.0
Windows half open	5 - 10
Windows fully open	9 - 15
Windows and doors open against each other	40

Absorption of gases by materials present indoors

When gas or particles penetrate inside a house, the contaminating substances come in contact with the materials used for construction and their coverings. Due to adhesive properties, the gases or the particles will fasten themselves on the surfaces of these materials. Such a process is defined as absorption. The properties of the contact surface of the material, such as porosity and above all the shape of the pores, play in this respect an important role. Also the nature of the gas and of the particles are determinant for the absorption. During the absorption process, the gas or particle molecules occupy the absorbing surface. Due to this, the absorbing surface is reduced and the speed of absorption slows down.

The degree of absorption – expressed by an absorption rate (see Par. 4.1) – is strongly dependent on the type of gas. Reactive gases absorb more on the materials present in a house than inert gases. Dockery (Ref. [14] has measured the following absorption factors (k) for particles:

particles smaller than $1\ \mu\text{m}$	$k = 0.05\ \text{h}^{-1}$
particles of the breathing fraction ($2.5 - 3.5\ \mu\text{m}$)	$k < 0.5\ \text{h}^{-1}$

Results of measurement of absorption rates for gases are scarce. This is due to the fact that these absorption rates are dependent on both gas and absorbing materials. Some values of absorption rates are given in Ref. [25,26] for gases out of indoors sources:

NO	absorption rate	$0-0.1\ \text{h}^{-1}$
NO ₂	"	$0.2-1.4\ \text{h}^{-1}$
Formaldehyde	"	$0.2-0.7\ \text{h}^{-1}$

For practical applications, the absorption rate for reactive gases, such as f.i. SO₂, NO₂ and O₃, can be set at an average value of 0.5. And, for inert gases, such as f.i. CO, at zero (0).

For a long exposure to a gas the absorbing surface becomes saturated. The absorption rates decrease with duration. The extent of such decrease is again dependent on gas and absorbing material. Measurements performed on different types of textiles are reported in Ref.[5]. For a standard distribution of wool, nylon and cotton in a room, it was found, for a 90 minutes duration, that the absorption rate is inversely proportional to the square root of the time.

Reduction of the background concentration

Due to traffic and emissions from industry, a continuous background concentration of certain contaminating substances is present. Measurements have shown that the inner concentration, due to this more or less continuous source, is generally lower than the outer concentration. The fact of remaining indoors offers, consequently, a certain degree of protection against the background concentration (pollution). This is principally caused by the absorption capacity of the materials in the houses, the deposit of particles and the decomposition of the gases. A commonly used measure to express the relationship between inner and outer concentrations is the so-called "indoors-outdoors" concentration ratio" C_i/C_o . The inverse of it (C_o/C_i) is called the protection factor. However, this type of measure is only really applicable to average values: a quick change in the value of C_o (for instance due to a change in wind direction) is followed by only a small change of the value of C_i and, consequently, the value of the ratio C_i/C_o then, changes appreciably. A few average values of measurements of the C_i/C_o ratio are presented in Table IV, taken from references [16,17,18,19,20,21,22 and 23]. The above measurements have principally been made in a big variety of furnished and lived-in houses, but only in those for which it was clearly established that the pollution was due to external sources. The measurements were performed with closed doors and windows and normally functioning ventilation systems.

Table IV Relationship between inner and outer concentrations for some gases and particles. Averages of various measurements

Contaminating substance	C_i/C_o	References
Sulphur dioxide (SO ₂)*)	0.1 - 0.5	16,17,19,20,23
Sulphur dioxide (SO ₂ **))	0.5 - 0.7	20
Nitrogen dioxide (NO ₂)	0.5	23
Ozone (O ₃)	0.2 - 0.5	18,23
Carbon monoxide (CO)	0.6 - 1.0	19,23
Sub-micron particles (Pb, Br)	0.4 - 0.7	21,22,23
Super-micron particles (Ca,Fe,Zn)	0.1 - 0.4	21,22

*) In areas with a low yearly-average SO₂ concentration (smaller than 10 µg/m³)
 **) In areas with a high yearly-average SO₂ concentration (10 - 60 µg/m³)

It can be seen, from this table, that the fact of staying indoors provides, generally, a protection factor (C_o/C_i) in the range of 2 against the background concentration of reactive gases. For sub-micron particles this factor is about 1.5 and for bigger particles it has an average value of 3.

Concentration indoors

If a building is overflowed by a toxic gas, then, dependent on the extent of exchange of inner and outer air, (ventilation), a concentration of polluted air will build-up indoors. Generally, this inner concentration will be lower than the maximum outer concentration. This is due to the fact that the outer air will always mix with the initially clean air inside the building. At the same time, the polluted gas or particles will also be absorbed by the materials present in the building. After the passage of the cloud the inner concentration remains relatively high. Thus, for optimum protection, it is necessary to ventilate immediately after the passage of the cloud.

The ventilation rate and, consequently, the maximum concentration are the highest in apartments located at the front side of the building. The apartments at the lee side obtain their fresh air principally out of apartments located more towards the front. Therefore, a better protection at the lee side can also be expected.

4.1 Mathematical model for the penetration of a gas cloud into a residence

The following assumptions have been made for the establishment of a mathematical model for the penetration of a gas cloud into a residence.

- Inside the residence an ideal mixing takes place between ventilation air and air which is present. Even though some investigators had measured appreciable differences of the ventilation rate inside a residence [12], Leach and Bloomfield [15] have measured and established, with the help of a diffusion model, that the concentration distribution is, on the whole, fairly homogeneous. Ref. [27] further indicates that, due to convective mixing, a heavy gas also spreads homogeneously inside a building.
- The absorbing surface is constant and desorption does not take place.

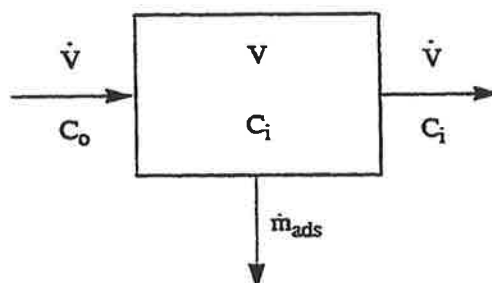


Fig. 2 Schematical representation of a ventilated space in which absorption takes place.

Fig. 2. shows schematically a room which is directly ventilated by the outer air and in which absorption takes place. An air flow \dot{V} , with a concentration C_o of contaminating substances, enters a room of volume V in which a concentration C_i is present. An absorption \dot{m}_{ads} takes place, after which the air flow leaves the room with a concentration C_i . The mass balance equation of this system is represented by the following relationship:

$$\dot{V} * C_o * dt = V * dC_i + \dot{m}_{ads} dt + \dot{V} * C_i * dt \quad (1)$$

or

$$\dot{V} * C_o * dt = V * dC_i + v_{ads} * A_{ads} * C_i * dt + \dot{V} * C_i * dt \quad (2)$$

where

- \dot{V} = air flow entering inside (m³/s)
- C_o = concentration in the outer air (kg/m³)
- t = time (s)
- V = volume (contents) of the room (m³)
- \dot{m}_{ads} = $V_{ads} * A_{ads} * C_i$ = the absorption loss flow (kg/s)
- v_{ads} = absorption speed (m/s)
- A_{ads} = absorption area (m²)
- C_i = concentration in the room (kg/m³)

We have further

$$\dot{n}_v = \frac{\dot{V}}{V} = \text{ventilation frequency (s}^{-1}\text{)}$$

$$\dot{n}_a = \frac{v_{ads} * A_{ads}}{V} = \text{absorption frequency (s}^{-1}\text{)}$$

$$\dot{n}_{va} = \dot{n}_v + \dot{n}_a \text{ (s}^{-1}\text{)}$$

Note:

A difference is made between the terminology “ventilation frequency” and “absorption frequency”, both expressed in s⁻¹, and the terms ventilation rate and absorption rate, both expressed in h⁻¹.

The solution of the differential equation with limit value $C_i = 0$ as $t = 0$ is:

$$C_i(t) = \dot{n}_v \int_0^t C_o(t') \text{EXP}(-\dot{n}_{va}(t-t')) dt' \quad (3)$$

For different time dependent outer concentrations, the inner concentration can be calculated with (3) above.

4.2

The concentration indoors as consequence of an external continuous source

The concentration at a height z in the center of a plume originating from a continuous emission of a neutral gas from a point source at height h is, according to [1]:

$$C_0(x,y,z) = \frac{\dot{m}}{2\pi u \sigma_y(x) \sigma_z(x)} * \text{EXP}\left(-\frac{y^2}{2\sigma_y^2(x)}\right) * \left[\text{EXP}\left(-\frac{(z-h)^2}{2\sigma_z^2(x)}\right) + \text{EXP}\left(-\frac{(z+h)^2}{2\sigma_z^2(x)}\right) \right] \quad (4)$$

in which:

$C_0(x,y,z)$ = concentration at a distance X from the source, at y from the plume axis and at height z (kg/m^3)

\dot{m} = source strength (Kg/s).

u = average wind speed at a 10m height (m/s)

h = emission height (m)

σ_y = standard deviation of the concentration distribution in the y -direction (m)

σ_z = standard deviation of the concentration distribution in the z -direction (m)

The concentration according to (4) can be eventually corrected for the initial dimensions of the source with the help of a virtual source distance (correction of the sigma's). At the same time, it can be corrected for the deposition by a reduction of the source-strength and/or for the plume rising by introducing a source height dependent on x – see, for this, for instance [1].

The concentration at the outside of a house, at a distance x from the source, can be approximated by a step function

$$C_0 = 0 \text{ for } t < 0$$

$$C_0 = C_0(x) \text{ for } t \geq 0$$

According to (3), the concentration indoors is then given by:

$$C_i(t) = \frac{\dot{n}_v}{\dot{n}_{va}} C_0 (1 - \text{EXP}(-\dot{n}_{va} * t)) \quad (5)$$

An example of the variation of the concentration caused by an external continuous source is reproduced in Figure 3. The ratio ventilation rate/absorption rate, in this example, is equal to 2.

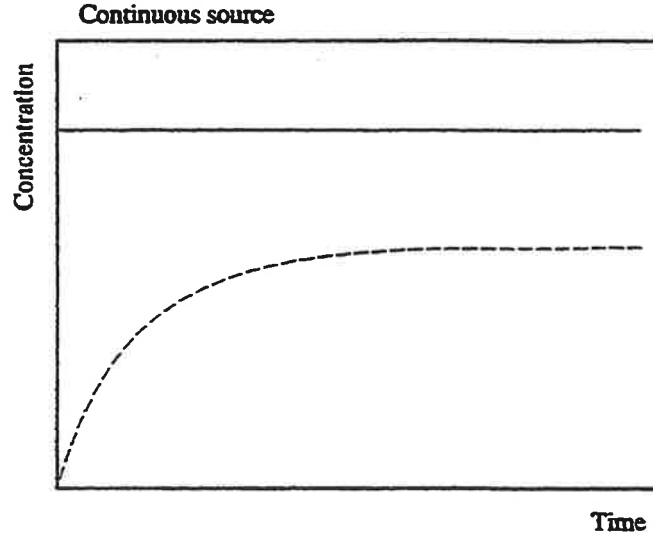


Fig.3 Outer (—) and inner (-----) concentrations, dependent on time, for a continuous constant emission.

By a constant absorption, the inner concentration, after a long time, is equal to:

$$C_i = \frac{\dot{n}_v}{\dot{n}_{va}} C_o \quad (6)$$

and the concentration reduction (see Paragraph 4.3) is equal to:

$$CR = \frac{C_o - C_i}{C_o} = 1 - \frac{\dot{n}_v}{\dot{n}_{va}} \quad (6a)$$

When the absorbing surface has been saturated, the inner concentration becomes equal to the outer concentration.

For the beginning stages we can determine, from (5), after how much time a given relationship between inner concentration and outer concentration will be reached. For a concentration ratio C_i/C_o we have, for time t^* :

$$t^* = -\frac{1}{\dot{n}_{va}} \ln \left(1 - \frac{\dot{n}_v}{\dot{n}_v} \frac{C_i}{C_o} \right) \quad (7)$$

4.3

The concentration indoors as consequence of an external temporary source

The terminology "temporary source" applies to a constant emission of a neutral gas which lasts a short period of time, but which is, however, longer than the time required for the gas cloud to travel to the house in question. The concentration by the house is again calculated according to (4). The outer concentration, in this case, is approximated by a block function:

$$C_o = 0 \quad \text{for } t < 0$$

$$C_o = C_o(x) \quad \text{for } 0 \leq t \leq t_1$$

$$C_o = 0 \quad \text{for } t > t_1$$

x is hereby the distance from the house to the source and t_1 the passage time. The time t is measured from the moment at which the cloud has reached the house, that means x/u s. after the beginning of the emission.

According to (3) the inner concentration is given by:

$$C_i(t) = \frac{\dot{n}_v}{\dot{n}_{va}} C_o (1 - \text{EXP}(-\dot{n}_{va} * t)) \quad \text{for } t \leq t_1 \quad (8a)$$

and

$$C_i(t) = \frac{\dot{n}_v}{\dot{n}_{va}} C_o (\text{EXP}(\dot{n}_{va} * t_1) - 1) \text{EXP}(-\dot{n}_{va} * t) \quad \text{for } t > t_1 \quad (8b)$$

An example of the variation of the concentration inside the house due to an external temporary source is reproduced in Fig.4. The ratio ventilation rate/absorption rate, in this example, is taken equal to 2.

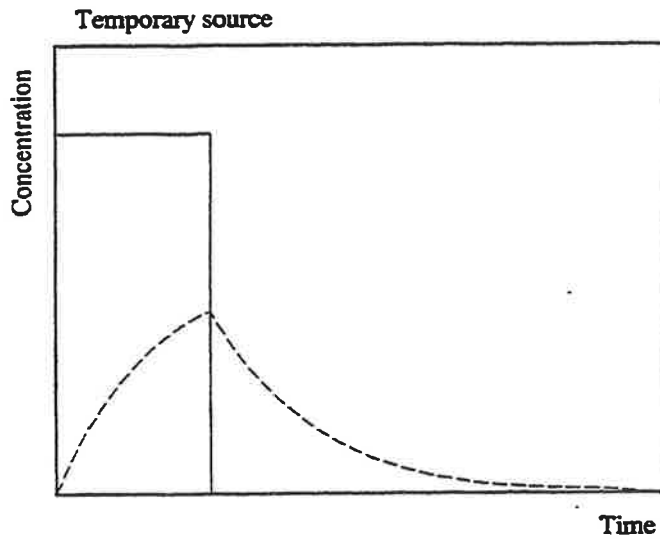


Fig. 4 Outer (—) and inner (---) concentrations, dependent on time, for an external temporary source

The maximum value of the inner concentration is reached at time t_1 and is calculated from (8a), whereby $t = t_1$. The ratio of the maximum inner concentration divided by the maximum outer concentration represents a measure of the reduction of the peak concentration which can be expected by staying indoors. This ratio is given by:

$$\frac{C_{i,max}}{C_{o,max}} = \frac{\dot{n}_v}{\dot{n}_{va}} (1 - \text{EXP}(-\dot{n}_{va} * t_1)) \quad (9)$$

If the reduction of the concentration is defined as the relative lowering of the maximum inner concentration versus the maximum outer concentration, then this reduction of the concentration (CR) is given by:

$$CR(t_1) = \frac{C_{o,max} - C_{i,max}}{C_{o,max}} = 1 - \frac{\dot{n}_v}{\dot{n}_{va}} (1 - \text{EXP}(-\dot{n}_{va} * t_1)) \quad (9A)$$

Curves for the concentration reduction, with dependency on passage time, for a temporary source and for the various parameters, are shown in diagrams 1 and 2.

In order to obtain maximum protection indoors ventilation should begin immediately after time t_1 . However, this precise time t_1 is not always known, so that in practice ventilation may begin later, at a time t_2 . It is then a question of a ventilation delay ($t_2 - t_1$).

The biological effect of toxic gases is, in many cases, not linear and cumulative. This implies that the toxic effect is proportional to the integration of the concentration up to a given power, over time (the probit dose); thus

$$D_i(t) = \int_0^t C_i^n(t') * dt' \quad (10)$$

The value to which the probit dose rises is jointly determined by the ventilation delay and by the dose-concentration relationship (n , the toxic load parameter). A measure of the protection indoors is given by the ratio between the doses to which people are exposed inside and outside, respectively. Similarly to the concept of "concentration reduction", we can now talk about a (probit)dose reduction concept, defined as the relative lowering of the optimum probit dose inside versus the probit dose to which people are exposed outside.

This dose reduction, for $n = 1$, is given by:

$$DR(t_1, t_2) = \frac{D_o(t_2) - D_i(t_2)}{D_o(t_2)} = 1 - \frac{\dot{n}_v}{\dot{n}_{va}} \left[1 - \frac{1}{\dot{n}_{va} t_1} (1 - \text{EXP}(-\dot{n}_{va} * t_1)) \text{EXP}(-\dot{n}_{va}(t_2 - t_1)) \right] \quad (11)$$

For integer values of n (1,2,3...) the following applies for the dose reduction:

$$DR(t_1, t_2) = 1 - \left(\frac{\dot{n}_v}{\dot{n}_{va}} \right)^n * \left[1 + \frac{1}{\dot{n}_{va} t_1} \sum_{i=1}^n (-1)^i \frac{1}{i} \binom{n}{i} (1 - \text{EXP}(-i \dot{n}_{va} t_1)) + \frac{1}{n \dot{n}_{va} t_1} (1 - \text{EXP}(-\dot{n}_{va} t_1))^n (1 - \text{EXP}(-n \dot{n}_{va} (t_2 - t_1))) \right] \quad (11a)$$

Hereby the $\binom{n}{i}$ are the binomial coefficients $\binom{n}{i} = \frac{n!}{(n-i)!i!}$

Curves for the dose reduction with dependency on passage time, for a temporary source and for the different parameters, are shown in diagrams 3a to 5c included.

Concentration indoors, as consequence of an external instantaneous source

The concentration at a distance x from an instantaneous emission, at a height h , of a neutral gas is given by:

(Reference [1])

$$C_o(x, y, z, t) = m * F_x(x, t) * F_y(y, t) * F_z(z, t) \quad (12)$$

with

$$F_x(x, t) = \frac{1}{\sqrt{2\pi\sigma_x(ut)}} * \text{EXP}\left(-\frac{(x-ut)^2}{2\sigma_x^2(ut)}\right)$$

$$F_y(y, t) = \frac{1}{\sqrt{2\pi\sigma_y(ut)}} * \text{EXP}\left(-\frac{y^2}{2\sigma_y^2(ut)}\right)$$

$$F_z(z, t) = \frac{1}{\sqrt{2\pi\sigma_z(ut)}} * \left[\text{EXP}\left(-\frac{(z-h)^2}{2\sigma_z^2(ut)}\right) + \text{EXP}\left(-\frac{(z+h)^2}{2\sigma_z^2(ut)}\right) \right]$$

where:

- x = downwind distance from the source (m)
- y = lateral distance (m)
- z = height (m)
- t = time measured from the beginning of the emission (s)
- u = average wind velocity (m/s)
- m = amount of instantaneous emission (kg)
- h = source height (m)
- σ_i = standard deviations from the concentration distribution for an instantaneous source - $i = x, y, z$ - (m)

The concentration, according to (12), can be corrected for the initial dimensions of the source with the help of the distance to a virtual source (correction of the sigma's). At the same time, a correction can be made for the deposition using a reduced source strength and/or for the plume rising by introducing a source height dependent on the distance - see, for this, for instance [1].

The inner concentration can be calculated with, for instance, (3) or (12). For a sufficiently big value of t the concentration indoors may be calculated using the time dependent standard variations of the concentration distribution, which means that in (12) $\sigma(ut)$ may be replaced by $\sigma(x)$.

Strictly speaking, t must be so large, that the cloud has already been passed, but the difference in the calculation of the outer concentration with $\sigma(ut)$ or $\sigma(x)$ is small. In this manner, the following analytical approximation for the inner concentration is found:

$$C_i(t) = \frac{\dot{n}_v m}{2u} F_y \left(y, \frac{x}{u} \right) F_z \left(z, \frac{x}{u} \right) \exp \left(\frac{1}{2} \left(K^2 - \frac{x^2}{\sigma_x^2} \right) \right) \exp(-\dot{n}_{va} * t) \left[\operatorname{ERF} \left(\frac{ut}{\sigma_x \sqrt{2}} - \frac{K}{\sqrt{2}} \right) + \operatorname{ERF} \left(\frac{K}{\sqrt{2}} \right) \right] \quad (13)$$

with :

$$K = \frac{\dot{n}_{va} \sigma_x^2 + ux}{u \sigma_x} \quad (13a)$$

We have, further :

$$\sigma_i = \sigma_i(x), \quad i = x, y, z$$

$\operatorname{ERF}(x)$ = the error function, defined as :

$$\operatorname{ERF}(x) = \frac{2}{\sqrt{\pi}} \int_0^x \exp(-t^2) dt$$

An example of the variation of the indoor concentration, as consequence of an external instantaneous source, is shown in Figure 5. The ratio ventilation rate/absorption rate, in this example, is taken equal to 2.

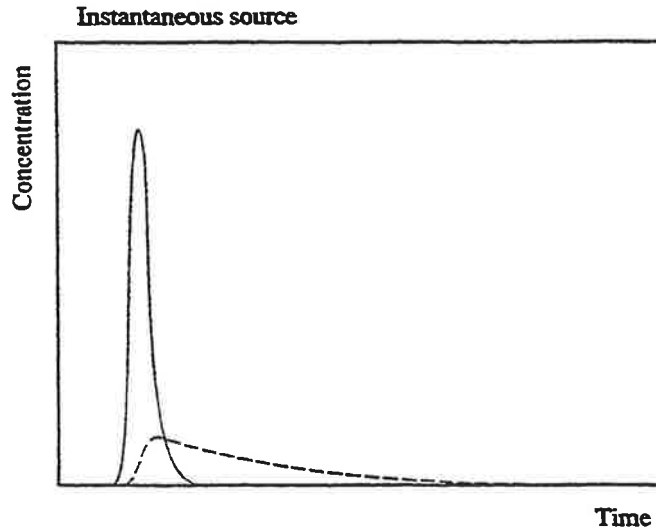


Fig.5. Inner (-----) and outer (——) concentrations, dependent on time, for an instantaneous source.

The maximum inner concentration is reached when the outer concentration becomes lower than the inner concentration. Differentiating (13) we find that the maximum inner concentration is reached at a time t_m given by the implicit equation:

$$\frac{u}{\sigma_x \sqrt{2\pi}} \exp \left[-\frac{1}{2} \left(\frac{u}{\sigma_x} t_m - K \right)^2 \right] = \frac{\dot{n}_{va}}{2} \left[\operatorname{ERF} \left(\frac{ut_m}{\sigma_x \sqrt{2}} - \frac{K}{\sqrt{2}} \right) + \operatorname{ERF} \left(\frac{K}{\sqrt{2}} \right) \right] \quad (14)$$

Another form of this equation is :

$$t_m = \frac{\sigma_x}{u} \left[\sqrt{-2 * \ln \left\{ \frac{\dot{n}_{va} \sigma_x \sqrt{2\pi}}{2u} * \left[\operatorname{ERF} \left(\frac{ut_m}{\sigma_x \sqrt{2}} - \frac{K}{\sqrt{2}} \right) + \operatorname{ERF} \left(\frac{K}{\sqrt{2}} \right) \right] \right\}} + K \right] \quad (14a)$$

According to Annex 1, σ_x is linearly proportional to x . Eq. (13a) shows that $K > x/\sigma_x$ and, therefore, $K > 7.6$ and, then, $\operatorname{ERF}(K/\sqrt{2}) = 1.0$. Further on, t_m is larger than x/u and certainly smaller than $2x/u$ (see, for this, Paragraph 4.6). The value of the argument in the first error function, in (13), lays then between $-\dot{n}_{va} \sigma_x/(u \sqrt{2})$ and $\dot{n}_{va} \sigma_x/(u \sqrt{2})$. Since \dot{n}_{va} is small, we can, for a value of x which is not too large, approximately set the value of the first error function as equal to zero (0). A restriction of the value of x , with dependency on \dot{n}_{va} and u , is given due to the fact that the argument of the log-function must be smaller than 1.0. We can then write, for the value of t_m , with which the maximum inner concentration must be calculated, approximately the following:

$$t_m \approx \frac{\sigma_x}{u} \left[\sqrt{-2 * \ln \left(\frac{\dot{n}_{va} \sigma_x \sqrt{2\pi}}{u} \right)} + K \right] \quad (15)$$

The maximum inner concentration can be approximated by (13), whereby $t = t_m$.

The concentration reduction is, with this:

$$CR = 1 - \frac{\dot{n}_v \sigma_x \sqrt{2\pi}}{2u} \operatorname{EXP} \left\{ \frac{1}{2} \left(K^2 - \frac{x^2}{\sigma_x^2} \right) \right\} \operatorname{EXP}(-\dot{n}_{va} t_m) \cdot \left[\operatorname{ERF} \left(\frac{ut_m}{\sigma_x \sqrt{2}} - \frac{K}{\sqrt{2}} \right) + \operatorname{ERF} \left(\frac{K}{\sqrt{2}} \right) \right] \quad (16)$$

The formulas show that, for a small amount of ventilation, the concentration reduction approaches 1.0. Equation (16) – and also – (17) are, with the common definition for σ_x (see Annex 1), homogeneous in x and u . Curves for the concentration reduction, with dependency on x/u , for an instantaneous source and for the various parameters, are shown in diagrams 6 and 7. The x/u ratio, hereby, represents the time required for the cloud to reach the house in question; this time is directly proportional to the passage time of the cloud, such as given in eq. (18).

The dose is calculated with the help of eq. (10). The dose reduction is dependent on the ventilation-delay and on the dose concentration relationship. The ventilation delay, in this, is the time difference between the time mark of complete ventilation and the time mark whereby the outer concentration, after passage of the cloud, becomes lower than the inner concentration. For $n = 1$, the dose reduction is given by:

$$DR(t_2) = \frac{D_o(t_2) - D_i(t_2)}{D_o(t_2)} = 1 - \frac{\dot{n}_v}{2\dot{n}_{va}} \left[\text{ERF} \left(\frac{ut_2 - x}{\sigma_x \sqrt{2}} \right) + \text{ERF} \left(\frac{x}{\sigma_x \sqrt{2}} \right) + \right. \\ \left. - \text{EXP} \left\{ \frac{1}{2} \left(K^2 - \frac{x^2}{\sigma_x^2} \right) \right\} * \text{EXP}(-\dot{n}_{va} t_2) * \left\{ \text{ERF} \left(\frac{ut_2}{\sigma_x \sqrt{2}} - \frac{K}{\sqrt{2}} \right) + \text{ERF} \left(\frac{K}{\sqrt{2}} \right) \right\} \right] \quad (17)$$

in which t_2 is the time mark of the delayed ventilation. We have, generally, for $n > 0$:

$$DR(t_2) = 1 - \left(\frac{\dot{n}_v}{2} \right)^n \left(\frac{\sigma_x \sqrt{2\pi}}{u} \right)^{n-1} \sqrt{n} \text{EXP} \left\{ \frac{n}{2} \left(K^2 - \frac{x^2}{\sigma_x^2} \right) \right\} * \\ \int_0^{t_2} \left[\text{ERF} \left(\frac{ut'}{\sigma_x \sqrt{2}} - \frac{K}{\sqrt{2}} \right) + \text{ERF} \left(\frac{K}{\sqrt{2}} \right) \right]^n \text{EXP}(-n\dot{n}_{va} t') dt' \quad (17a)$$

Curves for the dose reduction, with dependency on x/u , for an instantaneous source and for the different parameters, are given in diagrams 8a to 10c incl. The ventilation delay, hereby is measured from the time mark $t_1 = (3x)/(2u)$ - see, for this, Paragraph 4.6, equation (19).

4.5 Calculation examples for paragraphs 4.3 and 4.4

4.5.1 Calculation of the maximum indoors concentration and of the dose-reduction for a temporary emission

Given: an emission from a point source with a source-strength of 10 kg/s, lasting about one hour. At a 500 m distance a house is located. In this house, the ventilation rate is equal (on the average) to 1.0 h⁻¹, and the absorption rate can be set equal to 0.5 h⁻¹. The weather conditions are neutral, with a wind speed of 5 m/s. The wind direction is such that the house finds itself in the center of the plume. The roughness length is 0.1 m.

The following must be calculated: the 10 minutes average maximum concentration indoors and the dose reduction, considering that, after the passage of the cloud, one hour goes by before the house is ventilated.

Calculation:

According to Annex 1 : $\sigma_y(500) = 35.5$ m en $\sigma_z(500) = 22.5$ m.

If we choose, for z , a height of 1.0 m, then, according to (4), the outer concentration is equal to:

$$c_o = \frac{10}{2\pi * 5 * 35.5 * 22.5} \text{EXP} - \frac{1}{2 * 22.5^2} = 0.0008 \text{ kg/m}^3$$

The maximum indoors concentration is reached 1.0 h after the arrival of the cloud.

The ventilation frequency is : $\dot{n}_v = 1/3600 = 0.00028 \text{ s}^{-1}$

The absorption frequency is : $\dot{n}_a = 0.5/3600 = 0.00014 \text{ s}^{-1}$

The maximum inner concentration, according to (8a) is equal to:

$$C_{1,max} = \frac{0.00028}{0.00042} * 0.0008 * (1 - \text{EXP}(-0.00042 * 3600)) = 0.0004 \text{ kg/m}^3$$

The concentration-time variation, for this example, is shown in Figure 6.

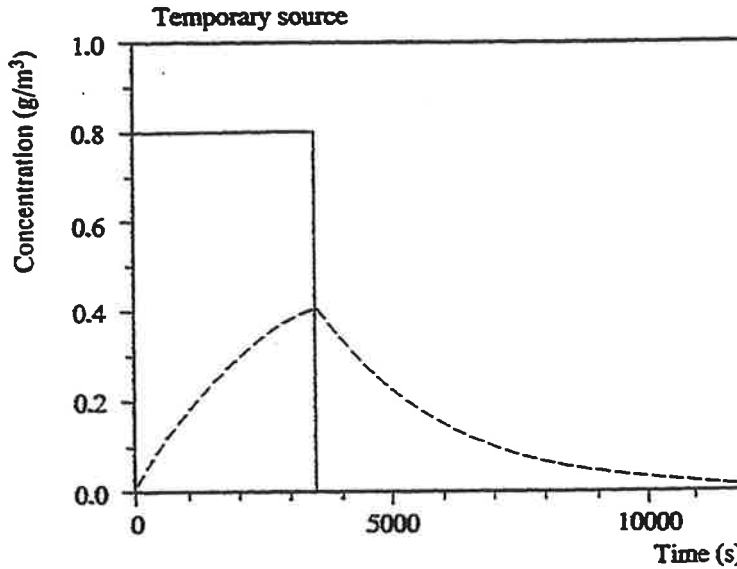


Fig. 6 Outer (—) and inner (----) concentrations, dependent on time, for a temporary constant emission of calculation example 4.5.1.

The dose reduction, for a ventilation delay of 1 hr (3600s) and for $n = 1$, is calculated according to (11):

$$DR = 1 - \frac{0.00028}{0.00042} \left(1 - \frac{1}{0.00042 * 3600} * (1 - \text{EXP}(-0.00042 * 3600)) * \text{EXP}(-0.00042 * 3600) \right) = 0.41$$

For $n = 2$, the dose reduction is calculated according to (11a):

$$DR = 1 - \left(\frac{0.00028}{0.00042} \right)^2 \left[1 + \frac{1}{0.00042 * 3600} \{ -2(1 - \text{EXP}(-0.00042 * 3600)) + \frac{1}{2}(1 - \text{EXP}(-0.00084 * 3600)) \} + \frac{1}{0.00084 * 3600} * (1 - \text{EXP}(-0.00042 * 3600))^2 (1 - \text{EXP}(-0.00084 * 3600)) \right] = 0.79$$

For a higher loading ($n > 1.0$) the dose reduction increases. The dose received indoors is higher for $n > 1$ than for $n = 1$. This actually applies, to a higher extent, to the dose received outdoors, so that the dose reduction increases with increasing n and decreases with decreasing n .

4.5.2

Calculation of the concentration reduction and of the dose reduction, by remaining indoors, for an instantaneous source

Given: an instantaneous emission of 1000 kg. A house is again located at a 500 m distance, in which the average ventilation rate is 1 h^{-1} and the absorption-factor can be set equal to 0.5 h^{-1} . The weather conditions are neutral and the wind speed is 5 m/s. The roughness length is 0.1 m.

To be calculated: the concentration reduction and the dose reduction, considering that the house will be fully ventilated 10 minutes after the emission.

Calculation:

According to Annex 1: $\sigma_x(500) = 65 \text{ m}$.

The time at which the inner concentration is maximum can be estimated with, for instance, (15). The unit K required for it must first be calculated.

the ventilation frequency is : $1/3600 = 0.00028 \text{ s}^{-1}$

the absorption frequency is : $0.5/3600 = 0.00014 \text{ s}^{-1}$

This gives, for the unit K:

$$K = \frac{0.00042 * 65^2 + 500 * 5}{5 * 65} = 7.698$$

while t_m , according to (15), is equal to :

$$t_m = \frac{65}{5} \left[\sqrt{-2 \ln \left(\frac{0.00042 * 65 * \sqrt{2\pi}}{5} \right)} + 7.698 \right] = 138 \text{ s}$$

The concentration reduction is then :

$$\begin{aligned} CR &= 1 - \frac{0.00082 * 65 * \sqrt{2\pi}}{2 * 5} \text{EXP} \left[\frac{1}{2} \left(7.698^2 - \frac{500^2}{65^2} \right) \right] \text{EXP}(-0.00042 * 138) * \\ &\left[\text{EXP} \left(\frac{5 * 138}{65 * \sqrt{2}} - \frac{7.698}{\sqrt{2}} \right) + \text{ERF} \left(\frac{7.698}{\sqrt{2}} \right) \right] \\ &= 1 - 0.00456 * 1.0448 * 0.9437 * (0.9965 + 1) = 0.99 \end{aligned}$$

The concentration variation with time, for this example, is given in Figure 7. The time axis as well as the concentration axis, in this figure, are logarithmic, so that the dose cannot be read directly from the figure.

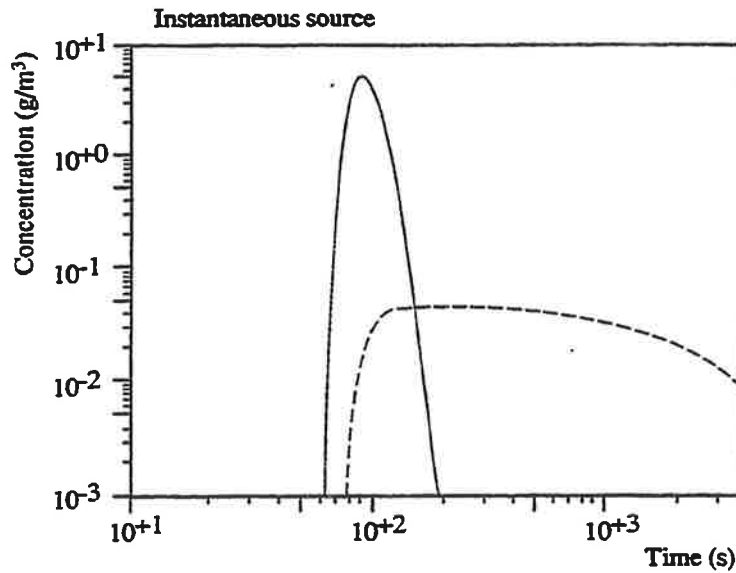


Fig.7 Outer (—) and inner (-----) concentrations, dependent on time, for the instantaneous source of calculation example 4.5.2.

The outer concentration, at the time mark of 10 minutes after the emission, is calculated with (12) with $t = 600$ s. Its value, from Figure 7, appears to be already negligibly small.

The dose reduction for $n = 1$ is calculated with the help of (17):

$$\begin{aligned}
 DR(600) &= 1 - \frac{0.00028}{2 * 0.00042} \left[\operatorname{ERF} \left(\frac{5 * 600}{65 * \sqrt{2}} - \frac{500}{65 * \sqrt{2}} \right) + \operatorname{ERF} \left(\frac{500}{65 * \sqrt{2}} \right) + \right. \\
 &\quad \left. - \operatorname{EXP} \left\{ \frac{1}{2} \left(7.698^2 - \frac{500^2}{65^2} \right) \right\} * \operatorname{EXP}(-0.00042 * 600) * \right. \\
 &\quad \left. \left\{ \operatorname{ERF} \left(\frac{5 * 600}{65 * \sqrt{2}} - \frac{7.698}{\sqrt{2}} \right) + \operatorname{ERF} \left(\frac{7.698}{\sqrt{2}} \right) \right\} \right] = \\
 &= 1 - 0.333 * \{ 1 + 1 - 1.0448 * 0.777 * (1 + 1) \} = 0.87
 \end{aligned}$$

For values of n not equal to 1, the dose reduction can be obtained from diagrams 8a to 10c incl., and can then be interpolated for the proper parameters.

4.6

Passage time of a cloud originating from an instantaneous source

The passage time of a cloud depends on many factors, and not in the last place on the presence of obstacles. By a free overflow, the passage time t_1 of the cloud can be approximated by the equation given in [1].

$$t_1 = \frac{2\sigma_x}{u} \sqrt{2 * \ln \left(\frac{c_{o,max}}{c_g} \right)} \quad (18)$$

in which:

- t_1 passage time of the cloud (s)
 σ_x standard deviation of the concentration distribution in the x-direction for $t = x/u$; eventually corrected for a virtual source distance (m)
 $C_{o,max}$ maximum concentration according to (12) calculated with $t = x/u$ (kg/m³)
 C_g limit concentration with which the beginning and the end of the cloud are defined (kg/m³)

If, for instance, 1% of the maximum concentration is considered to be the limit concentration, then (18) transforms into:

$$t_1 = \frac{6.1 \sigma_x}{u} \approx 0.8 \frac{x}{u}$$

The time, calculated from the moment of the instantaneous emission, during which the cloud is present over the house, is now given by:

an arrival time of $x/u - t_1/2$ (s)
 and a departure time of $x/u + t_1/2$ (s) (19)

4.7

Fraction of protected area and critical ventilation rate

The degree of protection provided, during the passage of a toxic cloud, by staying indoors, is described in paragraphs 4.3 and 4.5. If, in an area hit by a toxic cloud, a person remains indoors, the probit dose to which this person is exposed is smaller than the one received by a person outdoors. The probit dose decreases with an increase of the distance to the center of the cloud. If, at a certain distance from the center of the cloud, a given value of the dose is reached indoors, the same value of the dose, outdoors, will be reached at a further distance from this center of the cloud. The above is illustrated in Figure 8, with the distance A-O being larger than the distance B-O. The area around the trajectory of the center of the cloud, in which a given dose is exceeded by staying indoors, is then also smaller than the area in which the same dose is exceeded outdoors.

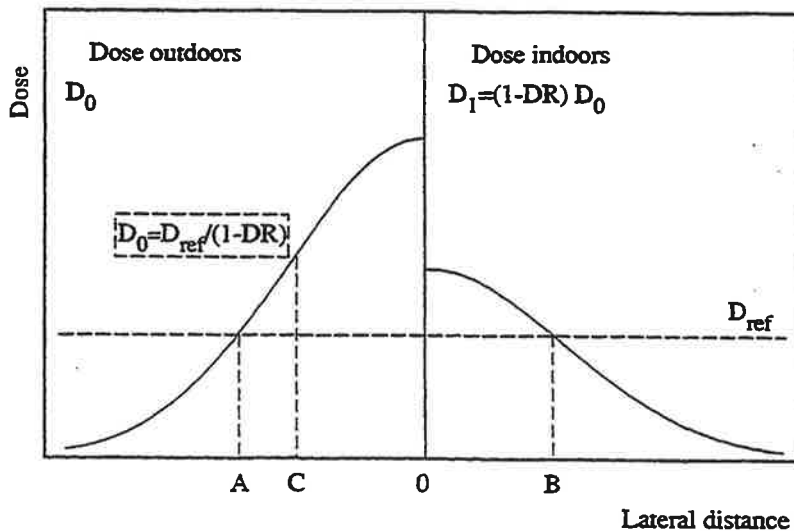


Fig. 8 Dose by staying indoors and by staying outdoors, as function of the lateral distance, for a temporary source.

The extent to which an area with a probit-dose higher than a given reference dose is reduced is expressed by the concept "fraction of protected area". It is assumed, hereby, that we are dealing with an average ventilation rate, an average absorption rate, and an average ventilation delay, all valid for the whole area. The fraction of protected area is a measure of collective protection received by a population, in case massive protection indoors is contemplated.

The fraction of protected area is defined as:

$$f_{pa} = \frac{A_o - A_i}{A_o} = 1 - \frac{A_o \left(\frac{D_{ref}}{(1-DR)} \right)}{A_o (D_{ref})} \quad (20)$$

in which:

f_{pa} = fraction of protected area

A_o = area in which the received probit dose outdoors exceeds the value D_{ref}

A_i = area in which the received probit dose indoors exceeds the value D_{ref}

The area in which the probit dose indoors exceeds the value D_{ref} , must be calculated as the area in which the probit dose outdoors exceeds the value $D_{ref}/(1-DR)$. This is in agreement with the equal distances C-O and B-O in Figure 8.

According to equation (10), the optimum probit dose outdoors, for a temporary source, is equal to $C_{ot}^n t_1$. Similarly to the equation, given in Reference [1], for the lateral distance to a reference concentration and the area inside the perimeter determined by the reference concentration, the area in which a probit dose $D^* = C_{ot}^n t_1$, coming from a temporary source, is exceeded, is given by:

$$A_o(D^*) = \frac{a' \sqrt{2\pi} \left(\frac{\dot{m}}{ua'c'} \right) \left(\frac{t_1}{D^*} \right)^{\frac{\alpha}{n}} \left(\frac{1}{\alpha} \right)^{\frac{3}{2}}}{b + d'} \quad (21)$$

with $\alpha = (b+1)/(b+d')$

Further values are:

a', b', c', d' Constants in the equations of the dispersion parameters in the y-, resp. z-direction, corrected respectively for the average time and, for the roughness length. (See, for this, Annex 1 and Ref. [1]).

D^* limit value of the probit dose

n power in the probit dose - concentration relationship.

From equations (20) and (21) it follows that, for a temporary source, the fraction of protected area is given by:

$$f_{pa} = 1 - (1 - DR)^{\frac{\alpha}{n}} \quad (22)$$

Via the dose reduction, the fraction of protected area is dependent on the ventilation rate, the absorption rate, the passage time and the ventilation delay. Through the power, the fraction of protected area is, at the same time, dependent on the meteorological stability. It is assumed, hereby, that the passage time of the cloud is equal to the source duration, thus independent of the distance to the point of emission. The spreading of the cloud in the average wind direction is hereby small according to the length of the cloud caused by the source duration.

For an instantaneous point-source at ground level we have, for the lateral distance for which the probit dose D^* is exceeded:

$$y(x) = \sigma_y(x) \sqrt{\frac{2}{n} \ln \left(\frac{D(x)}{D^*} \right)} \quad (23)$$

and for the area in which the dose D^* is exceeded

$$A_o(D^*) = \frac{a_l \sqrt{2\pi}}{b_l + d_l' + 1 - \frac{1}{n}} \left(\frac{2m}{(\sqrt{2\pi})^3 a_l c_l' e_l} \right)^\beta \left(\frac{e_l \sqrt{2\pi}}{u D^* \sqrt{n}} \right)^{\frac{\beta}{n}} \left(\frac{1}{\beta} \right)^{\frac{3}{2}} \quad (24)$$

in which:

- a_l, b_l, c_l', d_l' constants corrected for the roughness length in the equations of the dispersion parameters and e_l in the y-, z- and x- directions, respectively, for an instantaneous emission (see Annex 1 and Ref. [1])
- $D(x)$ optimum probit dose in the center of the cloud, at ground level and distance x from the emission point
- D^* limit value of the probit dose
- β $(b_l + 1)/(b_l + d_l' + 1 - 1/n)$

For an instantaneous emission, the passage time and, consequently, the dose reduction, are dependent on the distance to the emission point (see equation (18)). In order to calculate A_l , we must integrate equation (23) up to the distance at which $y(x)$ will be equal to zero. The dose D^* is given, hereby, by:

$$\frac{D_{ref}}{(1 - DR(x))}$$

The distance at which $y(x)$ will be equal to zero must be calculated with the help of an implicit equation:

$$x^* = \left(\frac{(2m)^n (1 - DR(x^*))}{(\sqrt{2\pi})^{3n-1} \sqrt{n} u a_l^n c_l'^n e_l^{n-1} D_{ref}} \right)^{\frac{1}{n(b_l + d_l' + 1) - 1}} \quad (25)$$

The fraction of protected area, for an instantaneous source at ground level, is calculated with :

$$f_{pa} = 1 - \frac{\int_0^{x^*} \sigma_y(x) \left[\frac{2}{n} \ln \left(\frac{(2m)^n (1 - DR(x))}{(\sqrt{2\pi})^{3n-1} \sqrt{n} u \sigma_x^{n-1}(x) \sigma_y^n(x) \sigma_z^n(x) D_{ref}} \right) \right]^{\frac{1}{2}} dx}{A_o(D_{ref})} \quad (26)$$

whereby $A_o(D_{ref})$ is calculated with equation (24).

Equation (26) must be solved numerically. In tables 2.Ia to c incl., in Annex 2, some values of the fraction of protected area are given, dependent on the ventilation rate, the absorption rate, the ventilation delay, the stability class and for various values of the reference dose. Within the different stability classes, we must work with the average wind speed corresponding to a given class. These are:

Very stable	(VS)	2 m/s
Neutral	(N)	5 m/s
Unstable	(U)	3 m/s

A source strength of 1000 kg. has been considered in the calculations. The numbers remain, however, valid when the ratio of the reference-dose versus the source strength up to power n is in agreement with the same value in the table; thus, for a limit dose D^* ($(\text{g}/\text{m}^3)^n \text{ s}$) and a source strength m (kg), we must refer, in Table 2. to a reference-dose $D_{\text{ref}}((\text{g}/\text{m}^3)^n \text{ s})$ which satisfies the following relationship:

$$\frac{D^*}{m^n} = \frac{D_{\text{ref}}}{1000^n}$$

By taking precautionary measures such as shutting the ventilation system and closing the openings it is possible to reduce the ventilation rate. The same types of measures increase the fraction of protected area. The latter is expressed by a critical ventilation rate, which is the ventilation rate whereby the fraction of protected area is exactly equal to 95%. This critical ventilation rate is obtained by interpolation out of the values of the fraction of protected area obtained as dependents of the ventilation rate. For a few cases, this critical ventilation rate is given, for various values of n , in Tables 2.II a, b and c, in Annex 2.

4.8

Calculation example for paragraph 4.7

We are considering, in this example, the emission described in the calculation example 4.5.1. For the case in which the probit dose has a square dependency of the concentration, it is asked to calculate the fraction of protected area and the critical ventilation rate.

The dose reduction calculated for the case under consideration was found equal to 0.79 (see Paragraph 4.5.1). From Annex 1 we find, for a neutral atmosphere, that

$$\alpha = \frac{(0.905 + 1)}{(0.905 + 0.76)} = 1.14$$

With the help of (22) it then follows that

$$f_{pa} = 1 - (1 - 0.79)^{\frac{1.14}{2}} = 0.59$$

For the determination of the critical ventilation rate, the fraction of protected area must be calculated for some values of the ventilation rate, after which the critical ventilation rate can be determined by interpolation. We find, for a ventilation rate of 0.1 h^{-1} a fraction of protected area of 94.9%. Consequently, the critical ventilation rate, by approximation, is equal to 0.1 h^{-1} .

We will now consider the situation of paragraph 4.5.2, and ask the same questions for a reference probit dose of $1.0 (\text{g}/\text{m}^3)^2 \text{ s}$ and a ventilation delay of 1 hour.

From Tables 2.Ib and 2.IIb we find that, for a ventilation delay of 1 hour, the fraction of protected area and the critical ventilation rate are, respectively, 97% and 1.6 h^{-1} .

Protection and protective measures

The degree of protection indoors against contaminating substances is determined by:

1. the duration of the emission; the passage time of the cloud
2. the ventilation rate
3. the absorption of the gases by materials available in the house; the deposit of particles
4. the ventilation delay

The protection indoors can be improved by shortening the passage time of the cloud, by shortening the ventilation delay, by decreasing the ventilation rate or and by increasing the absorption. In case of an accidental release of gases, a better protection can practically only be achieved by either the decrease of the ventilation rate and/or the shortening of the ventilation delay.

The closure of doors and windows; the shutting-off of the ventilation mechanism and the eventual taping of window and door joints already provide an appreciable reduction of the ventilation rate. Tests in which the window and door joints were sealed with tape and the ventilation openings were plugged with newspapers have shown, as result, a ventilation rate 0.35 to 0.80 times lower than the one without the above measures [2]. Measurements in a furnished and lived-in apartment [5] exhibited a ventilation rate reduction down to 25% of the original value. Thus, with simple measures, such as taping seams and joints and plugging the ventilation openings, the ventilation rate can be reduced by 50%.

A better protection is also provided by staying in rooms at the lee side of the building, providing that the doors in-between are closed. These rooms obtain their "fresh" air from the other rooms, located more towards the wind side of the building. According to results of measurements published in [2] and [5], the average ratio of the ventilation rate on the lee side versus the ventilation rate on the front side is equal to 0.6.

Equations have been derived for temporary sources, with the help of which the inner concentration can be calculated, with dependency on the ventilation parameters of a room at a wind side and of a room at the lee side [4]. See, for this, Annex 3.

The shortening of the ventilation delay is more difficult to achieve. It is necessary, for this, to know when the cloud has passed. The latter is possible when the cloud is visible, as, for example, through the presence of smoke in it, or if the cloud originates from a liquefied or condensed gas. In the last case, mist formation gives the cloud a visible shape. This mist formation, in turn, is dependent on the humidity present in the air. However, the visible shape of the cloud will not, generally, correspond with the toxic limit value of the released gas. For a cloud which is not visible to the naked eye, its passage time can be estimated if the distance to the source (x) and the wind speed (u) are known. For a temporary source the arrival and departure times of the cloud can be approximated with $x/(2u)$ and, respectively, $t_1 + (3x)/(2u)$, whereby t_1 is the source duration; the times, in this, are measured from the beginning of the emission. According to (19), the arrival and departure times, for an instantaneous source, can be approximated by $x/(2u)$ and, respectively, $(3x)/(2u)$, after the emission.

Density effects

The concept “non-neutral” gases refers to gases the density of which differs substantially from the air density. A difference must be made between light gases and heavy gases. The formulas derived in the preceding paragraphs principally only apply to neutral gases in a non-obstructed flow field.

In case of an emission of a heavy gas, the height of the cloud decreases rapidly due to gravity, while, along with this, the width and the length of the cloud increase. During the slumping process, air is taken-in at the boundaries of the cloud, the so-called “entrainment” process. The concentration in the cloud, close to the source, strongly depends on the speed of the slumping process, which, in turn, is determined by the difference in densities, the initial height of the cloud and the entrainment. The entrainment itself, finally, also depends on the turbulent properties of the atmosphere. Due to transfer of impulse, the cloud, as a whole, moves in the average direction of the wind, with a drift velocity which is a part of the wind speed at the height of the top of the cloud. By a small wind speed a heavy gas cloud can spread against the wind. After a sufficiently long time the height of the cloud again increases, due to neutral turbulent dispersion.

Several models have been developed in order to describe the spreading of a heavy gas [30,31]. These models, however, do not offer any analytical solution for the concentration dependent on location and time. It is then also not yet possible (as has been done in Chapter 4) to develop simple equations for the concentration and the dose reduction, for staying indoors, during the passage of a heavy gas cloud. Applying equation (3) to a numerical heavy gas model, it is possible (numerically) to calculate the inner concentration.

A few quantitative remarks are well worth mentioning. When a heavy gas spreads, the cloud in the immediate vicinity of the source has a very limited height. Tests on a large scale have shown a visible cloud with a height of 1 to 5 m. [30]. However, when such a cloud reaches a building, its height can increase up to a factor of 2 versus the original height [28]. This is dependent on the width of the building and the incident angle of the cloud with respect to the building. Even though a heavy gas cloud, due to its small height, has a high concentration, its penetration into the building is smaller since part of the cloud will not reach highly located joints and openings. The air exchange, for a one-family house, for instance, takes place for about 40% at the transition from walls to roof.

Reference [15] publishes test results of tests of emissions of heavy gases in closed spaces. These results indicate that a heavy gas can form a layer on the floor if the vertical velocity gradient is small. The spreading of the gas, then, is fully due to molecular diffusion. References [13] and [27] report on tests of emission of a heavy gas (Freon-12) coming from an external source at a 3 m height and at a 45 m distance from a building: the measured concentrations were equal at ground level, and on the first floor, both on the wind side of the building. A heavy gas cloud which penetrates a house at a substantial distance from the source is already diluted through atmospheric turbulence, so that, in this case, a model for a neutral gas can be used for calculation purposes. Reference [29] gives, for this distance, the following relationship: $x > 8 \dot{V}_r / u$, in which \dot{V}_r is the emission debit (m^3/s) and u the average wind speed (m/s).

Light gases raise upwards already during the emission and will, consequently, often pass over the houses. Inside a house, if affected, layers of gas may form near the ceiling. Similarly to heavy gases, the mixing is dependent on the density deficit. Reference [15] reports measurements performed with methane, in which the presence of such layers had been demonstrated. These layers, generally, mix poorly with the air in the rest of the room. Due to this poor mixing, the concentration in these layers themselves is relatively high.

Accuracy of the models for determination of the indoors protection against toxic substances

The degree of protection against toxic substances of external origin, offered by staying indoors, depends on the ventilation of the toxic substance towards the inside and on the absorption on objects present in the house. The determination of this degree of protection is based on the concentration outside of the toxic substance. This outer concentration is calculated, for instance, with the help of dispersion models.

The accuracy of the determination of the degree of protection indoors against toxic substances depends on the accuracy of the dispersion models, the accuracy of the ventilation models and on the determination of the absorption on objects inside.

Relatively little is known about the accuracy of the dispersion models used. The concentration calculated with the help of a model generally represents an average value for the center of the plume, for a non-changing wind direction and a flat ground without obstacles. An approximate evaluation of the Gaussian plume model shows that this model properly predicts the average concentration in 67% of all cases, this with a factor of 2 ($1/2$). This degree of inaccuracy does not have any consequences for the concentration - and dose reductions indoors, but well for the absolute values of the concentration and of the dose.

In many instances we must deal with the emission of a heavy gas. The spreading of a heavy gas cannot yet be reproduced by a simple analytical relationship. For this reason, no formula has been presented in this study allowing us to evaluate the concentration indoors on the basis of data about the source. In case of an emission of a non-neutral gas it is more difficult to predict the value of the concentration outdoors, unless the building is located at a big distance from the source.

The accuracy of the ventilation models is determined by the simplified assumptions used in the analysis. It is assumed, in this analytical treatment, that the infiltrating gas distributes instantaneously and homogeneously over the entire space. It is also assumed, at the same time, that the ventilation rate and the absorption rate are both time independent. Measurements indicate that this is not always the case.

Of more importance is the accuracy with which the ventilation rate and the absorption rate can be determined. The majority of the values of these two rates found in literature show a spread of plus-minus 70% of the average value. A ventilation rate which is twice as high leads to a concentration reduction which can be half of the original value. An absorption rate which is twice as high results, in the end, in a 1.5 times higher reduction.

The calculations of the fraction of protected area are based on the Gaussian plume model. The accuracy of the fraction of protected area and of the critical ventilation rate is also dependent on the accuracy with which the dispersion parameters, related to the distance to the source, are evaluated. The influence of the ventilation rate on the fraction of protected area is fairly big and dependent on the value of this ventilation rate. The changes in the fraction of protected area, dependent on the value of this ventilation rate, can be obtained through logarithmic interpolation of the values given in Tables 2.I and Annex 2.

Summarizing, it can be established, based on the above mentioned facts, that the accuracy of the determination of the degree of protection indoors is mainly dependent on the accuracy of the dispersion models. In case the concentration outside is known, then the spread of the estimated ventilation rates and absorption rates is determinant in the accuracy of the determination of the concentration indoors. The formulas which have been derived only provide average values which do not take into account items such as: differences in ventilation per room, fluctuations of the wind and fluctuations of the outer concentration. Due to the lack of large-scale test results, no judgement can presently be passed regarding these items.

Conclusions

Results of a study of the existing references, related to the protection against toxic substances of external origin offered by staying indoors, have been presented in this report. The degree of this type of protection depends on ventilation and absorption inside a house or building. A situation is first considered whereby no extra protective measures have been foreseen. The commonly used ventilation rates are then indicated for different types of buildings. A difference must be made, in this respect, between houses and public buildings.

Departing from a known concentration of contaminating substances outdoors, the concentration indoors can be calculated with the help of a mathematical model. Two sorts of emissions are considered in the study: a temporary, more or less constant emission in the orders of magnitude varying from a few minutes to several hours, and an instantaneous emission of a neutral gas.

In the first case, besides the ventilation and absorption rates, the degree of protection is also dependent on the duration of the emission. By non-changing meteorological conditions, this duration is equal to the passage time of the cloud. The longer the duration, the higher will be the concentration indoors. In such a situation, it is recommended to reduce the ventilation rate inside by shutting-off the mechanical ventilation and, eventually, taping seams and joints. With these measures, the ventilation rate can be reduced by 50%.

In case of an instantaneous emission the passage time of the cloud is mostly short, and the maximum concentration indoors is then only a fraction of the maximum concentration outdoors. For large distances, the ratio of inner concentration versus outer concentration is higher, but the absolute value of the outer concentration is smaller. By an increase of the wind speed the inner concentration is also reduced.

The concentration outside is not constant for a temporary source and, therefore, due to fluctuations of the wind direction and of the wind speed, the house does not remain constantly in the center of the plume. If, due to a change of wind direction, the concentration outdoors is brought back to zero, then, for a certain time, the concentration indoors will still retain the value it had already reached. The protection, in such a case, can be improved by fully ventilating and/or leaving the building, as soon as the plume no longer can reach it. The time difference between the time mark of full ventilation and the time mark by which the toxic cloud no longer reaches the house – the ventilation delay – is important in the evaluation of the received dose which has been reached inside. The shortening of the ventilation delay leads to an appreciable dose reduction.

The effect of the dose reached, dependent on concentration and time of exposure, is expressed by a so-called "probit" equation, in which the dose is proportional to the concentration to a power n . For a higher value of n the effect of the optimum dose is increasing. The dose reduction is larger for higher values of n (which is valid for both outer or inner optimum doses), even though the effect of the received dose indoors is higher than for smaller values of n .

It should be mentioned that tests have shown that the fact of staying in rooms located at the lee side of a building offers a better protection than in rooms at the wind side. Rooms at the lee side have a ventilation rate equal, on the average, to 0.6 times the ventilation rate at the wind side.

List of symbols

a, a', a_1	Constant in the dispersion parameter in the y-direction	$[m^{1-b}]$
b, b_1	Constant in the dispersion parameter in the y-direction	$[-]$
c, c', c_1	Constant in the dispersion parameter in the z-direction	$[m^{1-d}]$
d, d', d_1	Constant in the dispersion parameter in the z-direction	$[-]$
e_1	Constant in the dispersion parameter in the x-direction	$[-]$
f_{pa}	Fraction of protected area	$[-]$
h	Source height	$[m]$
\dot{m}	Source strength by a continuous emission	$[kg/s]$
m	Source strength by an instantaneous emission	$[kg]$
\dot{m}_{ads}	Absorption loss flow	$[kg/s]$
n	Power in the dose concentration relationship	$[-]$
\dot{n}_a	Absorption frequency	$[s^{-1}]$
\dot{n}_v	Ventilation frequency	$[s^{-1}]$
\dot{n}_{va}	Ventilation frequency plus absorption frequency	$[s^{-1}]$
t	Time	$[s]$
t^*	Time mark by which a given concentration ratio is reached	$[s]$
t_1	Passage time of the cloud	$[s]$
t_2	Time mark of delayed ventilation	$[s]$
t_m	Time mark by which the inner concentration is maximum	$[s]$
u	Average wind speed	$[m/s]$
v_{ads}	Absorption speed	$[m/s]$
x	Distance to the source measured along the average wind direction	$[m]$
x^*	Distance at which the lateral distance to a given dose becomes equal to zero	$[m]$
y	Horizontal coordinate perpendicular to the average wind direction	$[m]$
z	Vertical coordinate	$[m]$
A_{ads}	Absorbing surface	$[m^2]$
A_i	Area in which the dose reached indoors exceeds a given value	$[m^2]$
A_o	Area in which the dose reached outdoors exceeds a given value	$[m^2]$
C_i	Concentration indoors	$[kg/m^3]$
C_i/C_o	Ratio of inner to outer concentrations	$[-]$
C_o	Concentration outdoors	$[kg/m^3]$
CR	Concentration reduction	$[-]$
D_i	Time integration over the inner concentration (dose)	$[(kg/m^3)ns]$
D_o	Time integration over the outer concentration (dose)	$[(kg/m^3)ns]$
DR	Dose reduction	$[-]$
D_{ref}	Reference dose	$[(kg/m^3)ns]$
K	Auxiliary variable $(\dot{n}_{va} * \sigma_x^2 + u * x)/(u * \sigma_x)$	$[-]$
\dot{V}	Air flow	$[m^3/s]$
V	Contents (volume) of a room	$[m^3]$
\dot{V}_r	Emission debit	$[m^3/s]$
α	$(b + 1)/(b + d')$	$[-]$
B	$(b_1 + 1)/(b_1 + d_1 + 1 - 1/n)$	$[-]$
σ_x	Standard deviation of the concentration distribution in the x-direction	$[m]$
σ_y	Standard deviation of the concentration distribution in the y-direction	$[m]$
σ_z	Standard deviation of the concentration distribution in the z-direction	$[m]$

References

- [1] Methoden voor het berekenen van de fysische effecten van het incidenteel vrijkomen van gevaarlijke stoffen (gassen en vloeistoffen) - DGA (1979)
- [2] M. van Zelm
De penetratie van gaswolken in huizen en de bescherming van personen in huizen - Chem.Lab./TNO - Rapport 1976-2 (1976).
- [3] M. van Zelm
De penetratie van gaswolken in huizen - Chem.Lab./TNO - Rapport 1974-14 (1974)
- [4] A.C. van den Berg
De gevolgen voor de omwonenden van een calamiteit waarbij giftige stoffen vrijkomen en de bescherming die geboden wordt door een verblijf binnenshuis
PML/TNO Rapport 1978-11 (1978)
- [5] H.C. v.d. Weide
Voortzetting onderzoek van de penetratie van gaswolken in huizen en bescherming van personen in huizen.
PML/TNO Rapport PML 1978-38 (1978)
- [6] G. Huber
Minimale Lüftungszahlen in Wohn - und Arbeitsräumen.
Diss. ETH Nr. 7008 - Zürich (1982)
- [7] J.B. Dick
The fundamentals of natural ventilation of houses.
J. Inst. Heating and Ventilation Engineers 18, 123 (1950)
- [8] H.Ph.L. den Ouden, W.F. de Gids en J.A. Ton
Ventilatie van gebouwen - IG/TNO Afd. Binnenklimaat - Rapport C 348 Delft (1975)
- [9] W.F. de Gids, J.A. Ton en L.M. van Schijndel
Natural Ventilation of Dwellings. Investigation of the relationship between the ventilation of a flat and the meteorological conditions - IMG/TNO, Publ. 620 (1977)
- [10] W.F. de Gids, J.C. Phaff en B. Knoll
New ways to save energy - Proceed. of the Intern. Seminar, Brussels 23-25 Oct. 1979, pp. 1100-1106.
D. Reidel Publ. Comp., Dordrecht (1980), ISBN 90-277-1078-3.
- [11] J. Wegner
Untersuchungen des natürlichen Luftwechsel in ausgeführten Wohnungen, die mit sehr fugendichten Fenstern ausgestattet sind. Gesundheits-Ingenieur, Jg. 104, Heft 1, pp. 1-56 (1983).

- [12] H. Roetscher
Lueftungs- und Klimatechnik - Grundlagen
München, Wien: Hanser, 1982, ISBN 3-446-13498-0.
- [13] W. Richter
Lueftung im Wohnungsbau.
VEB - Verlag fuer Bauweisen, Berlin (DDR) (1983)
- [14] D.W. Dockery en H.D. Spengler
Indoor-outdoor relationship of respirable sulfates and particles.
Atm. Environm., Vol. 15, pp. 335-343 (1981).
- [15] S.J. Leach en D.P. Bloomfield
Ventilation in relation to toxic and flammable gases in buildings.
Building Science, Vol 8, pp. 289-310 (1973).
- [16] H. de Graaf en K. Biersteker
Luchtverontreiniging in Rotterdam, een vergelijkend onderzoek van luchtverontreiniging binnen
een buiten de woningen.
Ned. Tijdschr. voor Geneesk., 109.1.17, pp. 793-799 (1965).
- [17] I. Andersen
Relationship between Outdoor and Indoor Air Pollution - Technical Notes - Atm. Environm.,
Vol. 6, pp. 275-278 (1972).
- [18] F.H. Shair en K.L. Heitner
Theoretical Model for Relating Indoor Pollutant Concentrations to Those Outside - Environm.
Science & Technology, Vol. 8, Nr. 5, pp. 444-451 (1974).
- [19] H.W. Georgh
Über das Eindringen von Luftverunreinigung in Gebäude - Hygiene-Umwelt, Jg. 44, Heft 3, pp.
327-329 (1973).
- [20] J.D. Spengler, B.G. Ferris en D.W. Dockery
Sulfur Dioxide and Nitrogen Dioxide Levels Inside and Outside Houses and the Implications on
Health Effects Research
Environm. Science & Technology, Vol. 13, Nr. 10, pp. 1276-1280 (1979)
- [21] J. Alzona, B.L. Cohen, H. Rudolph, H.N. Jow en J.O. Frohlinger
Indoor-outdoor relationship for airborne particulate matter of outdoor origin - Atm. Environm.,
Vol. 13, pp. 55-60 (1979).
- [22] A.F. Cohen en B.L. Cohen
Protection from being indoors against inhalation of suspended particulate matter of outdoor
origin - Atm. Environm., Vol. 14, pp. 183-184 (1980).
- [23] J.F. Yocom
Indoor-Outdoor Airquality Relationship - A critical review.
JAPCA, Vol. 32, Nr. 5, pp. 500-520 (1982).
- [24] Discussion Papers (of above mentioned article of J.F. Yocom)
JAPCA, Vol. 32, Nr. 9, pp. 904-914 (1982).

- [25] W.J. Fisk
Building Ventilation and Indoor Air Quality Program University of California, LBL. - Proc. 3d Intern. Conf. Indoor Air Quality and Climate, Swedish Council for Building Research, Stockholm (1984).
- [26] G.W. Traynor, J.R. Girman, M.G. Apte, J.F. Dillworth, P.D. White
Indoor Air Pollution Due to Emissions from Unvented Gas-Fired Space Heaters.
JAPCA, Vol. 35, Nr. 3, pp. 231-237 (1985).
- [27] G. Purdy, P.C. Davies
Toxic Gas Incidents - Some Important Considerations for Emergency Planning.
Loss Prevention Bulletin, Nr. 062, The Institute of Chemical Engineering, Rugby, U.K. (1985).
- [28] J.W. Rottman, J.E. Simpson, J.C.R. Hunt, R.E. Britter
Unsteady Gravity Current Flows over Obstacles: Some Observations and Analysis Related to the Phase II Trials.
Journal of Hazardous Materials, Vol. 11, pp. 325-340 (1985).
- [29] P.A. Krogstad, R.M. Pettersen
Windtunnel Modelling of a Release of a Heavy Gas near a Building.
Atmospheric Environment, Vol. 20, Nr. 5, pp. 867-878 (1986).
- [30] J. McQuaid Editor
Heavy Gas Dispersion Trials at Thorney Island - 2.
proc. Symp. Univ. of Sheffield, UK, Sept. 1986.
Journal of Hazardous Materials, Vol. 16, Special Issue (1987).
- [31] D.L. Ermak, H.C. Rodean, R. Lange, S.T. Chan
A Survey of Denser-than-Air Atmospheric Dispersion Models.
Lawrence Livermore National Laboratory, UCRL-21024 (1988).

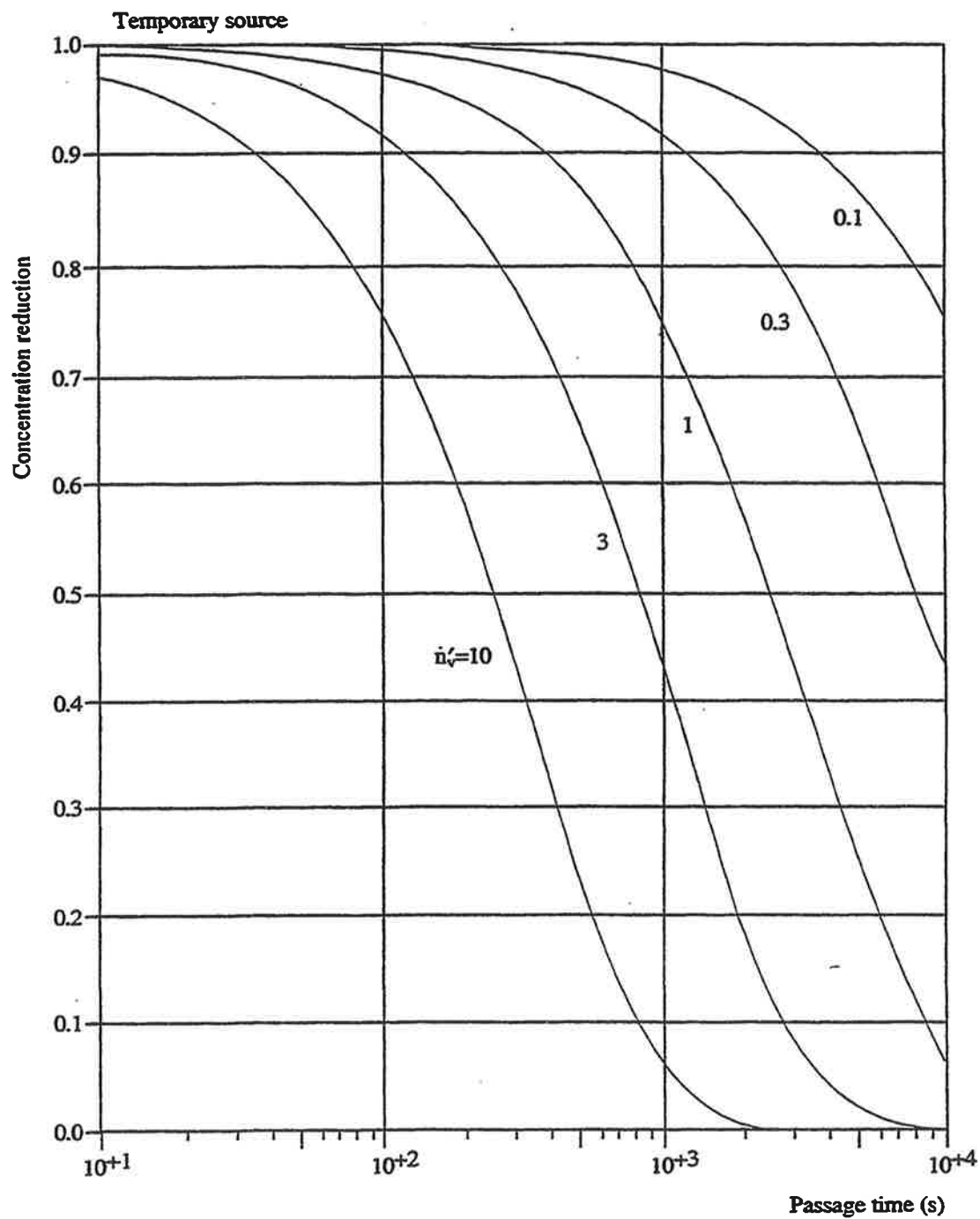


Diagram 1 Concentration reduction dependent on the passage time for a temporary constant source; parameter: the ventilation rate (\dot{n}_v') in h^{-1} ; no absorption.

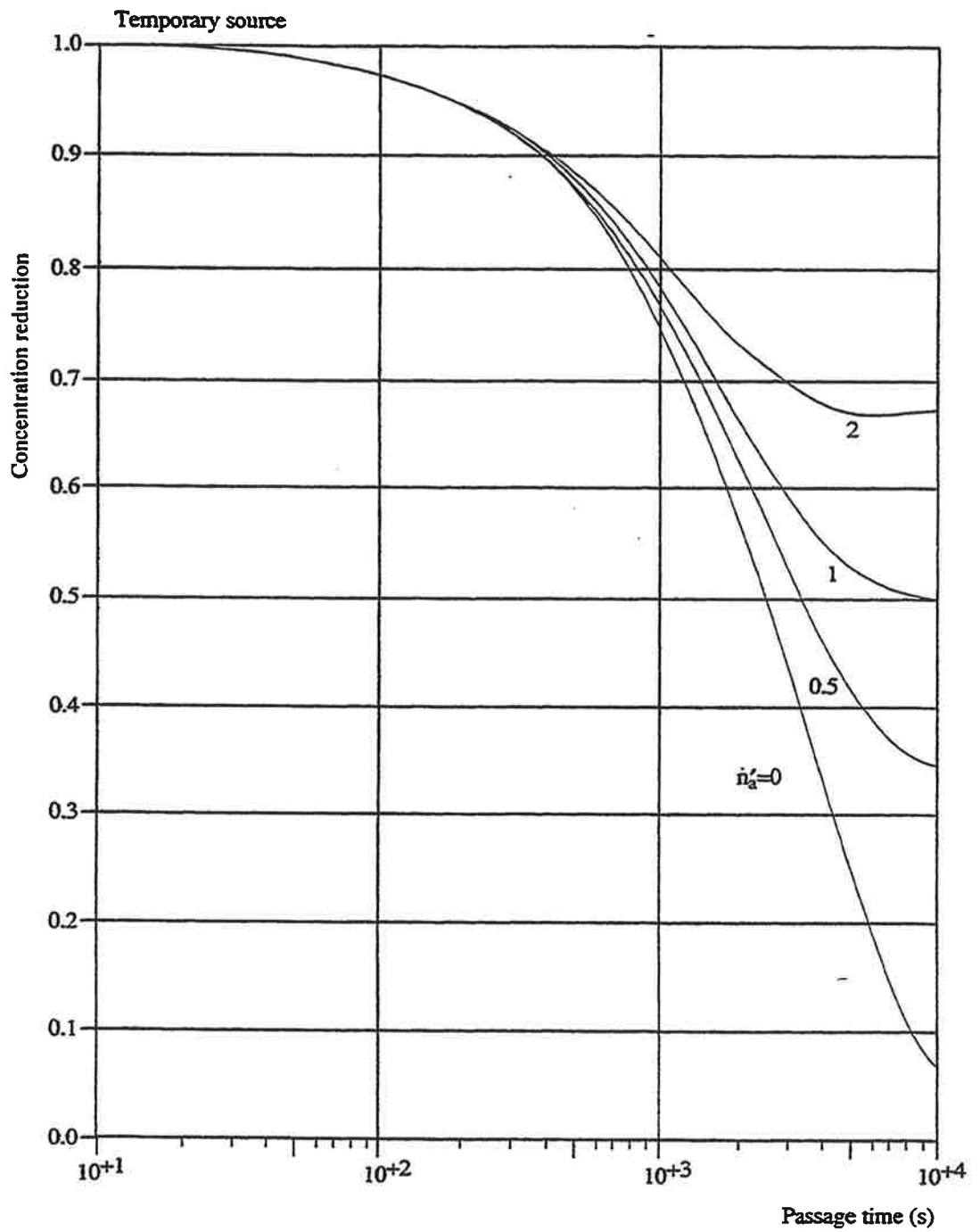


Diagram 2 Concentration reduction dependent on the passage time for a temporary constant source; parameter: the absorption rate (\dot{n}_a') in h^{-1} ; the ventilation rate is $1 h^{-1}$.

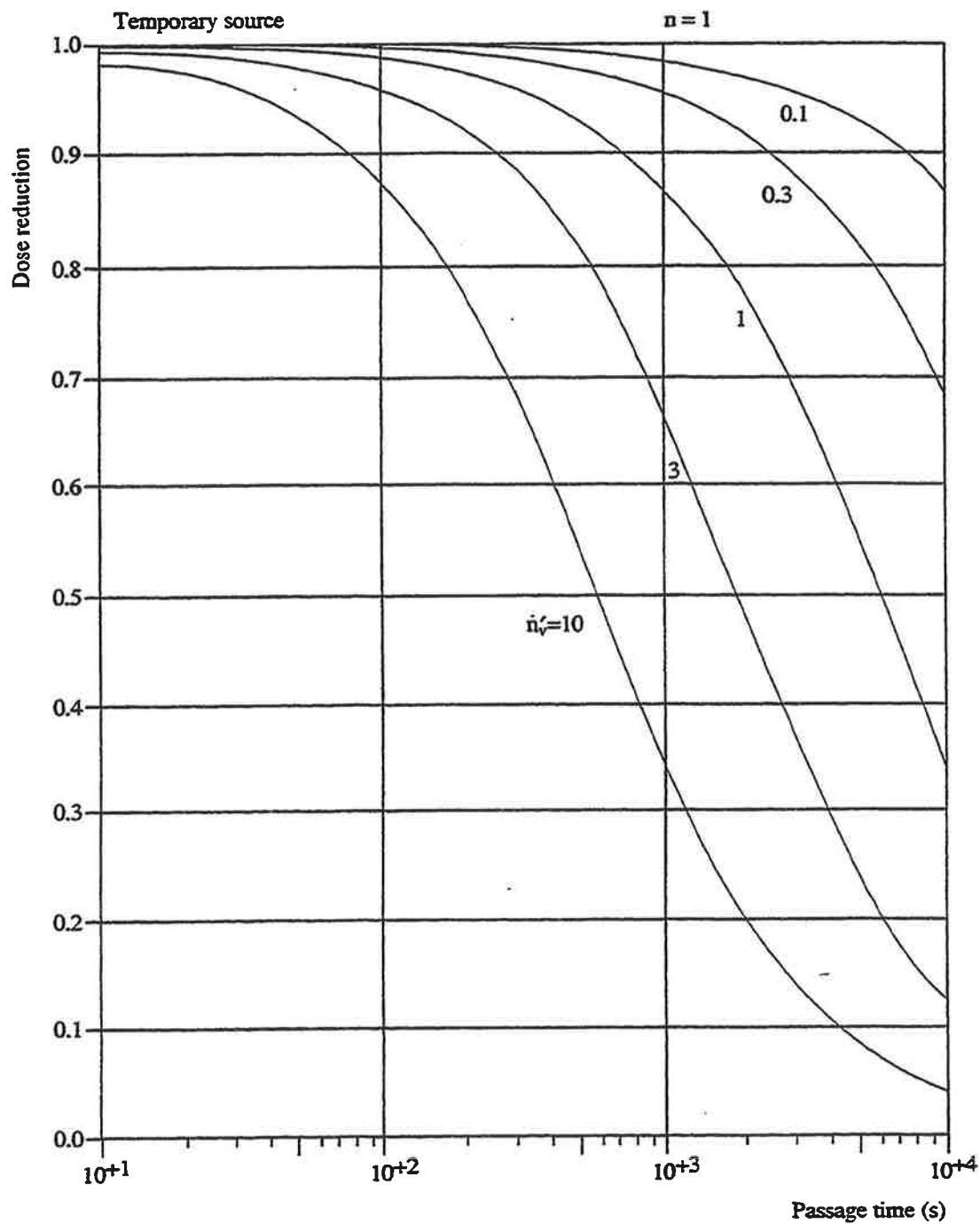


Diagram 3a Dose reduction dependent on the passage time for a temporary constant source for $n=1$; parameter: the ventilation rate (\dot{n}_v') in h^{-1} ; no absorption and no ventilation delay.

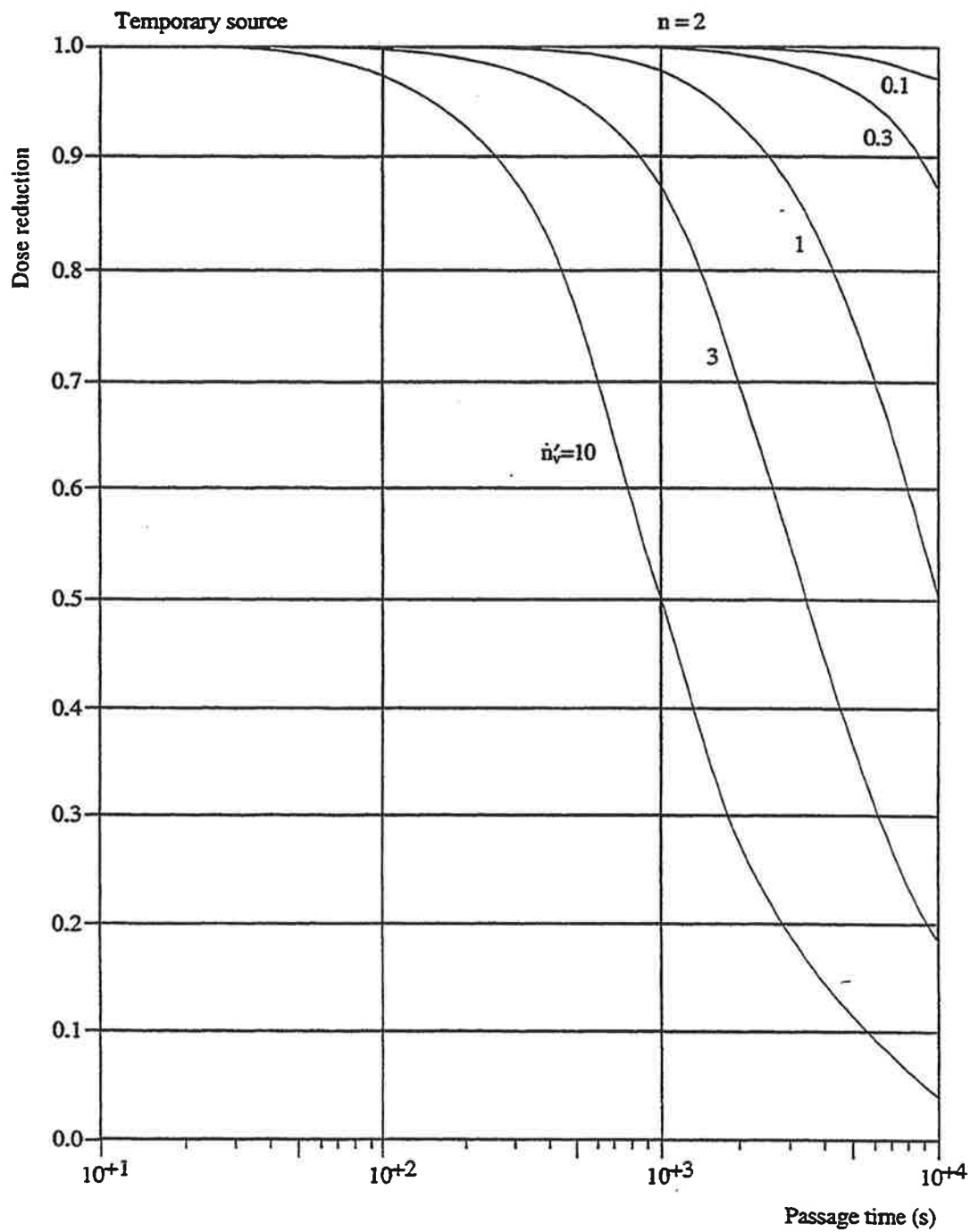


Diagram 3b Dose reduction dependent on the passage time for a temporary constant source for $n=2$; parameter: the ventilation rate (\dot{n}_v') in h^{-1} ; no absorption and no ventilation delay.

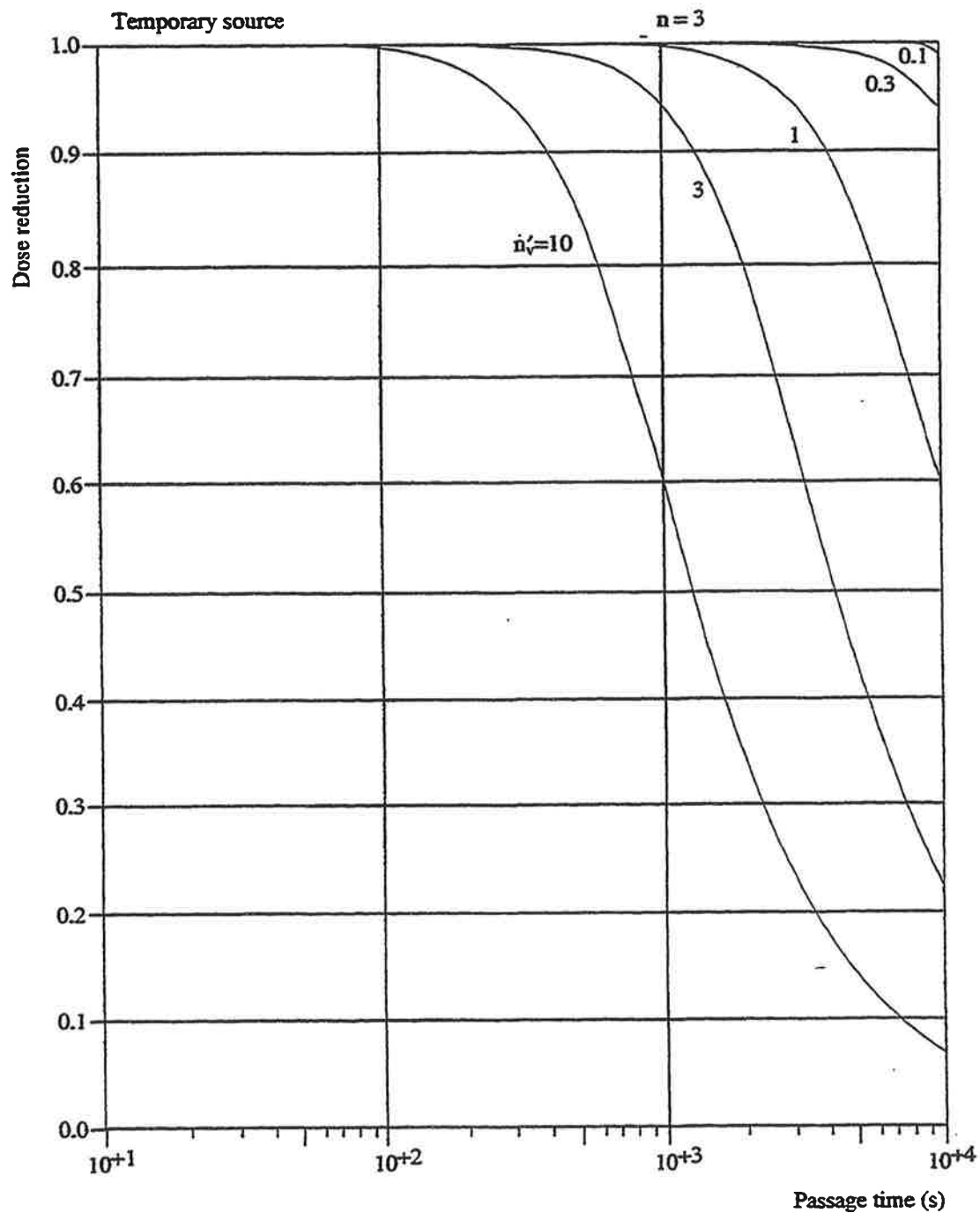


Diagram 3c Dose reduction dependent on the passage time for a temporary constant source for $n=3$; parameter: the ventilation rate (\dot{n}_v') in k^{-1} ; no absorption and no ventilation delay.

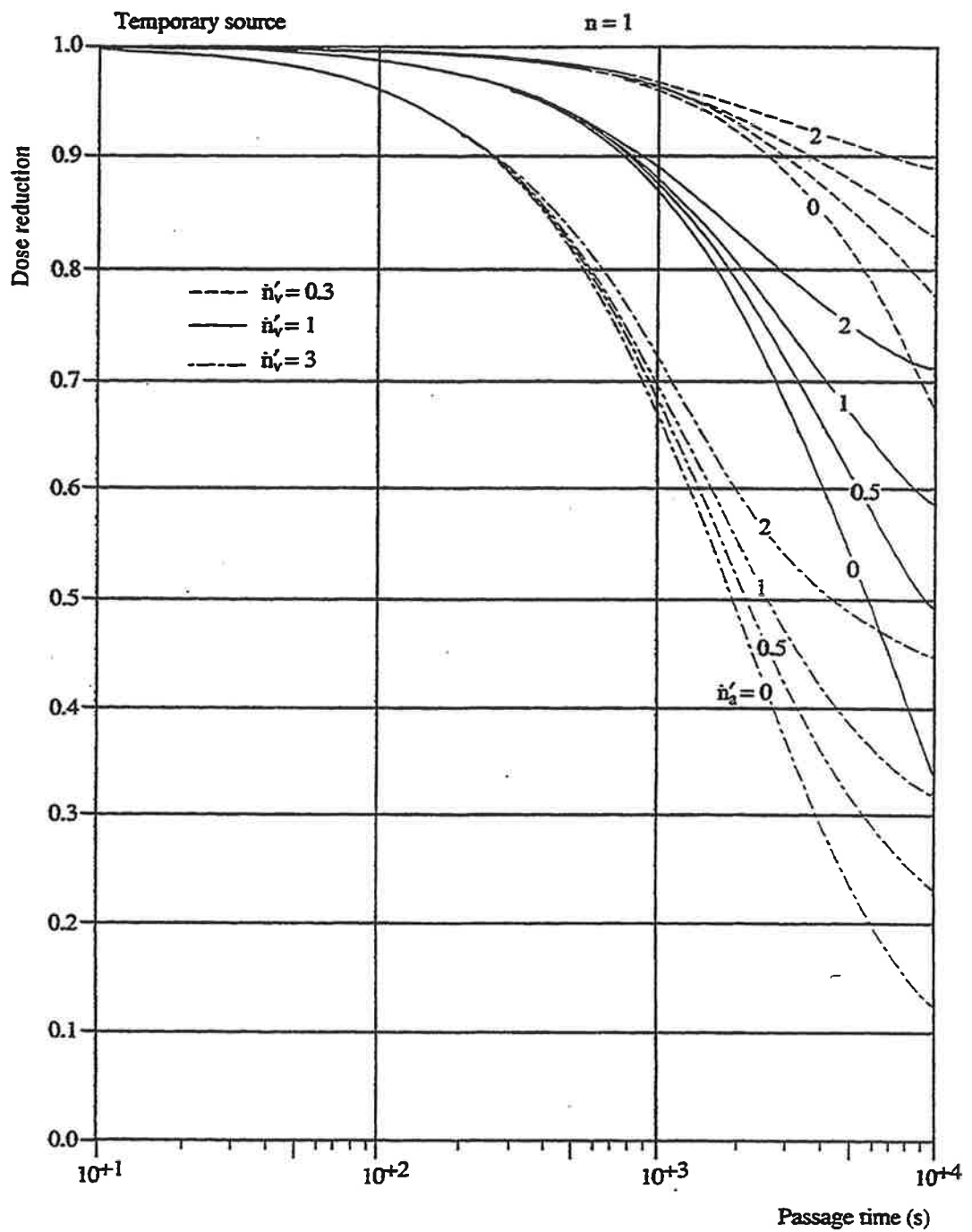


Diagram 4a Dose reduction dependent on the passage time for a temporary constant source for $n=1$; parameters: the ventilation rate (\dot{n}'_v) and the absorption rate (\dot{n}'_a) both in h^{-1} ; no ventilation delay.

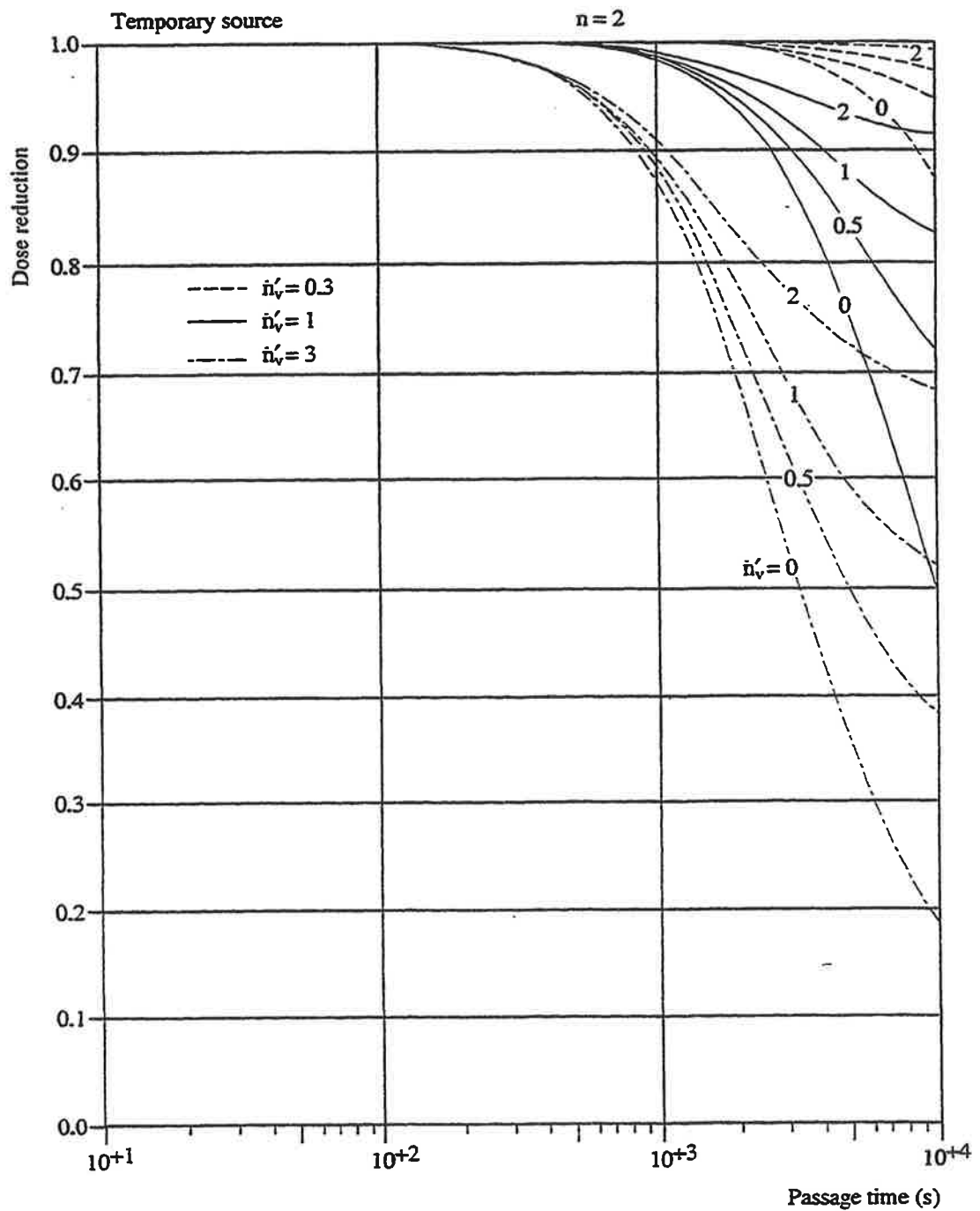


Diagram 4b Dose reduction dependent on the passage time for a temporary constant source for $n=2$: parameters: the ventilation rate (n_v') and the absorption rate (n_a') both in h^{-1} ; no ventilation delay.

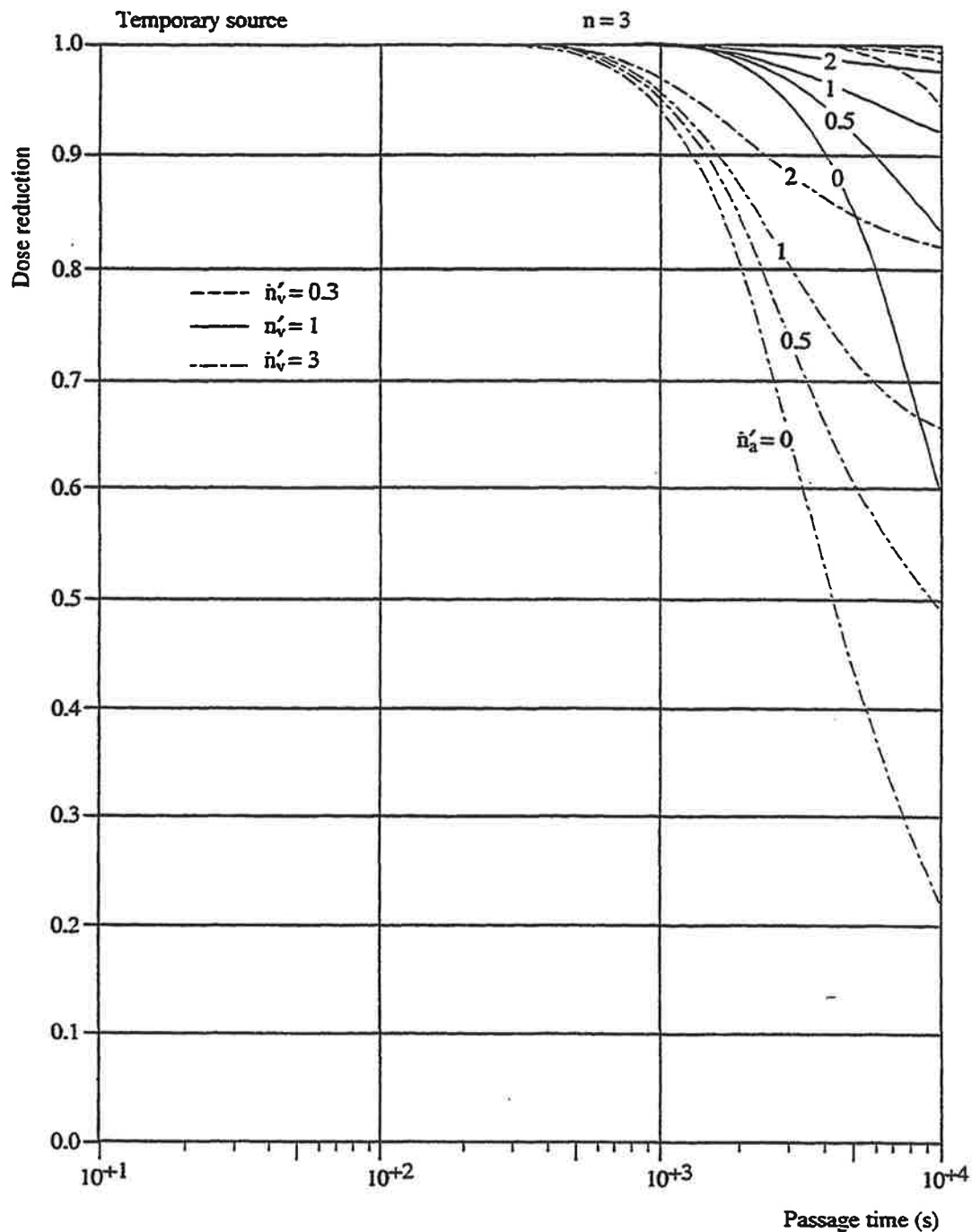


Diagram 4c Dose reduction dependent on the passage time for a temporary constant source for $n=3$; parameters: the ventilation rate (\dot{n}'_v) and the absorption rate (\dot{n}'_a) both in h^{-1} ; no ventilation delay.

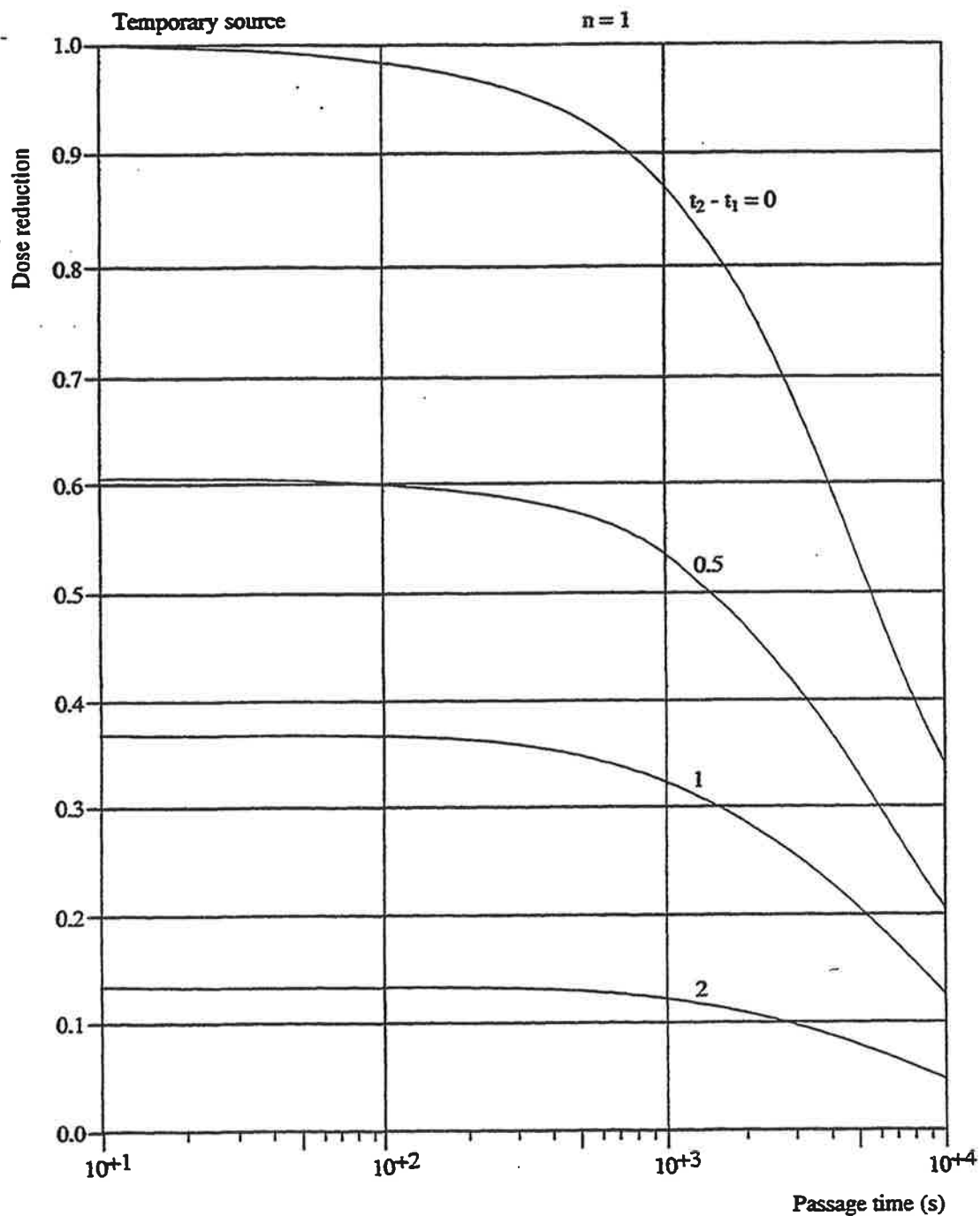


Diagram 5a Dose reduction dependent on the passage time for a temporary constant source for $n=1$; parameter: the ventilation delay (t_2-t_1) in h; the ventilation rate is 1 h^{-1} and there is no absorption.

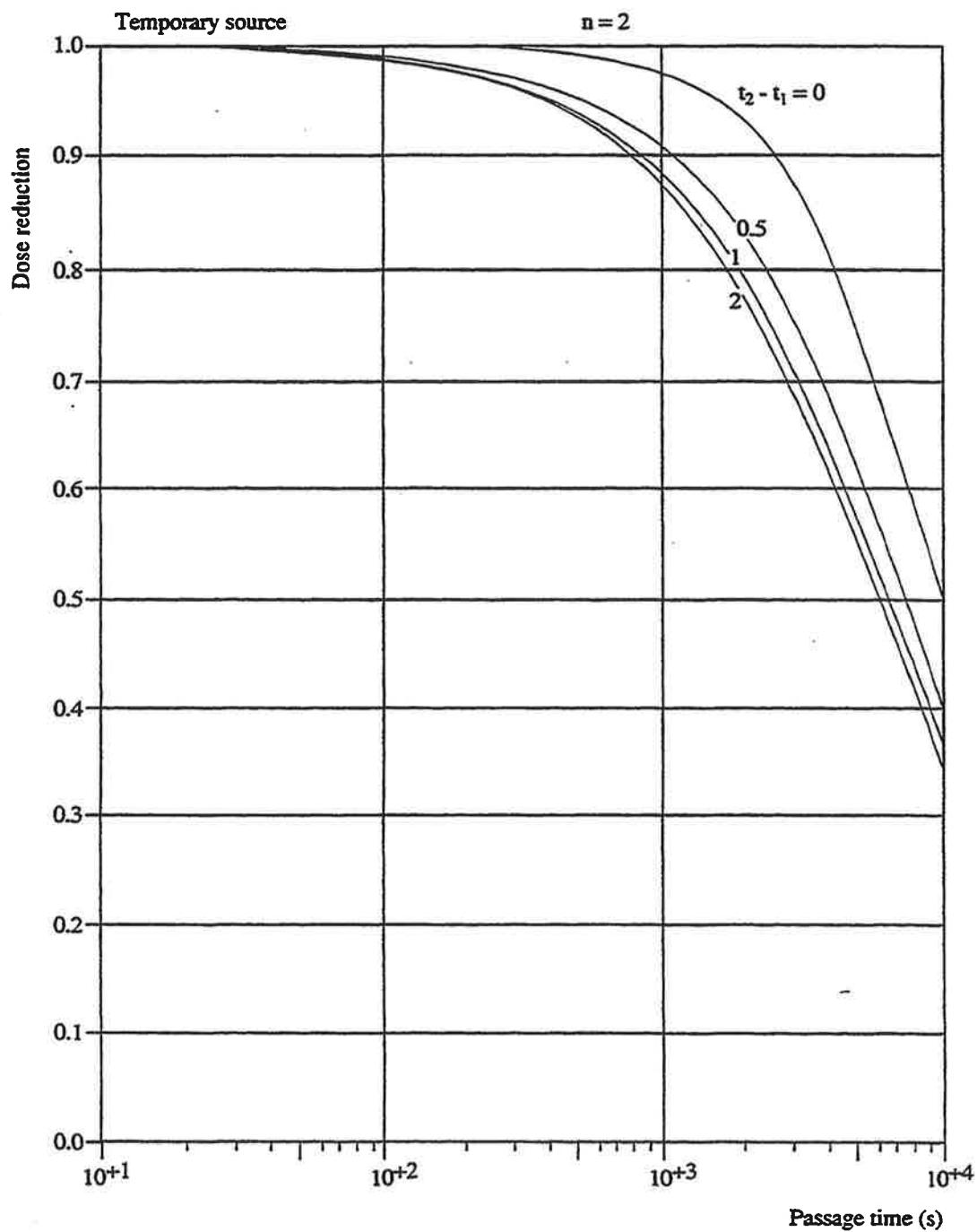


Diagram 5b Dose reduction dependent on the passage time for a temporary constant source for $n=2$; parameter: the ventilation delay ($t_2 - t_1$) in h; the ventilation rate is 1 h^{-1} and there is no absorption.

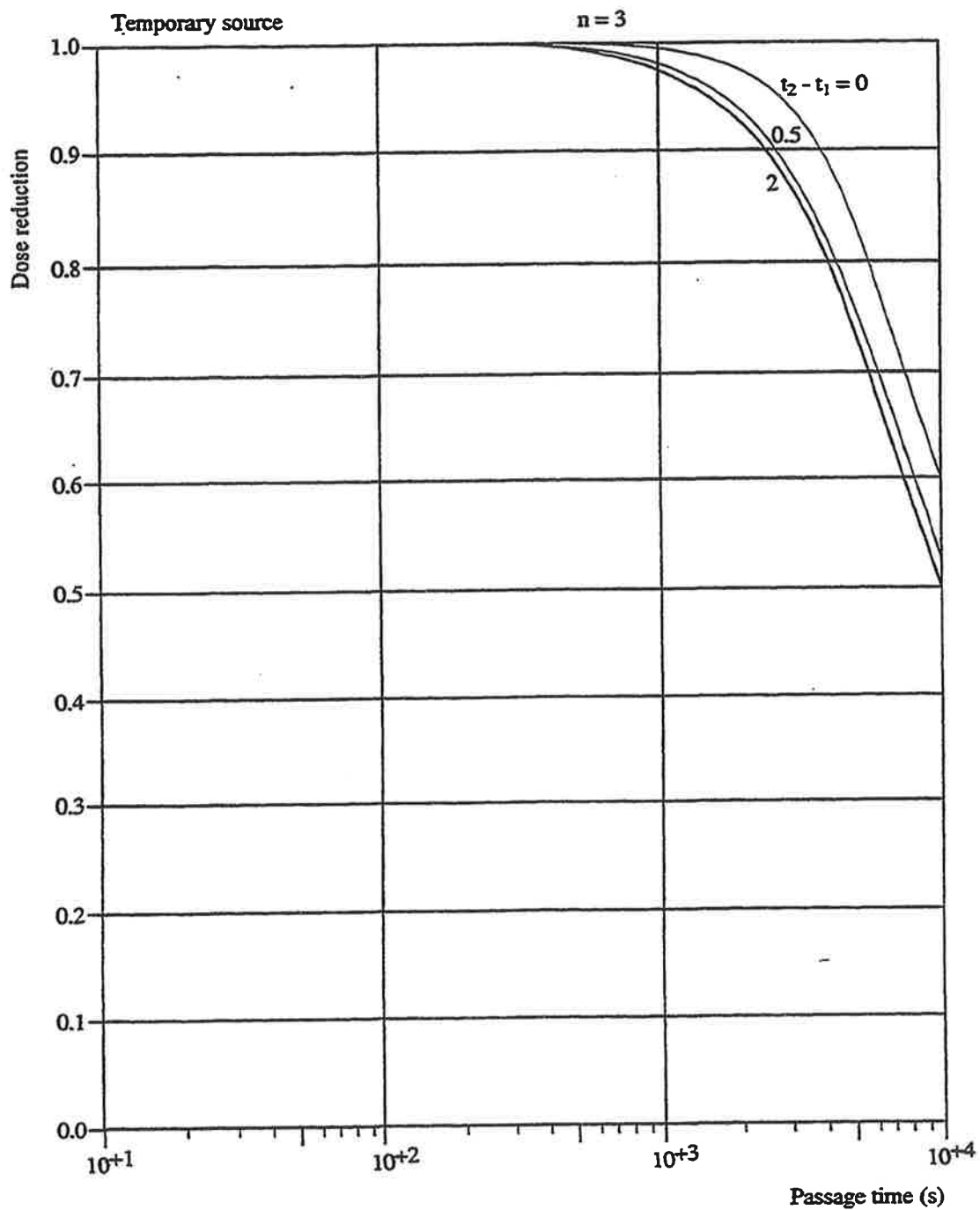


Diagram 5c Dose reduction dependent on the passage time for a temporary constant source for $n=3$; parameter: the ventilation delay (t_2-t_1) in h; the ventilation rate is 1 h^{-1} and there is no absorption.

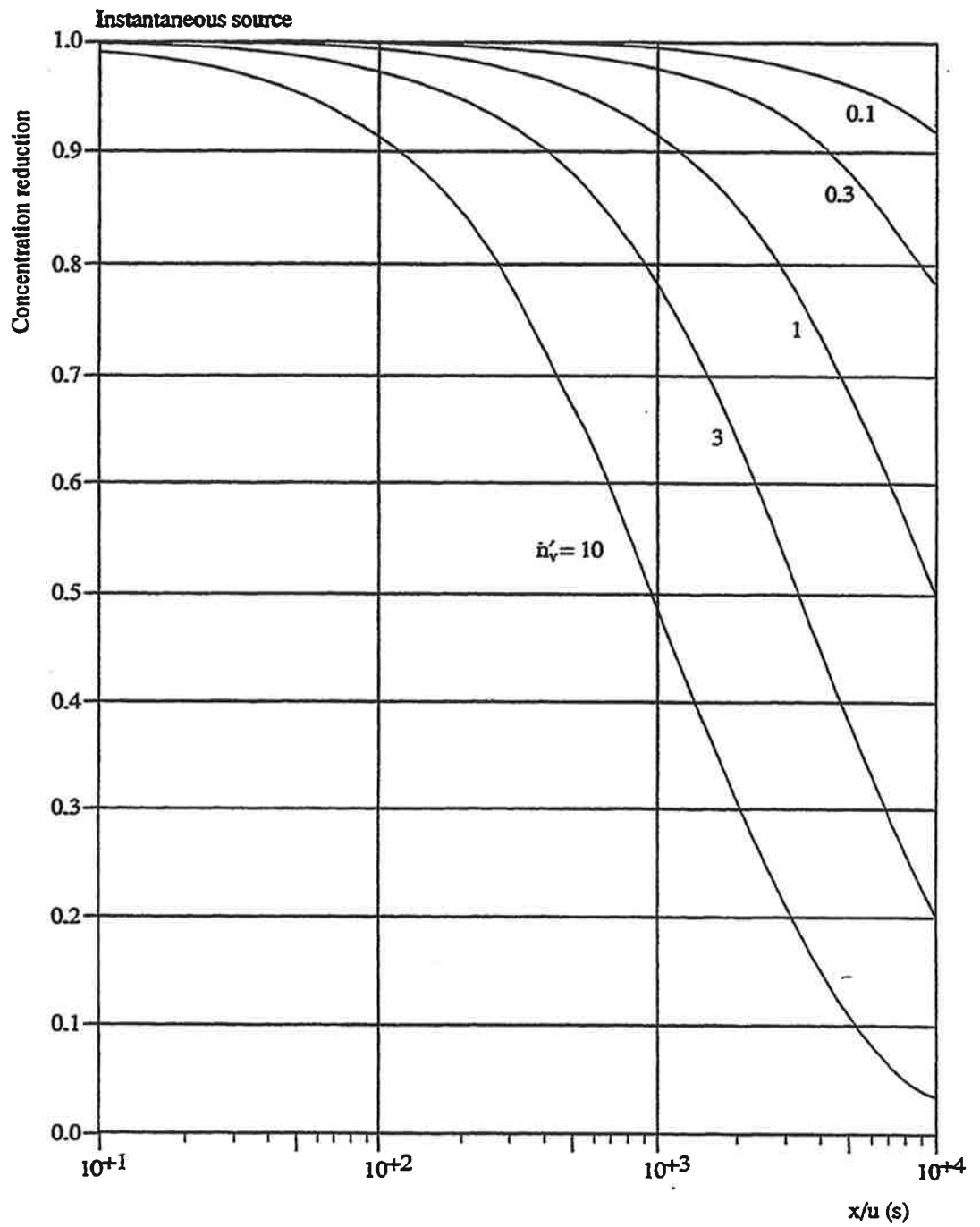


Diagram 6 Concentration reduction dependent on the x/u of an instantaneous source; parameter: the ventilation rate (\dot{n}_v') in h^{-1} ; no absorption.

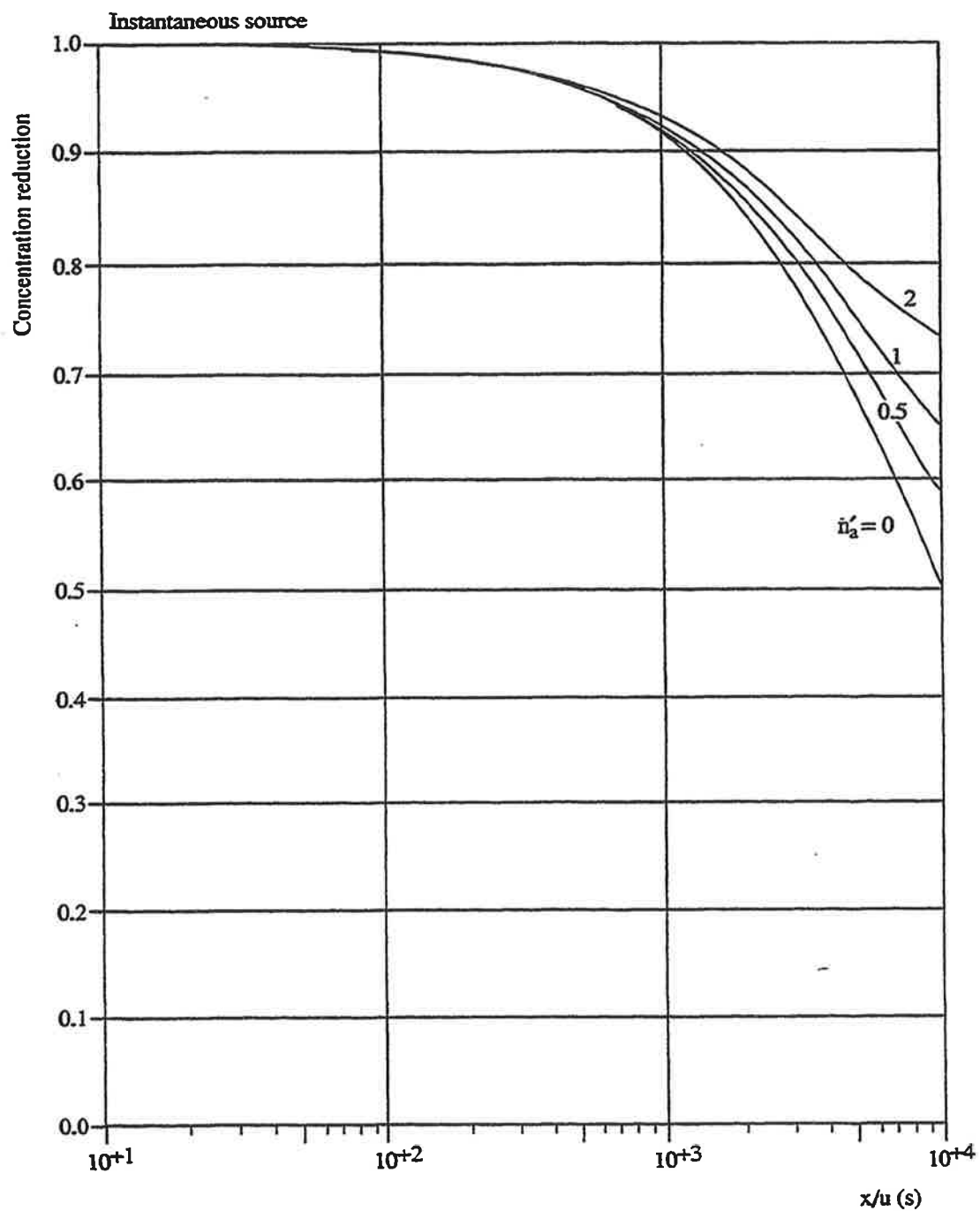


Diagram 7 Concentration reduction dependent on the x/u of an instantaneous source; parameter: the absorption rate (\dot{n}'_a) in h^{-1} ; the ventilation rate is $1 h^{-1}$.

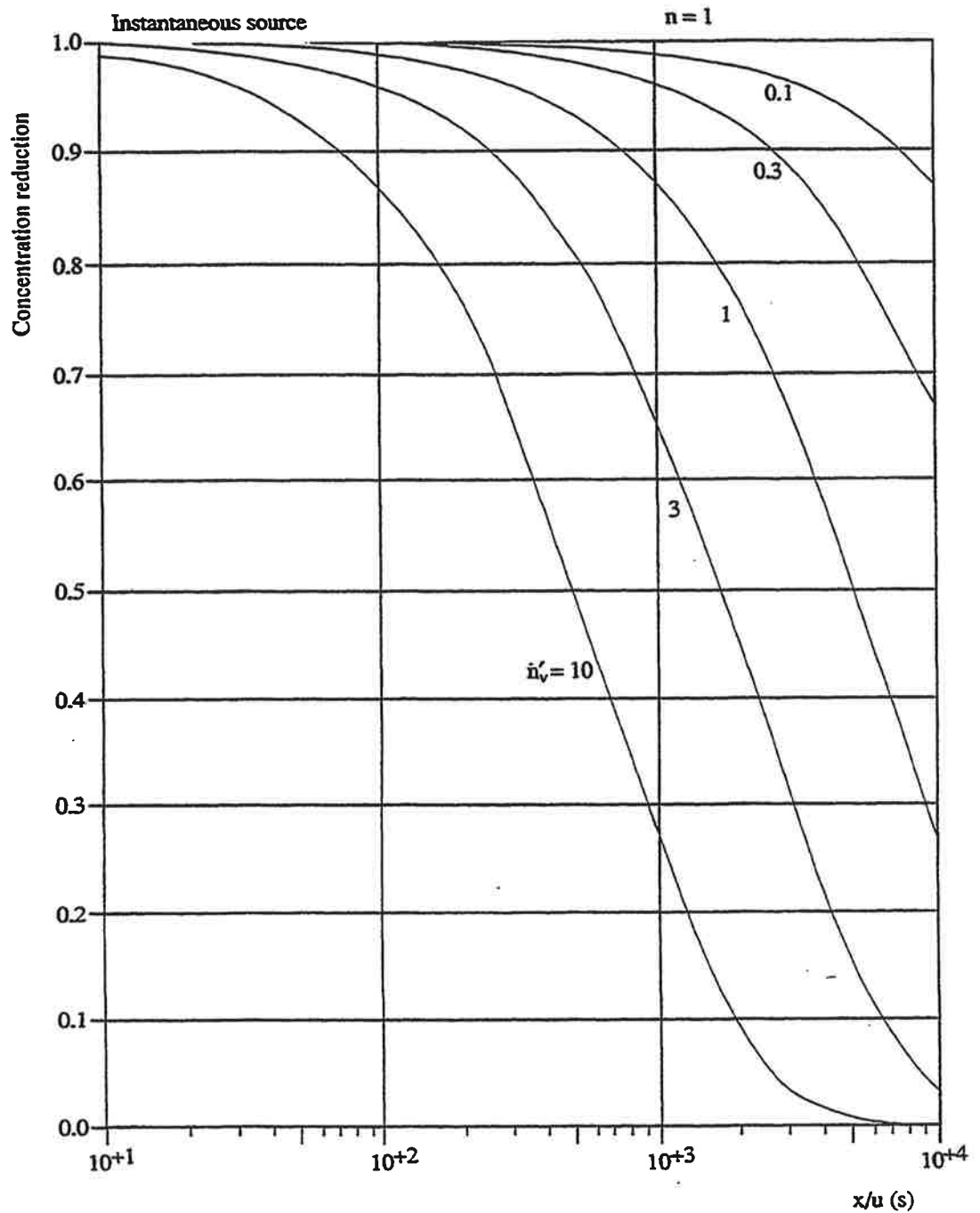


Diagram 8a Dose reduction dependent on the x/u of an instantaneous point source for $n=1$; parameter: the ventilation rate (\dot{n}_v') in h^{-1} ; there is no absorption and no ventilation delay.

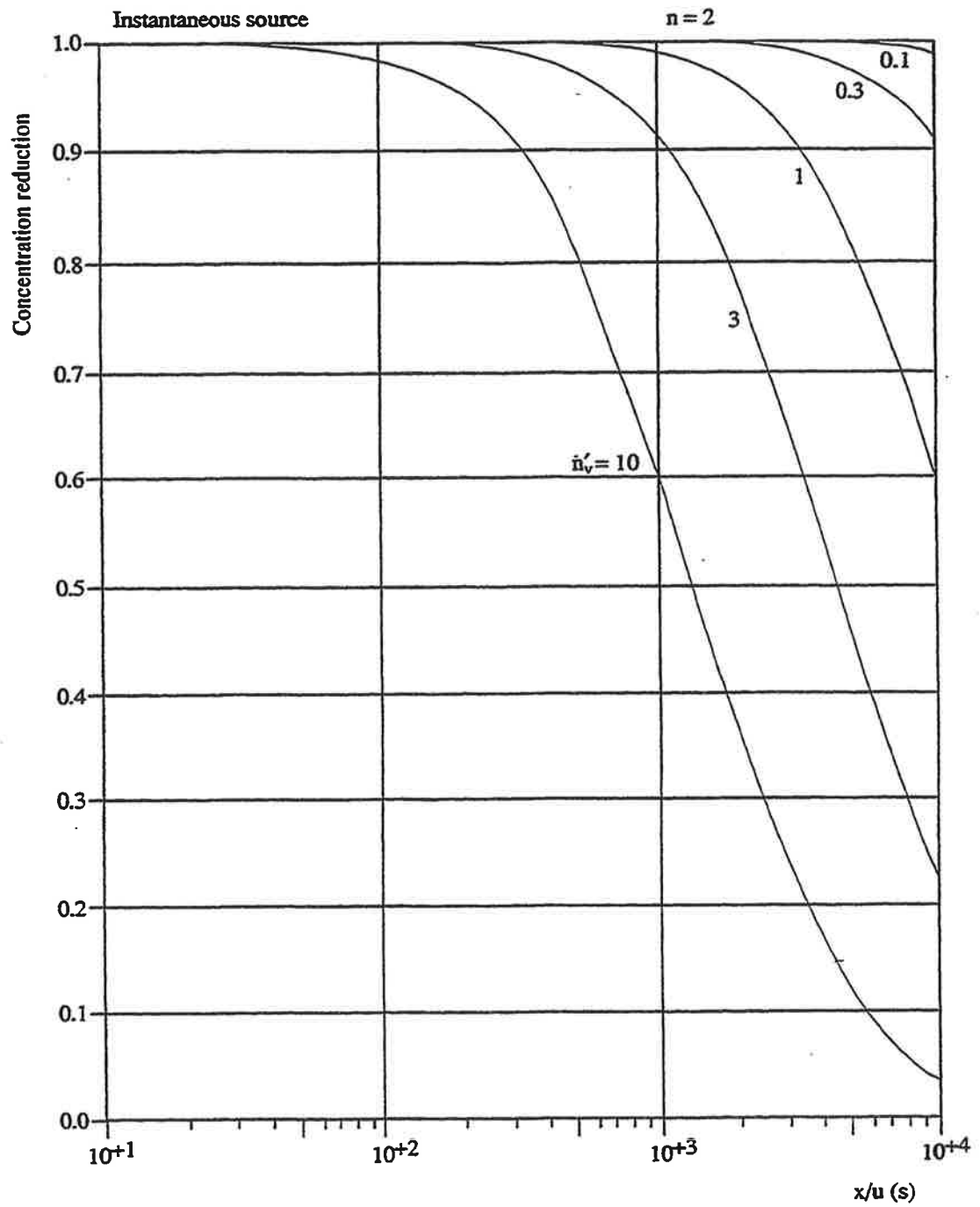


Diagram 8b Dose reduction dependent on the x/u of an instantaneous point source for $n=2$; parameter: the ventilation rate (\dot{n}_v') in h^{-1} ; there is no absorption and no ventilation delay.

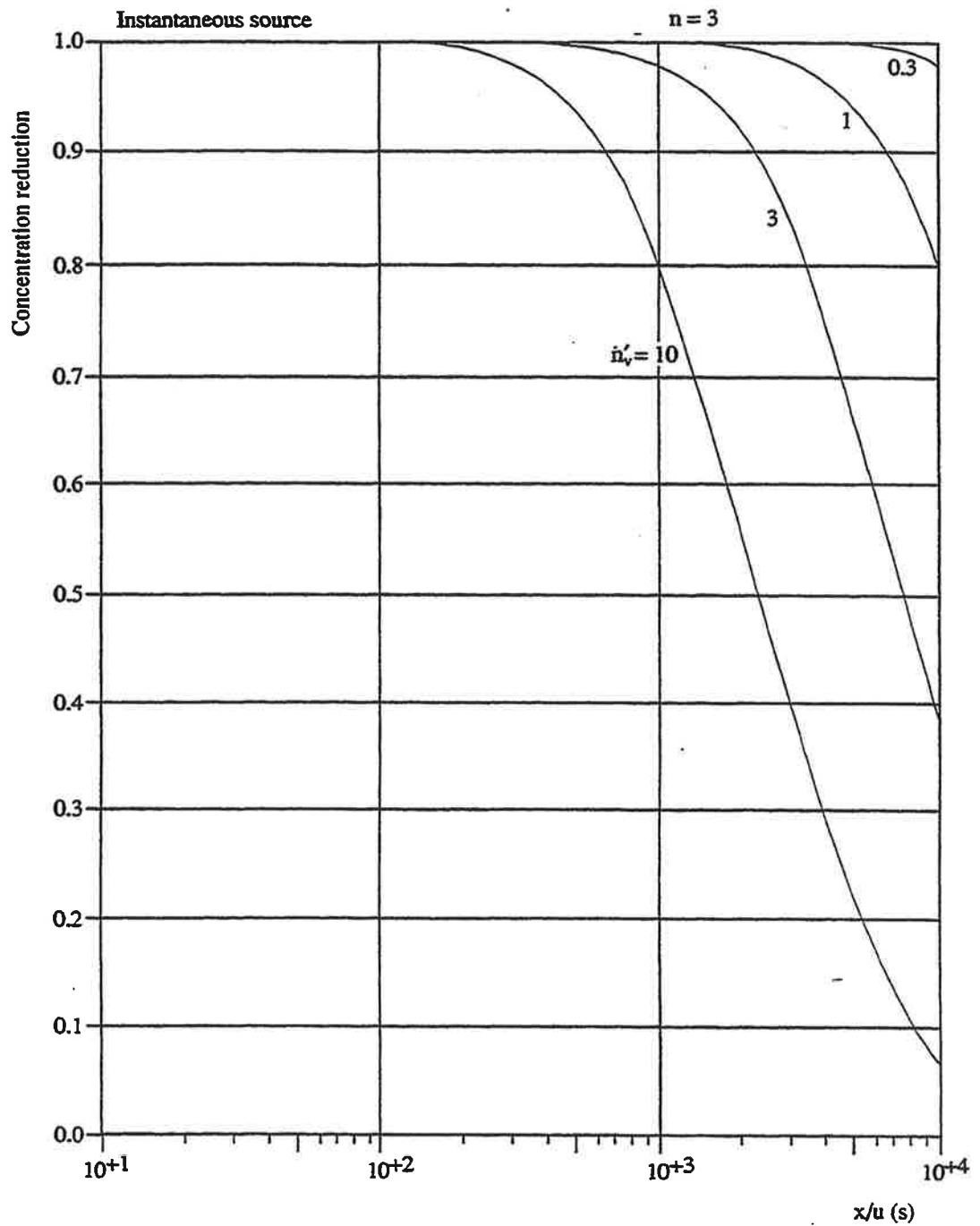


Diagram 8c Dose reduction dependent on the x/u of an instantaneous point source for $n=3$; parameter: the ventilation rate (n_v') in h^{-1} ; there is no absorption and no ventilation delay.

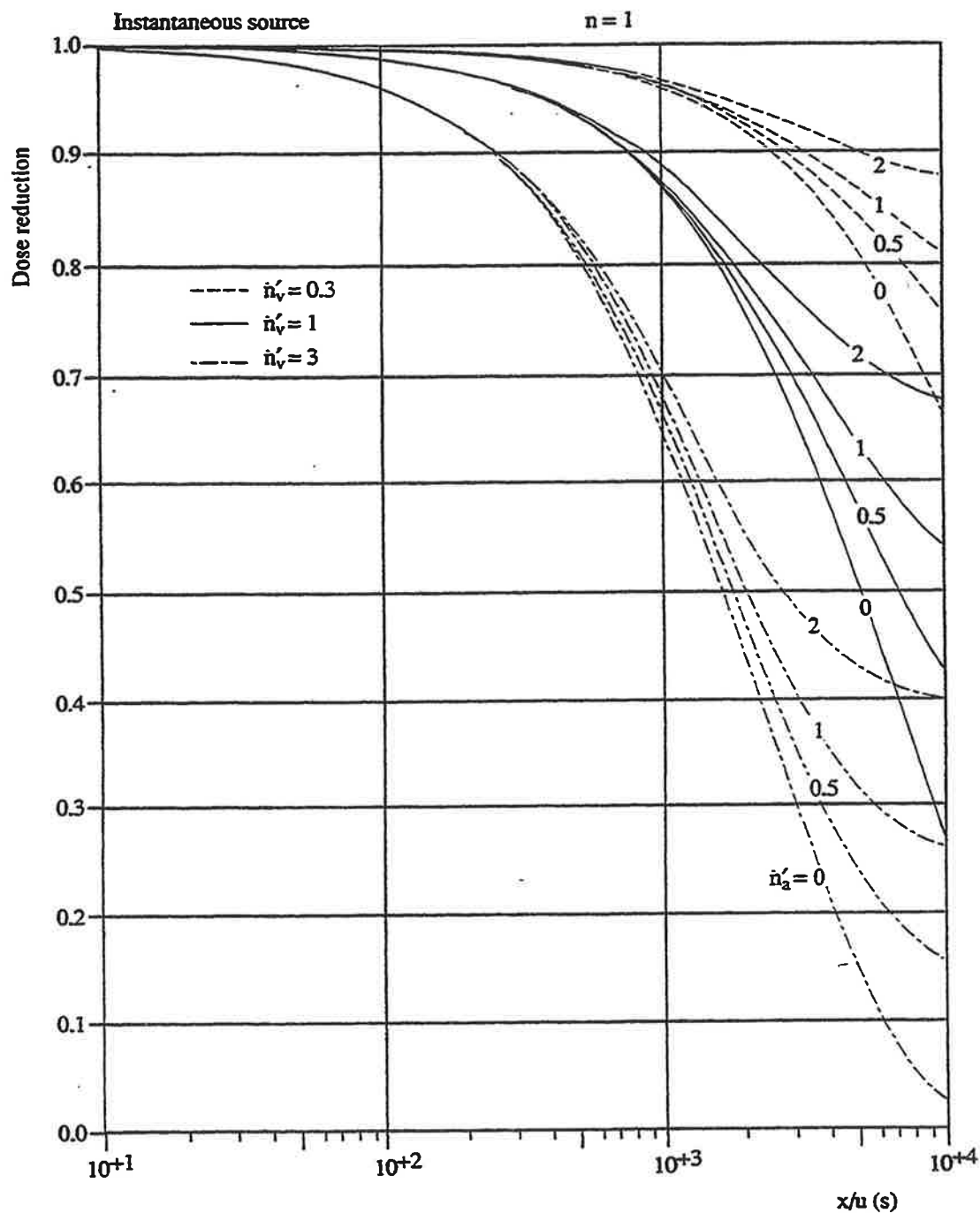


Diagram 9a Dose reduction dependent on the x/u of an instantaneous point source for $n=1$; parameters: the ventilation rate (\dot{n}_v') and the absorption rate (\dot{n}_a'), both in h^{-1} ; no ventilation delay.

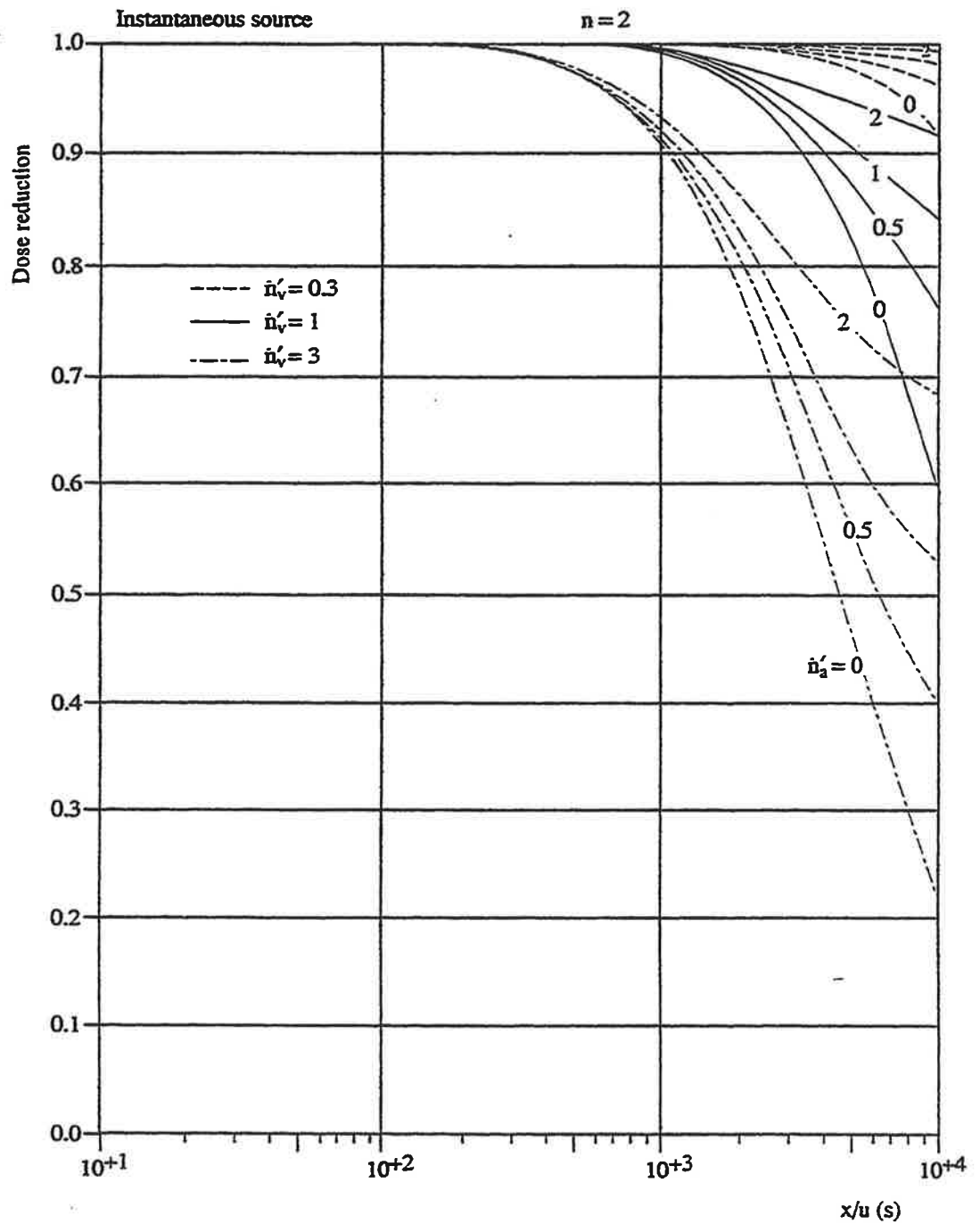


Diagram 9b Dose reduction dependent on the x/u of an instantaneous point source for $n=2$; parameters: the ventilation rate (\dot{n}'_v) and the absorption rate (\dot{n}'_a), both in h^{-1} ; no ventilation delay.

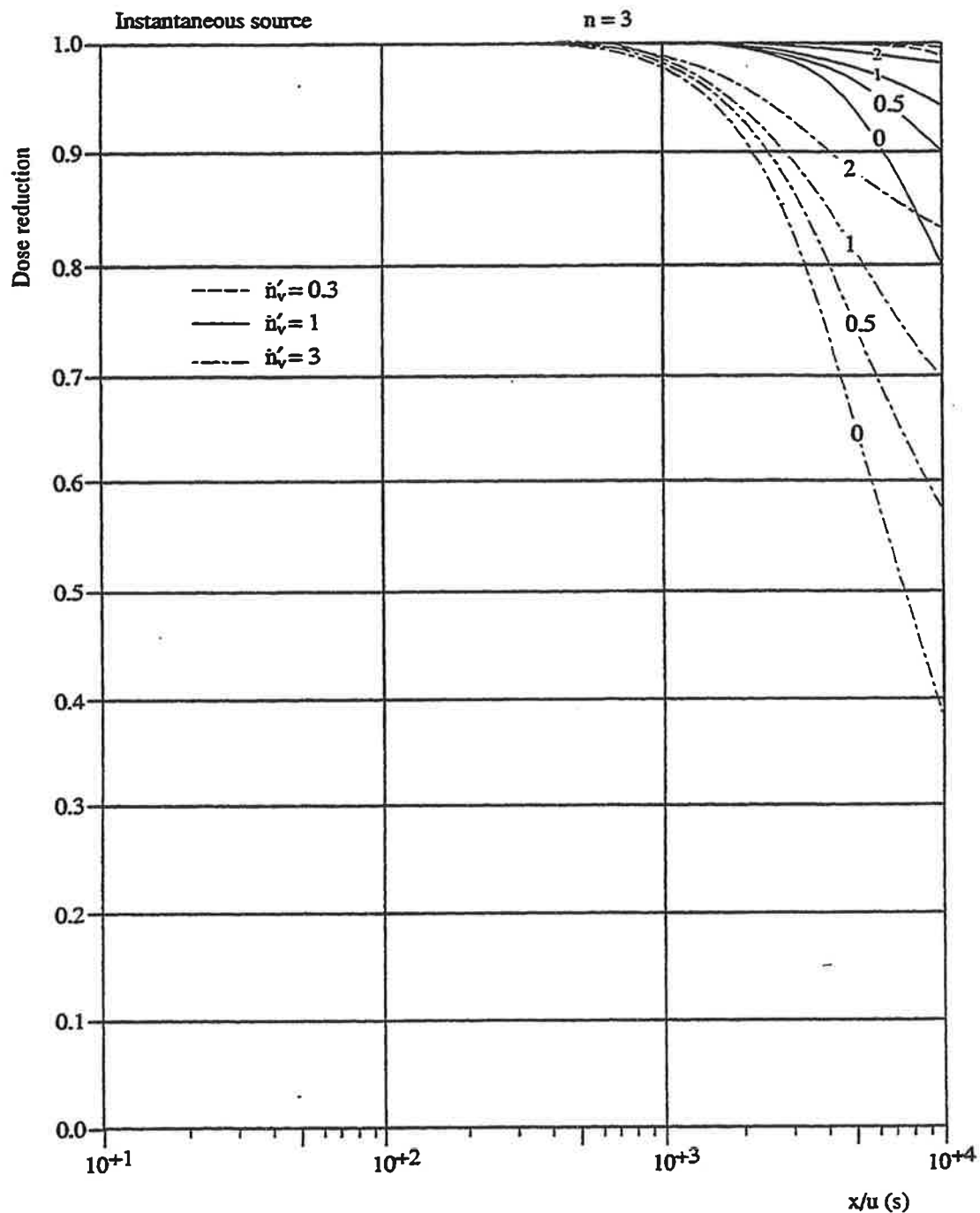


Diagram 9c Dose reduction dependent on the x/u of an instantaneous point source for $n=3$; parameters: the ventilation rate (\dot{n}_v') and the absorption rate (\dot{n}_a'), both in h^{-1} ; no ventilation delay.

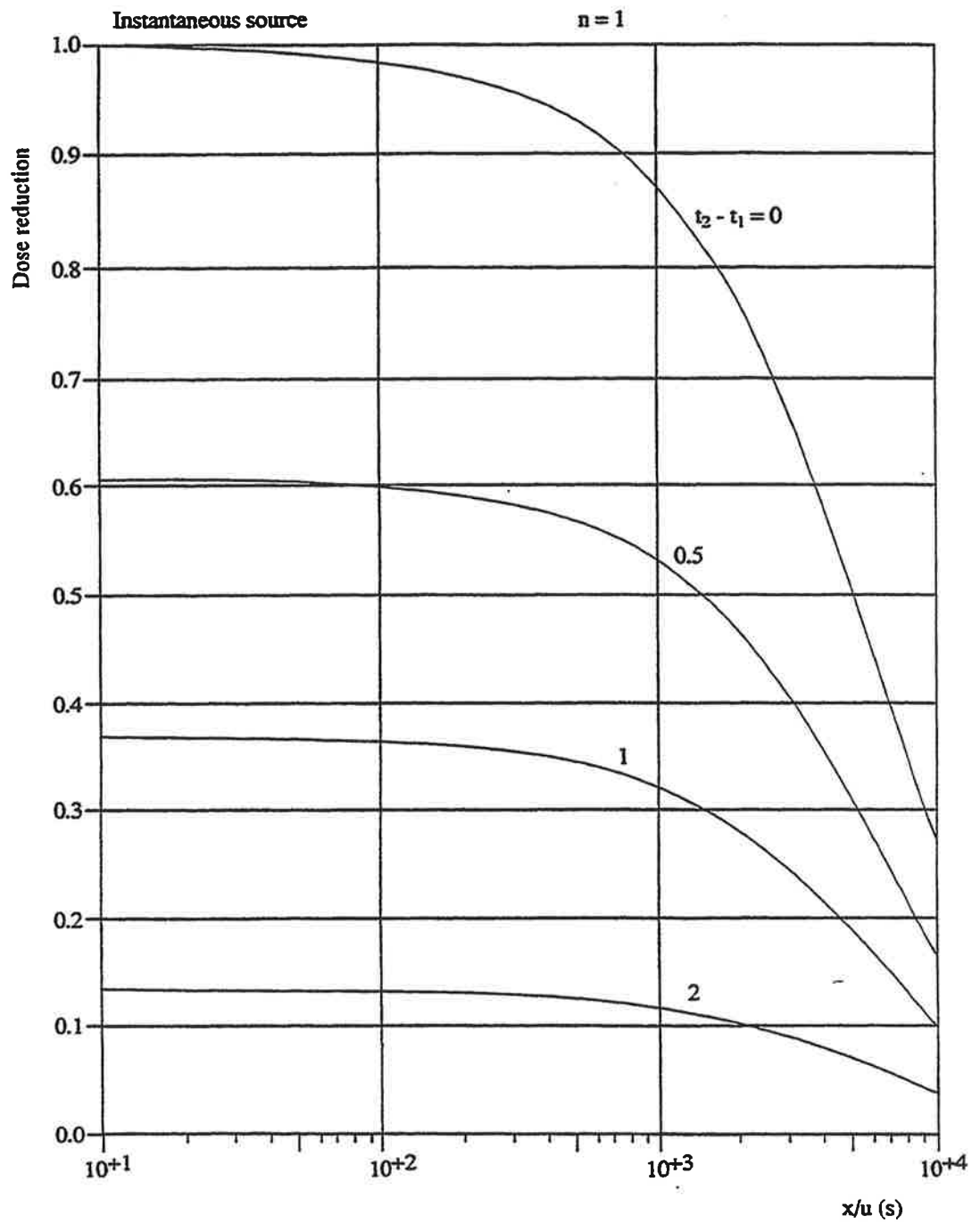


Diagram 10a Dose reduction dependent on the x/u of an instantaneous point source for $n=1$; parameter: the ventilation delay (t_2-t_1) in h; the ventilation rate is 1 h^{-1} and there is no absorption.

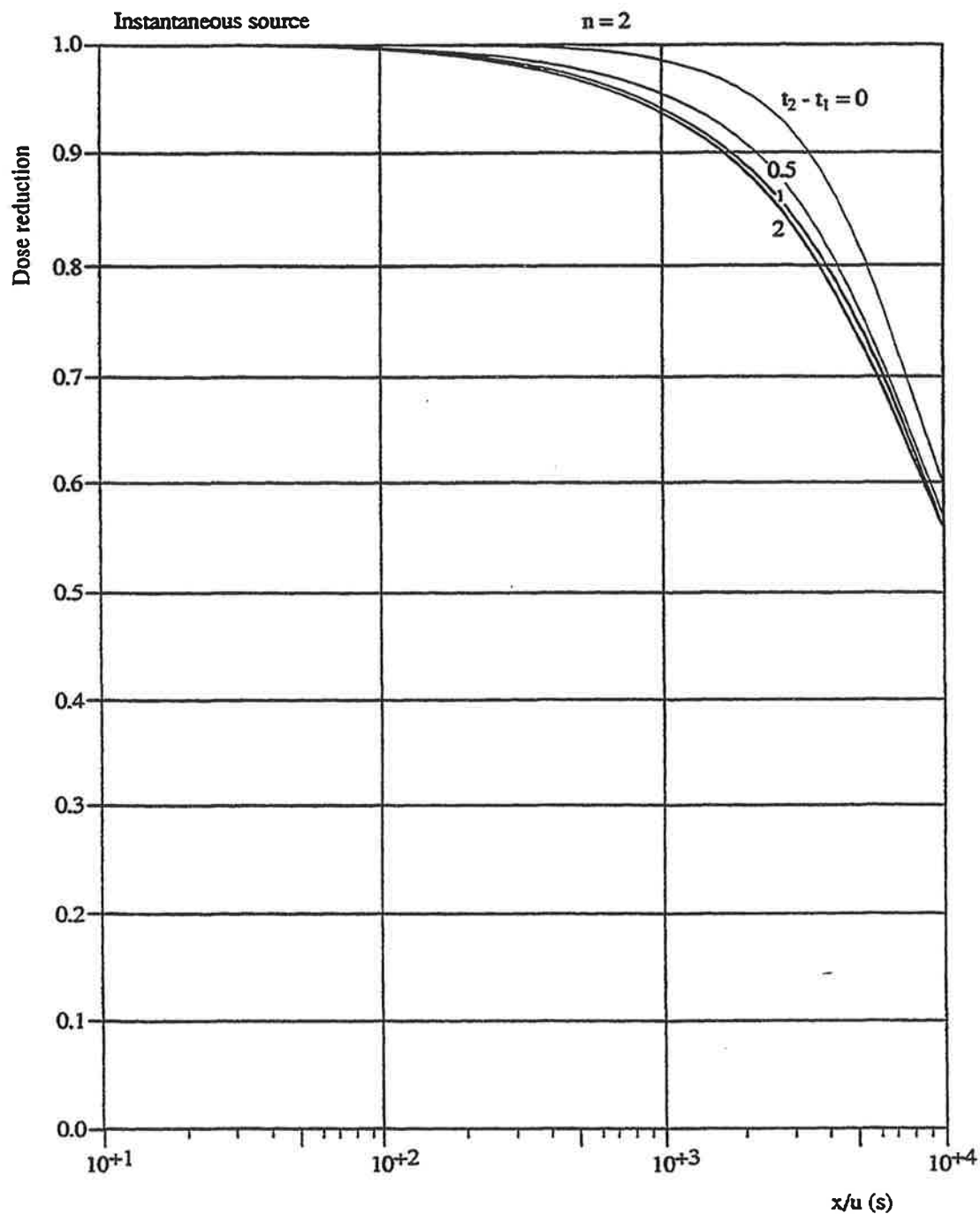


Diagram 10b Dose reduction dependent on the x/u of an instantaneous point source for $n=2$; parameter: the ventilation delay (t_2-t_1) in h; the ventilation rate is 1 h^{-1} and there is no absorption.

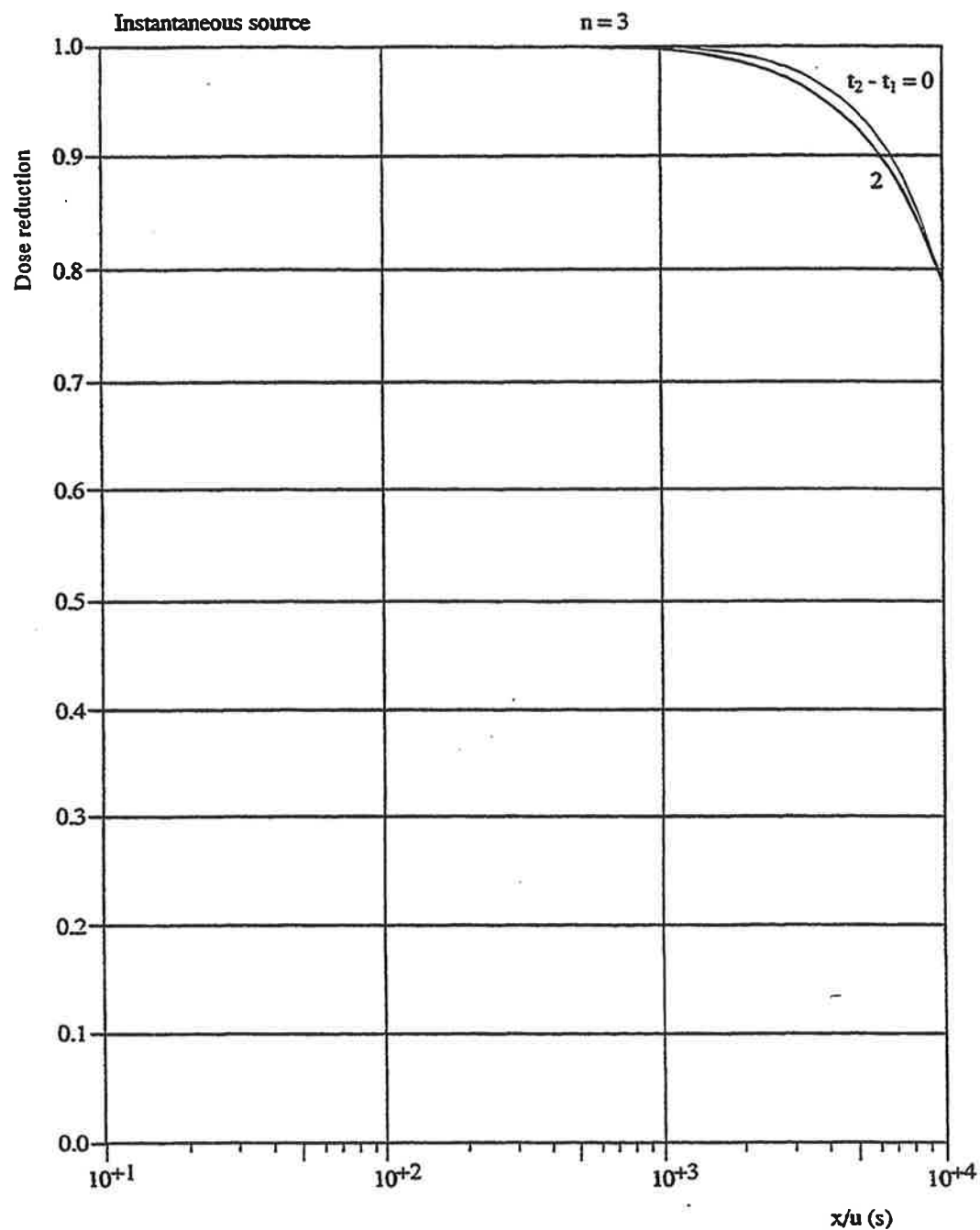


Diagram 10c Dose reduction dependent on the x/u of an instantaneous point source for $n=3$; parameter: the ventilation delay (t_2-t_1) in h; the ventilation rate is 1 h^{-1} and there is no absorption.

Annex 1

Review of the standard deviations of the concentration distribution (dispersion parameters), according to [1]:

The dispersion parameter in the x-direction $\sigma_x = e \cdot x^f$

The dispersion parameter in the y-direction $\sigma_y = a \cdot x^b$

The dispersion parameter in the z-direction $\sigma_z = c \cdot x^d$

The values of a to f(incl) are dependent on the stability of the atmosphere. For calculations for a continuous source the values given in the table below can be used.

Dispersion parameters for a continuous source according to [1].

Stability class		a	b	c	d	e	f
Very unstable	A)	0.527	0.865	0.28	0.90	0.13	1
Unstable	B)	0.371	0.866	0.23	0.85	0.13	1
Slightly unstable	C)	0.209	0.897	0.22	0.80	0.13	1
Neutral	D)	0.128	0.905	0.20	0.76	0.13	1
Stable	E)	0.098	0.902	0.15	0.73	0.13	1
Very stable	F)	0.065	0.902	0.12	0.67	0.13	1

For a instantaneous source we have:

$$\sigma_x = \sigma_x \text{ (continuous)} \quad e_I = e$$

$$\sigma_y = 0.5 \sigma_y \text{ (continuous)} \quad a_I = a/2, \quad b_I = b$$

$$\sigma_z = \sigma_z \text{ (continuous)} \quad c_I = c, \quad d_I = d$$

A correction for the average time t' (s), for a continuous source, is given by:

$$\sigma_y = c_{t'} \cdot a \cdot x^b \text{ with } c_{t'} = \left(\frac{t'}{600} \right)^{0.2}$$

(t' in s).

$$C_{t'} \geq 0.5$$

A correction for the roughness length z_0 (m) is given by :

$$\sigma_z = c_{z_0} \cdot c \cdot x^d = c' \cdot x^{d'} \text{ with } c_{z_0} = (10 z_0)^{0.53x^{-0.22}}$$

(z_0 in m).

Annex 2

Table 2.1a Fraction of protected area in % for an instantaneous source of 1000 kg., for different reference-doses (D_{ref}) and $n = 1$.

Absorption rate (h^{-1}):			0			0.5			1		
Ventilation delay (h):			0	1	2	0	1	2	0	1	2
D_{ref} ($g \cdot s/m^3$)	Stab.	Vent. (h^{-1})									
0.1	VS	0.1	34	30	26	90	89	89	95	95	95
		1	0	0	0	39	39	39	57	57	57
		10	0	0	0	6	6	6	11	11	11
0.1	N	0.1	99	92	83	99	94	91	99	96	94
		1	63	19	0	71	43	38	76	57	55
		10	1	0	0	6	5	5	11	10	10
0.1	U	0.1	99	91	82	99	93	90	99	95	93
		1	70	21	7	76	43	37	79	56	53
		10	2	0	0	7	5	5	11	10	10
1	VS	0.1	96	84	74	97	93	91	98	95	95
		1	8	2	1	42	39	39	59	57	57
		10	0	0	0	6	6	6	11	11	11
1	N	0.1	99	93	85	99	95	91	99	96	94
		1	98	34	12	98	50	40	98	60	55
		10	19	0	0	23	5	5	26	10	10
1	U	0.1	99	92	84	99	94	90	99	95	93
		1	98	34	12	98	48	38	98	58	54
		10	24	0	0	27	5	5	30	10	10
10	VS	0.1	99	92	85	99	95	92	99	96	95
		1	68	20	7	76	45	40	80	59	57
		10	1	0	0	7	6	6	12	11	11
10	N	0.1	99	93	86	99	95	91	99	96	94
		1	99	39	14	99	52	40	99	61	56
		10	83	0	0	83	5	5	83	10	10
10	U	0.1	99	92	84	99	94	90	99	95	93
		1	99	38	14	99	50	39	99	59	54
		10	85	0	0	85	5	5	85	10	10

100	VS	0.1	99	94	87	99	95	92	99	96	95
		1	99	36	13	99	52	42	99	62	57
		10	25	0	0	28	6	6	32	11	11
100	N	0.1	99	93	86	99	95	91	99	96	94
		1	99	40	15	99	53	41	99	61	56
		10	99	0	0	99	5	5	99	10	10
100	U	0.1	99	92	84	99	94	90	99	95	93
		1	99	39	14	99	51	39	99	59	54
		10	99	0	0	99	5	5	99	10	10

Table 2.Ib. Fraction of protected area in % for an instantaneous source of 1000 kg, for different reference-doses (D_{ref}) and $n=2$.

Absorption rate (h^{-1}):			0			0.5			1		
Ventilation delay (h):			0	1	2	0	1	2	0	1	2
D_{ref} ($g \cdot s/m^3$) ² s	Stab.	Vent. (h^{-1})									
0.1	VS	0.1	34	30	26	90	89	89	95	95	95
		1	0	0	0	39	39	39	57	57	57
		10	0	0	0	6	6	6	11	11	11
0.1	N	0.1	99	92	83	99	94	91	99	96	94
		1	63	19	0	71	43	38	76	57	55
		10	1	0	0	6	5	5	11	10	10
0.1	U	0.1	99	91	82	99	93	90	99	95	93
		1	70	21	7	76	43	37	79	56	53
		10	2	0	0	7	5	5	11	10	10
1	VS	0.1	99	99	98	99	99	99	99	99	99
		1	99	89	88	99	91	90	99	92	92
		10	70	54	54	70	55	55	70	56	56
1	N	0.1	99	99	99	99	99	99	99	99	99
		1	99	96	96	99	97	96	99	97	97
		10	98	83	83	98	84	84	98	84	84
1	U	0.1	99	99	99	99	99	99	99	99	99
		1	99	95	95	99	96	96	99	97	97
		10	97	82	82	98	83	83	98	83	84

10	VS	0.1	99	99	99	99	99	99	99	99	99
		1	99	92	91	99	93	93	99	94	94
		10	85	65	65	85	67	66	86	67	67
10	N	0.1	99	99	99	99	99	99	99	99	99
		1	99	97	97	99	97	97	99	98	98
		10	99	88	88	99	88	88	99	88	88
10	U	0.1	99	99	99	99	99	99	99	99	99
		1	99	96	96	99	97	97	99	97	97
		10	99	87	87	99	87	87	99	87	87
100	VS	0.1	99	99	99	99	99	99	99	99	99
		1	99	95	94	99	95	95	99	95	95
		10	94	75	75	94	75	76	94	76	76
100	N	0.1	99	99	99	99	99	99	99	99	99
		1	99	98	98	99	98	98	99	98	98
		10	99	91	91	99	91	91	99	91	91
100	U	0.1	99	99	99	99	99	99	99	99	99
		1	99	97	97	99	98	98	99	98	98
		10	99	90	90	99	90	90	99	90	90

Table 2Jc. Fraction of protected area in % for an instantaneous source of 1000 kg, for different reference-doses (D_{ref}) and $n = 3$.

Absorption rate (h^{-1}):			0			0.5			1		
Ventilation delay (h):			0	1	2	0	1	2	0	1	2
D_{ref} ($g \cdot s/m^3$) ^{3s}	Stab.	Vent. (h^{-1})									
0.1	VS	0.1	99	99	99	99	99	99	99	99	99
		1	99	96	96	99	96	96	99	97	97
		10	83	74	74	84	75	74	84	75	75
0.1	N	0.1	99	99	99	99	99	99	99	99	99
		1	99	99	99	99	99	99	99	99	99
		10	99	93	93	99	93	93	99	93	93
0.1	U	0.1	99	99	99	99	99	99	99	99	99
		1	99	99	99	99	99	99	99	99	99
		10	99	92	92	99	92	92	99	92	92

1	VS	0.1	99	99	99	99	99	99	99	99	99
		1	99	97	97	99	98	98	99	98	98
		10	90	80	80	90	81	81	90	81	81
1	N	0.1	99	99	99	99	99	99	99	99	99
		1	99	99	99	99	99	99	99	99	99
		10	99	94	94	99	95	95	99	95	95
1	U	0.1	99	99	99	199	99	99	99	99	99
		1	99	99	99	99	99	99	99	99	99
		10	99	94	94	99	94	94	99	94	94
10	VS	0.1	99	99	99	99	99	99	99	99	99
		1	99	98	98	99	98	98	99	98	98
		10	94	85	84	94	85	85	94	85	85
10	N	0.1	99	99	99	99	99	99	99	99	99
		1	99	99	99	99	99	99	99	99	99
		10	99	96	96	99	96	96	99	96	96
10	U	0.1	99	99	99	99	99	99	99	99	99
		1	99	99	99	99	99	99	99	99	99
		10	99	95	95	99	95	95	99	95	99
100	VS	0.1	99	99	99	99	99	99	99	99	99
		1	99	98	98	99	99	99	99	99	99
		10	96	88	88	96	89	89	96	89	89
100	N	0.1	99	99	99	99	99	99	99	99	99
		1	99	99	99	99	99	99	99	99	99
		10	99	97	97	99	97	97	99	97	97
100	U	0.1	99	99	99	99	99	99	99	99	99
		1	99	99	99	99	99	99	99	99	99
		10	99	96	96	99	96	96	99	96	96

Table 2.IIa. Critical ventilation rates in h^{-1} for an instantaneous source of 1000 kg and for different reference-doses (D_{ref}) and $n=1$.

Absorption rate (h^{-1}):		0			0.5			1		
Vent.-delay (h):		0	1	2	0	1	2	0	1	2
D_{ref} ($g \cdot s/m^3$)	Stab.									
0.1	VS	<0.1	<0.1	<0.1	<0.1	<0.1	<0.1	0.1	0.1	0.1
0.1	N	0.4	<0.1	<0.1	0.4	0.1	<0.1	0.4	0.1	<0.1
0.1	U	0.4	<0.1	<0.1	0.4	<0.1	<0.1	0.5	0.1	<0.1
1	VS	0.1	<0.1	<0.1	0.1	<0.1	<0.1	0.2	0.1	0.1
1	N	1.5	<0.1	<0.1	1.6	0.1	<0.1	1.7	0.13	0.1
1	U	2.2	<0.1	<0.1	2.4	<0.1	<0.1	2.5	0.1	<0.1
10	VS	0.4	<0.1	<0.1	0.5	0.1	<0.1	0.5	0.2	0.1
10	N	5.2	<0.1	<0.1	5.3	0.1	<0.1	5.4	0.1	<0.1
10	U	5.5	<0.1	<0.1	5.5	<0.1	<0.1	5.5	0.1	<0.1
100	VS	1.8	<0.1	<0.1	1.9	0.1	<0.1	2.0	0.2	0.1
100	N	23	<0.1	<0.1	23	0.1	<0.1	23	0.1	<0.1
100	U	23	<0.1	<0.1	23	<0.1	<0.1	23	0.1	<0.1

Table 2.IIb. Critical ventilation rates in h^{-1} for an instantaneous source of 1000 kg and for different reference-doses (D_{ref}) and $n=2$.

Absorption rate (h^{-1}):		0			0.5			1		
Vent.-delay (h):		0	1	2	0	1	2	0	1	2
D_{ref} ($g \cdot s/m^3$) ^{2s}	Stab.									
0.1	VS	1.7	0.3	0.2	1.7	0.4	0.3	1.7	0.5	0.5
0.1	N	10	0.9	0.8	10	1.0	1.0	10	1.3	1.3
0.1	U	10	0.7	0.6	10	1.0	0.9	10	1.1	1.1
1	VS	3.0	0.4	0.3	3.0	0.5	0.5	3.0	0.6	0.6
1	N	18	1.3	1.2	18	1.6	1.6	18	1.8	1.8
1	U	17	1.1	1.0	17	1.4	1.4	17	1.6	1.6
10	VS	5.1	0.6	0.4	5.1	0.7	0.6	5.1	0.9	0.9
10	N	31	2.1	2.0	31	2.4	2.4	31	2.7	2.7
10	U	29	1.7	1.6	29	2.0	2.0	29	2.4	2.3
100	VS	8.8	0.8	0.7	8.8	1.1	1.0	8.8	1.2	1.2
100	N	>40	3.4	3.4	>40	3.9	3.9	>40	4.1	4.1
100	U	>40	2.8	2.8	>40	3.2	3.2	>40	3.5	3.5

Table 2.IIc. Critical ventilation rates in h^{-1} for an instantaneous source of 1000 kg. and for different reference-doses (D_{ref}) and $n = 3$.

Absorption rate (h^{-1}):		0			0.5			1		
Vent.-delay (h):		0	1	2	0	1	2	0	1	2
D_{ref} ($g \cdot s / m^3$) ^{3s}	Stab.									
0.1	VS	4.5	1.2	1.2	4.5	1.4	1.4	4.5	2.1	2.1
0.1	N	23	6.3	6.1	23	6.4	6.3	23	6.8	6.6
0.1	U	21	5.4	5.3	21	5.5	5.5	21	5.8	5.7
1	VS	6.1	1.8	1.8	6.1	2.0	2.0	6.1	2.1	2.1
1	N	32	8.6	8.4	32	8.8	8.6	32	9.0	8.8
1	U	30	7.3	7.2	30	7.6	7.6	30	7.8	7.6
10	VS	8.5	2.4	2.4	8.6	2.6	2.6	8.6	2.9	2.9
10	N	>40	12	12	>40	12	12	>40	12	12
10	U	40	10	10	40	10	10	40	10	10
100	VS	12	3.5	3.5	12	3.7	3.7	12	3.9	3.9
100	N	>40	16	16	>40	17	17	>40	17	17
100	U	>40	14	14	>40	14	14	>40	15	15

Annex 3

For a temporary constant emission, which can be reproduced by a step function, such as described in Paragraph 4.4, the following equations for the inner concentration and for the dose reduction factor have been taken from Reference [4].

In these equations, index 1 refers to a room on the wind side and index 2 to a room on the lee side, which is ventilated exclusively by the air out of a room at the wind side of the building.

The inner concentration in a room at the front side:

$$C_{i2} = C_o \left[\frac{\dot{n}_{v1} \dot{n}_{v2}}{\dot{n}_{va1} \dot{n}_{va2}} + \frac{\dot{n}_{v1} \dot{n}_{v2}}{\dot{n}_{va1} (\dot{n}_{va1} - \dot{n}_{va2})} * \text{EXP}(-\dot{n}_{va1} t) + \frac{\dot{n}_{v1} \dot{n}_{v2}}{\dot{n}_{va2} (\dot{n}_{va1} - \dot{n}_{va2})} * \text{EXP}(-\dot{n}_{va2} t) \right] \text{ for } t \leq t_1 \quad (\text{A1})$$

and

$$C_{i2} = C_2^* * \text{EXP}(-\dot{n}_{va2} (t - t_1)) + C_1^* \frac{\dot{n}_{v2}}{\dot{n}_{va1} - \dot{n}_{va2}} [\text{EXP}(-\dot{n}_{va2} (t - t_1)) - \text{EXP}(-\dot{n}_{va1} (t - t_1))] \text{ for } t > t_1 \quad (\text{A2})$$

in which:

C_1^* = the concentration in room 1 (wind side) at time t_1 , to be calculated with, for instance, equation (8a).

C_2^* = the concentration in room 2 (lee side) at time t_1 , to be calculated with, for instance, equation (A1).

The other units are similar to the units given in Paragraph 4.

Annex 4

Table with error functions values for arguments $x + y$: $ERF(x+y)$

x:	y: 0.00	0.01	0.02	0.03	0.04	0.05	0.06	0.07	0.08	0.09
0.0	0.0000	0.0113	0.0226	0.0338	0.0451	0.0564	0.0676	0.0789	0.0901	0.1013
0.1	0.1125	0.1236	0.1348	0.1459	0.1569	0.1680	0.1790	0.1900	0.2009	0.2118
0.2	0.2227	0.2335	0.2443	0.2550	0.2657	0.2763	0.2869	0.2974	0.3079	0.3183
0.3	0.3286	0.3389	0.3491	0.3593	0.3694	0.3794	0.3893	0.3992	0.4090	0.4187
0.4	0.4284	0.4380	0.4475	0.4569	0.4662	0.4755	0.4847	0.4937	0.5027	0.5117
0.5	0.5205	0.5292	0.5379	0.5465	0.5549	0.5633	0.5716	0.5798	0.5879	0.5959
0.6	0.6039	0.6117	0.6194	0.6270	0.6346	0.6420	0.6494	0.6566	0.6638	0.6708
0.7	0.6778	0.6847	0.6914	0.6981	0.7047	0.7112	0.7175	0.7238	0.7300	0.7361
0.8	0.7421	0.7480	0.7538	0.7595	0.7651	0.7707	0.7761	0.7814	0.7867	0.7918
0.9	0.7969	0.8019	0.8068	0.8116	0.8163	0.8209	0.8254	0.8299	0.8342	0.8385
1.0	0.8427	0.8468	0.8508	0.8548	0.8587	0.8624	0.8661	0.8698	0.8733	0.8768
1.1	0.8802	0.8835	0.8868	0.8900	0.8931	0.8961	0.8991	0.9020	0.9048	0.9076
1.2	0.9103	0.9130	0.9155	0.9181	0.9205	0.9229	0.9252	0.9275	0.9297	0.9319
1.3	0.9340	0.9361	0.9381	0.9400	0.9419	0.9438	0.9456	0.9473	0.9490	0.9507
1.4	0.9523	0.9539	0.9554	0.9569	0.9583	0.9597	0.9611	0.9624	0.9637	0.9649
1.5	0.9661	0.9673	0.9684	0.9695	0.9706	0.9716	0.9726	0.9736	0.9745	0.9755
1.6	0.9763	0.9772	0.9780	0.9788	0.9796	0.9804	0.9811	0.9818	0.9825	0.9832
1.7	0.9838	0.9844	0.9850	0.9856	0.9861	0.9867	0.9872	0.9877	0.9882	0.9886
1.8	0.9891	0.9895	0.9899	0.9903	0.9907	0.9911	0.9915	0.9918	0.9922	0.9925
1.9	0.9928	0.9931	0.9934	0.9937	0.9939	0.9942	0.9944	0.9947	0.9949	0.9951
2.0	0.9953	0.9955	0.9957	0.9959	0.9961	0.9963	0.9964	0.9966	0.9967	0.9969
2.1	0.9970	0.9972	0.9973	0.9974	0.9975	0.9976	0.9977	0.9979	0.9980	0.9980
2.2	0.9981	0.9982	0.9983	0.9984	0.9985	0.9985	0.9986	0.9987	0.9987	0.9988
2.3	0.9989	0.9989	0.9990	0.9990	0.9991	0.9991	0.9992	0.9992	0.9992	0.9993
2.4	0.9993	0.9993	0.9994	0.9994	0.9994	0.9995	0.9995	0.9995	0.9995	0.9996
2.5	0.9996	0.9996	0.9996	0.9997	0.9997	0.9997	0.9997	0.9997	0.9997	0.9998
2.6	0.9998	0.9998	0.9998	0.9998	0.9998	0.9998	0.9998	0.9998	0.9998	0.9999
2.7	0.9999	0.9999	0.9999	0.9999	0.9999	0.9999	0.9999	0.9999	0.9999	0.9999
2.8	0.9999	0.9999	0.9999	0.9999	0.9999	0.9999	0.9999	1.0000	1.0000	1.0000
2.9	1.0000	1.0000	1.0000	1.0000	1.0000	1.0000	1.0000	1.0000	1.0000	1.0000
3.0	1.0000	1.0000	1.0000	1.0000	1.0000	1.0000	1.0000	1.0000	1.0000	1.0000

$$ERF(X) = \frac{2}{\sqrt{\pi}} \int_0^X \exp(-t^2) dt$$

Chapter 7

Population data

Contents

	Page
1. Introduction	4
2. Residential areas	5
2.1 Detailed data	5
2.2 Global data	6
3. Other areas	8
3.1 Industrial area	8
3.2 Recreational area	9
4. Presence indoors/outdoors, day/night	11
5. Recommended methodology	13
6. References	15

1

Introduction

Within the framework of risk analysis, the effects consequent to the escape of hazardous materials in the surroundings are translated, into the damage caused by this. Damage models, for this purpose, are presented in this edition. In the determination of the degree of injury which can be sustained, data about the presence of people in the surroundings and about their stay are necessary. An inventory is presented, in this chapter, of data available for use in risk analysis studies.

In order to determine the number of persons who might be affected, knowledge about the population density in the surroundings is required.

For an estimate with regard to the presence of people, difference is made between the function of the area, such as:

- Residential areas, sub-divided into sparsely and densely populated areas.
- Industrial areas, sub-divided into industrial installations and offices.
- Recreational areas.

In the same time, we also must estimate the presence of people distributed indoors and outdoors, as well as during the day and night.

The information used in this report originates from previously performed studies and projects and, also, from census data. A computer literature research has also been carried out, from which some articles have been selected from planning and nuclear energy files.

Residential areas

In order to determine the number of people which might be affected within a calculated damage distance, reference is made, most of the time, to population data per type of residential area or buildings.

The accuracy of such a determination depends on the detail of the available population data.

If the damage area is of restricted nature, then local conditions play an important role and, consequently, sufficient accuracy can only be obtained from properly detailed data, see paragraph 2.1.

If the damage affects a larger area, then data of a more global nature can be sufficient, see paragraph 2.2. Inaccuracies per parts of the area, over - and under estimations, can, as much as it is possible, be averaged-out. However, every situation must be considered on its own. A global division into types of residential areas will be then, often more efficient, since a detailed inventory relative to presence of people is generally too time-consuming.

It is concluded, in reference [7], that an acceptable reliability in risk estimations can be obtained if, within a 400 meters distance, detailed population data, such as from census, will be used. For distances larger than 400 meters global data, relative to types of residential areas, can be used.

2.1.

Detailed data

Detailed population data are often available in municipalities, governmental planning services and provincial planning services.

The Dutch Ministry of VROM* is presently working on a database of population data per 100 x 100 meters squares for all of the Netherlands.

When detailed and up-to-date population data are available, it can be recommended to make use of it, for small as well as large damage areas.

Also, a difference can be made between the presence of people during day-time and night-time.

The number of people present can be established by counting the persons who, at a given moment, are present in a given area. If, in the area under consideration, only housing is located, then the number of houses can be counted. Thereafter, this number is multiplied by the average number of people per house. According to reference [5], this was equal to 3.0 in 1975 and 2.6 in 1984. During the day, not all of the inhabitants are in or near the house. This number, is estimated to be of 1 or 2 per house.

Taking the above into consideration, the distribution between people present in the houses during day or night is, respectively, 30 - 70% and 100%.

The above-mentioned methodology is applied in the LPG, a study [8]. The areas considered for this purpose are split into 100 x 100 meters squares. Following that, an estimate is made of how many people are located in every given square. Such an inventory had been made by the information department of the Governmental planning service. They established the number of mailing addresses per square. Each mailing address counts for 3 inhabitants present at this address.

*) Ministry of Housing, Physical Planning and the Environment.

The counting of the number of people present in a given area can also be conducted according to reference [3]. In this case, a number of different land-use patterns differentiated, information with which data on the number of people is established by professional planners. Table 1 (at the end of this chapter) contains a short summary of these data.

This procedure leads to duplications, since people present in, for instance, shops, schools and businesses are also counted as present in their homes.

The number of people present in their homes is taken equal to 100% in ref. [3], which represents 3 persons per residence. In order to avoid the problem of duplication it would appear reasonable to calculate with, for instance, 1 to 2 persons per residence.

2.2.

Global data

Population density in cities

According to reference [1], it appears that the population density in the cities, at different distances from the center, satisfies reasonably well the following exponential function:

$$D(x) = D_0 \exp(-D_1 x) \quad (1)$$

in which:

$D(x)$ = population density at distance x [persons/ha]

D_0 = population density in the center of the city [persons/ha]

D_1 = density gradient [km^{-1}]

x = distance from the center [km]

An inventory of population densities in cities in the United-Kingdom, West-Germany and the USA [1] leads to the following average values for D_0 and D_1 :

$D_0 = \pm 100$ persons/ha.

$D_1 = \pm 0.25 \text{ km}^{-1}$

These values are higher in cities in Japan, but the town planning, in this case, departs more from the one in cities in the Netherlands.

The above-given averages appear to agree with the ones in Dutch cities. The average value of D_0 (100 persons per hectare) has a wide spreading: for dense cities D_0 , on the average, is equal to ± 130 persons/ha, while for cities more sparsely set-up D_0 has an average value of ± 70 persons/ha.

Formula 1 is adequate for cities which regularly expand from the center, with the center being the most densely populated. Formula 1 is, however, less applicable when, for instance, green areas are provided, or when a city expands from different suburbs, whereby an agglomeration is formed. Also, formula 1 is not adequate when the city expansion consists of ribbon building.

Population density per type of residential area

Only a city, as a whole, has been considered in the previous paragraph. When the damage area only affects part of a city or a village with its surroundings, a better estimate of the number of people present can be obtained, then, by using values of population densities for different types of residential areas.

The values have been established with the help of inventories of Dutch population data per partial areas/districts of South-Holland (obtained by the TNO Emission Registration project) and of the municipalities of Apeldoorn, Enschede and Dalfsen (obtained via the municipality of Apeldoorn and the Overijssel province).

The following types of residential areas are differentiated:

- nature areas: woods, water, moorland and similar
- remote area: agricultural
- scattered housing
- quiet residential area: 0% of high buildings
- busy residential area: 25% of high buildings
- urban area: 85% of high buildings

The percentages of high buildings named above are merely global indications. The population densities in the inventories are compared with the values evaluated in ref. [3], see table 1 and ref. [7]. The different values are placed next to each other in table 2. The average population densities which typify the different residential areas are given in the last column.

Table 2 - Population densities per type of housing area

Type of residential area	Population density (persons/ha)						
	Note [3]	Reference[7]	South-Holland	Apeldoorn	Dalfsen	Enschede	"Recommended" averages
Nature area (woods, water, moorland etc)		0	0	0	0		0
Remote area (agricultural)		1	1	1	1	1	1
Scattered housing	10	10	4	5	6	3	5
Quiet residential area (0% high buildings)	40	40	20	30	20	30	25
Busy residential area (25% high buildings)	80		70	60	70	70	70
Urban area (85% high buildings)	120-255	100-150	130			110	120

In chapter 4 we will deal in more details with the aspects of presence during day-time and night-time, as well as the distribution of people indoors and outdoors.

Other areas

3.1. Industrial area

In part 2 of the 4th general business composition status prepared by the Central Bureau of Statistics [4] information is available relative to the number of working people and to the ground areas of the different SBI business classes (SBI = standard business classification).

The concept "working people" applies to all persons who are actually working, on the average, 15 hours or more per week.

The "ground area" includes not only the built-up area, but also the area in the vicinity of the buildings which is being used.

Global personnel densities, for the different business branches, are obtained from the above data.

Business branch	Ground area (ha) per establishment	Number of working people per esta- blishment	Personnel density (persons/ha)
0. Agriculture and fishing (except agricultural and gardening industries)	2	6	3
1. Exploration of minerals	10	30	3
2/3. Industry	0.6	25	40
4. Public utilities	9	50	6
5. Construction and installation industries	0.16	12	75
6.1/6.6 Commerce	0.1	4	40
6.7 Hotels and restaurants	0.4	3	8
6.8 Repairs of consumer goods	0.1	5	50
7. Transportation and storage	0.7	11	15
8. Banking and insurance business-services (except government)	0.1	8	85
9. Other services (partially) (except, among others, education, health- care)	0.1	3.5	35

From this inventory, 3 categories can globally be distinguished:

Personnel density		Business branch
Low	5 pers./ha	0-1-4-6.7-7
Medium	40 pers./ha	2/3-6.1/6.6-6.8-9
High	80 pers./ha	5-8

Within the business branches, large differences can be found in personnel density per type and size of business. The numbers given, consequently, can only be used as global indications.

Intensively working businesses and offices in banking or insurance entities the personnel density can raise up to 200 persons/ha or more.

Generally, in offices people are present only during the day, but in businesses with work in shifts there are also people present during the night.

In the data from ref. [3] no personnel densities are given for industries or offices, but only indications regarding the number of employees per office or per industry. However, indications regarding the number of people present during day or night and indoors or outdoors are provided, see table 1. This shows that during the day 100% are always present, and that during the night 1% of office personnel and 21% of personnel from industry are present. In the 100% figure during the day, part-time jobs or other absences are not taken into account.

3.2

Recreational area

The number of people present in a recreational area is very difficult to estimate. People are not always present in such areas, so that a given probability of presence must be established.

Presence of people in recreational areas is strongly dependent on season, weather conditions and on the day of the week.

Various types of recreational areas can be differentiated, such as covered areas (less dependent on the season) and open areas, such as beaches, playgrounds, zoological gardens and parks.

Some municipalities were asked to provide data about the capacities of camping businesses. The following global data have been obtained from this:

Widely-spaced camping businesses: + 17 locations/ha and 3.5 persons per location = 60 persons/ha.

Other camping businesses: 37 locations/ha and 3.5 persons per location = 130 persons/ha.

The last data are in agreement with the estimate made in ref. [3].

The following global evaluations regarding data on presence are provided in ref. [3].

Land-use pattern no. 14: campings, bungalows, standard trailers, public gardens with garden-houses.

– bungalows:

25 units/ha and 3 to a max. of 6 persons/unit = 125 persons/ha

– standard trailers:

40-50 units/ha and 3.5 to a max. of 5 persons/unit = 200 persons/ha.

– tourist areas:

60 units/ha and 2.5 to a max. of 4 persons/unit = 180 persons/ha.

Remarks: These data on presence relate to a summer period ($\pm 40\%$ of the year). There are peaks during vacation periods and weekends. On peak days in attractive areas we find 75 units/ha = 225 persons/ha.

Land-use pattern no. 15 : outdoor sport and recreation, in the weekends, evenings and summers.

- little use: 36 persons/ha
- intensively use, for instance: an open swimming pool: 500 persons
- very intensively use, for instance: a zoological garden, an attraction park: 2500 persons/day

Presence indoors/outdoors, day/night

In order to be able to determine the number of people affected by an accident we need, besides data on population density, also data relating to presence of people indoors or outdoors.

Depending on the effect, the fact of remaining indoors may, or may not, offer protection.

In cases of heat radiation or toxic gas clouds staying indoors does offer protection. A reduction factor for the consequences is often applied in studies. This reduction factor, for a toxic gas cloud, depends on the ventilation rate of the building, the passage time of the cloud and the time during which people remain indoors.

The fact of remaining indoors can also lead, however, to personal injury, for instance, due to smoke formation inside and due to the collapse of a building caused by an explosion.

In the TNO studies, in the past, the following values had mostly been used:

during day-time: 80% indoors and 20% outdoors

during the night: 95% indoors and 5% outdoors

In the Covo-study [6] and in the Technica-program use is made of a number of people outdoors equal to 1% of the total population and of a number of people indoors equal to 99% of this total.

An inventory is made in ref. [2] regarding how a person, on the average, splits its time and where this person is staying:

home, indoors:	69% of the time
somewhere else, indoors:	24% of the time
outdoors (inclusive of travel time):	7% of the time

These figures are, among others, dependent on wheather conditions and seasons and, also, on personal characteristics such as age and occupation.

Article [7] indicates how many people are present in a given residential area at different times of the day:

school time 8.00 - 16.00 hours:	50%
work time 8.00 - 18.30 hours:	70%
at night 18.30 - 8.00 hours:	100%

Differences between seasons or differences during a week are not taken into account in the above figures.

Reference [7] also differentiates a more vulnerable group of people, such as young children, old people and sick people. Such a group forms about 25% of the total population. This group will be outdoors for about half an hour per day, while the remainder will be about one hour per day outdoors. During the night 1% of the population will be outdoors (not the vulnerable group). It follows, from all of the above, that 7% of the population will be outdoors during the day.

In table 1, for various land-use patterns, a distribution indoors/outdoors for the day and the night is presented, taken from reference [3].

Inventories regarding presence which are found in literature can differ appreciably. Figures on presence vary, among others, with the time of the year, the weather conditions, the day of the week and the time during the day. The data, consequently, can only be used to provide global indications. For damage calculations it is presently assumed, for simplification, that people remain at the same place where they are located. But people, in reality, move and travel. Proper disaster combatment plans can substantially limit the number of victims by foreseeing appropriate measures related to escape possibilities of people, such as, for instance : staying indoors or going outdoors, closing windows and doors and sealing slits or evacuating to a safe location.

Recommended methodology

In the preceding paragraphs, different data about presence, as found in inventories from literature, have been presented and evaluated.

Based on the above inventories, a methodology is recommended in this paragraph, to be used in risk analysis studies.

The required data are: number of people present during day and night and percentages of presence indoors and outdoors in the damage area under consideration.

Uncertainties with regard to population data lead, in turn, to proportional uncertainties in a risk analysis with regard to the number of fatalities.

However, uncertainties in damage distances, in their turn, lead to uncertainties which are much larger than proportional.

As shown in reference [7], detailed population data are necessary for a reliable estimate of the damages if the damage area is small. If, on the other hand, the damage area is large, a reasonably reliable estimate of the damages can be obtained with only global population data.

Methodology regarding population data

Generally speaking, it is, of course, preferable, for purposes of risk analysis, to be able to obtain detailed and up to date population data which, most of the time, are available at municipalities and planning services.

If, however, these data are not available, the following procedure will suffice:

In a restricted area (a limit of 400 m is used in ref [7]), all-around the considered installation, detailed population data must be provided for a risk analysis. For this purpose, having recourse to the map of the surroundings, the number of houses can be counted and this number, then, must be multiplied by 3 (average number of people present per house).

For a larger damage area, it is sufficient to classify the area according to its type of use, whereby the following global inventory of population densities is provided:

Type of area	Population density (persons/ha)
– residential area:	
nature area	0
remote area	1
scattered housing	5
quiet residential area	25
busy residential area	70
urban area	120
– industrial areas:	
low density of personnel	5
medium	40
high	80
– recreational area:	
camp site	130
(only during tourist spot	200
summer period)	

Presence during day/night, indoors/outdoors

For residential areas a percentage of presence during the night equal to 100% is being used. During the day-time 30% to 70% of the people will be present in residential areas.

However, if within the residential area schools and/or employment are also present, then the percentage of presence can be taken equal to about 100%.

For industrial areas, a percentage of presence of 100% during the day-time is valid. If, in some companies, people are working during the night, this percentage of presence is equal to about 20%, but, if not, then it is equal to about 0%.

Presence in a recreational area during the day or the night highly depends on the type of recreation. If this is difficult to estimate, a figure of 100% is considered for the day as well as for the night.

On the average, 7% of the people are staying outdoors during the day, and 1% is outdoors during the night [7]. This distribution can be used for both residential and industrial areas, unless other figures are known, for instance, for specific work outside.

For recreational areas an inventory of the types of recreations is necessary, specifically with reference to indoor or outdoor recreation.

The data presented in this study can only represent global indications, since population data, within the various categories, can vary substantially and are dependent on a large number of factors which must be further quantified, such as:

- time of the year
- wheather conditions
- day of the week
- time of the day
- age, profession and life habits of different people.

References

- [1] N.J. Glickman, M.J. White.
Urban land-use patterns: an international comparison.
Environment and Planning A, 1979, volume 11, pages 35-49.
- [2] K. Sexton, R. Letz, J.D. Spengler.
Estimating human exposure to NO₂: An indoor/outdoor modelling approach.
Environmental Research, 1983, volume 32, pages 151-166.
- [3] D. v.d. Brand, mw. S. Fiebelkorn.
Notitie: Aanwezigheidsgegevens ten behoeve van schadeberekeningen. (Note on presence data for damage calculations) Provinciale Waterstaat Zuid-Holland, Provinciale Planologische Dienst, februari 1985.
- [4] Centraal Bureau voor de Statistiek.
4e Algemene Bedrijfstelling 1978.
Deel 2. Algemene sectorale gegevens.
- [5] Centraal Bureau voor de Statistiek.
Statistisch Zakboek 1985.
- [6] A report to the Rijnmond public authority. ("Covo study")
Risk analysis of six potentially hazardous industrial objects in the Rijnmond area, a pilot study.
November 1981.
- [7] J.I. Petts, R.M.J. Withors, F.P. Lees.
The assessment of major hazards: the density and other characteristics of the exposed population around a hazard source. Journal of Hazardous Materials, 14 (1987) 337-363.
- [8] LPG, a study
Comparative risk analysis of the storage, the transshipment, the transportation and the use of LPG and motor spirit. MT-TNO, may 1983.

Table 1 Summary of the note: Data on presence for damage calculations.
D.v.d. Brand and Mrs. S. Fiebelkorn [3].

Land-use pattern	Number of people present				%In/outdoors	
					day	evening +night
1. Housing, 3 inhabitants/housing unit - scattered house-building, low buildings - very low density house-building, low buildings - quiet housing district, scattered flats - busy housing district, low buildings + flats - highest density, flats	very small scattered	small	medium	large	36/64	92/8
2. Lived-in trailers and ships 3. Hospital, nursing home, old age people home, sanatorium 4. Infants-, basic school 5. Advanced education 6. Shopping centers, -streets 7. Office 8. Industry or trade	20 pers. 10/shop	9/location 60 beds= 240 pers. 50 pers. 200 pers. 100/ha 10 pers. 5 pers.	30/location 300 beds = 1500 pers. 200 pers. 500 pers. 500/ha 100 pers. 100 pers.	120/loc. 600 beds= 3000 pers. 500 pers. 1000 pers. ≥1000 1000 pers. 500 pers.	38/62 70/10 67/33 71/29 33/46 86/14 78/22	93/7 33/6 5/11 8/11 7/8 0/1 11/10

Table 1 (Contd.)

(cont. tabel 1)

Land-use pattern		very small scattered	Number of people present				%In/outdoors	
			small	medium	large	very large	day	evening +night
9. Hotel and catering industrie			10 pers.	50 pers.	250 pers.		17/21	91/2
10. Theatre/cinema			50 pers.	100 pers.	200 pers.		41/10	27/9
11. Church			10 pers.	50 pers.	250 pers.		48/12	29/7
12. Sport-hall, covered swimming-pool			50 pers.	100 pers.	1000 pers.		67/25	25/13
13. Station			50 pers.	500 pers.	1000 pers.		25/25	8/7
14. Camping, public garden + garden house							12/88	76/24
– bungalows				125/ha				
– trailer parks (standard trailers)				200/ha				
– touristic locations				180/ha, on peak days	225/ha			
15. Sport and recreation outdoors							0/95	0/19
– extensive use				25/ha				
– intensive use				500 pers.				
– very intensive use				2500/day				
16. Important auto-routes				16.000 cars/24 hours/lane			50	50
– line up				100 cars/km/lane				
– normal circulation				20 cars/km/lane				

Remarks with reference to table 1.

*

The table has been established by planners. Data on presence are presented for 16 different land-use patterns (purpose of the area/building). A number of such pattern is further sub-divided into some presence classes.

*

The percentages indoors and outdoors for day and night have been obtained from ref. [3], using the following distribution of the 24 hours period for the day and for the night:

- day: 8.00 - 18.00 hours
- night : 18.00 - 8.00 hours

*

The sum of the percentages indoors and outdoors gives the average percentage of people present. This does not, consequently, always have to be equal to 100%, since, for many land-use patterns, the numbers of persons present which are mentioned do not have to correspond to a presence during the whole day or the whole night.

*

For land-use pattern 14 (campings) and 15 (sport and recreations outdoors) the percentages of presence indicated correspond to a summer period (about 40% of the year).